The Effects of Seating on the Acoustics of Auditoria

by

William Jonathan Davies

Submitted for the degree of Doctor of Philosophy in

the Department of Applied Acoustics of the University of Salford.

June 1992

Contents

Part II

Table of Illustrations

Acknowledgements

I am greatly indebted to Dr. Rafal J. Orlowski and Dr. Y. W. Lam, who supervised the work described in this thesis. They gave encouragement, advice, practical help and intellectual guidance. Many thanks are also due to my colleagues and friends at Salford who submitted to numerous subjective experiments and provided vital assistance for the measurements in auditoria. Trevor Cox should be singled out for his collaboration in the development of the concert hall simulator. A lot of the measurements would also not have been possible without the cooperation of the acoustic consultants, architects, seating manufacturers, and hall owners associated with the auditoria visited. I am grateful to the Department of Building at Heriot-Watt University for the loan of much of the equipment for the concert hall simulator, and to the Acoustics Laboratory at the Technical University of Denmark for the use of their computer program Odeon. Financial support for much of the work was gratefully received from the Science and Engineering Research Council. Finally, I should like to thank my wife Jane, who saw me through the production of this thesis.

Abstract

The two main attributes of seating in auditoria have been investigated. The first is random incidence absorption. The second is the low-frequency selective attenuation which seating can impart to sound travelling over it at grazing incidence: the so-called "seat dip" effect.

It was found that there was a need for a more accurate laboratory measurement method to predict auditorium seat absorption. The traditional method tended to overpredict the absorption of the exposed front and sides of seating blocks. A new method was studied which involves the use of barriers to obtain realistic measurements of front and side absorption. The new method was validated by comparing measurements of seats made in a reverberation chamber with *in-situ* absorption data for the same seats, calculated from reverberation time measurements in ten auditoria with and without the seats present. The accuracy of the new method was found to be satisfactory in all cases, although a severe lack of diffusion in two of the halls hindered the validation process.

The important physical factors affecting seat dip attenuation were investigated by measurements in a concert hall and on scale model seats. A scheme for reducing the attenuation with resonant absorbers was evaluated, and a simple theoretical model developed. The subjective significance of the effect was established with a panel of ten subjects and a fully simulated auditorium sound field. The absolute threshold of perception of the seat dip effect was found to be 7.1 ± 0.6 dB attenuation in the 200 Hz octave band of the early field. It was found that seat dip attenuation might be made less audible in a hall by: (i) supplying early energy along paths remote from the seating, (ii) increasing the vertical angle of incidence of the direct sound and (iii) installing resonant absorbers in the floor between seat rows.

Chapter 1

Introduction

In the last twenty years, much progress has been made in understanding the importance and subjective perception of the early sound field in auditoria. This has led to a number of design criteria dealing principally with the early field, such as Early Lateral Energy Fraction. These researches have been driven by the need to obtain subjectively preferred listening conditions in modern auditoria which often have considerably greater seating capacities and radically different shapes from the venerated classical rectangular concert halls.

Yet the oldest parameter in room acoustics is still the one which hall designers turn to first. This is reverberation time which, as Sabine established empirically in 1923, should depend solely on the volume and total absorption of a room. Of all the parameters in common use in auditorium design today, reverberation time was the first to be established and it is one of the most subjectively important. Because the total absorption in a hall is dominated by that of the seating and audience, it is essential that these can be measured or predicted accurately in the early stages of design. However there is at present no wholly accepted standard test method for measuring seating absorption and the data quoted in the literature varies widely.

The traditional method of measuring seating absorption involves placing a small array of seats in the centre of a reverberation chamber. The main problem with this arrangement is that it exaggerates the absorption of the exposed front and side of the seating array, compared to the larger seating blocks commonly found in auditoria. This results in errors in the predicted reverberation time for the auditorium.

A modification of the traditional reverberation chamber test method for seating absorption was proposed by Kath and Kuhl as long ago as 1964. Though this seemed to offer the possibility of greater accuracy by correctly allowing for the absorption of the exposed front and sides of seating blocks in auditoria, it has not been widely taken up. This may have been due to the absence of any large-scale validation of the method, and a lack of understanding of the effects of the various measurement parameters. The work reported here aims to clarify this situation.

The first part of this thesis covers the investigation and validation of a reverberation room method of measuring seating absorption. New investigations which concentrate on many of the parameters pertaining to it are presented. The choice of the optimised parameter values is justified by comparisons between reverberation chamber measurements and accurate *in-situ* seating absorption measurements in ten auditoria. It is concluded that the new method is significantly better than the traditional method and that it can provide accurate predictions of seating absorption so that the chance of a subjectively significant deviation from the design value of reverberation time is minimised.

A second and more subtle effect of seating in auditoria is the selective low-frequency attenuation it imparts to sound travelling over it at grazing incidence. This is quite separate from, and largely unrelated to, the statistical absorption coefficient of the seating. This so-called "seat dip" effect was first quantified during measurements in New York Philharmonic Hall made by two teams of researchers, Schultz and Watters, and Sessler and West, both in 1964. Their reports communicated the somewhat alarming fact that the attenuation could be as severe as 20 dB around 150 Hz. The authors conjectured as to the subjective significance of the phenomenon, one team concluding more pessimistically than the other. It is certainly true that seat dip attenuation must occur on the flat stalls floors of some of the best concert halls in the world, but nobody knew whether it could be detected by listeners and, if it could, how important it was subjectively.

Recently, there has been a resurgence of interest in the problem of seat dip attenuation with the ever closer examination of the early sound field and reflection sequences in auditoria. Two theoretical models of the attenuation and some new measured data have appeared in the literature. It is also now possible to make some inferences of the subjective importance of the phenomenon from the work of Morimoto and Maekawa (1988), amongst others. This demonstrates that low-frequency early energy is of great importance in establishing the desirable attribute of auditory spaciousness. Following the work of Barron and Marshall (1981), it is known that early *lateral* reflections are crucial too. Since seat dip attenuation affects the early lateral reflections passing over seating as well as the direct sound, it seems likely to have some significance for the listener. However, there are no

direct measurements in the literature of the subjective effect of seat dip attenuation in a typical concert hall. Another development has been the suggestion by Ando (1982) of a method for reducing the measured attenuation by making the floor between seat rows absorbent at low frequencies. This was based on theoretical calculations only and no full practical investigation of the advantages and disadvantages of such a scheme has been published to date.

The second part of this thesis is concerned with a comprehensive investigation, both subjectively and objectively, of seat dip attenuation. The main aims were to establish how the phenomenon occurs, whether it can be detected by the audience in a typical hall, and how it might be reduced. To this end, new measurements of the seat dip effect in a concert hall and on scale model seating are presented. The extent to which the attenuation can be altered by different types of floor absorber is also investigated by measurement. Subsequent chapters elaborate on the physical mechanism underlying the seat dip effect, leading to the development of a simple computer model. The subjective significance of the measured attenuations is evaluated from tests on a panel of subjects in a completely simulated concert hall sound field which included variable seat dip attenuation. It is concluded that seat dip attenuation probably is an audible concern in many concert halls, though a relatively minor one. The wide plan shapes with nearly flat stalls floors found in some modern auditoria are likely to be troublesome, however. Several ways of ameliorating the attenuation are examined in this thesis. Each of these methods has its drawbacks, so that a combination will usually be the best approach for design.

Part I

Chapter 2

Methods of Measuring Seating Absorption and their Parameters

This chapter compares a new reverberation room method of measuring seating absorption, based on a proposal by Kath and Kuhl (1964), with other methods. An investigation of the parameters affecting the new method is presented. Besides the new method, there are four others available: the traditional reverberation room method, a rather lengthier reverberation room method due to Bradley (1992), and two more approximate prediction methods based on average seat absorption coefficients.

2.1 The Traditional Method

The aim of measuring the random incidence absorption of a small sample of seats in a reverberation chamber is to predict the absorption which a large area of the same seats will exhibit when installed in an auditorium. The traditional method, as recommended by BS 3638: 1987, is to place a rectangular array of the seats with a plan area between 10 and 12 m^2 in the centre of the reverberation chamber, using the same row spacing as is found in the real theatre. Hence the largest typical sample is likely to be about 24 chairs; in the current work, the standard sample was four rows of six chairs. When this is scaled up to a large block of seats every fourth

row is in effect a front one, and every sixth seat is on the edge of an aisle. This over-emphasis of the absorption of the front row and side aisles leads to a predicted absorption coefficient higher than that which will be exhibited in the auditorium.

2.2 Average Seat Absorption Methods

2.2.1 Kosten's α_{eq}

There are two methods of predicting the reverberation time (RT) in an auditorium which do not rely on a measurement of the actual seat absorption, but instead use averaged data from many halls already built. The simplest of these is due to Kosten (1965). From published RT, volume and seating area data for more than 40 concert halls, Kosten calculated an average absorption coefficient α_{eq} assuming that the seats are the only significant absorber in a hall. He drew a cumulative distribution plot of mid-frequency α_{eq} for all the halls, and eliminated the extremes. The average mid-frequency values of α_{eq} were found to be 0.81 ± 0.11 for unoccupied halls, and 1.07 ± 0.07 for occupied ones. The reverberation time T in a new hall can then be predicted thus:

$$T = \frac{0.161\,V}{S_A\,\alpha_{eq}} \qquad (2.1)$$

where V is the hall volume and S_A is the audience and orchestra area including aisles up to one metre wide.

Kosten's prediction method is best suited to early design calculations. Because seating absorption can vary significantly between different seat types and other

significant absorbing surfaces are often present in halls, a high enough accuracy for a finished design cannot be guaranteed. The method does seem to be robust across a wide range of halls, however. Kosten's calculations have been repeated in British halls by Barron (1988), who arrived at the remarkably similar figure of 1.06 ± 0.07 for occupied α_{eq}.

2.2.2 Beranek's α_S and α_T

In 1960, 1962 and 1969, Beranek published average absorption data for occupied and unoccupied seats calculated from a large number of halls. The data in the 1969 paper includes that from the other two publications and so it will be used here as the most complete. These figures are still widely used in hall design, and have now found their way into commercial room acoustic computer modelling programs, such as the one described by Rindel (1991).

To obtain the audience absorption coefficient, α_T, (that is, for occupied seating) Beranek averaged values calculated from reverberation times measured in a studio, a reverberation chamber (by Kath and Kuhl (1964)) and in halls (by himself). Next, an average absorption coefficient, α_R, for all the surfaces in a hall other than the seating, audience and orchestra, was calculated by Beranek. This was done by using α_T, an average RT from measurements in many occupied halls, an average value for the ratio of hall volume to seating area, V/S_T, and an average value for the ratio of areas not covered and covered by audience, S_R/S_T. Finally, an average unoccupied absorption coefficient for upholstered seats, α_S, was calculated by Beranek using all the above data along with Kosten's α_{eq}. No uncertainty estimates

are given for all these averages, though, as Bradley (1992) has noted, the errors are likely to be quite large due to the uncertain accuracy of the many measurements, the use of different measurement methods, the varying states of diffusion of all the halls and rooms (though Beranek's RTs are for large halls only) and the use of average values for V/S_T and S_R/S_T.

The RT in a new hall can now be predicted in the normal manner, except that α_T or α_S is used in place of the actual seating absorption coefficient. RT predictions made using Beranek's data are likely to be more accurate than those made using Kosten's because Beranek's scheme does away with the assumption in Kosten's method that the seating is the only absorber in the hall. However, the method is still not totally reliable for finished designs unless one can be confident that the seats to be used in a particular hall will have an absorption close to Beranek's average. Since modern seat designs can vary greatly, this will be doubtful in many cases.

2.3 The Need for Greater Accuracy

None of the methods described above can be completely relied upon for predicting seating absorption accurately. This has been remarked upon by Kuttruff (1991, p. 164) and Nagata (1990), amongst others. The question of how much accuracy the designer needs arises here. An estimated answer can be given from the difference limen for reverberation time T obtained by Seraphim and quoted by Cremer and Müller (1982a, pp. 505-506). Seraphim measured the smallest percentage change $\delta T/T$ which could be correctly identified by 75% of his subjects for reverberated

band pass noise with various values of T and centre frequency. For the mid-frequency octave between 800 and 1600 Hz, $\delta T/T$ is between 3 and 4% for values of T between 0.6 and 4 seconds. Since the reverberation time in a hall is governed by the audience and seating absorption, this indicates that one should aim to measure seating absorption to an accuracy of 3 to 4%, at least at mid frequencies. This level of accuracy is unlikely to be achieved by the average seat absorption methods, unless one is lucky with the actual seat absorption for Beranek's method, or with all the hall absorption coefficients for Kosten's method. Such an accuracy is also often not found with small samples of seats measured with the front and sides exposed according to the traditional reverberation chamber method.

2.4 Bradley's Method

Very recently, Bradley (1992) published details of a seating absorption measurement method which attempts to take account of the variation of seating absorption coefficient with sample size - the failing of the traditional method. This involves making measurements on five or six differently sized arrays of a seat type. The variation of absorption coefficient with the ratio of array perimeter length to area, E, is assumed to be linear, so that a straight line may be fitted to the data. This is extrapolated back to the smaller values of E which characterise large seating blocks in auditoria. Bradley found that this method could give accurate results when compared with measurements of the same seats *in situ* in auditoria.

Though it seems that this method can offer superior accuracy over the other three methods discussed above, it does require a considerable number of tests for each type of seat measured. Bradley also recommends a more economical but less accurate approach. This is to measure one small sample of a seat type in a reverberation chamber and then apply an average correction to obtain the absorption coefficient of a larger sample. This correction is calculated from the average of the absorption coefficient versus E characteristics of the five seat types which Bradley measured. Because this characteristic varies considerably over different seat types, however, the use of an average would seem to be rather hazardous.

2.5 Kath and Kuhl's Method

Kath and Kuhl (1964, 1965) also thought that the over-valuing of front and side absorption in the traditional method was one of the main reasons for poor prediction of auditorium absorption coefficients. They proposed an alternative method which requires fewer measurements than Bradley's and yet may be at least as accurate. In this method the seating array is placed in the corner of the reverberation chamber, and the exposed edges obscured with barriers, as in the photograph in figure 2.1. Though it is true to say that the array is mirrored in the adjacent walls of the chamber, thus effectively increasing its size, it is not effectively infinite as Kath and Kuhl thought. Diffraction effects must still be present at the two free edges and so the measured absorption coefficient may still vary with sample size. The significance of these effects is dealt with in full in chapter 4.

Figure 2.1: An array of 24 seats surrounded by barriers in the corner of the reverberation chamber for an absorption measurement.


No6

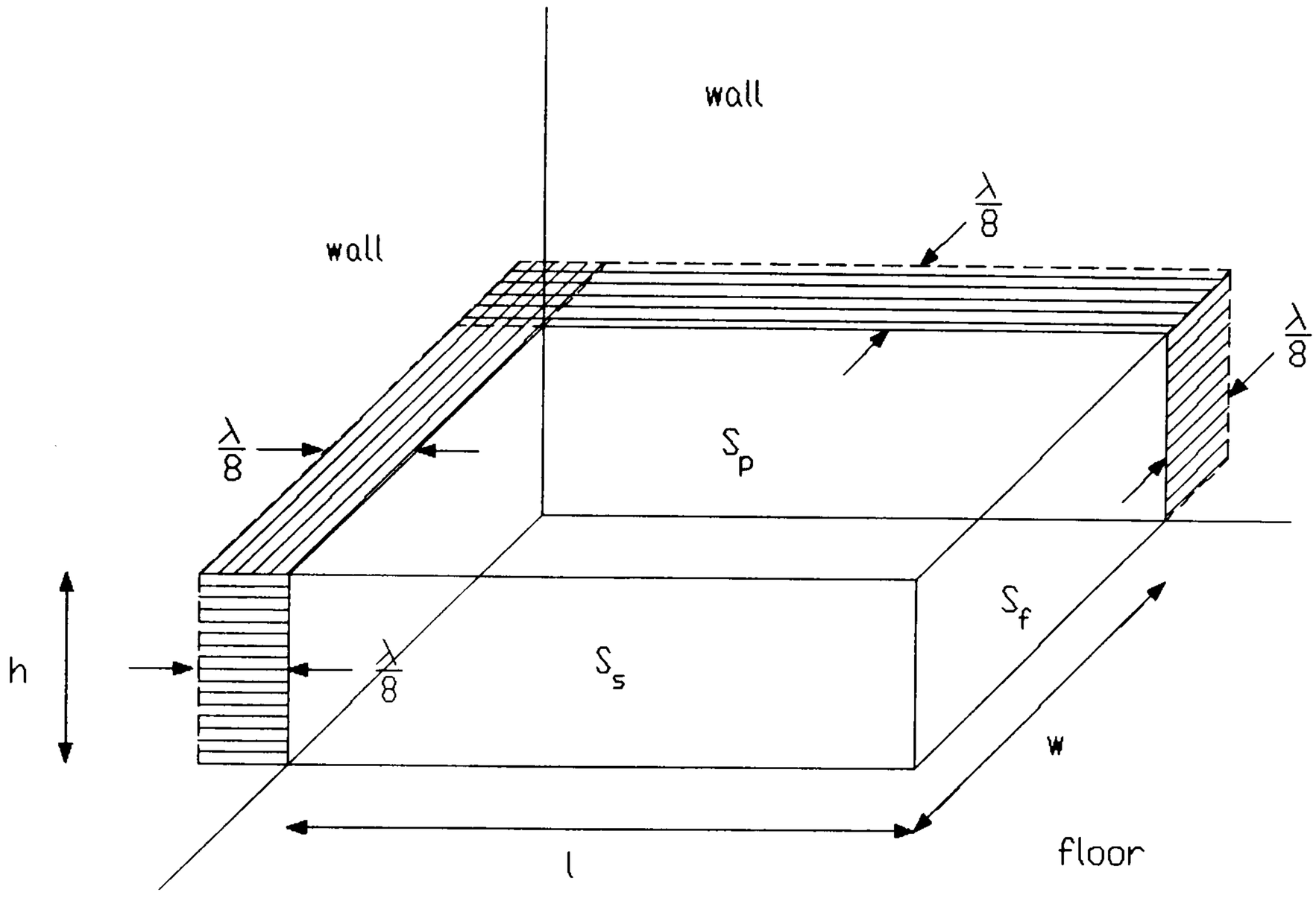

Figure 2.2: Schematic diagram of an array of seats in the corner of the reverberation chamber, showing the strips needed to correct for pressure doubling; after Kath and Kuhl (1964).

Ignoring diffraction effects for the time being, this arrangement allows us to measure three absorption coefficients of the seating array shown schematically in figure 2.2: α_p with barriers covering both the front row and side aisle, α_1 with barriers covering the side aisle only, and α_2 with barriers covering the front row only. If diffraction can be ignored, then α_p is the absorption coefficient for an infinite sample. These absorption coefficients are found from the plan area and measured total absorptions:

$$\alpha_p = \frac{A_p}{S_p} \tag{2.2}$$

$$\alpha_1 = \frac{A_p + A_f}{S_p} \tag{2.3}$$

$$\alpha_2 = \frac{A_p + A_s}{S_p} \tag{2.4}$$

where the suffix p refers to plan, f to front and s to side.

Hence the absorption coefficients of the front row and side aisle may be found:

$$\alpha_f = (\alpha_1 - \alpha_p)\frac{S_p}{S_f} \tag{2.5}$$

$$\alpha_s = (\alpha_2 - \alpha_p)\frac{S_p}{S_s} \tag{2.6}$$

Because the SPL in a reverberant field is increased at the boundaries (Waterhouse, 1955), the absorption coefficients measured will be higher than those found when the sample is in the centre of the chamber. To compensate for this, Kath and Kuhl (1961) proposed that the absorber area used in the calculation should be increased by strips of width $\lambda/8$ as shown in figure 2.2, where λ is the wavelength corresponding to the centre frequency of the measurement. This extra absorbing area accounts for the increase in measured total absorption due to the increase of up to 3 dB in SPL close to the wall. In a corner, the increase is greater, and a correction of $(\lambda/8)^2$ is needed. Hence, the effective test areas become:

$$S_p = lw + \frac{\lambda}{8}(l+w) + \left[\frac{\lambda}{8}\right]^2 \qquad (2.7)$$

$$S_s = lh + \frac{\lambda}{8}h \qquad (2.8)$$

$$S_f = wh + \frac{\lambda}{8}h \qquad (2.9)$$

where all symbols are defined in figure 2.2.

Now, if the areas of the front row (S_{fa}), side aisles (S_{sa}) and plan area (S_{pa}) of a particular large seating block in the theatre are known then its absorption coefficient α_m, expressed as the total absorption which would be measured *in situ* divided by the plan area of the large block, can now be predicted with the laboratory absorption coefficients to give

$$\alpha_m = \alpha_p + \alpha_f\frac{S_{fa}}{S_{pa}} + \alpha_s\frac{S_{sa}}{S_{pa}} \qquad (2.10)$$

Thus, α_m should incorporate the correct amount of absorption due to the exposed front row and side aisles. Alternatively, α_f and α_s can be used to calculate the widths of correction strips to be added to the plan area to take account of front row and side aisle absorption when designing auditoria. For the front row, the strip width in metres is k_f, such that

$$\alpha_1 S_p = \alpha_p(S_p + k_f l) \qquad (2.11)$$

$$\Rightarrow \quad k_f = l\left[\frac{\alpha_1}{\alpha_p} - 1\right] \qquad (2.12)$$

Similarly, the width of the correction strip for the side aisles is

$$k_s = w\left[\frac{\alpha_2}{\alpha_p} - 1\right] \tag{2.13}$$

where α_p, α_1 and α_2 are the measured reverberation chamber coefficients from equations (2.2), (2.3) and (2.4). Note that if we are not interested in examining α_f and α_s by themselves, α_m in equation (2.10) can also be expressed in terms of α_p, α_1 and α_2:

$$\alpha_m = \alpha_p(1-p-q) + \alpha_1 p + \alpha_2 q \tag{2.14}$$

$$\text{where} \quad p = \frac{S_{fa}S_p}{S_f S_{pa}} \quad \text{and} \quad q = \frac{S_{sa}S_p}{S_s S_{pa}} \tag{2.15}$$

2.6 The Reverberation Chamber Measurement System

It was thought that Kath and Kuhl's method offered the basis for an accurate way of predicting seat absorption in an auditorium without making too many measurements. To investigate the method further, it was determined to attempt to validate it and therefore to make many measurements of seat absorption in a reverberation chamber. In validating a variation of a technological testing method, it is important that the accuracy of the equipment and facilities used should have a traceable standard. To this end, it was ensured that the reverberation chamber and equipment used for the laboratory measurements of seating absorption complied with BS 3638: 1987. This standard recommends the traditional method of testing seats with their edges left exposed, for which it has been criticised above in section 2.1. However, it is thought to be perfectly adequate in other aspects of

equipment and method specification. The standard recommends a room volume of approximately 200 m^3. The room used at the Department of Applied Acoustics at Salford has a volume of 224 m^3 and a surface area of 226 m^2. The room plan in figure 2.3 shows that it has one slanting wall to aid diffusion; the ceiling is horizontal.

In accordance with BS 3638, the aspect ratio of the room is not far from unity, and

$$l_{max} < 1.9V^{1/3} \quad (2.16)$$

where V is the volume of the room and l_{max} is the length of the longest straight line which fits inside it. Eleven fixed diffusers were suspended in the room. These consisted of curved and varnished plywood sheets with a total two-sided area of 67.1 m^3 oriented and hung at random throughout the room. Two of the diffusers can be seen in the photograph of a seat absorption measurement in figure 2.1.

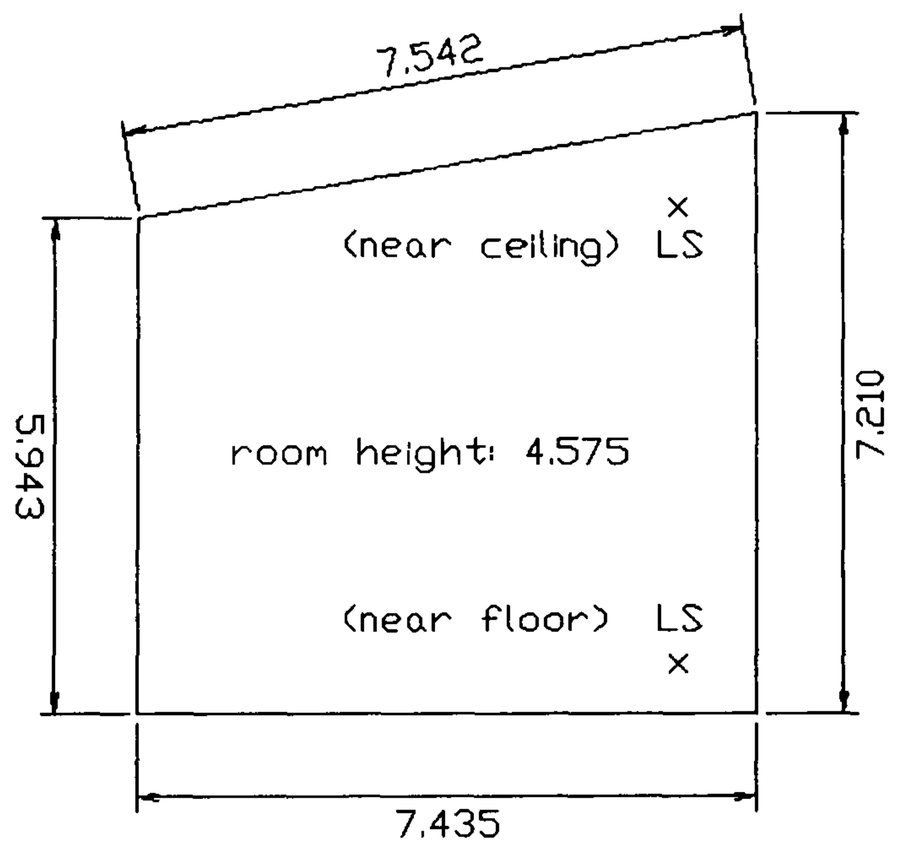

Figure 2.3: Plan of reverberation chamber.

To measure sound decays in the room, two loudspeakers, indicated in figure 2.3, and five microphones, all at known positions were used. Broadband pink noise was radiated from one loudspeaker, interrupted, and the decay recorded at one

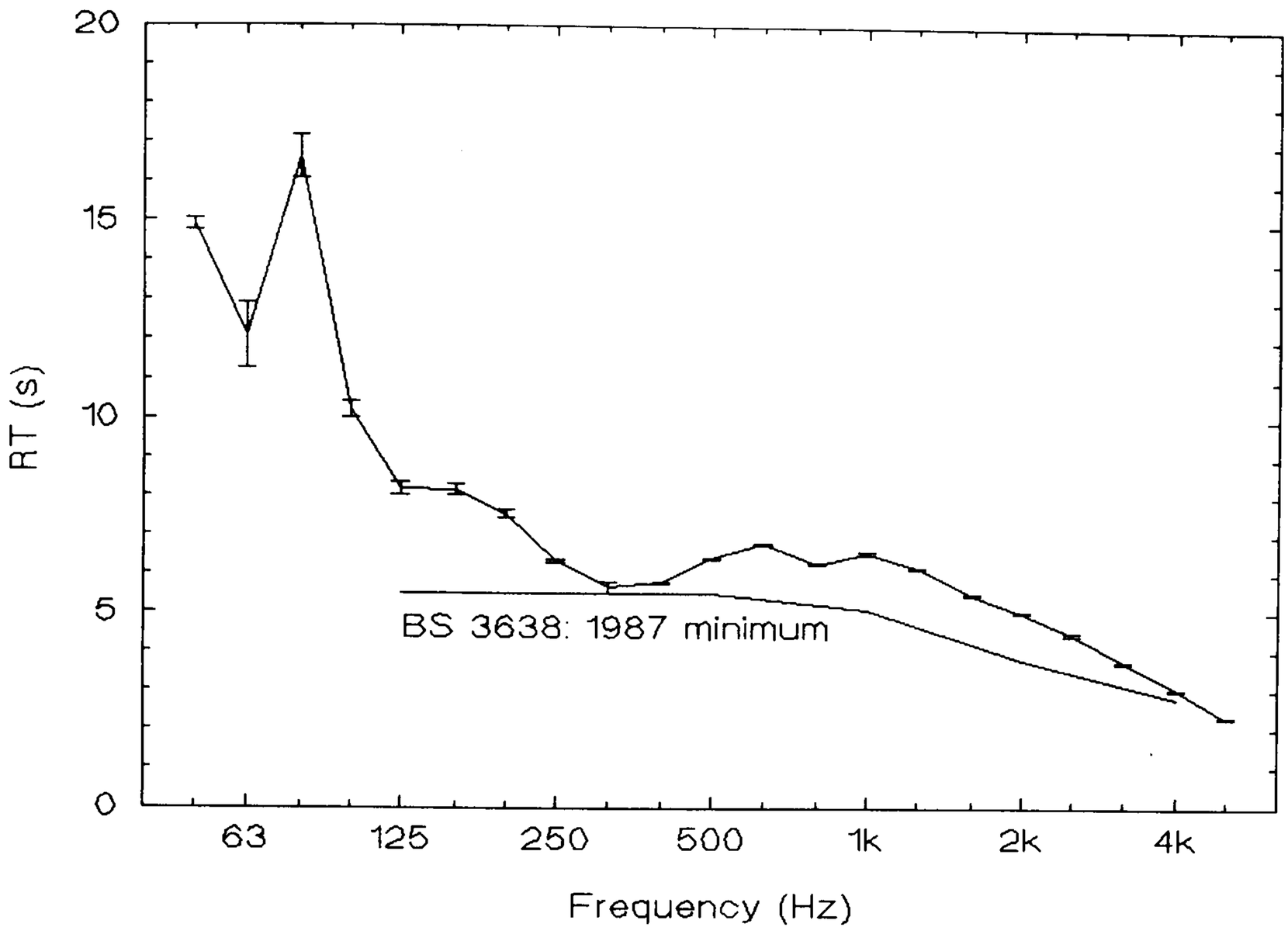

Figure 2.4: Averaged Reverberation Time in empty chamber plotted with BS 3638: 1987 minimum curve. The error bars represent ± one standard error.

microphone. This was done five times and the five decay curves were averaged in 1/3 octave bands by a Norwegian Electronics NE830 real-time analyser. The analyser was then used to calculate the RT in each frequency band for this loudspeaker and microphone combination by fitting a straight line between the -5 and -35 dB points of the averaged decay curve. This procedure was repeated at the other four microphones. Next the microphones were moved to new known positions and the second loudspeaker was used to generate another five decays for each microphone. This process resulted in ten RTs in each frequency band which were used to give an ensemble average in each band. The measurement process

thus involved averaging across time and space. Because all the evaluated RTs were recorded and kept, any systematic variations between different loudspeaker and microphone position combinations could be examined if poor homogeneity was suspected. It was assumed that any variations between the five decays at any one measuring position would be essentially random, and so these raw decays were averaged without being stored. Figure 2.4 shows a typical RT spectrum for the empty room, along with the BS 3638 minimum curve for the particular room volume and surface area.

2.7 Absorption Coefficient Formula

Sabine's formula was used to calculate the absorption coefficient α of a sample of seats from reverberation time measurements made with and without the seats present in the chamber:

$$\alpha = \frac{55.3V}{S(331+0.6t)}\left[\frac{1}{T_s}-\frac{1}{T_e}\right] \qquad (2.17)$$

where S is the plan area of the seating in m^2;

t is the average ambient air temperature in ^{o}C;

T_s is the reverberation time measured with the sample in the chamber, in seconds;

T_e is the reverberation time measured in the empty chamber, in seconds.

It should be remembered that this formula, though originally derived empirically by Sabine (1923), is a product of statistical room acoustics which requires a

perfectly diffuse sound field and ignores wave effects. There has been much criticism of its widespread use in room acoustics because of this (by Gomperts (1965), for example) and many authors have proposed alternative formulae and methods. These range from the widely-accepted equation of Eyring (1930), often used where average absorption is high, through less well-known and more complicated formulae like that of Arau-Puchades (1988), to the complete refutation of theoretical statistical room acoustics by Gomperts (1965). Certainly, it is true that perfect diffusion cannot be obtained with a highly-absorbing surface in the room, but the criticisms of Gomperts seem overstated. Because Sabine's formula remains dominant, at least for technological testing, it was felt important that any adaptation of the method for measuring seating absorption should also use it. It seemed that Kath and Kuhl's method for measuring seating absorption might offer increased accuracy while still allowing a simple calculation formula. As with all statistical room acoustic methods, the main proviso is that errors in absorption coefficients estimated from the reverberation time variances may be smaller than the real uncertainties at low frequencies due to a low modal density in the measuring room. Kuttruff (1991, p. 256) has contributed a formula for the lowest frequency at which the modal density in a room is high enough for statistical equations to be used with confidence:

$$\sqrt[3]{V} f_{min} \approx 1000 \qquad (2.18)$$

For the reverberation chamber used here, f_{min} is 165 Hz. It should be noted that reverberation rooms are often used below this limiting frequency. BS 3638: 1987

stipulates a lower ⅓ octave measurement band of 100 Hz, but recommends a room volume of 200 m^3, for which f_{min} is 171 Hz.

2.8 Repeatability of Measured Absorption Coefficients

In order to check that the measurement system described above was consistent in itself, a short run of repeatability measurements was made, as recommended by BS 3638. A sample of twenty-four auditorium seats was measured six times in the same configuration, being removed from the chamber and replaced for each measurement. The repeatability r of the system was then found from

$$r = t\sqrt{2}\,\sigma_{n-1} \tag{2.19}$$

where t is Student's factor for 95% probability and five degrees of freedom and σ_{n-1} is the standard deviation of the six measurements.

The six absorption coefficients are plotted in figure 2.5, along with r and a typical standard error curve from one of the measurements. The standard error curve was computed from the variance of the measured RTs according to the formulae derived in Appendix A. Because it is not significantly less than half the 95% r curve, the calculated standard error is a reasonable estimate of the uncertainty in the measurement. In other words, the standard error from Appendix A is a reasonable prediction of the uncertainty which is actually found if a given measurement is repeated several times.

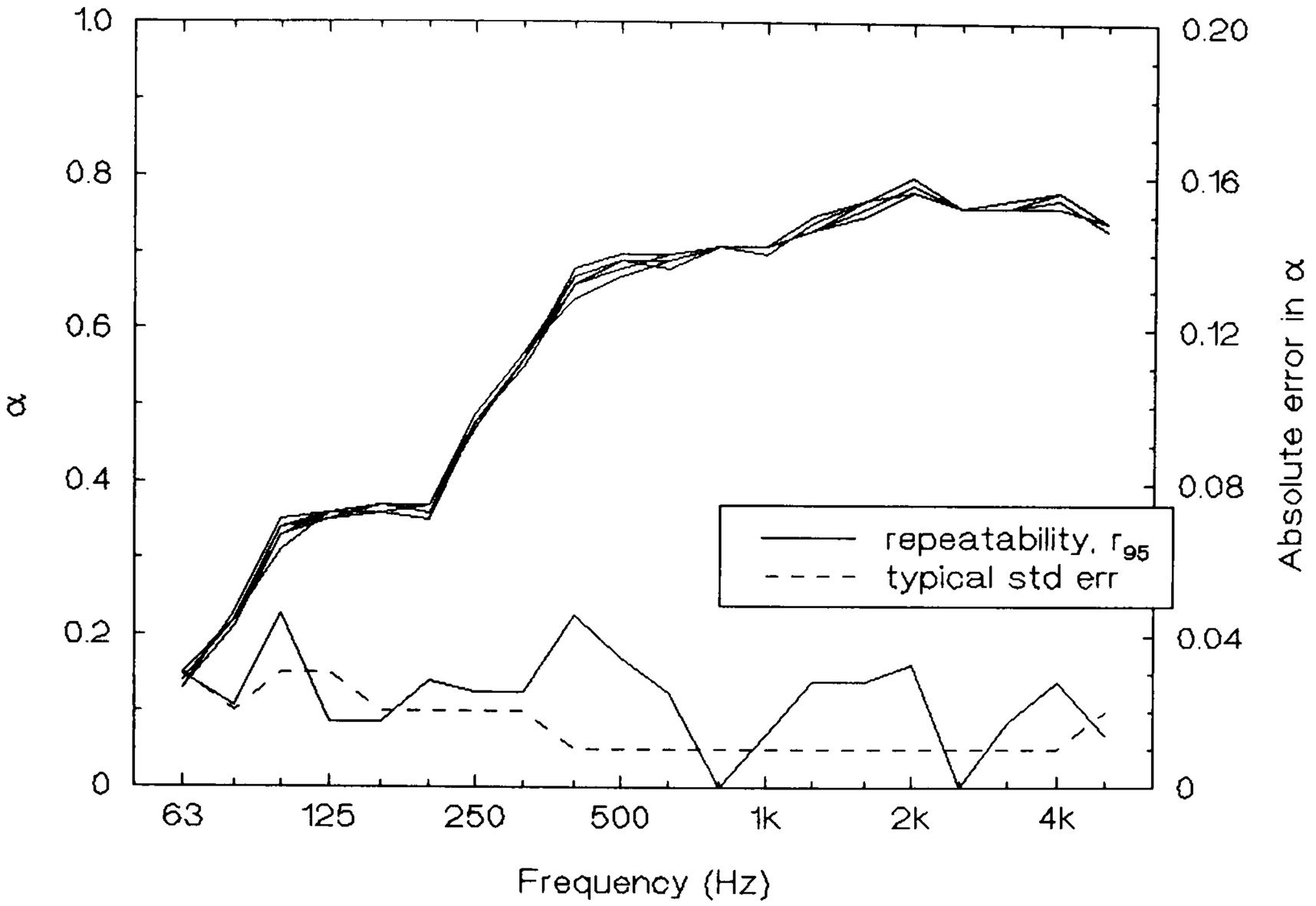

Figure 2.5: Repeatability (95%) of six seating absorption measurements and typical standard error of one.

2.9 Parameters of the New Measurement Method

For comparison with the *in-situ* absorption measurements made in auditoria, many reverberation chamber measurements were made on samples of seating. As part of the optimisation process for the measurement method, the following parameters were investigated: row spacing, array position in chamber, barrier height, number of sides obscured by barriers, the pressure doubling correction, the "large finite area" correction (i.e. using α_m from equation (2.10) rather than α_p from equation (2.2)), the effect of carpet under the seats, and the effect of occupancy. Measurements were made over two years on samples of twelve different auditorium seats, both lightly and heavily upholstered and covered with a variety of materials.

Table 2.1 lists the materials forming the major components of the twelve seat types. The seat types are sorted by their mid-frequency (average of 500 and 1000 Hz octaves) values of α_p, in descending order.

Name	Seat back	Rear back	Squab	Squab underside	Armrest	α_{mid}
A	CF	wood	CF	CW	CF	0.70
D2	CF	wood	CF	wood	CF	0.69
O	CF	metal	CF	wood	-	0.68
B2	CF	wood	CF	wood	CF	0.68
D1	CF	wood	CF	wood	CF	0.67
L	CF	wood	CF	CW	CF	0.67
G1	CF	CW	CF	CW	CF	0.66
G2	CF	CW	CF	CW	CF	0.66
B1	CF	metal	CF	metal	-	0.59
C	CF	plastic	CF	metal	plastic	0.56
H	CF	metal	CF	metal	-	0.55
M	VF	metal	VF	metal	-	0.37

Table 2.1: Materials composing the twelve seat types. (CF = cloth (woven) on foam, CW = cloth (woven) on wood and VF = impervious vinyl on foam.)

Because of time limitations, it was not possible to examine the effect of every combination of parameters on each seat type. However, most parameters were investigated for most seats, using an array of four rows of six in almost all cases. Because of the difficulty of obtaining test persons, it was only possible to determine the effect of occupancy with two seat types.

Since only the effects of the various parameters are discussed in this chapter, most of the following graphs use a "standard" measurement as a baseline: that is, the seats were placed in the corner of the chamber, at 900 mm row spacing, surrounded by 0.9 m high barriers, corrected for pressure doubling at the walls, but with no corrections for front and side absorption. Figure 2.6 shows the range of absorption coefficients from the ten seat types which were measured in this configuration. Most of the seat types have an absorption profile not unlike that of a homogeneous porous absorber. The most notable exception is seat type D2 which was a standard well-upholstered model, except that its squab was hollow. The bottom of this squab consisted of a 350 by 330 by 45 mm air volume covered with 5 mm thick stiff plywood, and this seems to have produced an effective low-frequency resonant panel absorber. Seat type B2 is picked out as representative of the well-upholstered cloth-covered seats often installed in concert halls. It was a standard model from a large manufacturer.

Any error bars in the following graphs represent ± one standard error, calculated according to the formula derived in Appendix A. The barriers were constructed from sheets of 18 mm thick chipboard.

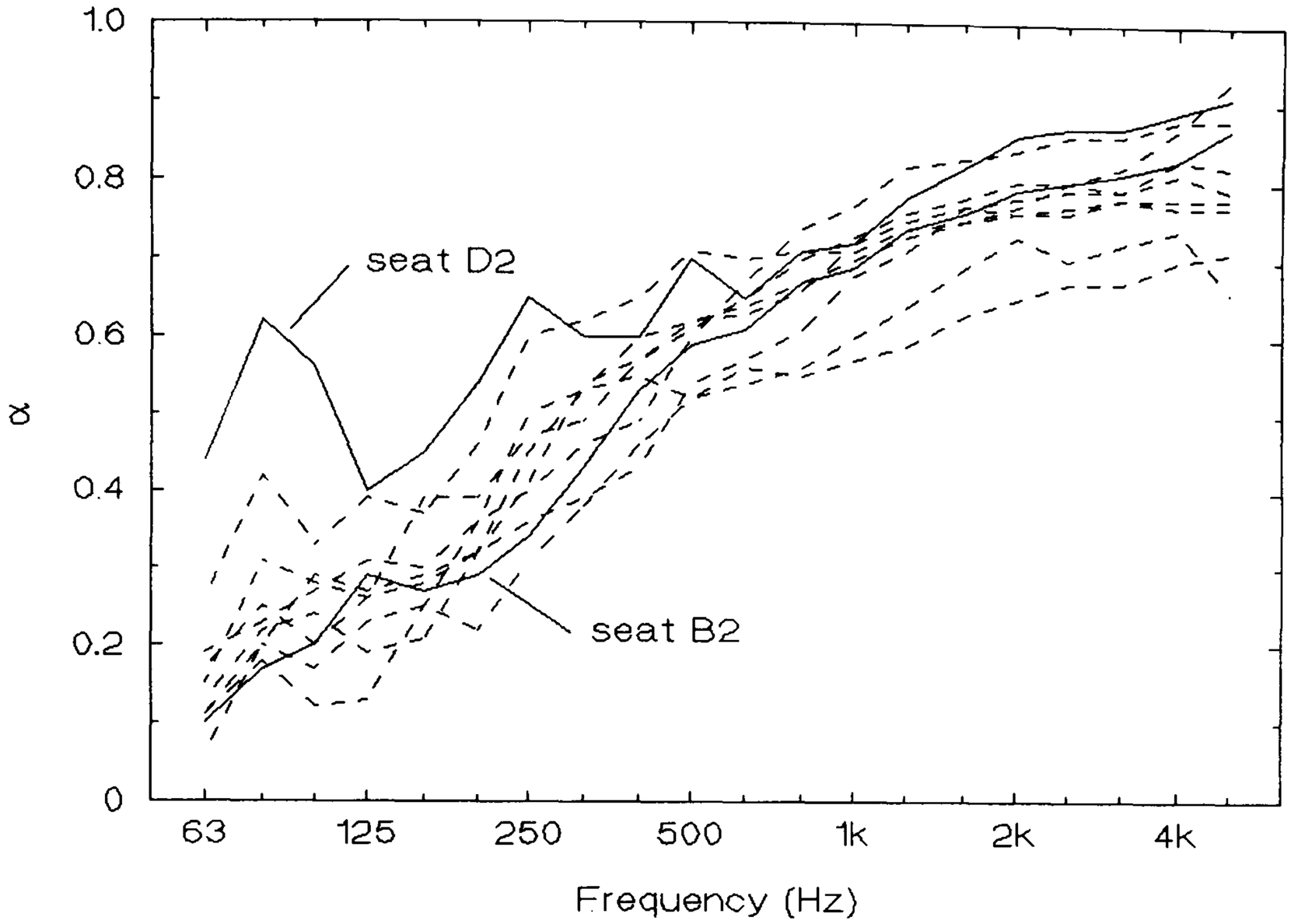

Figure 2.6: Reverberation chamber absorption coefficients of ten different seat types, measured using the "standard" version of the new method at 900 mm row spacing.

2.9.1 Row Spacing

Figure 2.7 shows the effect of varying the row spacing over a small range commonly found in auditoria, on the absorption coefficient of seat B2. The effect is significant compared to the magnitude of one standard error. It should be noted that increasing the row spacing *increases* the total absorption of the seat array, but the plan area increases faster, and so the combined effect is to *decrease* the absorption coefficient.

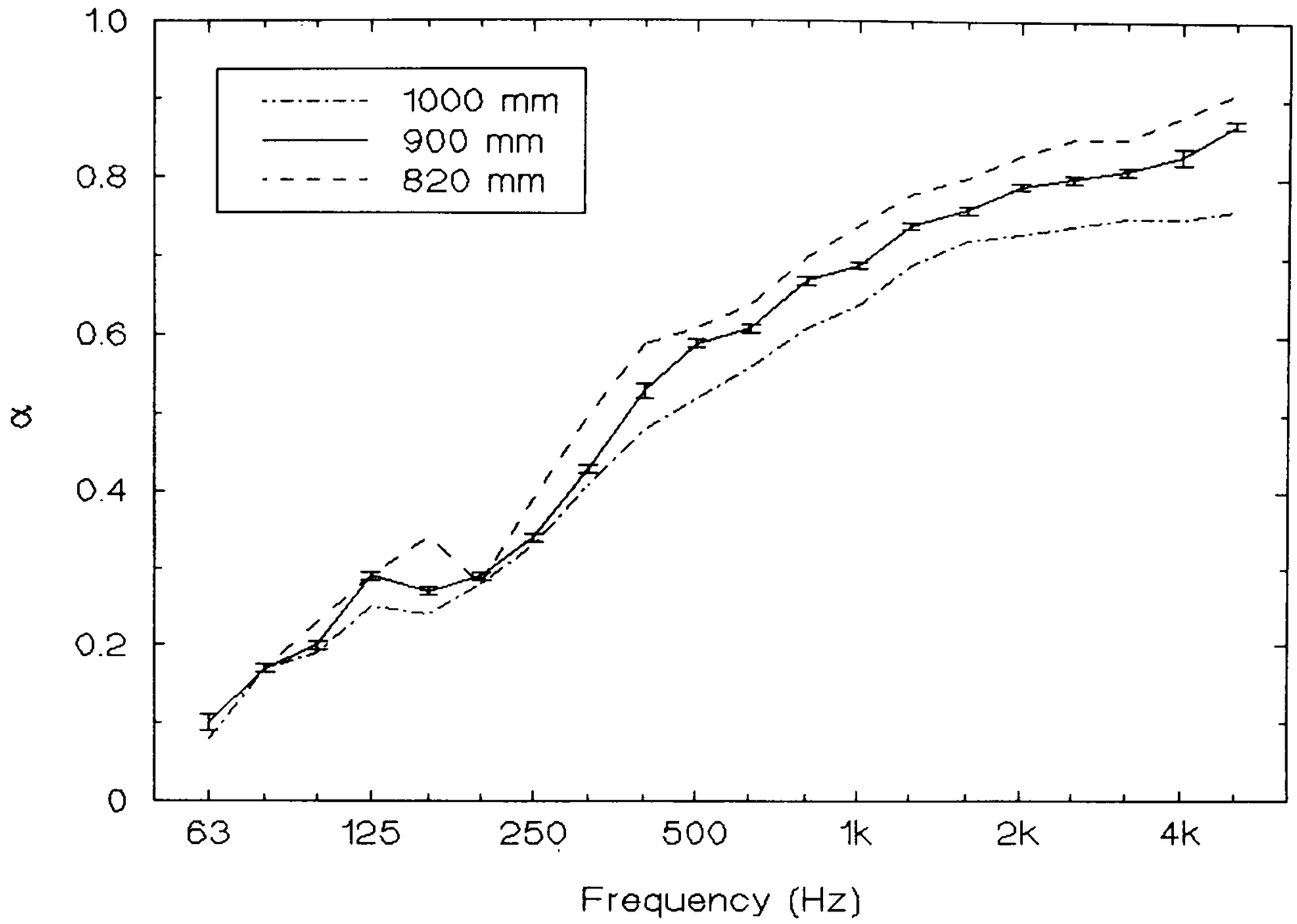

Figure 2.7: Effect of row spacing on the α_p of an array of 24 seats of type B2, measured in the corner and surrounded by 0.9 m barriers.

Though the lines in figure 2.7 are different, they are all highly correlated with each other (the lowest correlation coefficient is 0.9938). This indicates that it should be possible to predict absorption at one row spacing from a measurement of absorption at another. No attempt has been made to produce a straight line regression for prediction, however. The magnitude of the effect of row spacing depends, not surprisingly, on how absorbent the seats are. There was not enough time to make measurements on several seats at say, six different row spacings each. Nevertheless, if data is supplied for the absorption of seats at two different row spacings and a hall designer requires it for a third spacing, then linear extrapolation should be a good first approximation.

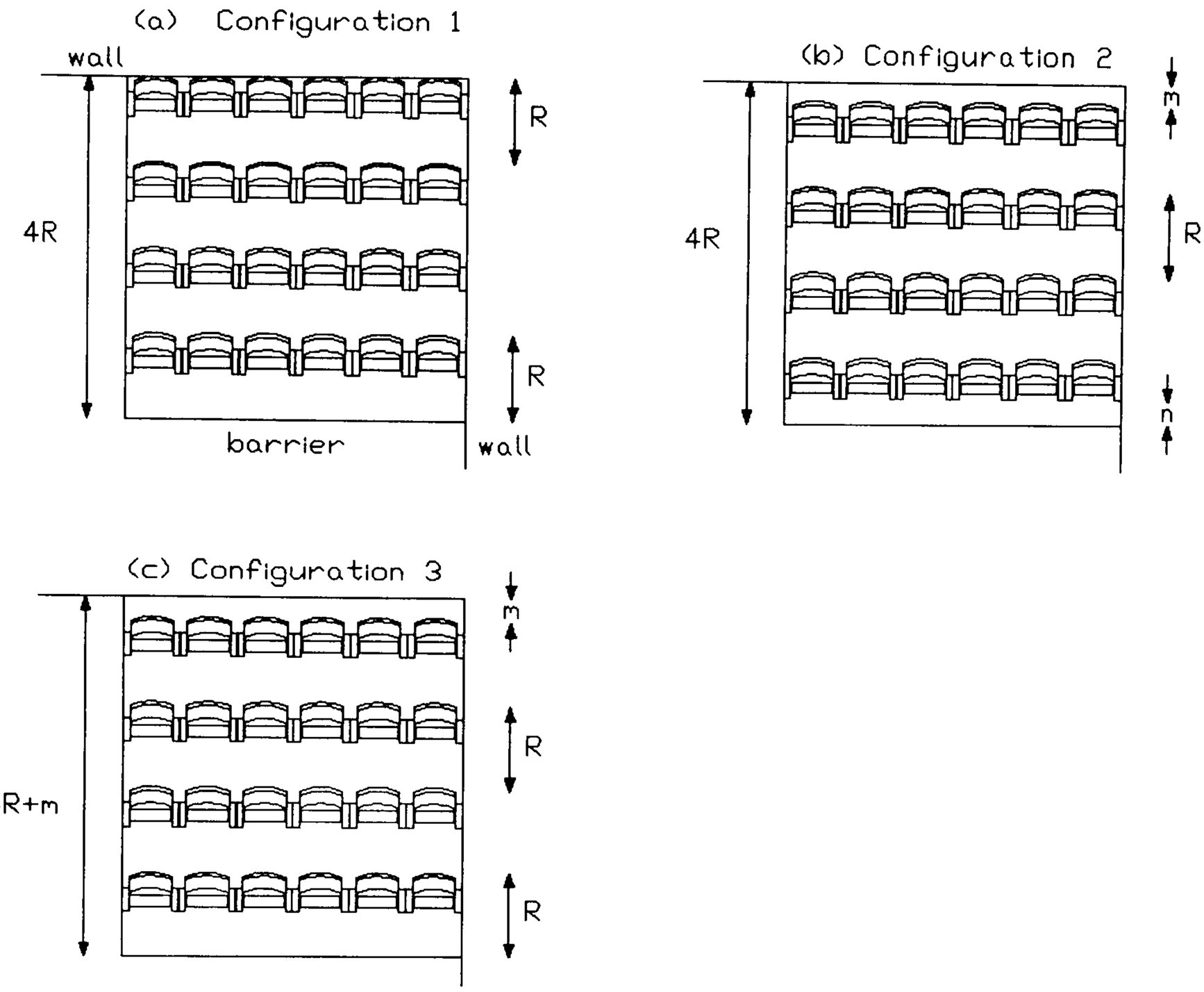

Figure 2.8: Plan view of three different configurations for measuring seating enclosed by barriers.

2.9.2 Array Configuration

It was thought that one of the parameters which might affect α is the test array configuration. The three configurations investigated here are shown in figure 2.8. Configuration 1 was the one used by Kath and Kuhl. It accurately represents the size of a 24 seat array plucked from a larger block, and it allows the correct front row leg room for occupied measurements. However, it misrepresents the absorption of the back of the back row, which would be more exposed in the theatre than it is in configuration 1. Configuration 2 also accurately represents the

array length of 4R (R = row spacing), with the additional advantage of exposing the back of the back row. However, it restricts front row leg room. Configuration 3 exposes the back of the back row and allows leg room at the front. It does, though, misrepresent the length of a 24 seat array by increasing it to 4R + m.

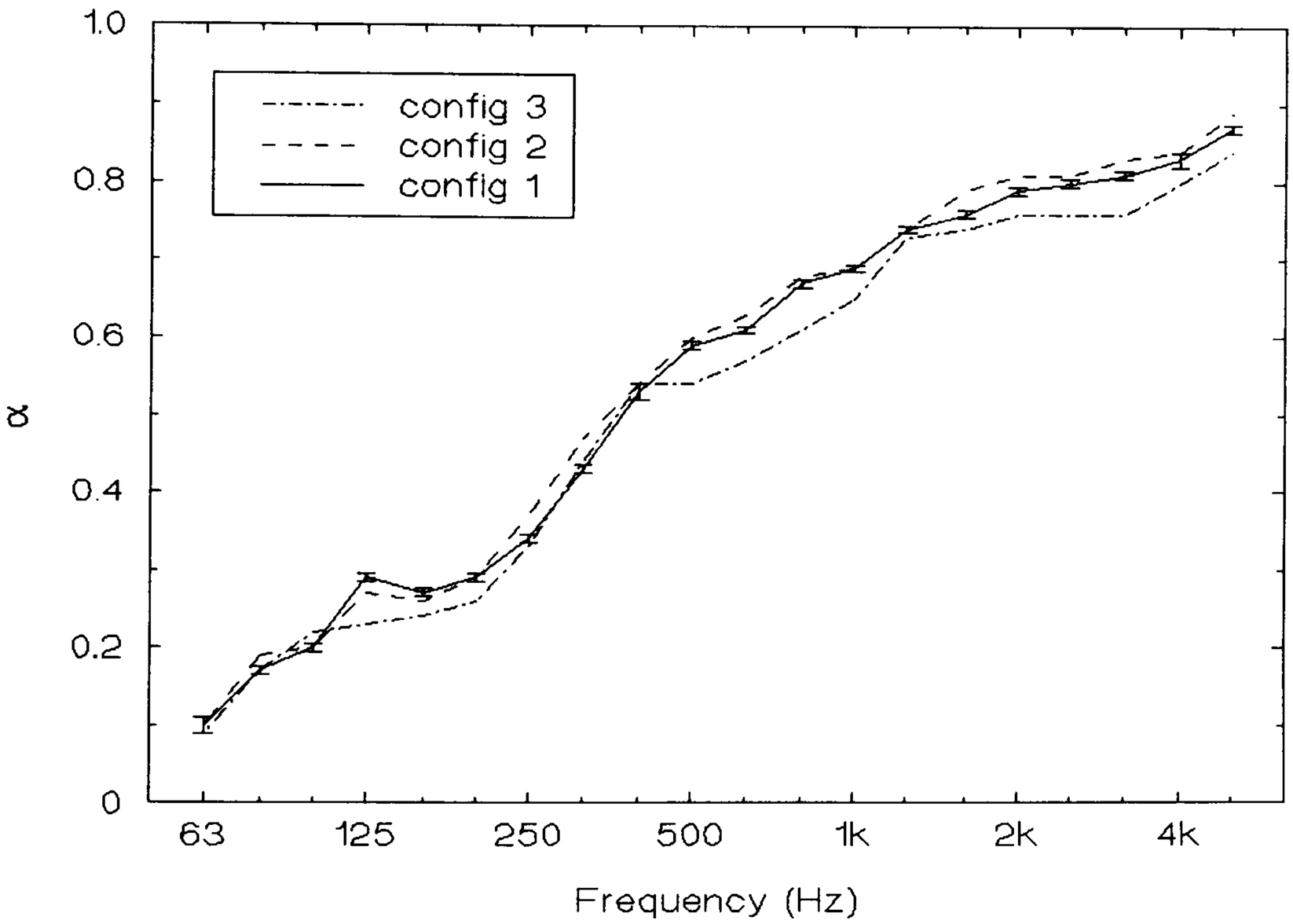

Figure 2.9: α_p for 24 seats of type B2 measured in the corner, with 0.9 m barriers, at 900 mm row spacing; parameter: array configuration (see figure 2.9).

The effect of varying the array configuration on the absorption coefficient of seat B2 is small, as shown in figure 2.9. In configuration 2, the array was placed equidistant from the rear wall and front barrier, so that m = n = 23 cm. At a 95% confidence level (two standard errors) configurations 1 and 2 are certainly identical.

Configuration 3 is very close, except perhaps at the extremes of the frequency range, though its greater plan area would be expected to make a difference. Not surprisingly, the differences are even smaller for less well-upholstered seats. This indicates that enclosing the correct plan area with the barriers is more important than the size of any gap between the seats and walls of the chamber. This finding would be of interest where a chamber is used which has no right-angled corners and hence cannot accommodate a rectangular array exactly.

2.9.3 Barrier Height

One aspect of Kath and Kuhl's method which has given rise to some confusion in the literature is the question of specification of the barrier height. Bradley (1992) has published results from enclosing some seats with a 0.6 m high barrier, where the seats seem to be about 0.9 m high. This will leave absorbing material exposed at the sides, defeating the object of the method.

To investigate the influence of barrier height, measurements were made on some relatively lightly-upholstered seats, from hall H. These seats are 840 mm high. Modular barriers were used, in the form of sheets of chipboard 300 mm high and 18 mm thick. The barrier surface was left untreated. The results are shown in figure 2.10. Consider the mid and high frequencies only first. When the barrier height is increased from 0 to 300 mm, there is little difference in α_p because a 300 mm barrier obscures only the non-absorbent chair legs (these seats did not have a tippable squab). As the barrier height is increased from 300 through 600 to 900 mm, though, α_p decreases first at high and then at mid frequencies. Now the

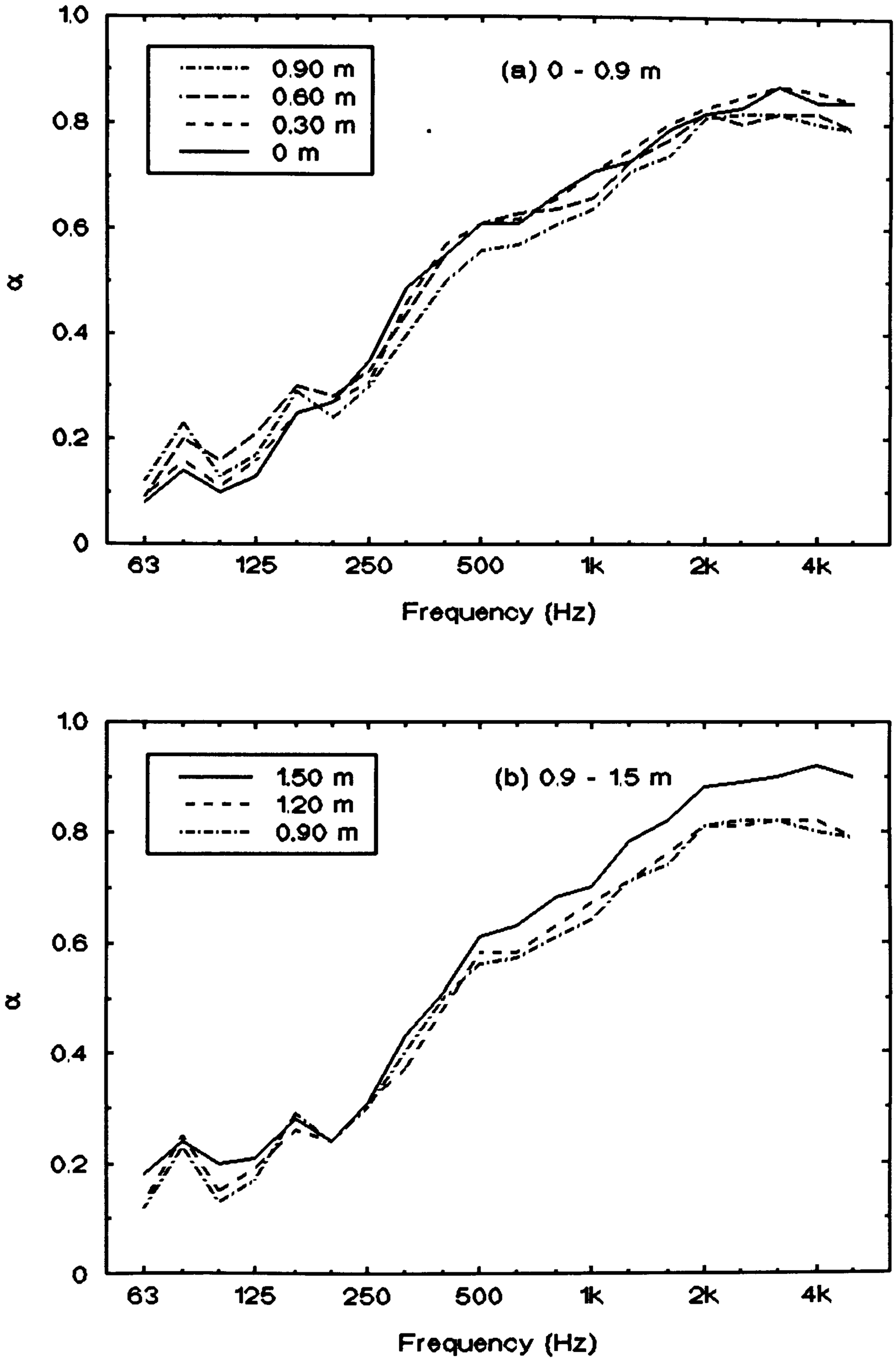

Figure 2.10: α_p for 24 seats of type H measured in the corner at 800 mm row spacing in configuration 1; parameter: barrier height.

barriers are progressively obscuring the absorbing surfaces of the squab and back of the seats.

When the barrier height is increased from 900 to 1200 mm there is little change in α_p at mid and high frequencies. This seems reasonable, since there are no more absorbing surfaces on the front and side of the array to be covered. With an increase to 1500 mm, however, there is a significant jump in α_p at mid and high frequencies. The barriers are now some way above the seat tops, so it is possible that the absorbing array is no longer in a diffuse field. As the barriers are extended further and further above the absorber, any sound rays entering this enclosure are less likely to leave, and so the apparent absorbing power of the array will increase. This situation is analogous to that of seating under a deep balcony overhang. Cremer and Müller (1982a, p. 408) say that such seating is no longer in the diffuse hall field, and recommend ascribing an absorption coefficient of 1.0 to the opening under the overhang, as one might to an open window. The high frequency absorption in figure 2.10(b) is also probably due in part to the surface absorption of the untreated chipboard.

There is also evidence of an increase in low-frequency absorption due to the barriers in figure 2.10. This has been remarked upon by Bradley (1992) too. The peak in absorption here suggests that this is a resonant effect. This might be caused by strong modes propagating in the enclosure formed by the barriers and being absorbed by the seats, or by resonant modes of the barriers themselves, or perhaps by a combination of both. Because this anomalous low-frequency absorption

seemed a real defect of the method, it was investigated in some detail: the results appear in chapter 3.

The unwanted high-frequency barrier absorption seems easier to deal with: the barriers should be at least as high as the seating plus any auditors, but excessive extra height (say > 100 mm above the top of the absorbers) should be avoided. Note that the lowest values of α_p at mid and high frequencies in figure 2.10 are for 900 mm barriers. Since most of the seat types measured in this work were a little below a height of 900 mm, two sets of barriers were commonly used: 900 mm high for unoccupied measurements and 1200 mm high for occupied work.

2.9.4 Array Position in Chamber

Since placing a seating array in the corner of a chamber necessitates applying a correction for the pressure doubling phenomenon, it may be thought preferable to use a more conventional position in the centre of the chamber while still using barriers to obscure the front and sides. Because the absorber is no longer mirrored in the adjacent walls, moving it to the centre should also reduce the effective acoustic size of the array. Due to the diffraction effects discussed in chapter 4, the measured absorption might then be expected to be higher in the centre of the chamber, especially at mid and high frequencies. There is some evidence of this in the measurements made on seat H in figure 2.11, though the decrease in absorption at the highest frequencies is hard to explain and was not typical of other seats measured. However, the most dramatic increase in the measured absorption of seat H when the array is moved to the centre is at the low-frequency resonant

peak. Since four barriers are needed to surround the array in the centre and only two in the corner, this effect is probably due to an increase in resonant barrier absorption.

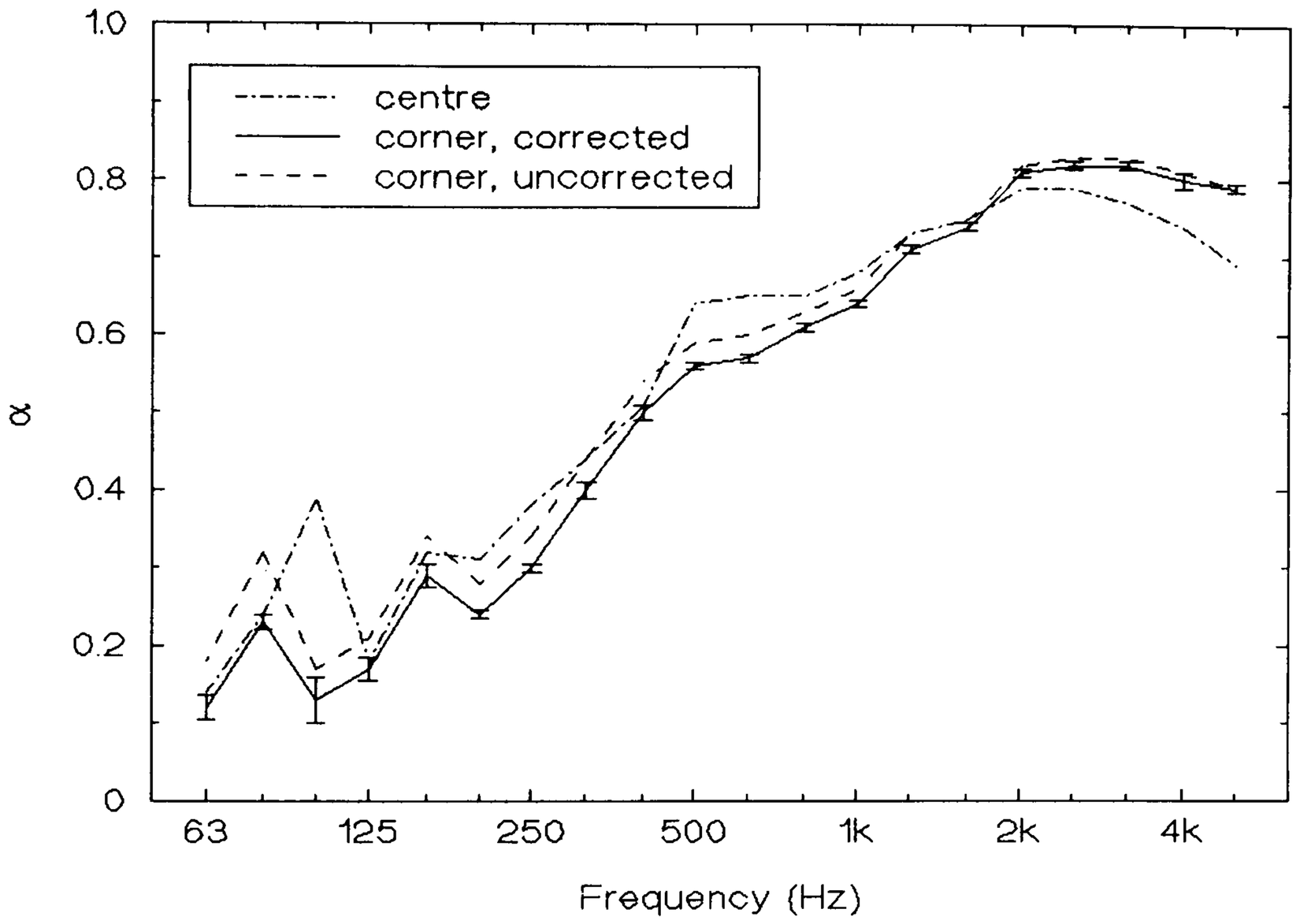

Figure 2.11: α_p for seat H at 800 mm row spacing, enclosed by barriers in configuration 1; parameters: array position in room, and correction for pressure doubling.

2.9.5 Pressure Doubling Correction

Also shown in figure 2.11 is the typical effect of the pressure doubling correction of equation (2.7) on the absorption coefficient of an array of four rows of six chairs. Compared with the anomalous barrier effects it is slight, and only really significant below 250 Hz. Of course, the correction will be more significant if there is greater

low-frequency absorption, as with occupied chairs (see below), or if a smaller test array is used. For the four rows of six seats used here, the correction increases the plan area used in the absorption calculation by 31% at 100 Hz. If three rows of four were used the increase would be 45%, and for two rows of three chairs it would be 65%. It should be remembered that due to the problem of low modal density at low frequencies, the uncertainty in the measured absorption coefficient is quite possibly larger than that estimated by the standard error in figure 2.11 at low frequencies. It is not therefore always possible to be certain when evaluating whether a low-frequency absorption effect will have a significant effect on the reverberation time in a real hall.

2.9.6 Occupied Seats and the Effect of Carpet

In a previous work on seating absorption by Subagio (1986) it was found that placing high-quality carpet under unoccupied upholstered seats increased their absorption coefficient until it was nearly the same as that measured when the seats were occupied. Little difference was then found between occupied and unoccupied absorption with the carpet in place. This is a potentially useful result to a hall designer who wishes the reverberation time of an auditorium to remain constant whatever its percentage occupation. Further light may be shed on this by the data in figures 2.12 and 2.13.

In figure 2.12, arrays of 24 seats of two different types have been measured in the corner of the reverberation chamber, with 1.2 m barriers surrounding them and 24 adults (mostly male) occupying them. The test on seat type B2 was conducted in

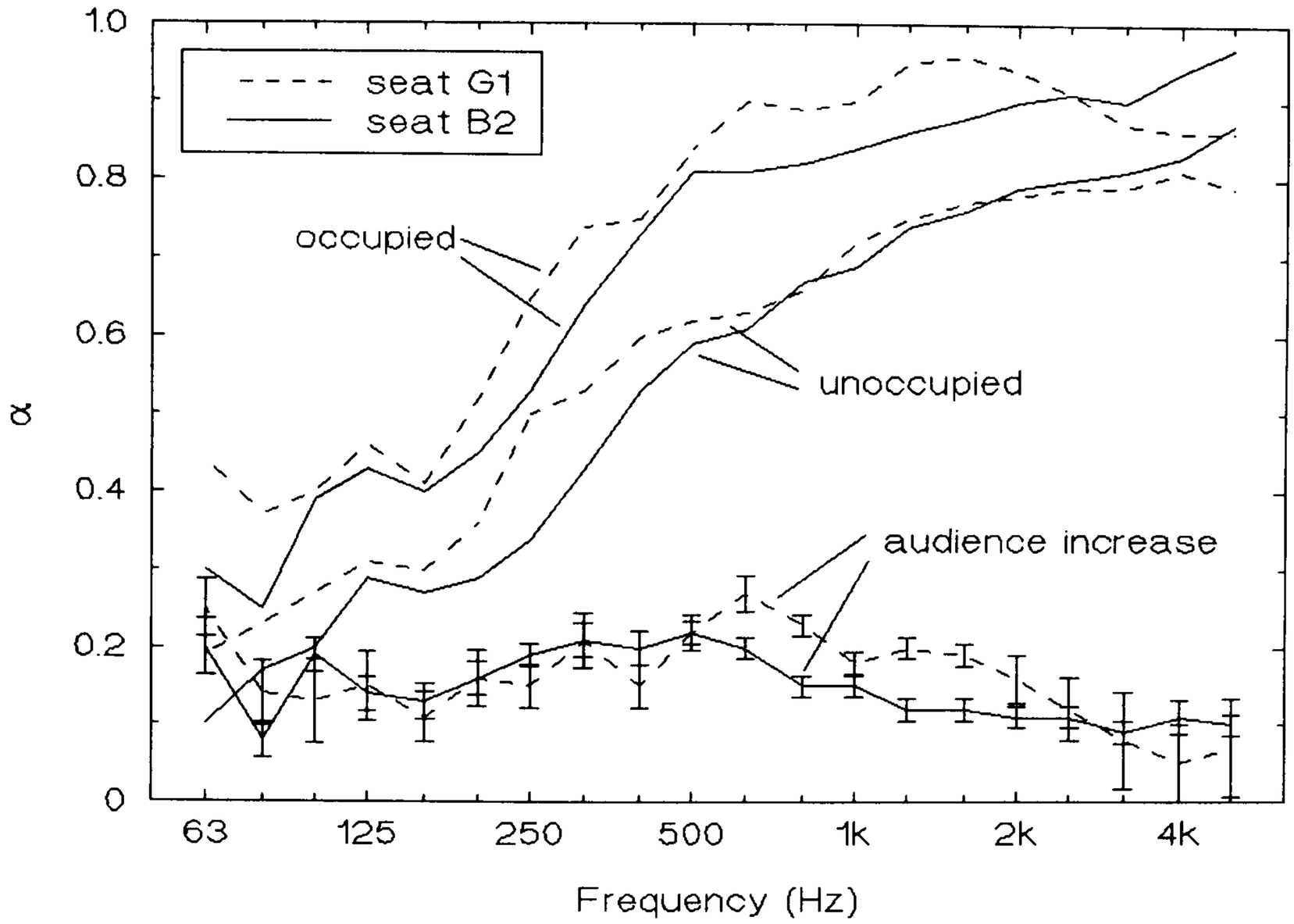

Figure 2.12: α_p for two seat types in both unoccupied and occupied states, measured at 900 mm row spacing in configuration 1.

Autumn and that on seat type G1 in Winter, so the test persons may have been wearing slightly more absorbing clothing for the G1 test, though a jacket and thick jumper were typical for both measurements. Because time was short, no measurements were made on occupied seats without barriers and so no estimate of the absorption of the front and side of the array could be formed. Hence the data in figure 2.12 applies effectively to an infinitely large area of seating, barring diffraction effects. Absorption coefficients for the two seat types measured unoccupied with 0.9 m barriers but otherwise identical conditions are also shown. Although both seat types were modern well-upholstered cloth-covered designs, the addition of an audience has substantially increased the absorption coefficient of

their plan area. The bottom two lines in figure 2.12 give the additional absorption obtained by subtracting the unoccupied data from the occupied data for each seat type. Though the seats were of similar design, these two curves are not the same in the mid and high frequency region. The difference is probably partly accounted for by differences in clothing. Hence only a rather rough guide for the additional absorption due to an audience on modern seats could be obtained: for this reason the two "additional absorption" curves have not been averaged.

Unfortunately it was not possible to test either of the above two seat types with carpet due to the poor availability of test samples, so figure 2.13 shows measurements made on a different well-upholstered cloth-covered seat with and without carpet under the seat array. The carpet was a high-quality 9 mm thick "Axminster" type laid over a 5 mm rubber underlay. As well as the increase in absorption caused by the carpet to that of the seats, figure 2.13 also shows the fairly substantial absorption coefficient of the carpet alone. By comparing figures 2.13 and 2.14, it can be seen that the effect of carpet on seat D1 was not as great as the effect of occupancy on seat types B2 and G1. It should be noted that the data for seat type D1 was obtained for a row spacing of 780 mm only, compared to the more common 900 mm for seat types B2 and G1. Because the seats will obscure the carpet, it is expected that the effect of the carpet would be greater for a greater row spacing. The effect of occupancy on the other hand would probably remain nearly constant with row spacing, as the relative exposure of the seats and occupying persons to the sound field should not change much with row spacing. It can be concluded therefore, that thick floor carpet under seats will increase their

absorption, but whether it is increased to the value for the occupied seats may depend on the row spacing.

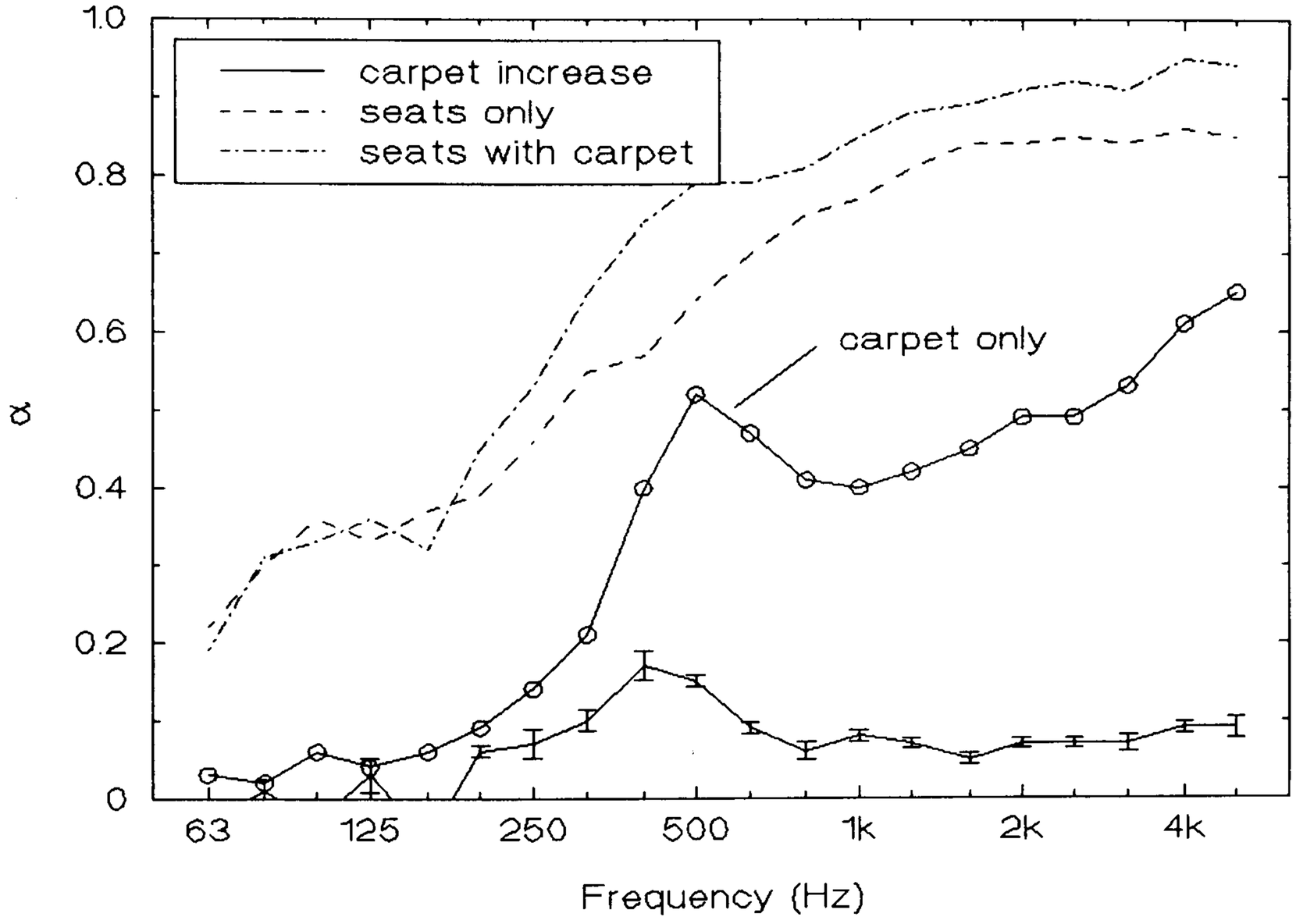

Figure 2.13: α_p for seat D1 with and without high-quality carpet, at 780 mm row spacing.

2.10 Comparison with Beranek

Figure 2.14 shows the range of absorption coefficients taken from figure 2.6, their mean, and Beranek's figures for α_S. Considering the range of the current data, the agreement between the mean and Beranek's values is surprisingly good up to 1 kHz. At higher frequencies, as Bradley (1992) explains, Beranek's absorption data is quite possibly affected by differences in air absorption between the many hall measurements he used. Beranek's data is below the mean of the present data at

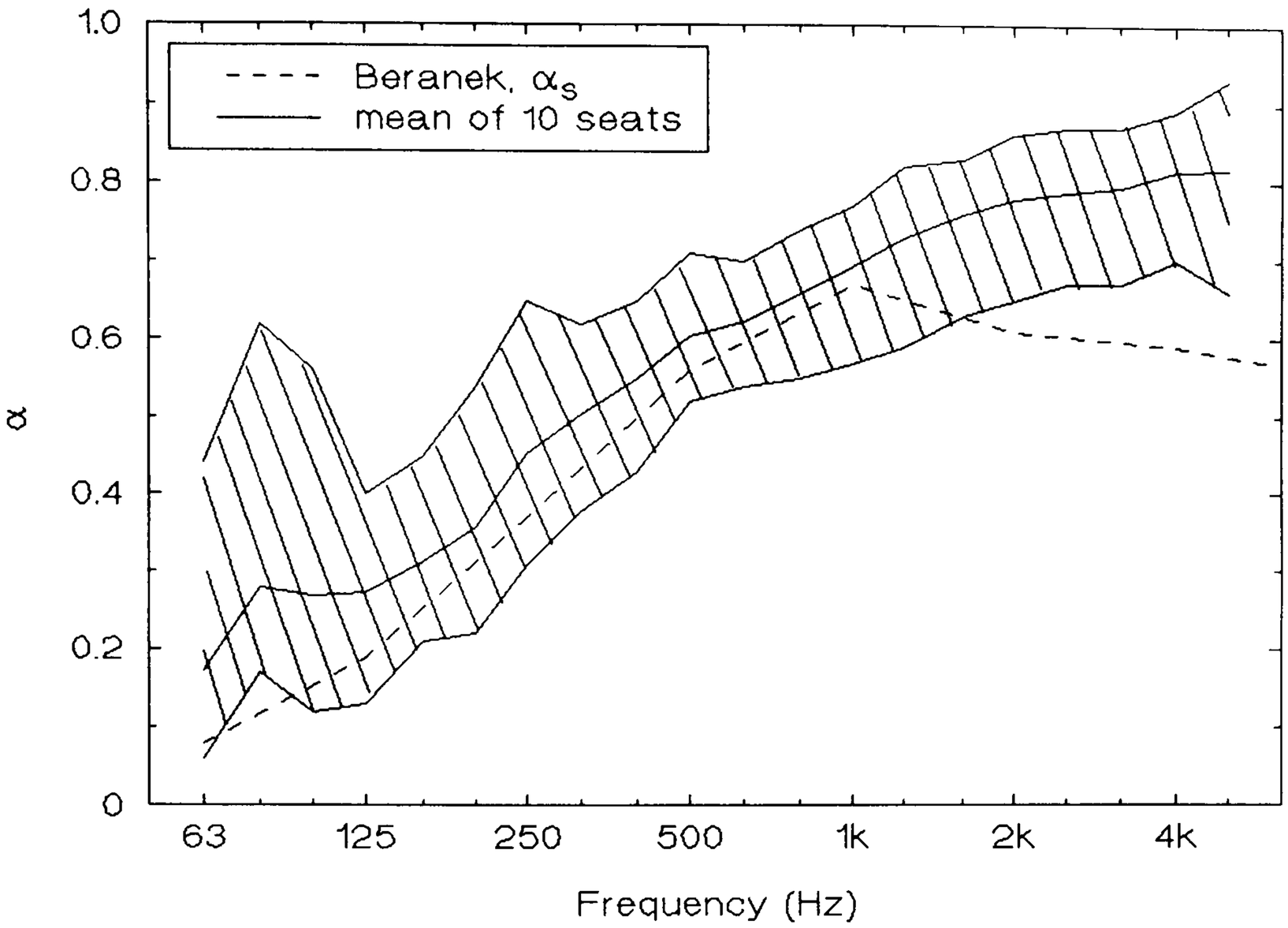

Figure 2.14: Mean, minimum and maximum absorption data for ten unoccupied upholstered seat types compared with Beranek's average, α_S.

all frequencies. This could be due to differences in diffusion between Beranek's halls and our reverberation chamber. In general, because most of the floor of a hall will be covered by a highly absorbing surface, it is less likely to meet the conditions for a diffuse field than a reverberation chamber. Embleton (1971) has shown that less diffuse fields can yield lower absorption coefficients for samples measured in them. It may also be true that modern theatre seating has slightly more padding than the ones forming the bulk of Beranek's data. What the spread of data in figure 2.14 also emphasises is that the use of an average absorption coefficient should be for rough early design figures only, at least for unoccupied RT prediction in a hall. For example, the highest unoccupied value of α_p in the present

data at 1 kHz is 0.77 while Beranek gives α_S = 0.67 at the same frequency. Thus a predicted RT based on α_S for a hall filled with these seats could be as much as 15% higher than the value which would be measured in the hall. This error is considerably greater than the difference limen of 3 - 4% for mid-frequency RTs quoted in section 2.3.

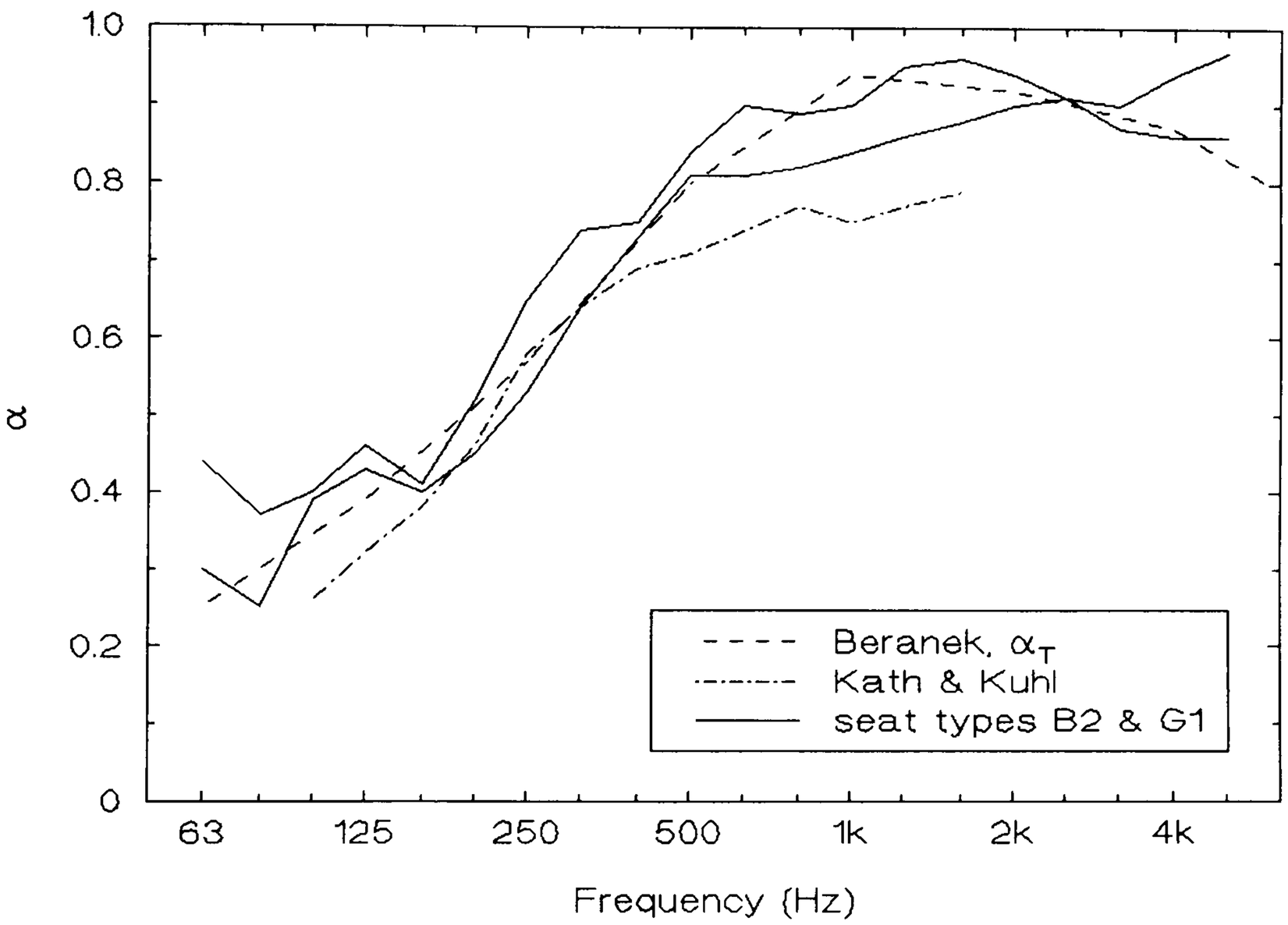

Figure 2.15: Two sets of occupied values for α_p compared with Beranek's average audience absorption coefficient, α_T, and a measurement by Kath and Kuhl.

The comparison of the present occupied data from figure 2.12, with Beranek's average is very interesting. In figure 2.15 it can be seen that Beranek's α_T is very close to being the mean of the two measured data sets for seat types B2 and G1.

It is unfortunate that there were no opportunities to obtain more occupied data, since this raises the possibility that the average absorption coefficient may be accurate enough to give good predictions of occupied hall RT, at least for some types of seat. A measurement of occupied seats from one of the original papers of Kath and Kuhl (1965) is also shown, and this too agrees with the present data, at least up to 500 Hz. The lower absorption of the Kath and Kuhl data above this frequency might be accounted for by less absorbent audience clothing. Hence the data in figure 2.15 accords quite well with the supposition that the absorption of occupied upholstered seats is dominated by the absorption of the occupying people and so should not vary much over different seat types.

It therefore seems that average absorption coefficients can give a reasonable but rough prediction for an unoccupied hall RT and possibly a good prediction for an occupied hall. In the absence of further occupied seating absorption data measured in a diffuse reverberation chamber with barriers, it is still best to measure a sample of seats destined for an auditorium both unoccupied and occupied if possible, for accurate design figures.

Chapter 3

The Effects of Barriers on Seat Absorption Measurements

It was found in section 2.5.4 that the barriers used in Kath and Kuhl's method to surround the exposed edges of a seating array could contribute anomalous low-frequency absorption themselves. Since this extra absorption would not be present for a real seating block in an auditorium, it limits the accuracy of the reverberation chamber measurements made according to Kath and Kuhl's method. In order to find the reasons for the unwanted absorption, several different measurements have been made on the type of seats which demonstrated the problem to the greatest extent. These were the D2 seats which, as mentioned in section 2.5, have a cavity in the base of the squab. This gives rise to a resonant low-frequency peak in the absorption coefficient of the seats in the reverberation chamber even without any barriers. The peak in the absorption coefficient and the further low-frequency increase caused by the introduction of barriers can be seen in figure 3.1

3.1 Steady-State Pressure Maps over Seats in the Reverberation Chamber

The first conjecture about the cause of the low-frequency absorption was that it might be due to the enclosure formed by the barriers changing the amplitude of the low-frequency room modes in such a way as to increase the measured absorption

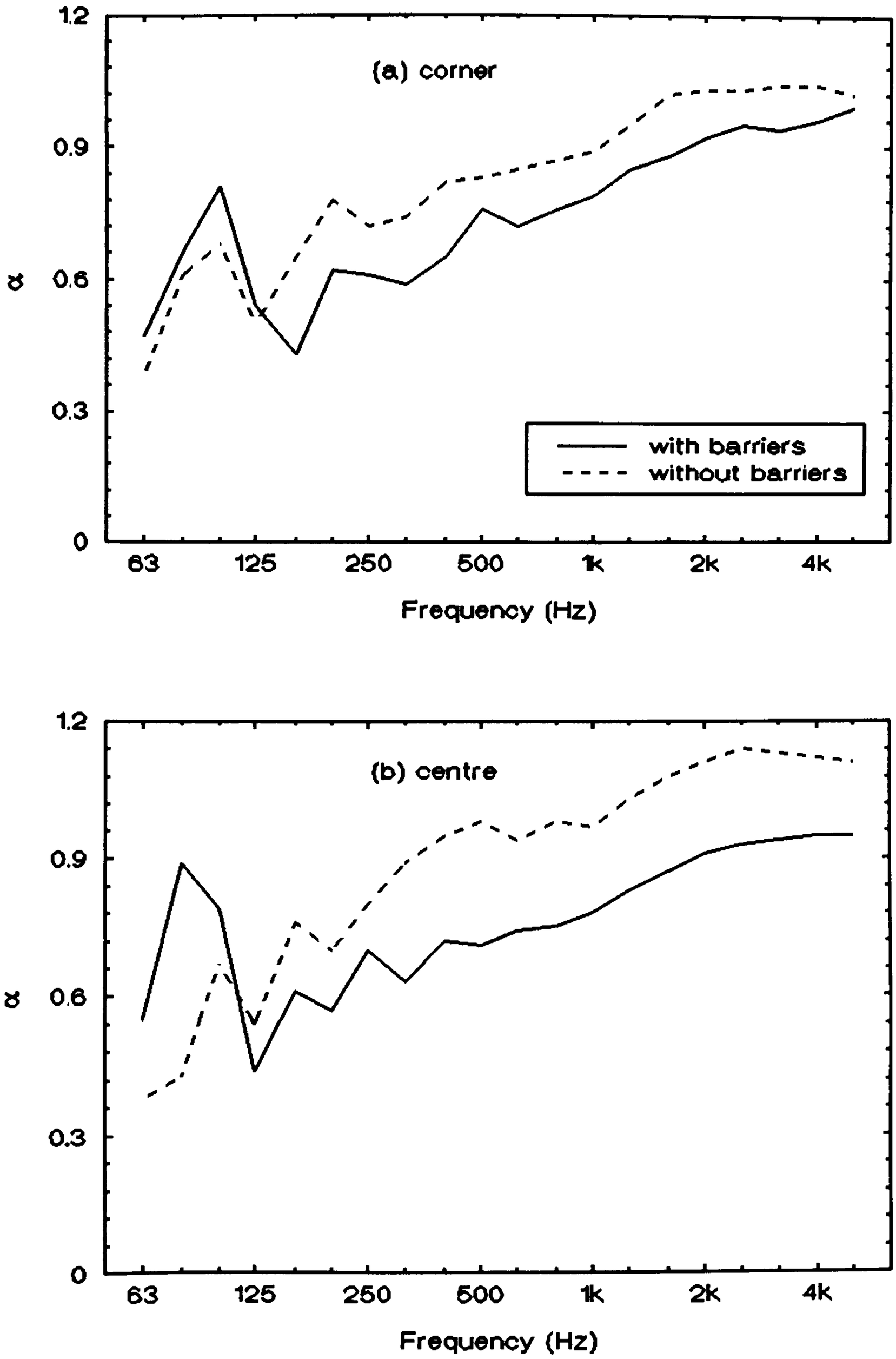

Figure 3.1: Absorption coefficient of seat D2 at 780 mm row spacing; (a) in the corner and (b) the centre of the chamber, with and without barriers.

of the seats. The biggest change in absorption was found with an array of 24 seats of type D2 measured in the centre of the chamber with and without barriers, in figure 3.1(b). To try and give clear measurements of any pressure wave changes, it was therefore decided to measure the steady-state sound pressure level distribution over this seating configuration in the reverberation chamber. Of course, absorption measurements are made with a decaying sound field, not a steady-state one, but it was thought that any strong pressure variations would be similar in either. Making measurements on a steady-state field would also be quicker and easier to interpret.

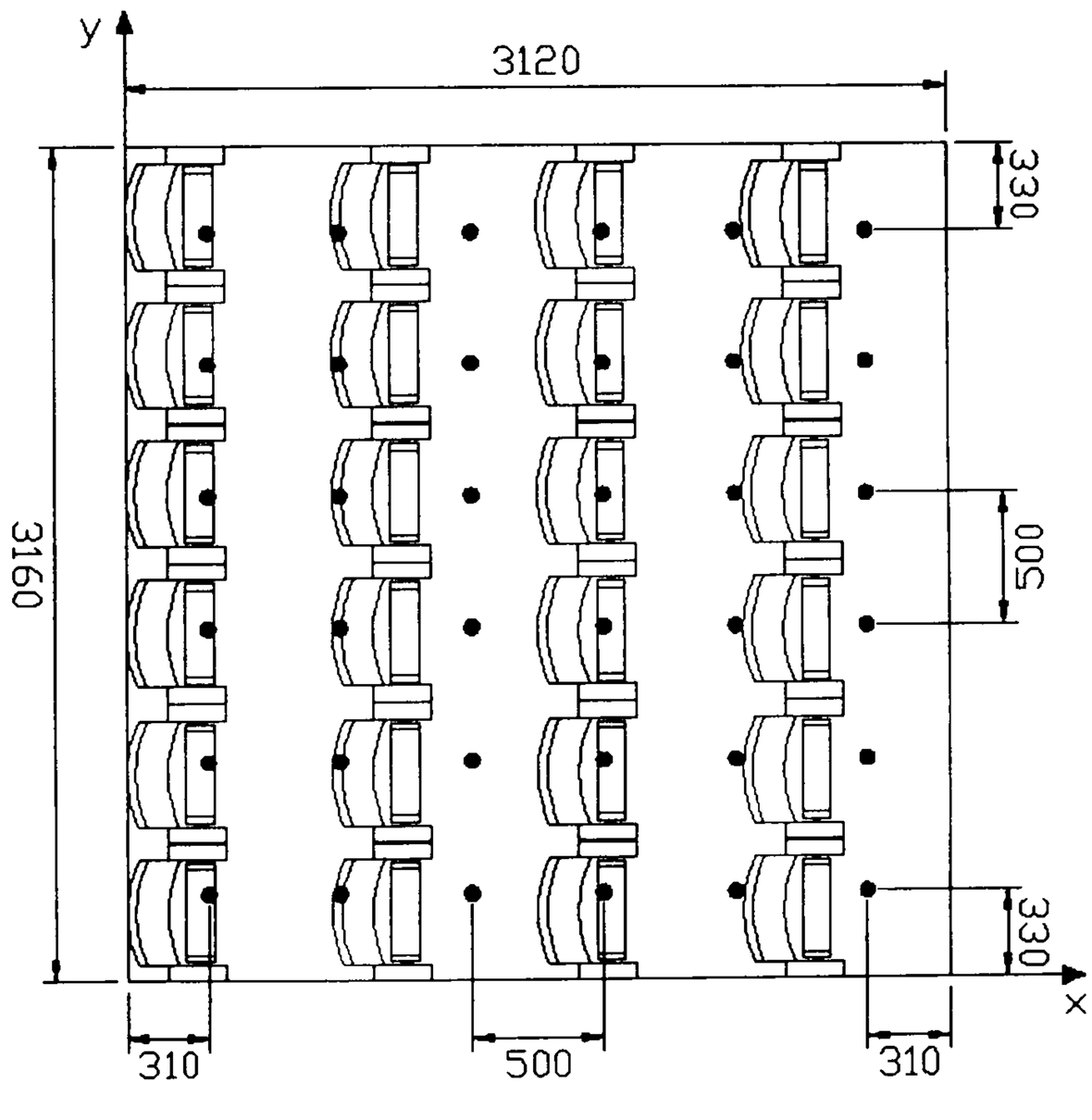

Figure 3.2: The 36 measurement positions for a pressure map over an array of 24 type D2 seats, surrounded by barriers on all four sides in the centre of the reverberation chamber.

The seating array comprised four rows of six seats, measuring 3120 mm in the x direction (rows) and 3160 mm in the y direction (seats), as shown in figure 3.2. Because low-frequency pressure variations were of prime importance, relatively widely spaced measurement points over the array were used. Strictly speaking, at least four equally spaced points a distance $\lambda/4$ apart would be needed to identify a pure standing wave with a wavelength of λ. To speed up the measurements, an interval of 50 cm was chosen so the highest frequency standing wave which could have been reliably identified was 172 Hz. This frequency is some way above the main absorption peaks at 80 and 100 Hz in figure 3.1.

The procedure followed was this: the reverberation chamber with the seating array inside was excited with broad-band pink noise from a loudspeaker in the corner. After allowing 10 seconds for a steady state to be achieved, a 10-second L_{eq} was evaluated at one of the microphone positions shown in figure 3.2, in ⅓ octave bands from 50 Hz - 5 kHz using a real-time analyser. The microphone was then moved to the next position and the measurement repeated until all 36 measurement points had been covered. This was done with all four sides of the array covered by barriers, at the height of the barriers (z = 0) and halfway down inside the enclosure formed by the barriers (z = - 450 mm). Some of the positions inside the enclosure were adjusted slightly from the regular grid shown in figure 3.2 in order to fit the microphone round the seats. A third set of measurements was made over the seating array at z = 0 with the barriers removed.

The results are shown in figures 3.3 - 3.7 in the form of a surface of L_{eq} values over the grid of 36 measuring points for one particular ⅓ octave band. Consider first the

pressure maps at the height of the barriers, i.e. at z = 0. In figure 3.3 it can be seen that there is little variation in pressure at 1 kHz, with or without barriers round the array. Though the measurement spacing is not fine enough to pick out all the possible detail at such a frequency, it is unlikely that the graphs would appear much rougher at a smaller resolution. This is because there are a large number of room modes in the steady-state field at this frequency which will be averaged out in a ⅓ octave band. For a rectangular room of volume V the modal density at frequency f is, from Kuttruff (1991, p.61), approximately

$$\frac{dN_f}{df} = 4\pi V \frac{f^2}{c^3} \qquad (3.1)$$

Thus for the reverberation chamber used, the modal density is 69 modes per Hertz at 1 kHz, and the number of modes in the 1 kHz ⅓ octave is approximately 15,900.

At the bottom end of the frequency spectrum, the results are different. The map for 63 Hz without barriers in figure 3.4(a) shows good evidence for quite a smooth standing wave pattern over the seats. As the wavelength of sound at 63 Hz is 5.46 metres, the curve for y = 330 mm is likely to be half of a standing wave. The standing wave pattern is more prominent in the x direction because the walls of the reverberation chamber in the y direction are parallel. In the x direction, the walls are not parallel (see the plan of the chamber in figure 2.3) and so would tend to inhibit standing waves along the y axis between them. When the barriers were introduced, in figure 3.4(b), the standing wave was still present and the pressure variation along the y axis was more marked. It seems as though the barriers may have encouraged standing waves to form in the y direction.

The graphs for the next ⅓ octave up demonstrate larger variations in pressure without barriers for 80 Hz in figure 3.5(a) than for 63 Hz. The extremes of pressure over the array without barriers are now 6.8 dB apart. Again, these variations, particularly in the y direction, look very much like portions of standing wave patterns. When barriers were placed round the array, the pressure variation increased quite dramatically to that shown in figure 3.5(b). It was found in figure 3.1(b) that the biggest increase in absorption coefficient which occurs with the introduction of barriers comes in the 80 Hz ⅓ octave.

If the analysis is shifted up the frequency band again, it can be seen that the maps for 100 Hz are not so dramatic. The introduction of barriers in figure 3.6(b) has slightly accentuated a wave pattern already present over the seats in figure 3.6(a). This tallies with the absorption coefficient graph where the anomalous barrier increase is not nearly so great at 100 Hz as it is at 80 Hz.

Finally, two graphs from the map at z = - 450 mm (that is, halfway down inside the barrier enclosure) are presented. At 80 Hz, the pressure distribution of figure 3.7(a) has a similar shape to the corresponding one at z = 0 in figure 3.5(b). The central dip is not so large though and the overall values are higher, probably because of pressure doubling at the very close surfaces of the seat squabs and the inside of the barriers. The map for 100 Hz inside the enclosure, figure 3.7(b) also has a similar shape to its counterpart at the top of the array, figure 3.6(b). This time, the pressure values are an average 3.8 dB higher.

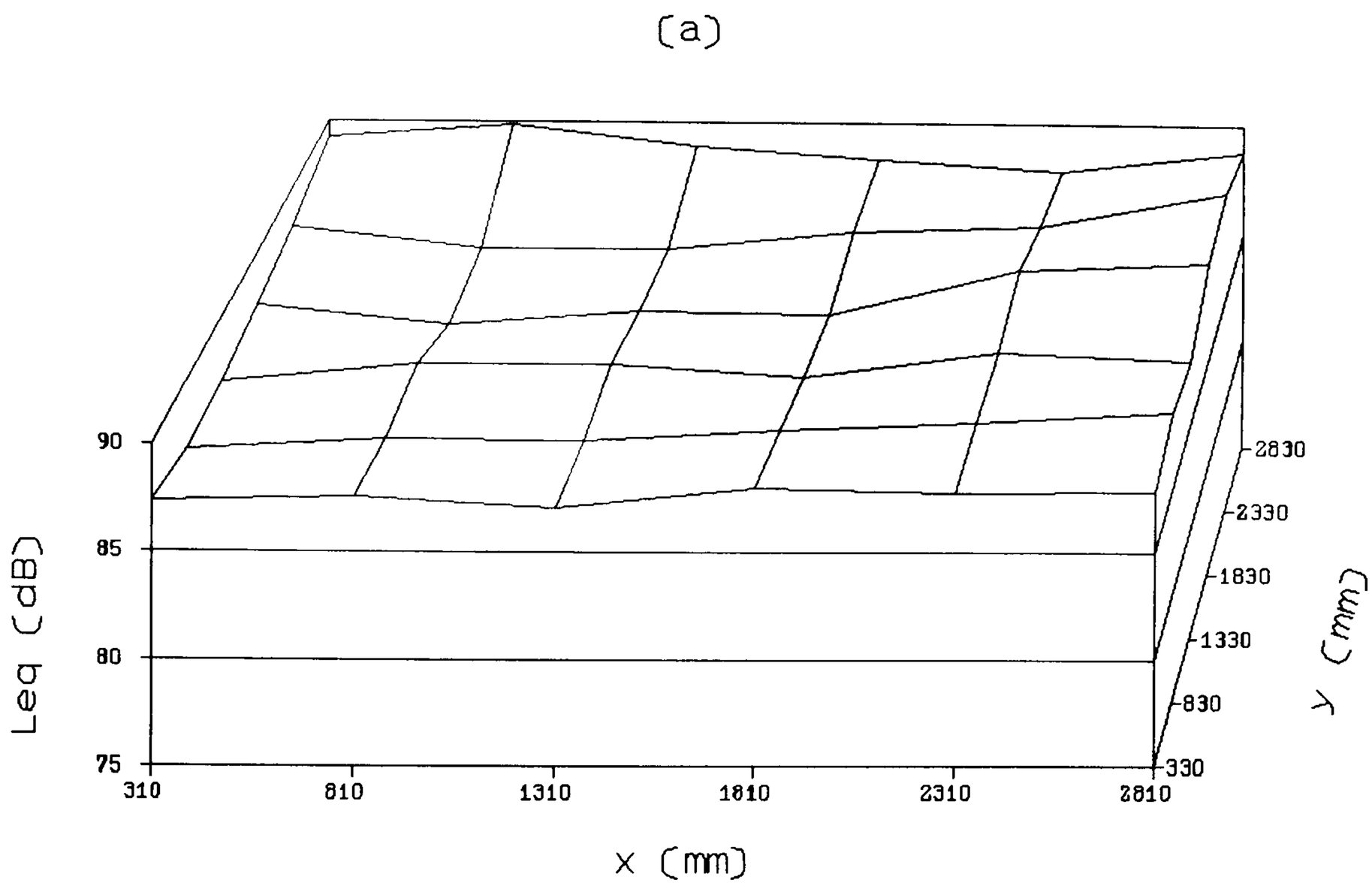

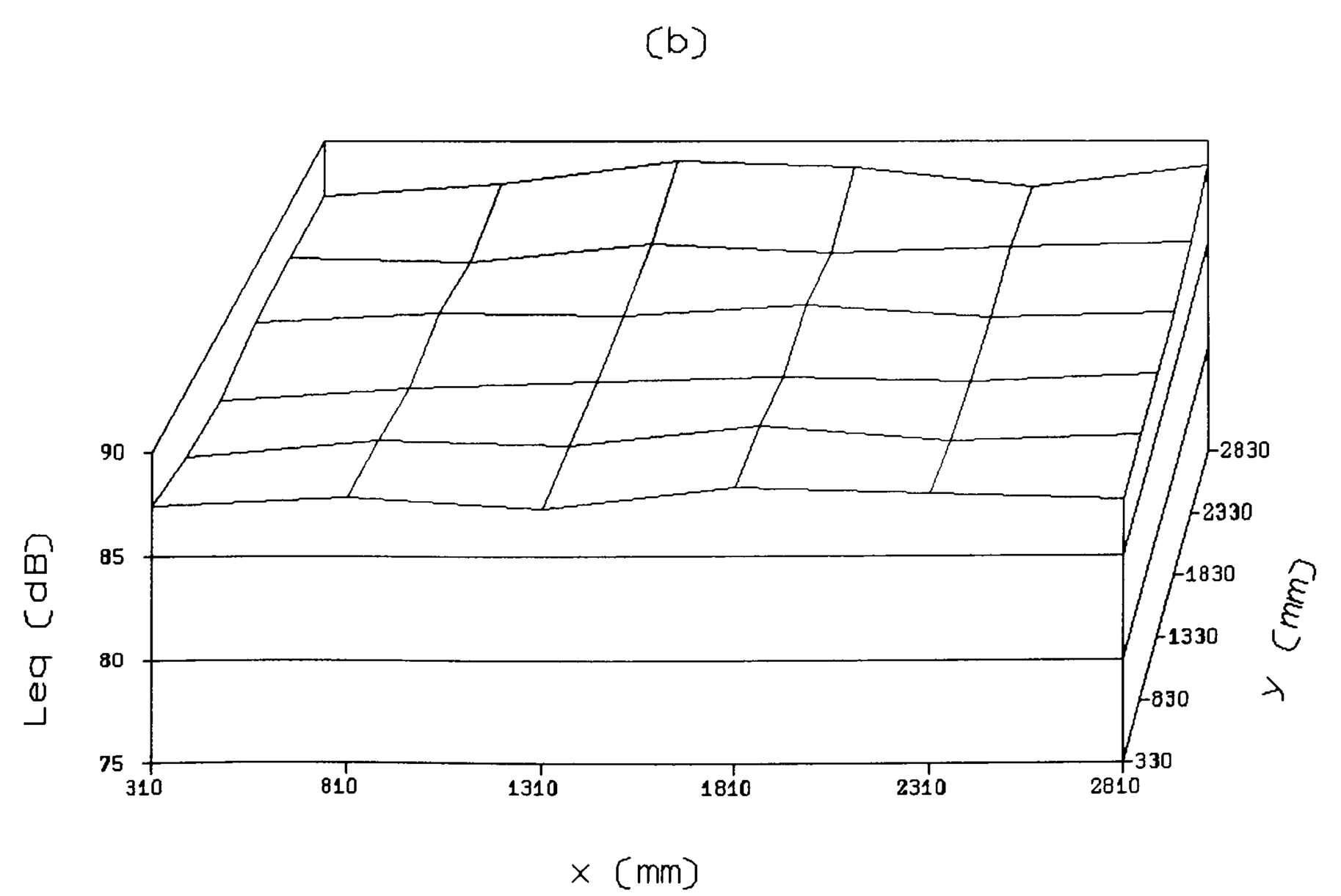

Figure 3.3: Pressure map over array of D2 seats at z = 0 for 1 kHz, (a) without barriers, and (b) with barriers.

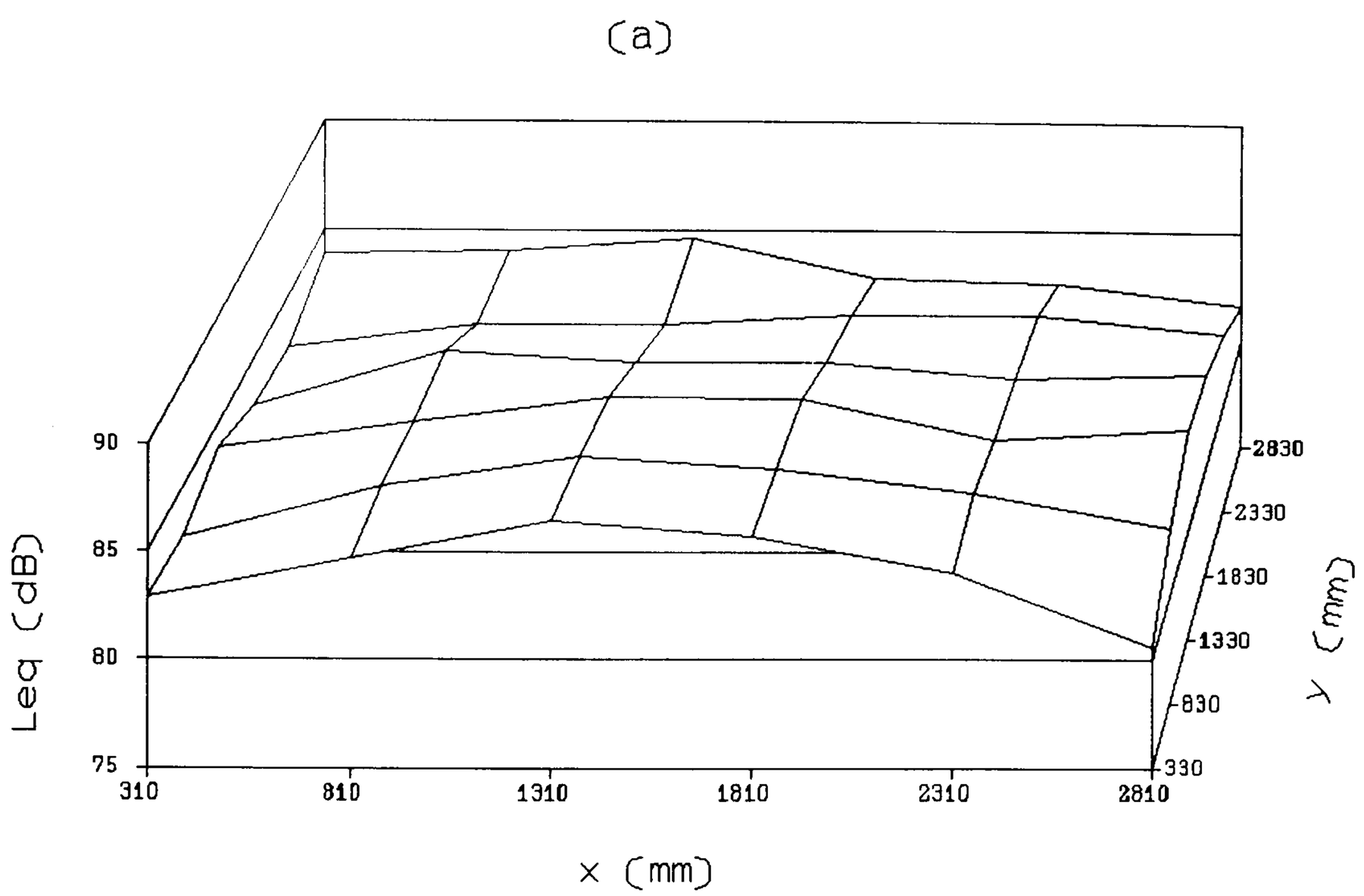

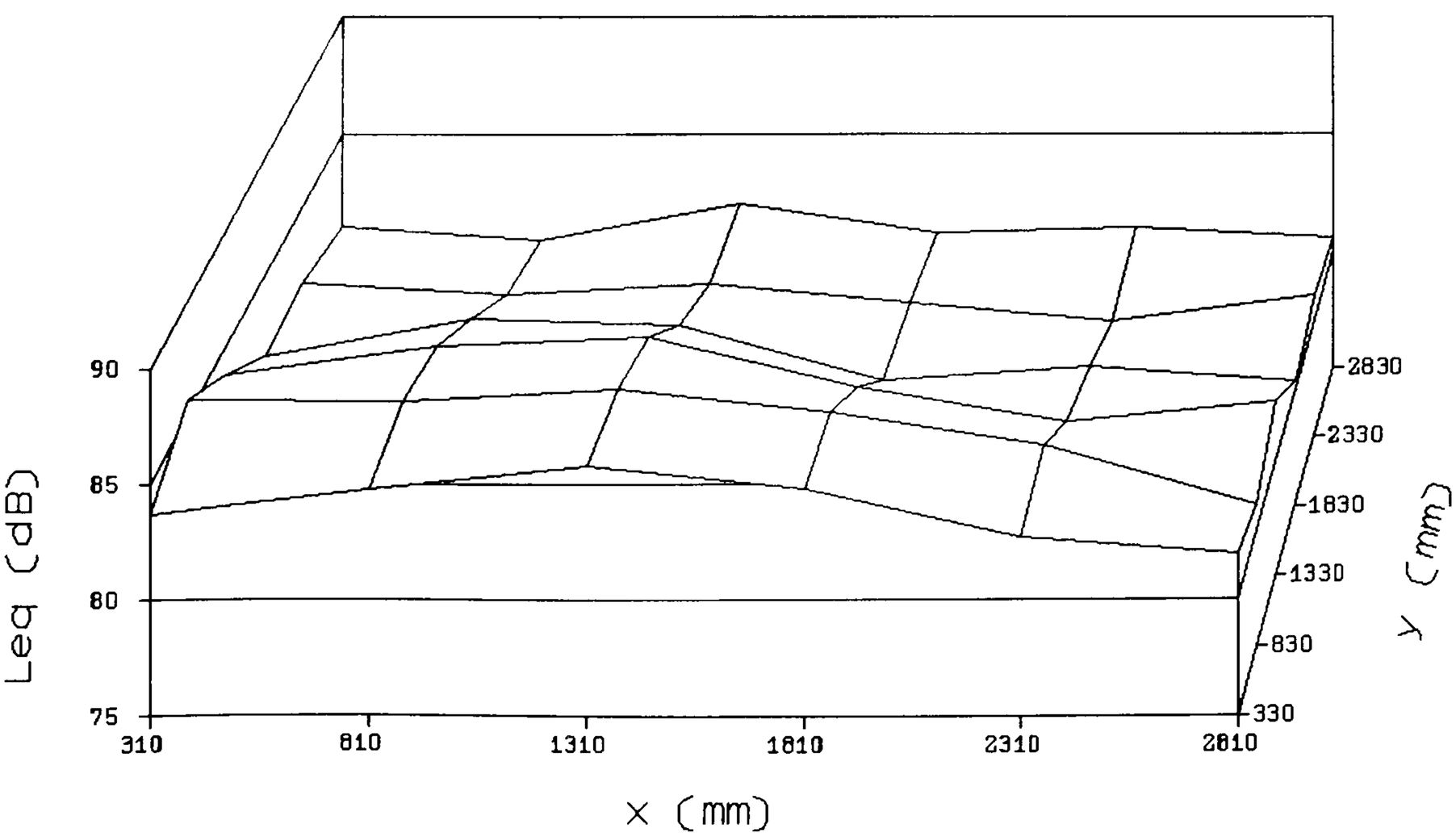

Figure 3.4: Pressure map over array of D2 seats at z = 0 for 63 Hz, (a) without barriers, and (b) with barriers.

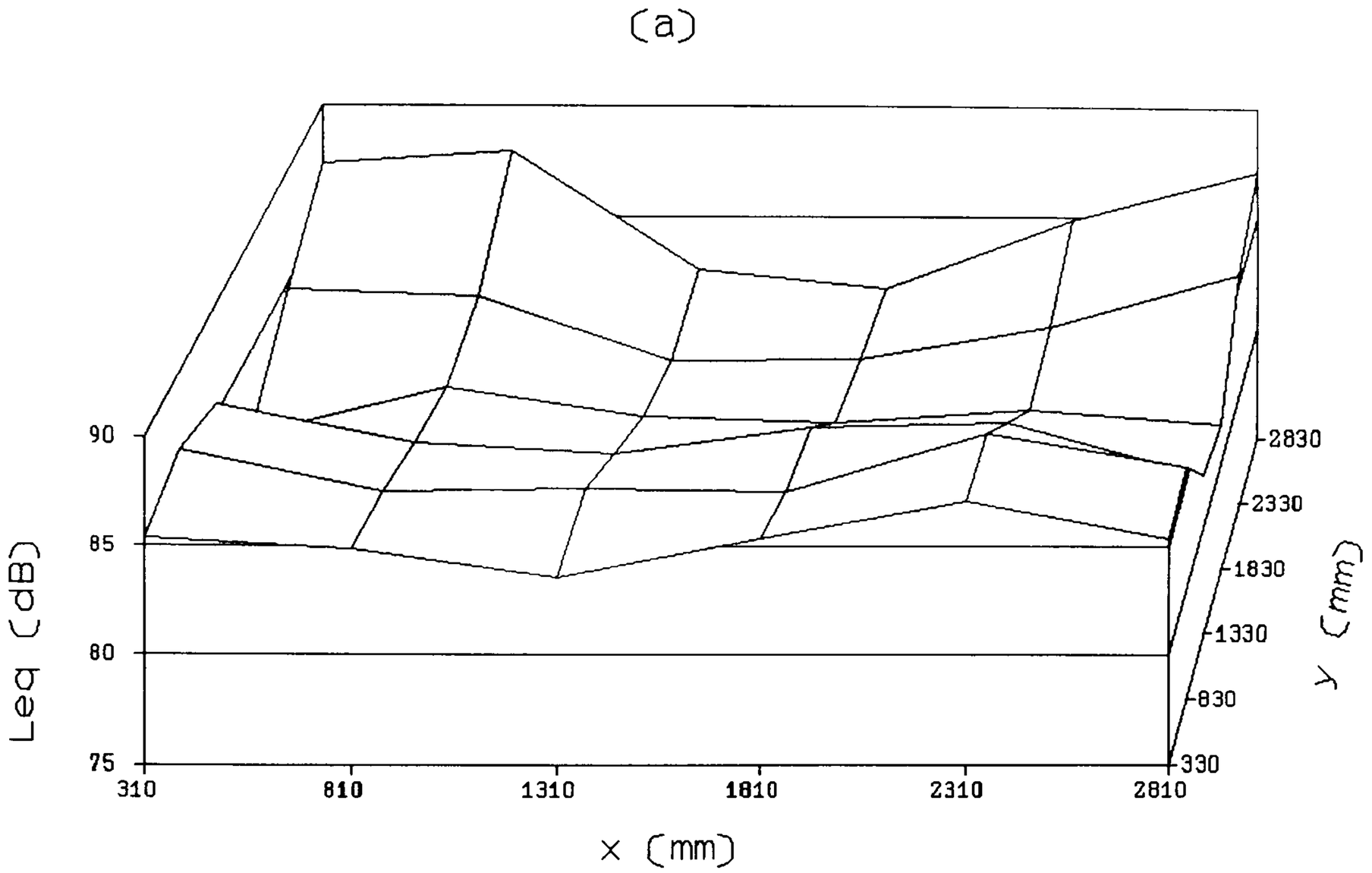

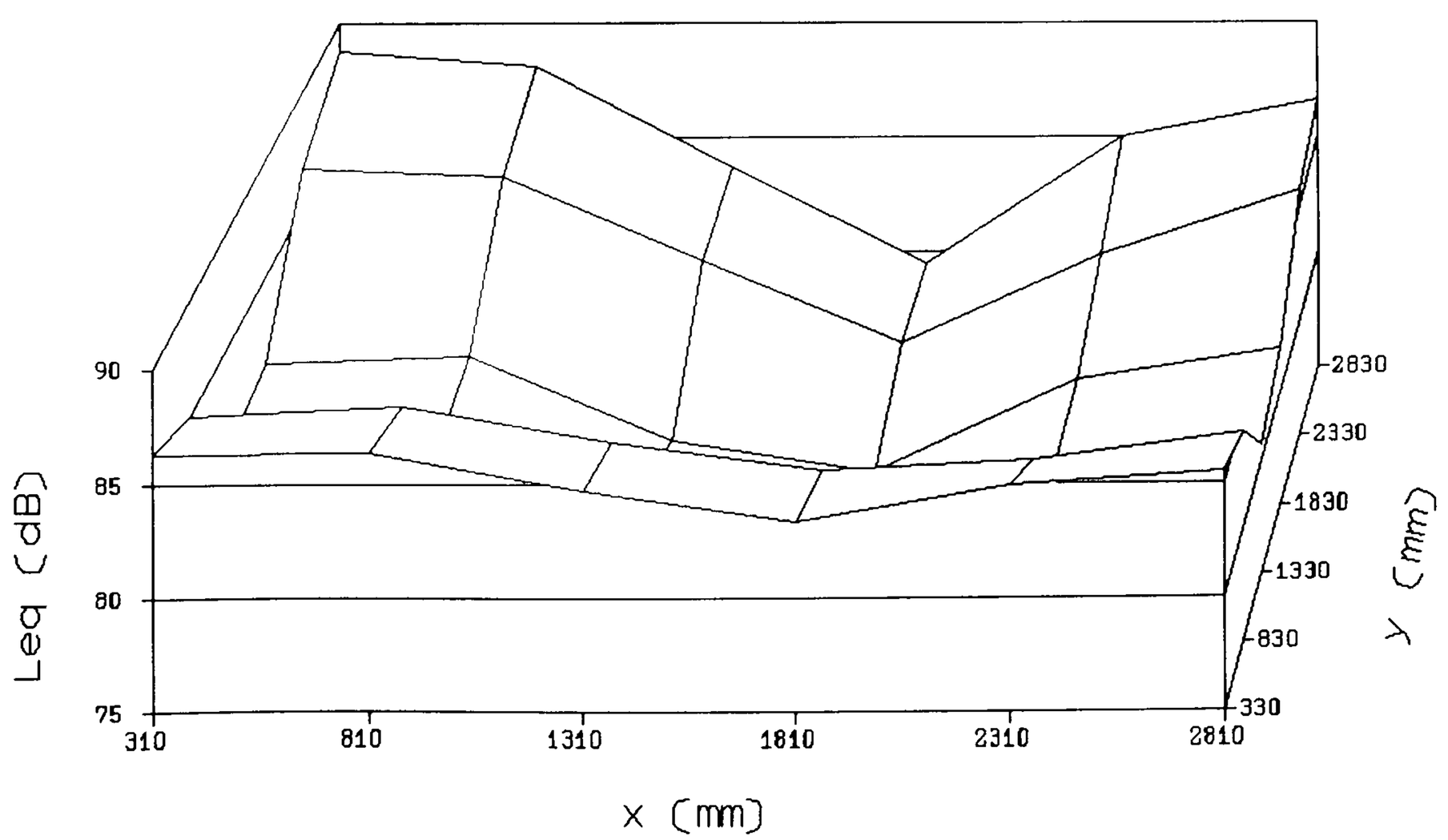

Figure 3.5: Pressure map over array of D2 seats at z = 0 for 80 Hz, (a) without barriers, and (b) with barriers.

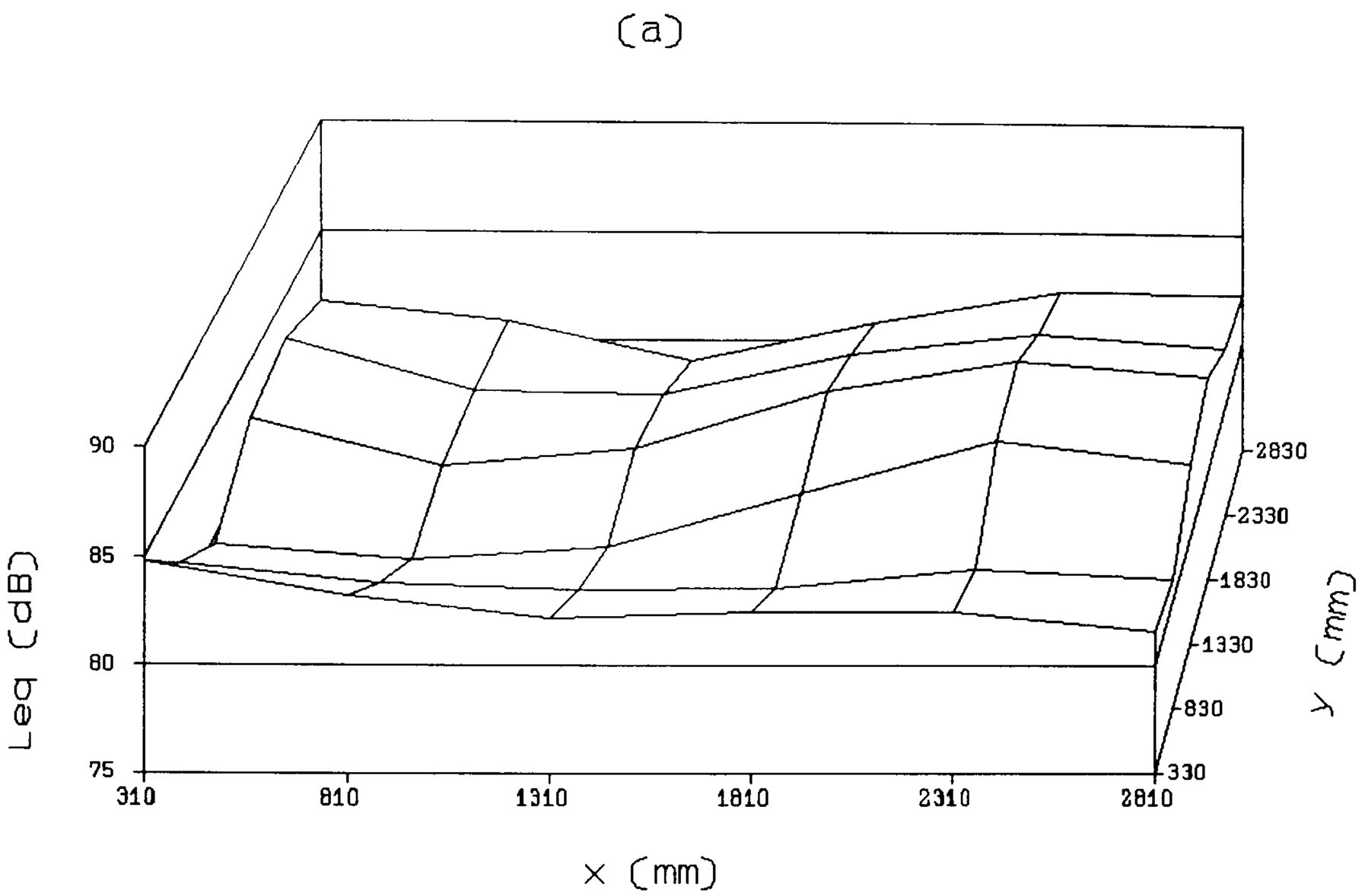

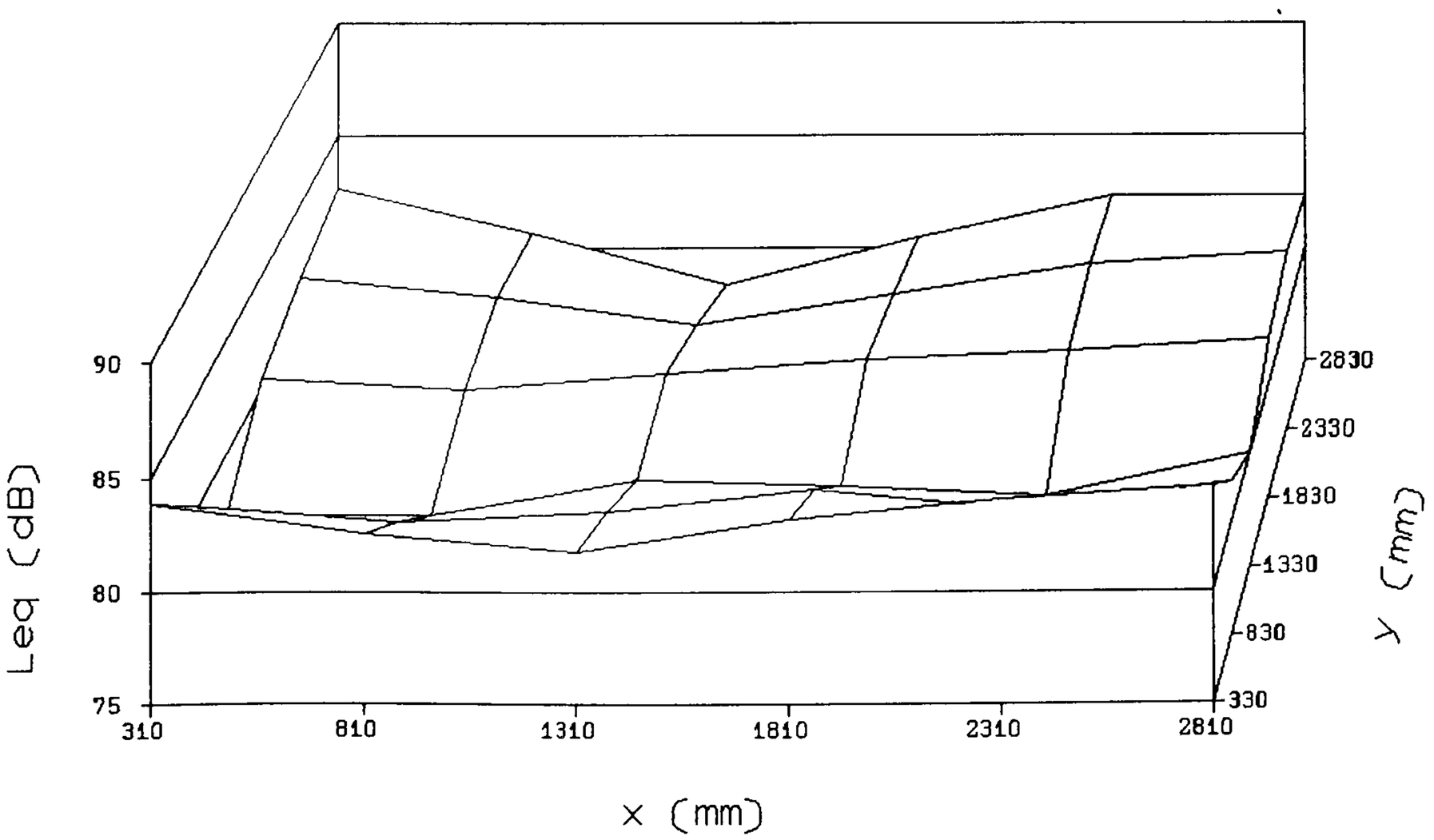

Figure 3.6: Pressure map over array of D2 seats at z = 0 for 100 Hz, (a) without barriers, and (b) with barriers.

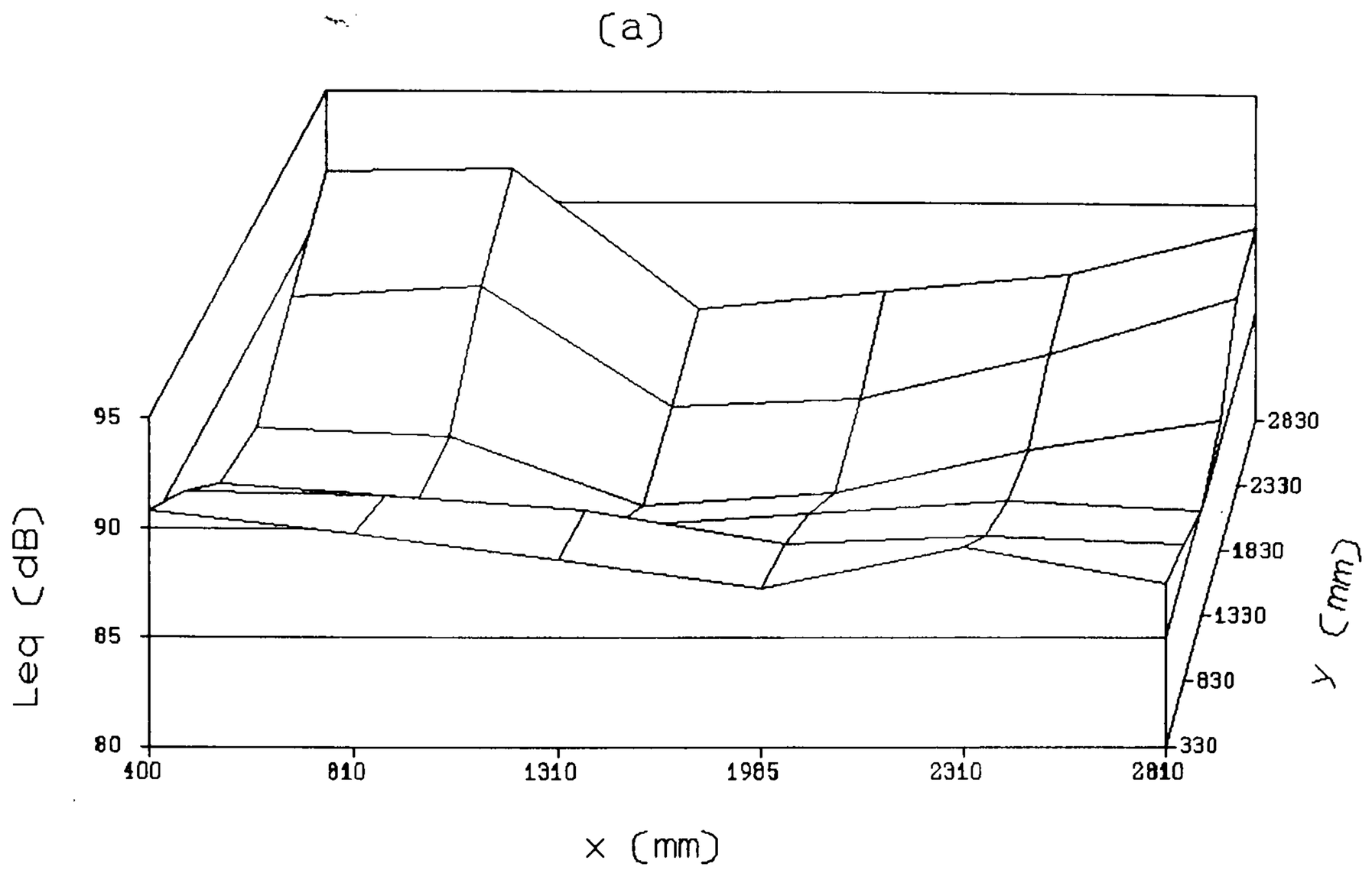

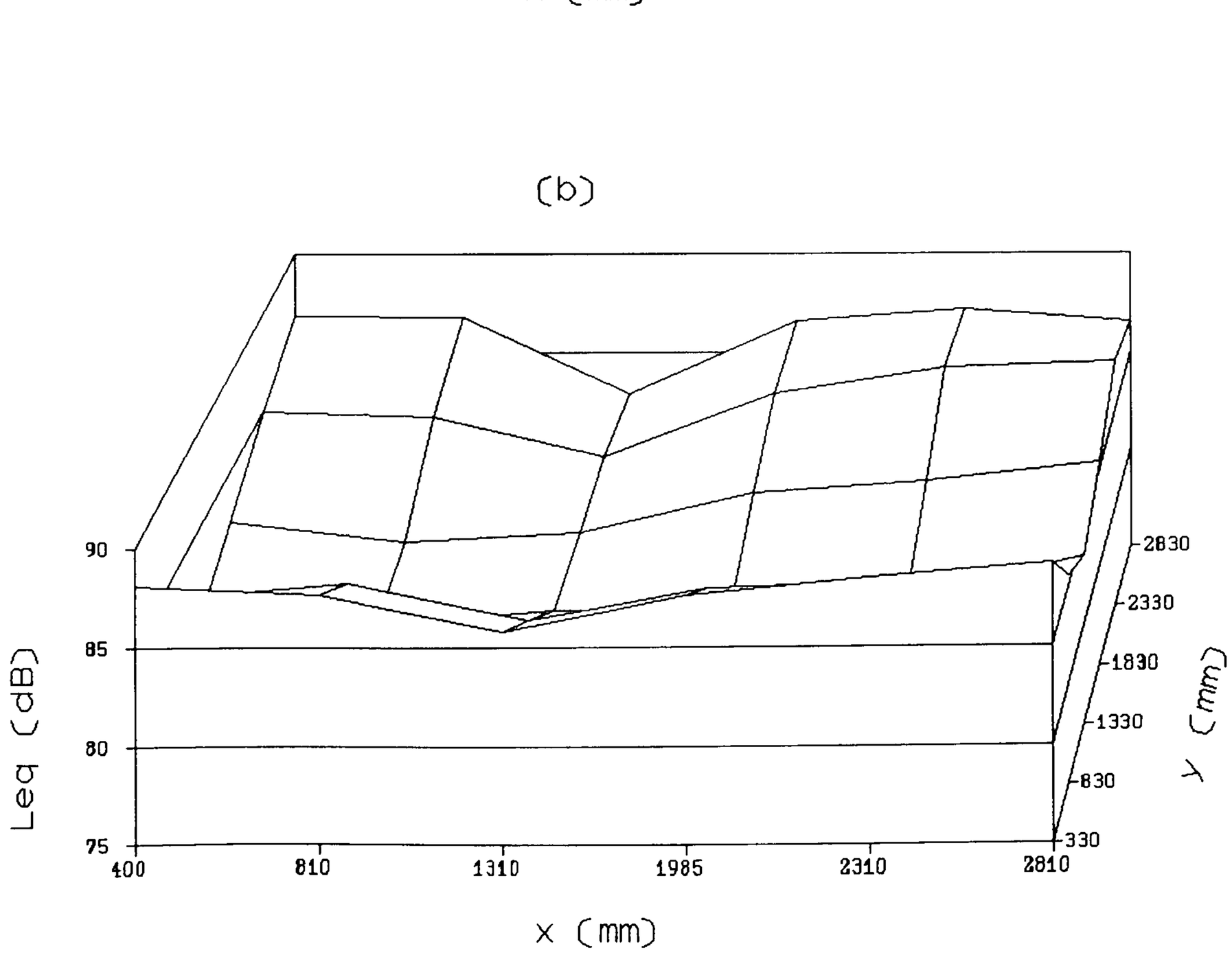

Figure 3.7: Pressure map over array of D2 seats at z = - 450 mm with barriers, at (a) 80 Hz and (b) 100 Hz.

Hence, it seems that putting barriers round the seating array accentuates room modes which are already present. The biggest change in pressure distribution occurs at the frequency where the barriers cause the greatest increase in the measured absorption coefficient. It is likely that the first phenomenon causes the second. How this happens is not yet clear: it is conceivable that either the seats or the barriers themselves could be absorbing the extra energy. It is thought that the seats could be providing at least part of the extra absorption because the barriers have changed the modal amplitudes over them. Dowell (1978) has shown theoretically and Taylor (1985) has confirmed practically that measured sound absorption can depend substantially on the standing wave pattern over the area of the absorber. This is particularly true for lower order modes. The next two sections investigate the possibility of the barriers absorbing sound themselves.

All the pressure maps discussed here are probably typical in overall form to any absorption measurement with barriers in any reverberation chamber, at least on upholstered seats. The magnitude of the pressure changes caused by the introduction of barriers might be different for other seat types: the D2 seats were specifically picked for the large anomalous barrier absorption they exhibited. However, it is thought that the phenomenon itself is not peculiar in any way to the particular combination of reverberation chamber and barriers used here, since Bradley (1992) has also remarked on the problem and some of the original absorption results of Kath and Kuhl (1965) exhibit a low-frequency peak.

3.2 Impulse Response of Barriers

As a first step in determining whether the barriers themselves could be absorbing energy at 80 Hz, it was decided to measure their resonance behaviour using a hammer and an accelerometer connected to a FFT (Fast Fourier Transform) analyser. The barriers were set up as usual in the centre of the chamber (since this position gave the bigger absorption increase in figure 3.1) to form a rectangular enclosure, but without the seats inside. Because the seats are not usually in close contact with the barriers they should not have a large effect on the impulse response of the barriers. The equipment arrangement is shown in figure 3.8.

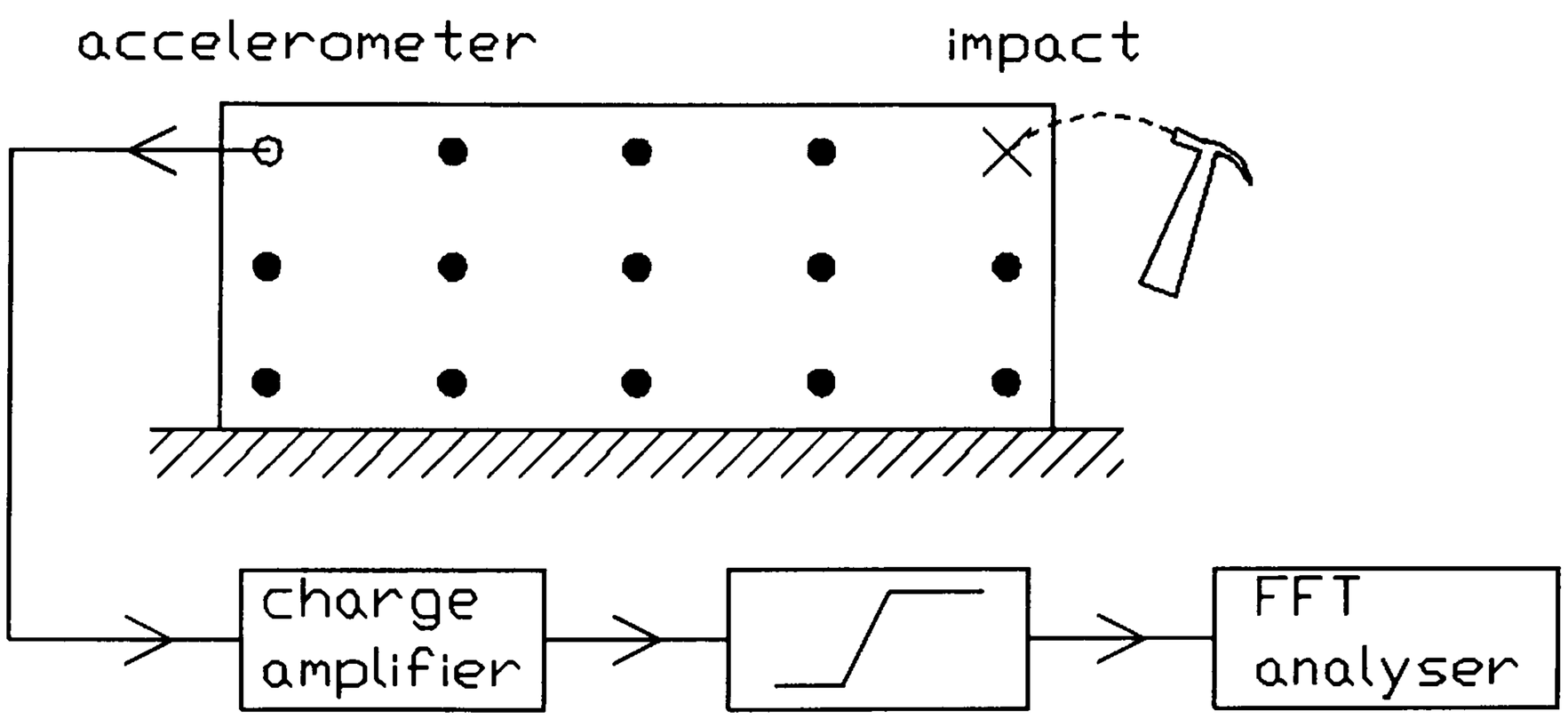

Figure 3.8: Apparatus for measuring impulse response of barriers used in seating absorption measurements.

Barrier resonances were detected from the FFT of the captured impulse response. Since the region of interest here was a fairly narrow low-frequency one, the analysis was performed in the frequency range from 50 to 200 Hz. Measurements were

made at fifteen equally-spaced points on the surface of one of the 2320 x 900 x 18 mm chipboard panels making up the barriers, as shown in figure 3.8. The top of the panel was free to vibrate and the bottom was resting on the ground.

A sample of the results is shown in figure 3.9. These are spectra for five equally-spaced points on a horizontal line along the centre of the barrier. The first and last points are close to the edges of the barrier, where it was screwed to other panels in the enclosure. The first point is near a corner joint, and the last is near a flat joint. In most of the spectra, the amplitude of low-frequency modes is relatively high. There seem to be strong modes at about 65 and 85 Hz at the first four points and also at 105 Hz at the middle three measurement points. In the last spectrum, the response of the panel is more complicated: this is perhaps due to the slightly different modes of the other panel to which it is clamped at this point. With only five measuring points, it is difficult to see mode shape patterns on the panel surface.

It can be concluded from this experiment, then, that the panels making up the barriers do have resonances in the frequency range of interest. In particular, a strong mode around 85 Hz was detected which seems to correspond to the biggest effect on seating absorption caused by the barriers, which is in the 80 Hz ⅓ octave band. From the pressure map experiment in part 3.1, it seemed that the addition of barriers accentuated room modes already present. If these room modes are considered as a resonant force, then it is quite possible that absorption may be occurring because of the coincidence between the frequency of a resonant force and the modal frequencies of a lossy vibrating body.

(a)

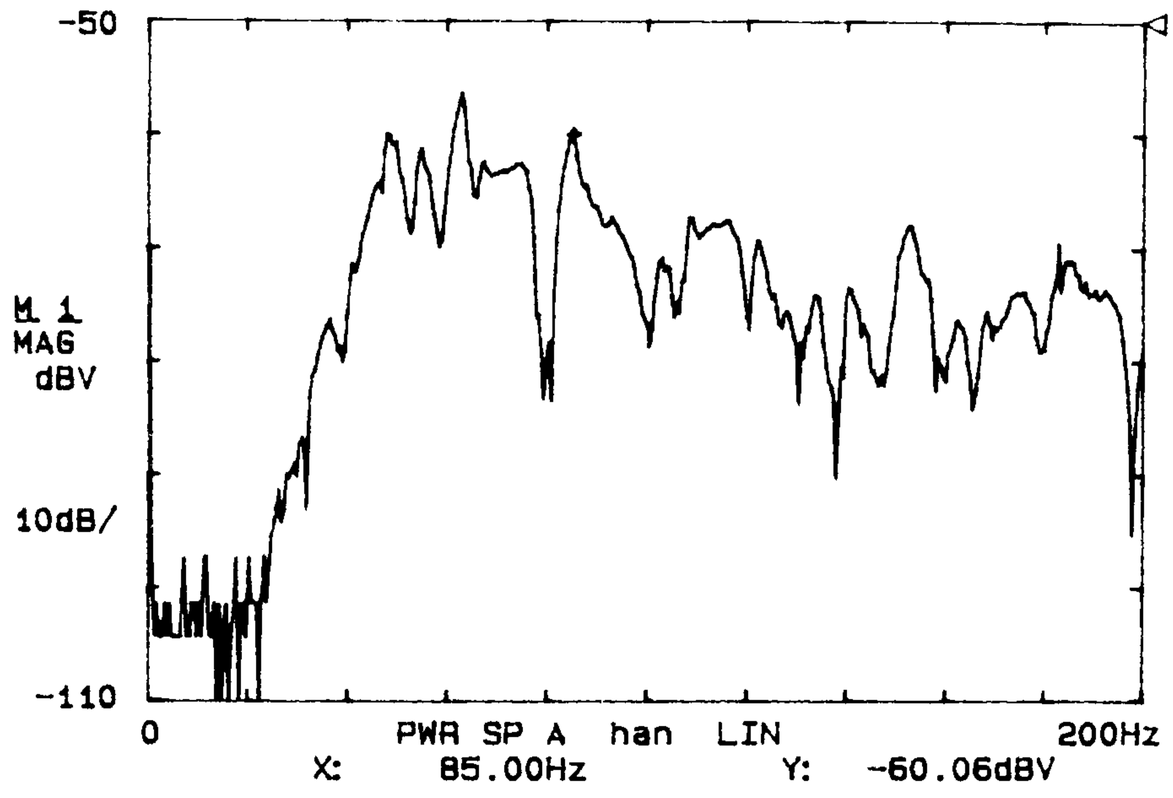

(b)

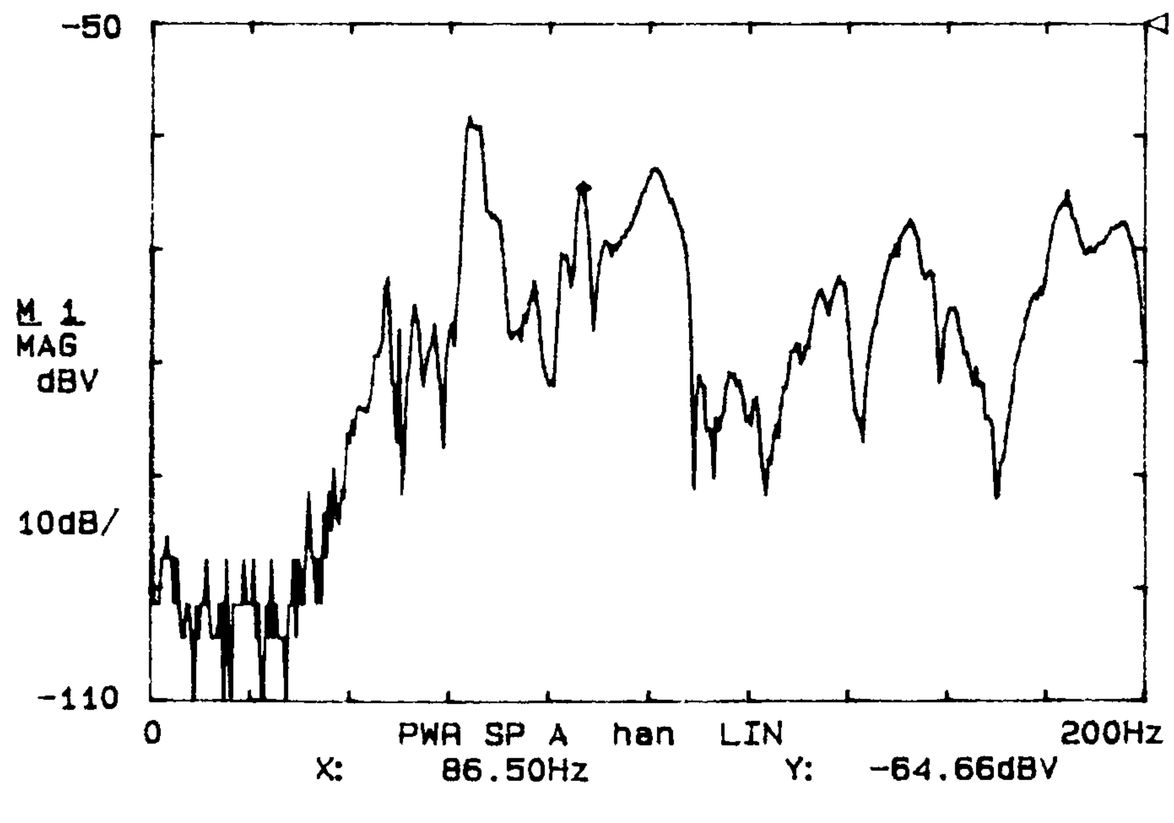

Figure 3.9: Impact response of barrier panel measured at evenly-spaced positions along its centre line as indicated in figure 3.8. The spectra range from the left of the panel (a) to the right (e).

(c)

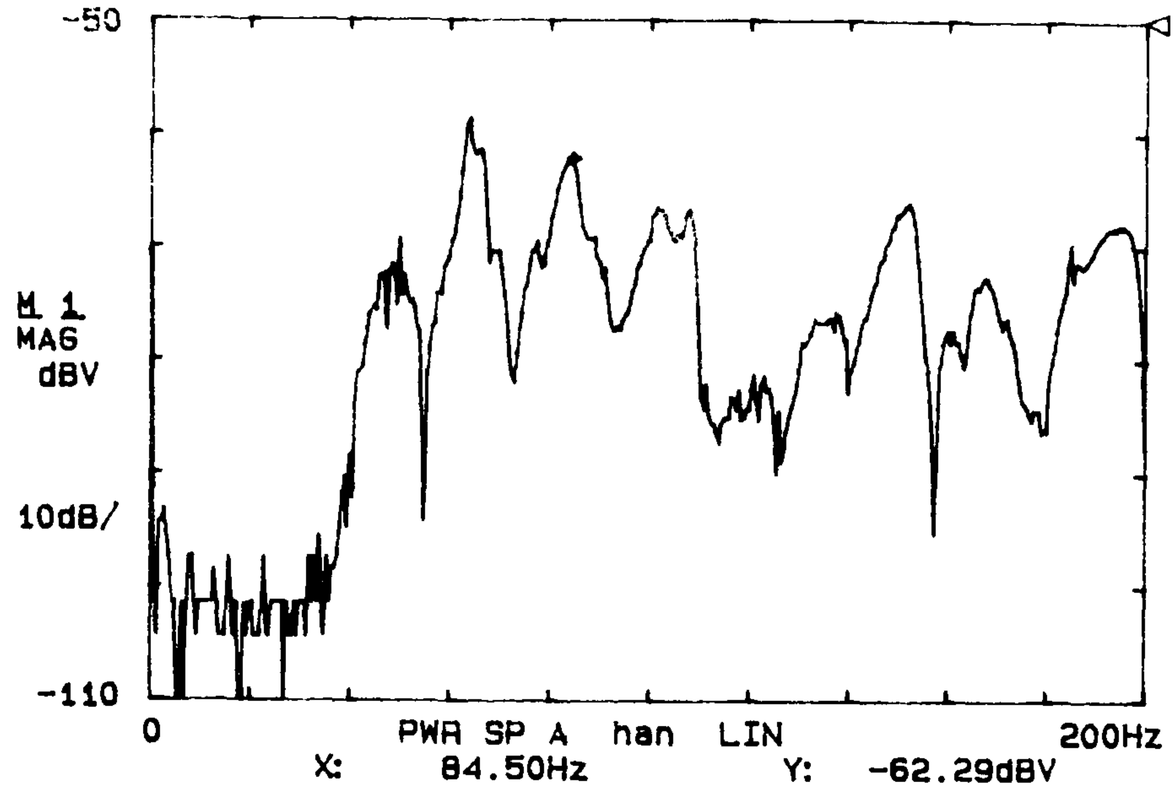

(d)

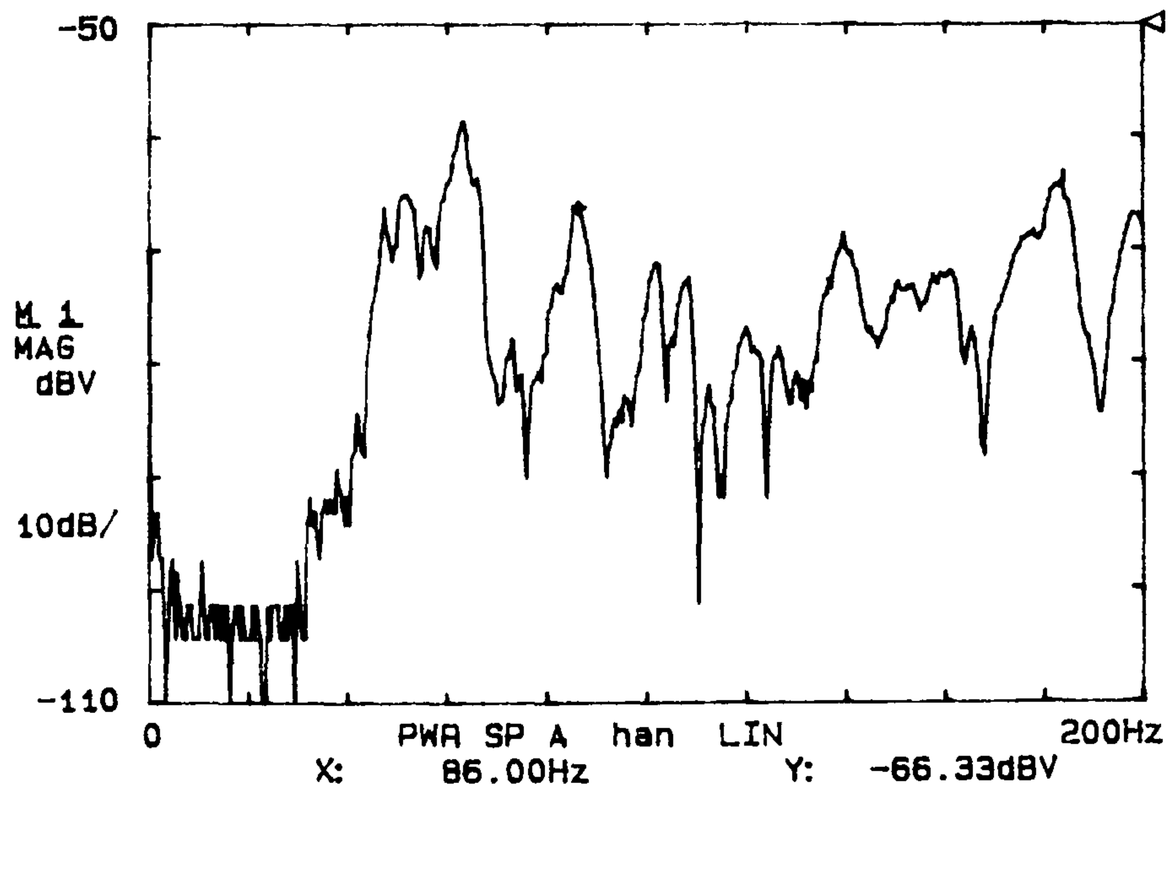

Figure 3.9 (continued).

(e)

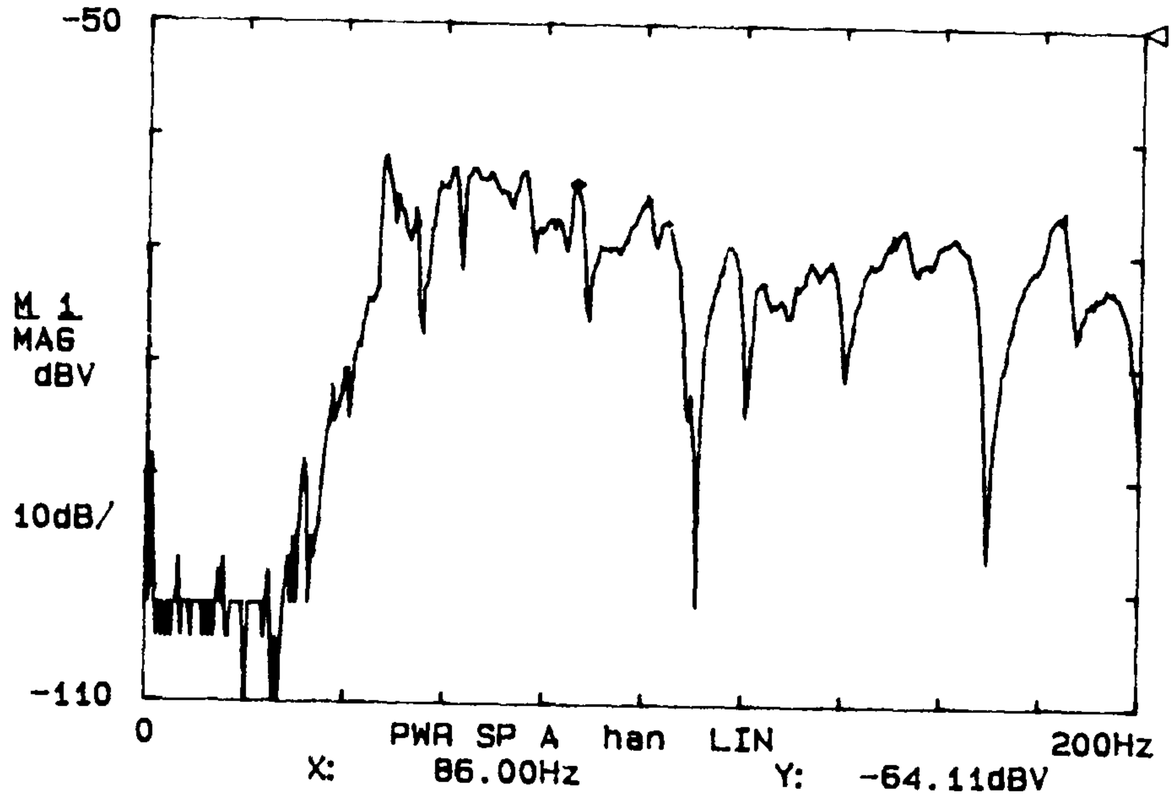

Figure 3.9 (continued).

3.3 The Transfer Function from Reverberation Chamber to Barriers

In order to test further the possibility that the combination of reverberation room and barriers might be forming a resonant system, measurements were made of the total transfer function from the loudspeaker in the corner of the room to the barrier surface. This was done using the same equipment as above set up as in figure 3.8, except that the FFT analyser was replaced with a maximum length sequence analysis system. This measurement technique is described fully by Rife and Vanderkooy (1989): it is a way of quickly obtaining the impulse response of a linear system with a high signal-to-noise ratio. The maximum length sequence signal was amplified and used to drive a loudspeaker in the corner of the reverberation chamber. The impulse response of the loudspeaker - room - barrier system was

obtained by cross-correlating the input maximum length sequence with the output from an accelerometer fixed to the barrier as in figure 3.8. Fourier Transforming this gave the magnitude of the acceleration transfer function of the system. The influence of the loudspeaker and amplifier was then removed by making a separate anechoic measurement of their combined frequency response and normalising the acceleration transfer function to this.

It was assumed that most of the energy lost in the barrier would be due to linear viscous damping, so that this energy would be proportional to the root mean square velocity at the surface of the panel (Meirovitch, 1967, pp. 388-389). Therefore, the magnitude of the velocity transfer function of the room - barrier system was obtained by dividing the acceleration function by $2\pi f$ at all frequencies f.

As in part 3.2, measurements were made at fifteen equally-spaced positions on the surface of the barrier panel. Figure 3.10 shows the velocity transfer function at the centre of the barrier panel. The frequency resolution of the spectrum is 0.98 Hz. The graph is dominated by the strong resonances at 65 and 83 Hz, the peaks of which are 29 and 26 dB higher respectively than the average level at higher frequencies. These peaks are nearly always present in the transfer functions for the other fourteen measuring positions on the barrier. Some of the other positions also have peaks at frequencies such as 116 Hz, though these are less common. This means that if the transfer function is energy-averaged over the barrier area, then the low frequency resonances stand out even more clearly, as can be seen in figure 3.11.

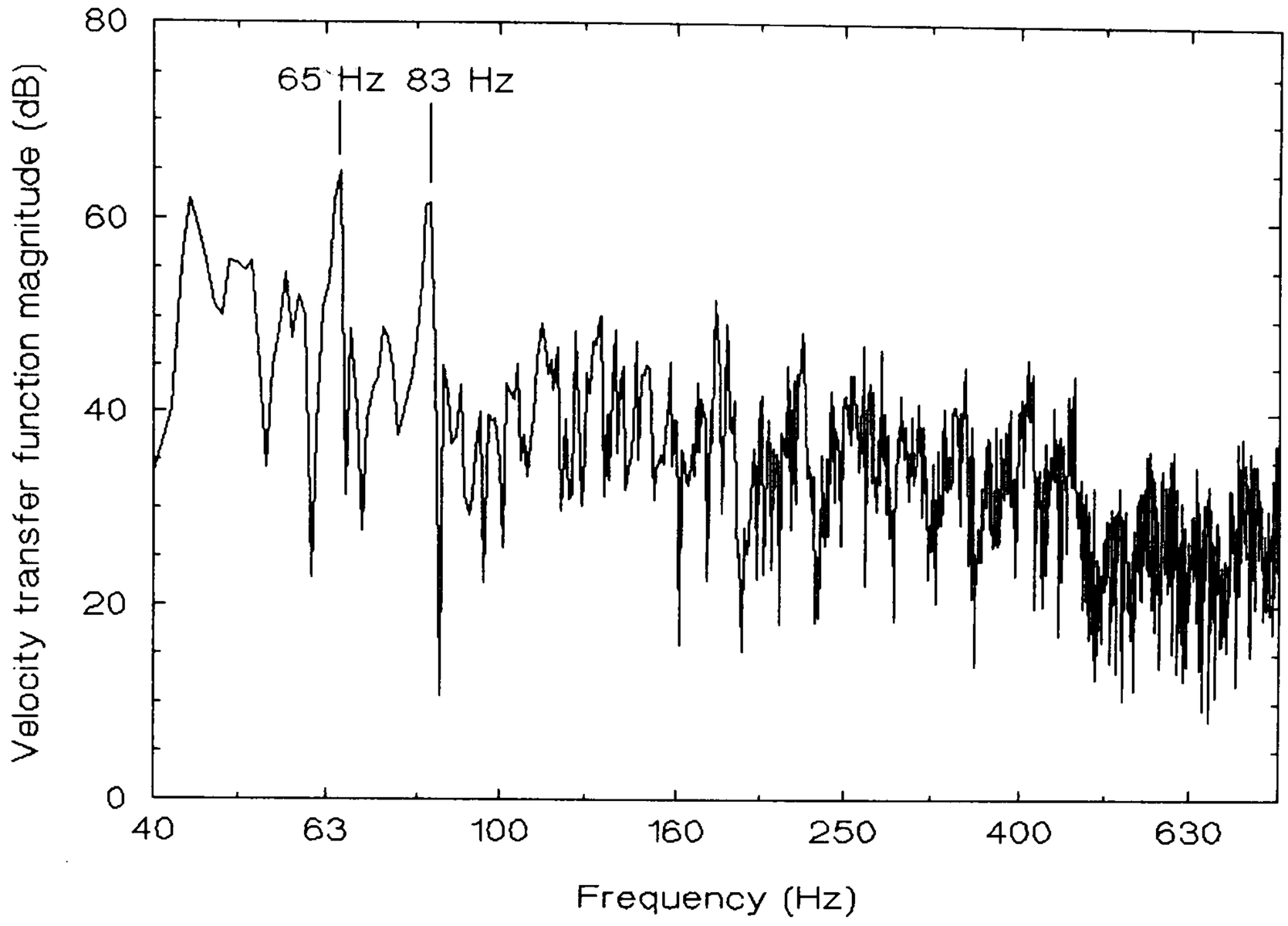

Figure 3.10: Magnitude of the velocity transfer function from reverberation room to the centre of the barrier surface.

The frequencies of these resonances accord with those found in a rough subjective check of the phenomenon. For this, the barriers were left set up and a sine wave generator was used to drive the loudspeaker in the corner of the reverberation chamber via a powerful amplifier. With one hand on the barrier, the frequency of the sine wave was increased. The barrier could easily be felt to be vibrating strongly in the region from 55 to 90 Hz.

The area-averaged velocity transfer function magnitude can now be compared with the absorption coefficient of the barriers alone. An attempt was made to measure this in the reverberation chamber from reverberation time measurements of the

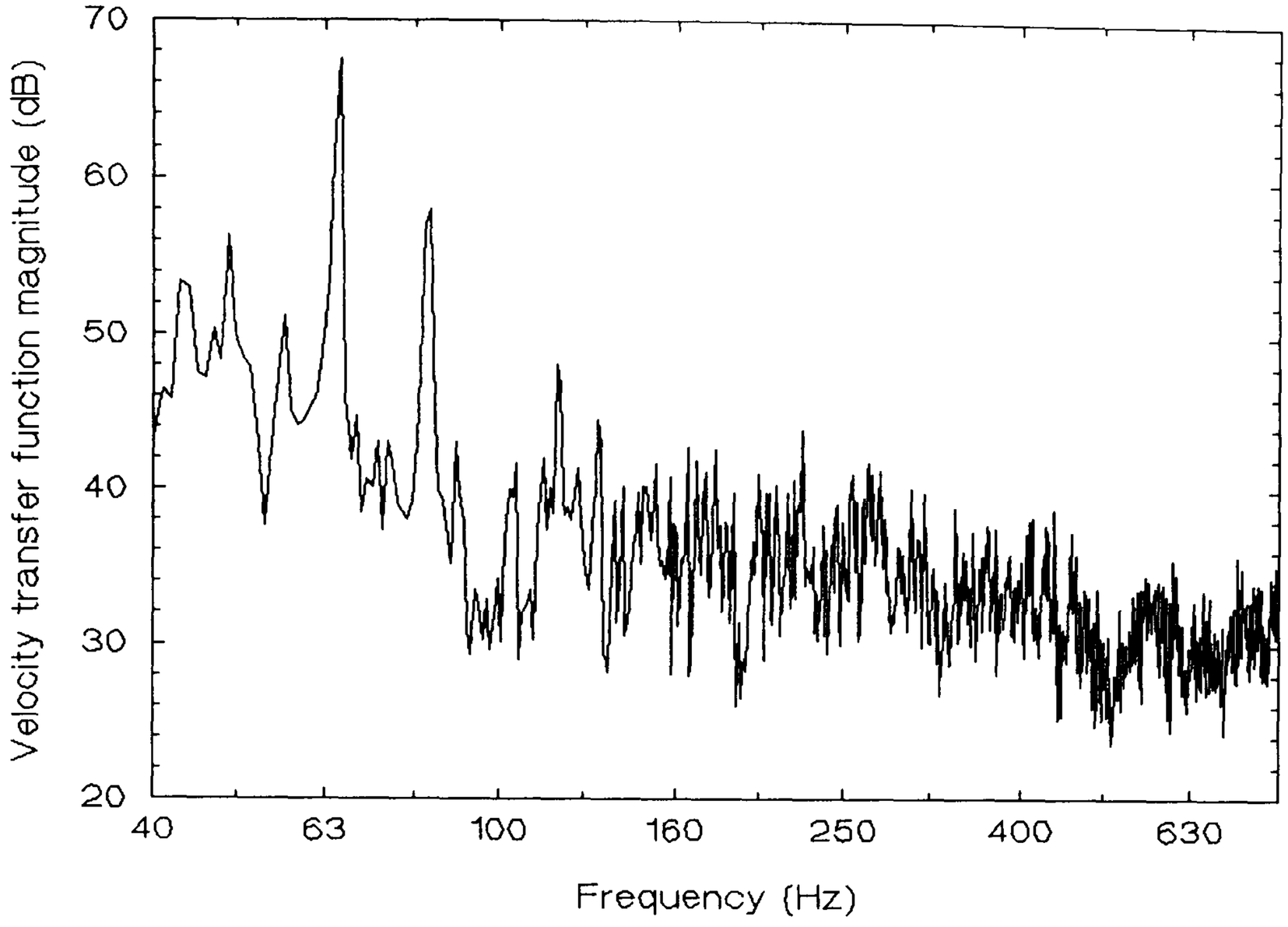

Figure 3.11: Velocity transfer function from the reverberation room to the barrier, averaged across the surface of the barrier.

empty room and the room with just the barrier enclosure set up in the centre. Of course, the uncertainties in this measurement are quite large since the barriers have relatively little total absorption. The absorption coefficient has been calculated in figure 3.12 relative to the plan area of the barrier enclosure. This is the same area used in seating absorption coefficient calculations.

As in the seating absorption measurements with and without barriers in figure 3.1(b), the barrier absorption coefficient has a substantial peak at 80 Hz. This tallies well with the second resonant peak in the area-averaged velocity transfer function in figure 3.11. This is good evidence for barrier absorption being caused

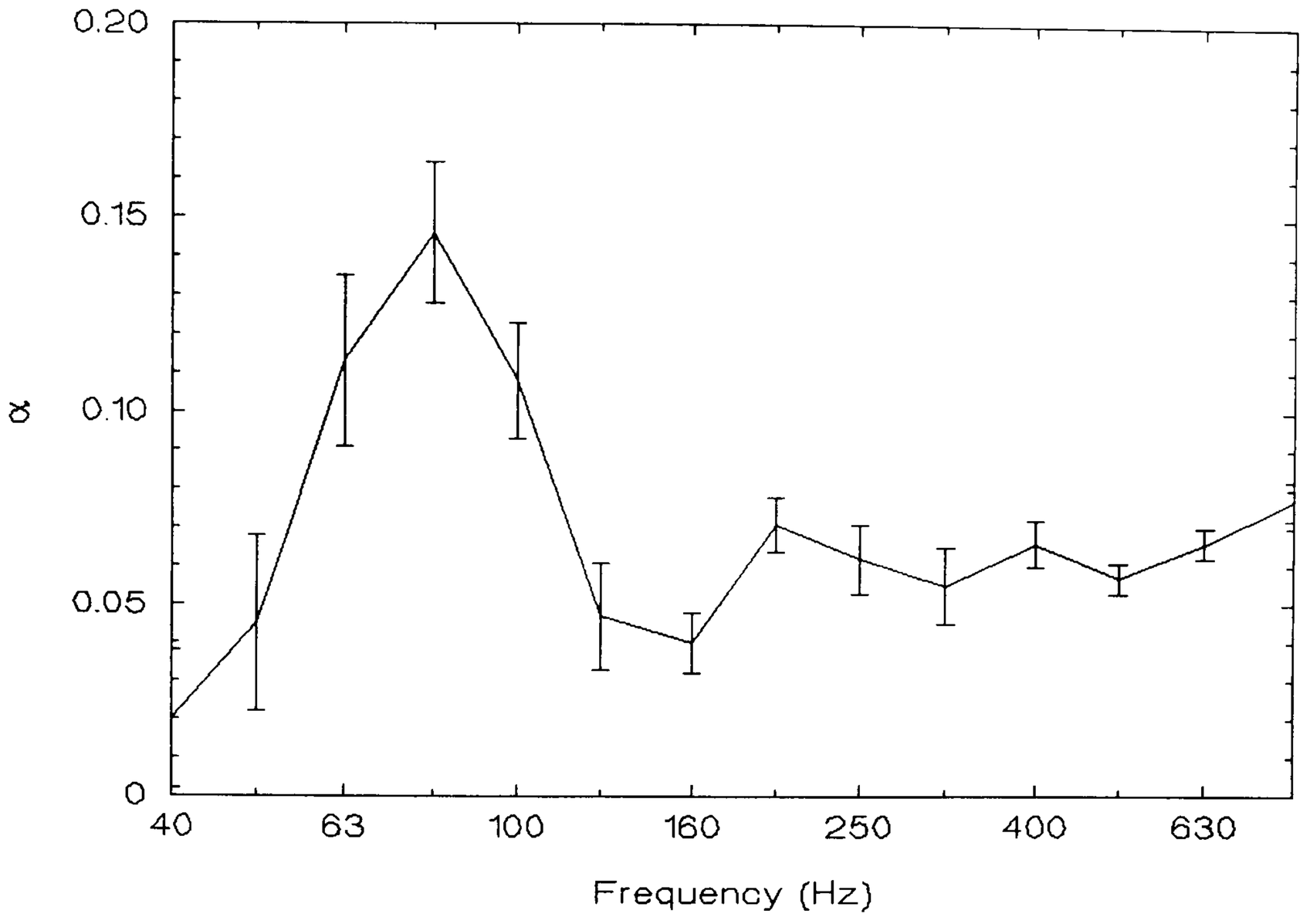

Figure 3.12: Absorption coefficient of the four-sided barrier enclosure alone, in the centre of the chamber. The error bars represent ± one standard error.

by the transfer of energy from room modes to the vibrating barrier - a panel absorption mechanism. Energy is lost inside the barrier panel due to its damping, due to poor coupling with other barrier panels, and in friction with the chamber floor. The absorption of the barriers is quite large in the 63 Hz ⅓ octave, though not as large as the first peak in figure 3.11 might suggest. It seems that, though a room mode can make the barrier vibrate well at this frequency, not quite as much energy is lost inside the barrier as at 80 Hz.

3.4 Summary of Absorption Mechanisms

The results depicted above provide good evidence that the unwanted low-frequency absorption occurring when a seating array is surrounded by barriers occurs at least partly due to the barriers behaving as a panel absorber in the reverberation chamber. More specifically, section 3.1 showed that there were pressure variations in the frequency range of interest over the seats without the use of barriers, and that these variations increased with the introduction of the barriers. Section 3.2 showed that the barriers had a resonance at the frequency where the absorption increased. Section 3.3 showed that the combined room - barrier system had a transfer function with a strong resonant peak at the frequency of maximum barrier absorption.

The unwanted low-frequency absorption probably also involves the seats themselves, since the amount of extra absorption varies for different seat types. This part of the extra absorption is measured because the barriers change the pressure distribution over the seats. It was stated in the introduction to this chapter that seat type D2 had the highest low-frequency absorption to start with, and that it showed a greater absorption increase with the introduction of barriers than did seat B2 in figure 2.7, for example.

3.5 Minimising Barrier Absorption

Anomalous low-frequency barrier absorption is lessened by using a position in the corner rather than the centre of the reverberation chamber for seat absorption

measurements. This requires two rather than four barriers and so roughly halves the problem. Reducing it further seems to be less simple. Because at least part of the unwanted absorption seems to be due to interaction between barrier and room modes, it would be advantageous to suppress the most prominent barrier modes or move them out of the frequency range of interest. Unfortunately, in the course of this work, suitable materials were too expensive to buy in an area large enough to form seating barriers.

If the problem cannot be tackled at source, then a crude correction can be made to seating absorption measurements by subtracting the absorption coefficient of the barriers measured separately, as in figure 3.12, from the absorption coefficient of the seats with barriers. This is not entirely satisfactory for two reasons: firstly the "barriers only" absorption measurement will not be very accurate due to the low absorption being measured, and so the corrected absorption will be equally inaccurate; and secondly it takes no account of the increase of the measured seat absorption due to the barriers changing the distribution of room modes over the seats.

It should be remembered that the barrier absorption problem is not as bad as it might be, since it occurs at the lower end of the frequency spectrum. Low frequency absorption measurements are always less accurate, especially in rooms with less then perfect diffusion like auditoria. Also, fortunately, the human ear is also less discriminating in this region: Cremer and Müller (1982a, p. 507) quote results from Plenge showing that the subjective limen for relative change in

reverberation time increases with decreasing frequency below 1 kHz. Hence, no further investigations of the problem were made.

Chapter 4

Side Absorption and the Edge Effect

An awkward problem in measuring the absorption coefficient α of a three-dimensional object in a reverberation chamber is that the measured coefficient is found to vary with the size of the sample. This is often expressed as the dependence of α on E, the ratio of the total plan edge length of the sample to its plan area. If the absorbing edges of a sample are exposed, then this variation is due to two components:

(i) the absorption of the front row and side of the seating array, causing α to increase as E increases;

(ii) diffraction of sound waves at the edges of the array, again causing α to increase with E.

The first component is here referred to as side absorption and is simply taken into account in Kath and Kuhl's method by obscuring the exposed sides of the seating array with non-absorbent barriers. Measurements of side absorption and predictions of equivalent corrections to the plan area for seating absorption calculation are examined later in this chapter. The term edge effect is reserved for the second component, as this nomenclature usually implies a diffraction phenomenon. This effect is not taken into account in Kath and Kuhl's method and

so may limit the accuracy of the method. It is therefore examined in detail in the following section.

4.1 The Edge Effect

Of the edge effect, Bartel (1981) has written:

> "The apparent linear relationship between the absorption coefficient and the relative edge length of the specimen is often written in the form
>
> $$\alpha = \alpha_\infty + \beta E \qquad (4.1)$$
>
> where α is the absorption coefficient of a given specimen as obtained by measurement in a reverberation room, α_∞ is the true absorption coefficient, a result that would be obtained in the absence of any diffraction effect at the edges, ß is a constant, and E is the ratio of the specimen perimeter to area."

This relationship was first proposed by Kosten (1960) and has been investigated experimentally by several others, notably Kolmer and Krnak (1961), Daniel (1963), Gomperts (1965), ten Wolde (1967) and Dekker (1974). All measured α for a range of E never exceeding $1.1\ m^{-1} < E < 9\ m^{-1}$, for different plane absorbers. All then fitted a straight line to the data, assumed that equation (4.1) was true outside their observed ranges of E, and extrapolated to $E = 0$ to obtain α_∞. Only Gomperts disagreed with the values of α_∞ found thus. In each case, ß was found to be characteristic of the test material and varied with frequency. Similarly, Bartel (1981) measured α for $1.3\ m^{-1} < E < 3.3\ m^{-1}$, for three types of plane absorber, and fitted a straight line regression for each. For one of the materials, however, the graph of α versus E showed a trace of non-linearity towards $E = 1.3\ m^{-1}$. Now, a

prediction of the results based on impedance tube measurements of the three materials and using a theory developed by Northwood (1963), gave very good agreement with the observed data for 1.3 m^{-1} < E < 3.3 m^{-1}. However, for E < 1.3 m^{-1}, the theoretical graphs of α versus E become non-linear. Bartel therefore concluded that it is *not* possible to infer α_∞ for locally-reacting plane absorbers from reverberation chamber measurements of α with E varied.

Up until this year, the only investigation of the relationship between α and E for auditorium seating had been carried out by Hegvold (1971) using 1:8 scale model auditors on unupholstered chairs. He measured α for seating arrays whose edges were obscured by barriers, for 1.5 m^{-1} < E < 8.5 m^{-1} (full scale). He then assumed that the straight-line relationship of equation (4.1) applied for E < 1.5 m^{-1} and extrapolated to obtain α_∞. However, the auditoria used for the present work had large seating blocks with values of E considerably less than 1.5 m^{-1}. For instance, for a typical block from hall B2, a multipurpose hall used primarily for concerts, E = 0.46 m^{-1}. Until very recently then, the relationship between α and E for large areas of seating had still not been investigated, and it was not clear whether it would follow Bartel's predictions for large locally-reacting plane absorbers.

This year, Bradley (1992) published a paper in which he investigated α for full-size auditorium chairs over 1.4 < E < 2.4 m^{-1}. The sides of the array of seats were not obscured by barriers. Over this range, the variation of α with E was approximately linear, so Bradley fitted equation (4.1). The absorption coefficient of the same seats was also calculated from RT measurements in the corresponding auditorium

with and without the seats present. The reverberation chamber measurements were linearly extrapolated to give a value of α at the average value of E of all the seating blocks in the auditorium. The two absorption coefficients were then compared. This was done for four auditoria, and the agreement between the in-situ measurement and the extrapolated reverberation chamber α was very good for two of them. The value of E extrapolated to for both these measurements was 0.8 m^{-1}. Bradley therefore concluded that the linear extrapolation method works and that it is the best way of predicting seat absorption in auditoria.

Bradley's is a useful result, but his method of measuring seating absorption involves too many tests at different values of E for it to be used as a standard technological method. Kath and Kuhl's method necessitates fewer tests on a given seat type and it can take side absorption into account, but it does not correct for any variation of α with E due to diffraction. It would be advantageous if the likely error caused by neglecting the edge effect in Kath and Kuhl's method could be shown to be small. This can indeed be partially demonstrated from Bradley's work: namely that the influence of the edge effect must be small *if it is non-linear*. This is because Bradley's results are for seat arrays with the sides left exposed. Thus the variation of α with E in his results should have been due to both the edge effect and side absorption. Yet it is easy to show that one would expect to obtain a linear relationship of the form of equation (4.1) for the effects of side absorption only.

Consider a rectilinear locally-reacting absorbing block of dimensions w x l in plan and of height h metres. When measured in a diffuse reverberation chamber, the total absorption is

$$A = A_p + A_s \tag{4.2}$$

where A_p is the total absorption of the plan (top) area and A_s is the total absorption of the four sides. If diffraction effects are ignored,

$$A_p = \alpha_\infty wl \tag{4.3}$$

$$A_s = 2\alpha_s h(w+l) \tag{4.4}$$

where α_s is the absorption coefficient of the sides of the absorber, assumed to be unaffected by diffraction and equal for all four sides.

If the absorption coefficient for the whole absorber is now calculated as a function of the plan area wl then equations (4.3) and (4.4) may be substituted into (4.2) to obtain

$$\alpha = \frac{A}{wl} = \alpha_\infty + 2\alpha_s h\frac{w+l}{wl} \tag{4.5}$$

We now introduce the ratio of perimeter length to plan area,

$$E = \frac{2(w+l)}{wl} \tag{4.6}$$

Substituting equation (4.6) into (4.5) gives

$$\alpha = \alpha_\infty + h\alpha_s E \tag{4.7}$$

At a given frequency, $h\alpha_s$ will be a constant (ß), so equations (4.7) and (4.1) are equivalent. Hence, if an array of seats can be likened to a block in this way and if any non-linear edge effect is small, then this relationship is a consequence of measuring different sizes of seating arrays with the sides exposed. Bradley did obtain such a linear relationship for measurements of real seats and he found that extrapolation to small values of E gave the correct results compared with in-situ auditorium measurements. This means that the assumptions made in deriving equation (4.7) are probably true.

To summarise: Bradley's work shows that the combined effect of (side absorption + edge effect) is probably linear for at least $E > 0.8\ m^{-1}$. But equation (4.7) shows that the effect of side absorption only is expected to be linear over all E. Two possibilities therefore remain. Either the edge effect on its own is also linear for at least $E > 0.8\ m^{-1}$, or it may be non-linear but insignificant over the same range of E. Since Hegvold's results show that the edge effect is linear for $1.5\ m^{-1} < E < 8.5\ m^{-1}$, the first possibility is the more likely. This still leaves room for Bartel's predictions of non-linearity for very large seating blocks, where $E < 0.8\ m^{-1}$.

4.1.1 The Implications of the Edge Effect for Kath and Kuhl's Method

It was stated above that Kath and Kuhl's method does not specifically take into account the edge effect for a particular auditorium. This is true, but the edge effect can still be minimised. When the seating array is placed in the corner of the chamber it is effectively mirrored in the two adjacent walls. Sound cannot diffract into the array at the edges adjoining the walls, so E is halved. This has the same

effect as quadrupling the size of the sample. If the test sample extended over the whole of the chamber floor, sound could no longer diffract into it at any edge, so α_∞ would be measured. In all of the absorption coefficient data presented here, an array of four rows of six chairs was used, with a typical plan area of 3.3 by 3.6 m. In the centre of the chamber this gives E = 1.16 m^{-1}, but in the corner of the chamber the effective value is 0.58 m^{-1}. Thus, by using a reasonably large array of 24 seats and placing them in the corner, the edge effect has probably been reduced to a negligible level. If the variation of α with E due to the edge effect is linear in this region, and we assume the values of ß obtained by Bradley (1992) for screened seats, then the biggest edge effect error in α is 0.02, at 4 kHz. This is the predicted absolute error in α due to assuming that α measured at E = 0.58 m^{-1} is the same as the α which would be measured at the typical auditorium value of E = 0.46 m^{-1}. This is on the order of the standard errors obtained in a reverberation chamber measurement, and is smaller than those usually found in RT measurements in auditoria, so it is unlikely to be important.

It may be speculated that the differences between values of E in auditoria and those of test samples in reverberation chambers may be becoming smaller with the trend towards the subdivision of the audience area into smaller blocks in modern concert halls - see Cremer (1989) for an example. This "vineyard steps" arrangement is of course adopted to achieve high levels of early lateral energy, but it may also give a small benefit in the fundamental task of predicting the *in-situ* absorption coefficient of the seating.

4.2 Side Absorption and Edge Correction Strips

In the past, acousticians have usually attempted to make an allowance for the absorption of the sides and front of a seating block by increasing the seating area used in calculations from the actual plan area. These corrections usually take the form of a strip of constant width into which the plan area of the seating block is supposed to extend at all its exposed sides. Because the width used is constant with frequency, the assumption is made that the exposed sides have an absorption coefficient proportional to that of the plan area of the block. Also, the same strip width is used for the exposed front row and sides, so the absorption coefficients of the front and sides are assumed to be the same. However, even once these assumptions have been made, it is not clear what the width of the strip should be.

The subject of aisle and perimeter corrections is a confused one in the literature and two authors have each proposed two different methods to use when calculating seating area. In one paper, Barron (1988a) assigns a 0.5 m wide strip to the perimeter of all seating blocks (including aisles). The choice of 0.5 m is based on the well-known paper by Beranek (1969), though Barron notes that Beranek has never stated the origin of this figure. In his earlier book though, Beranek (1962, p. 571) has prescribed a width of 3.5 feet (1 m):

" S_A = Audience seating area in square feet. It includes the sum of: (a) the area of floor covered by the audience; (b) the area of aisles for widths up to 3.5 feet if they lie within the audience area or around the edge of an audience area (no aisle allowance is made at the front edge of a balcony where the audience is seated against a balcony rail; if the aisles are wider

than 3.5 feet, the excess is not included as part of the audience area); and (c) the area used as standing room."

To further confuse the matter, Barron (1988b) has used this value (1 m) in a different paper.

When the absorption coefficients of the front and side of seating blocks was measured using the method described in section 2.5, it was found that the results were quite different from the absorption coefficient of the plan area of the same block. Consequently, the edge correction strip widths calculated from the same measurements using equations (2.12) and (2.13) are not constant with frequency. The original papers of Kath and Kuhl (1964, 1965) included results demonstrating this for one measurement of people on unupholstered seats and one of upholstered seats, both occupied and unoccupied. In the present work, measurements of front and side absorption were made on blocks of ten types of seats, and these were mostly found to have a broadly similar shape to Kath and Kuhl's data.

4.2.1 Measurements of Front Row and Side Area Absorption Coefficients, α_f and α_s

It was found that the front row absorption coefficients α_f of seven seat types could be put into one of three groups and averaged, according to the seat construction. All the seats had at least some upholstery and were covered with cloth. The first group comprises two well-upholstered seat types with upholstered armrests and a tippable squab, the bottom of the squab being covered with cloth. These seats were identified as G2 and A in table 2.1. The second group is composed of two similar

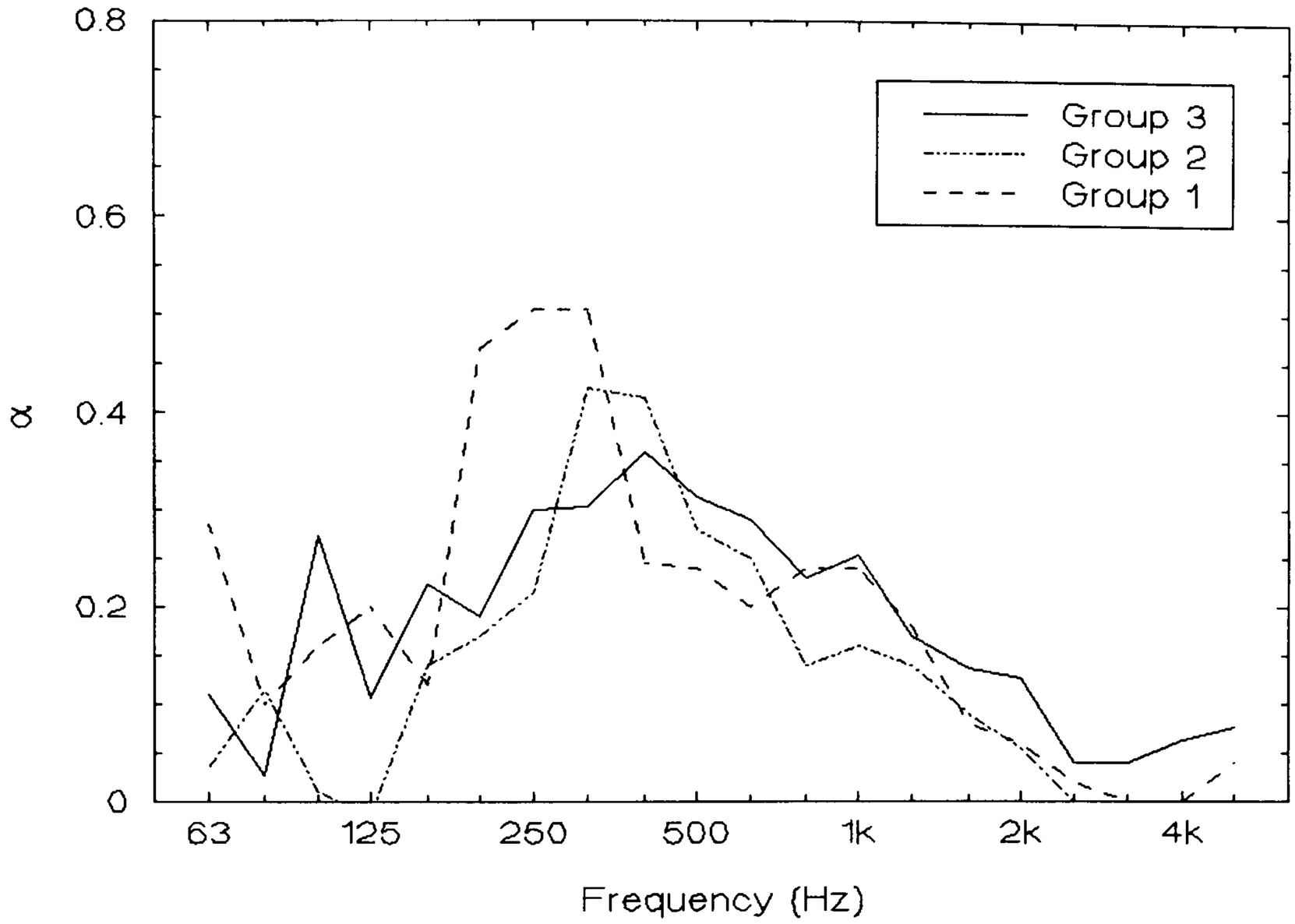

Figure 4.1: Estimates of exposed front row absorption coefficient for different seat types, grouped according to seat construction (see text for group definitions).

seat types (B2 and D1 in table 2.1), but the bottom of their squabs were wooden. The third group is made up of three seat types (B1, O and H in table 2.1) with no armrests, and medium upholstery on the back and the fixed squab only. Figure 4.1 shows that the main difference between the groups is the frequency and magnitude of the maximum value of α_f. Not surprisingly, group 1 seats have the highest peak -their front view is composed almost entirely of absorptive surfaces.

The total range of α_f for the seven seat types was large, particularly at low frequencies, as figure 4.2 shows. Some of this variation must be due to the large

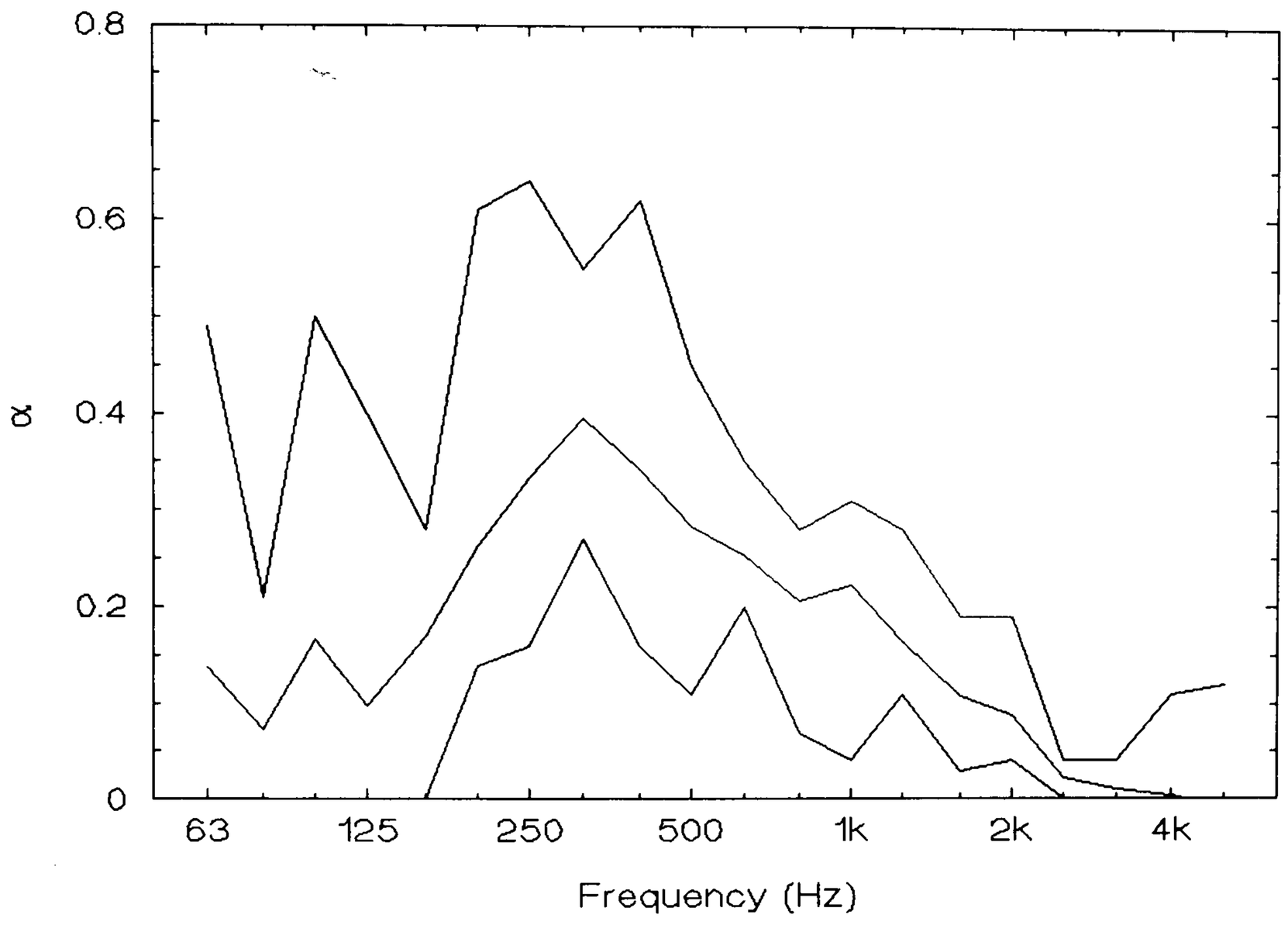

Figure 4.2: Minimum, mean and maximum front row absorption coefficient at each frequency, obtained from measurements on seven seat types.

uncertainties in α_f, which occur because it is formed from the difference of two measured absorption coefficients in equation (2.8). The rest of the variation, however, must be due to considerable differences in front row absorption between seat types. This means that the use of an average front row absorption coefficient for design problems may only be justified where the ratio of exposed front row area to plan area is very small, or for rough calculations.

The range of absorption coefficients α_s for the side area of the five of the seven seat types which were measured at a row spacing of 900 mm, is presented in figure 4.3. Since the average lines in figures 4.2 and 4.3 are very similar, one can say that

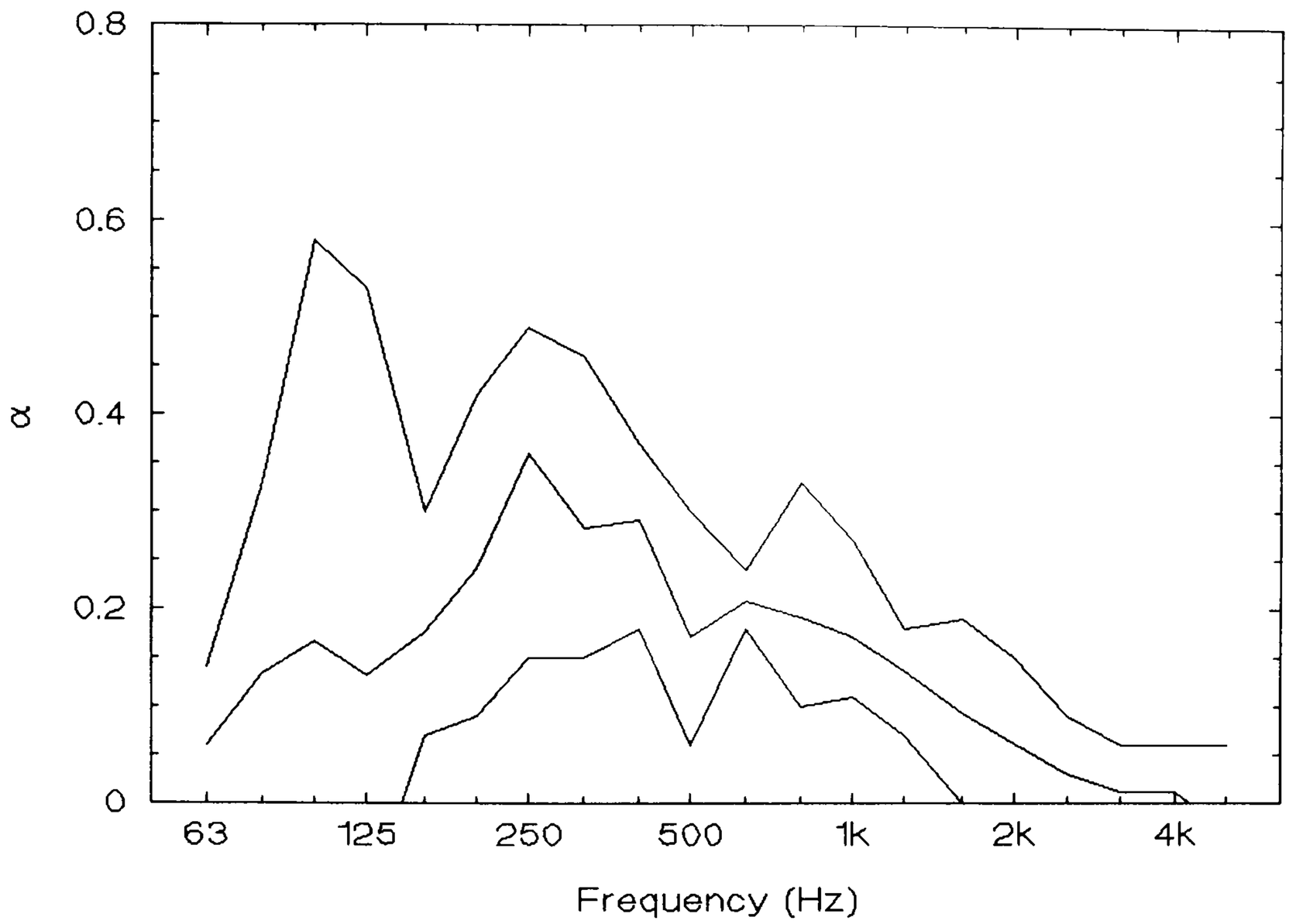

Figure 4.3: Minimum, mean and maximum side area absorption coefficient at each frequency, obtained from measurements on five seat types at 900 mm row spacing.

if an average absorption coefficient is to be used for exposed seating block edges, then the same one might be used for all edges. However, the similarity of the means hides the difference between front and side absorption which can occur at some frequencies for an individual seat type. The front row and side area absorption coefficients for a seat from group 3 are shown in figure 4.4. Though broadly similar, the two coefficients are very different at 80, 315 and 400 Hz.

Figure 4.4 also shows a typical example of the magnitude of the standard error calculated for side area absorption coefficients. According to equation (2.6), the

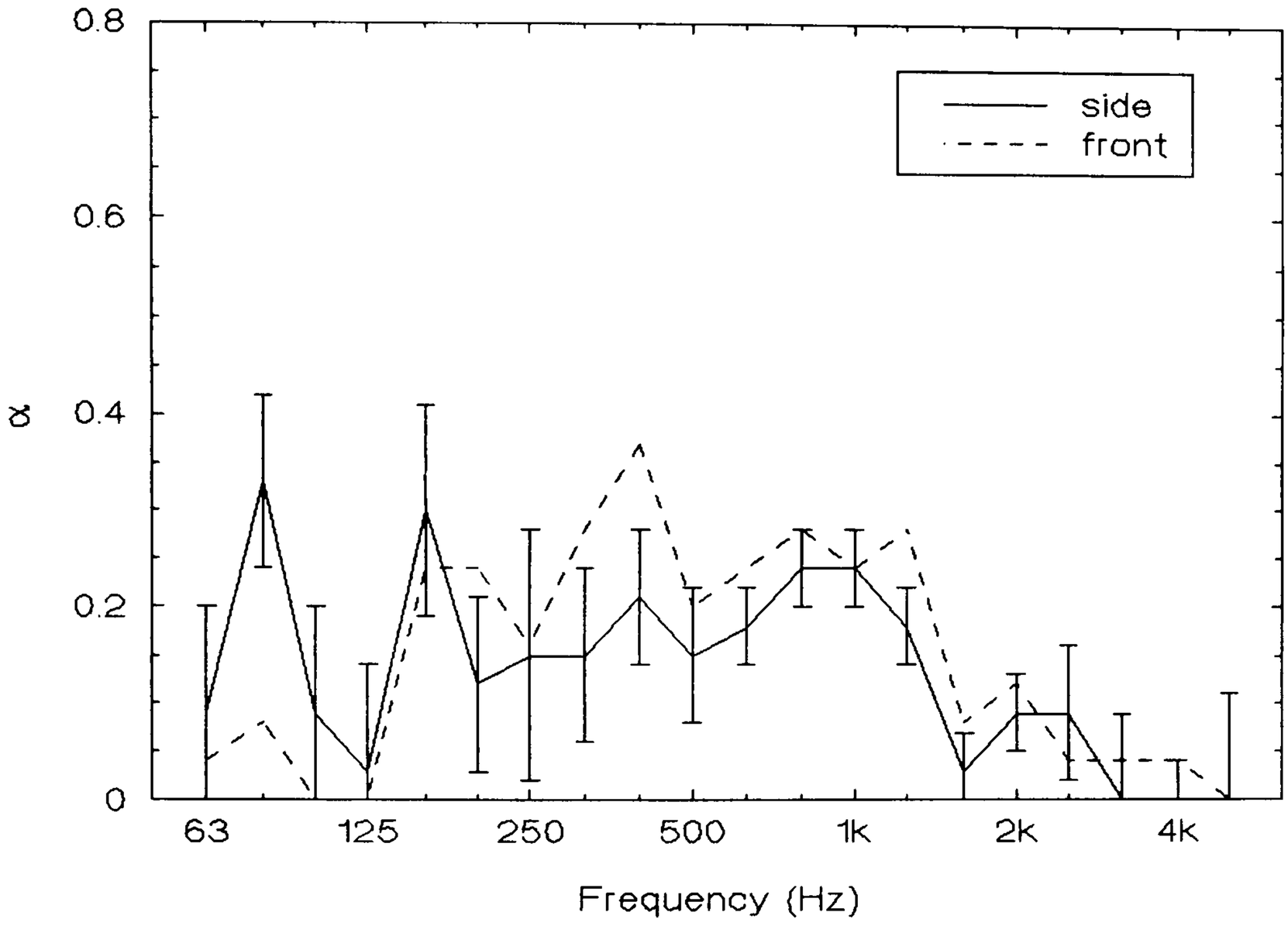

Figure 4.4: Front row and side area absorption coefficients for seat type B1 at 900 mm row spacing.

standard error is found from

$$e_s = \sqrt{e_2^2 + e_p^2}\ \frac{S_p}{S_s} \qquad (4.8)$$

where e refers to a standard error and the other symbols and subscripts are the same as in equation (2.6). This error is considerably larger than that for a single absorption measurement made in the ISO reverberation chamber. The size of the uncertainty should be reduced by using a smaller array of seats for the measurement of α_f and α_s, so that exposing an edge makes a bigger difference to the measured total absorption. Most of the data presented here used a standard

array of four rows of six chairs, so that the more important α_p would be as accurate as possible.

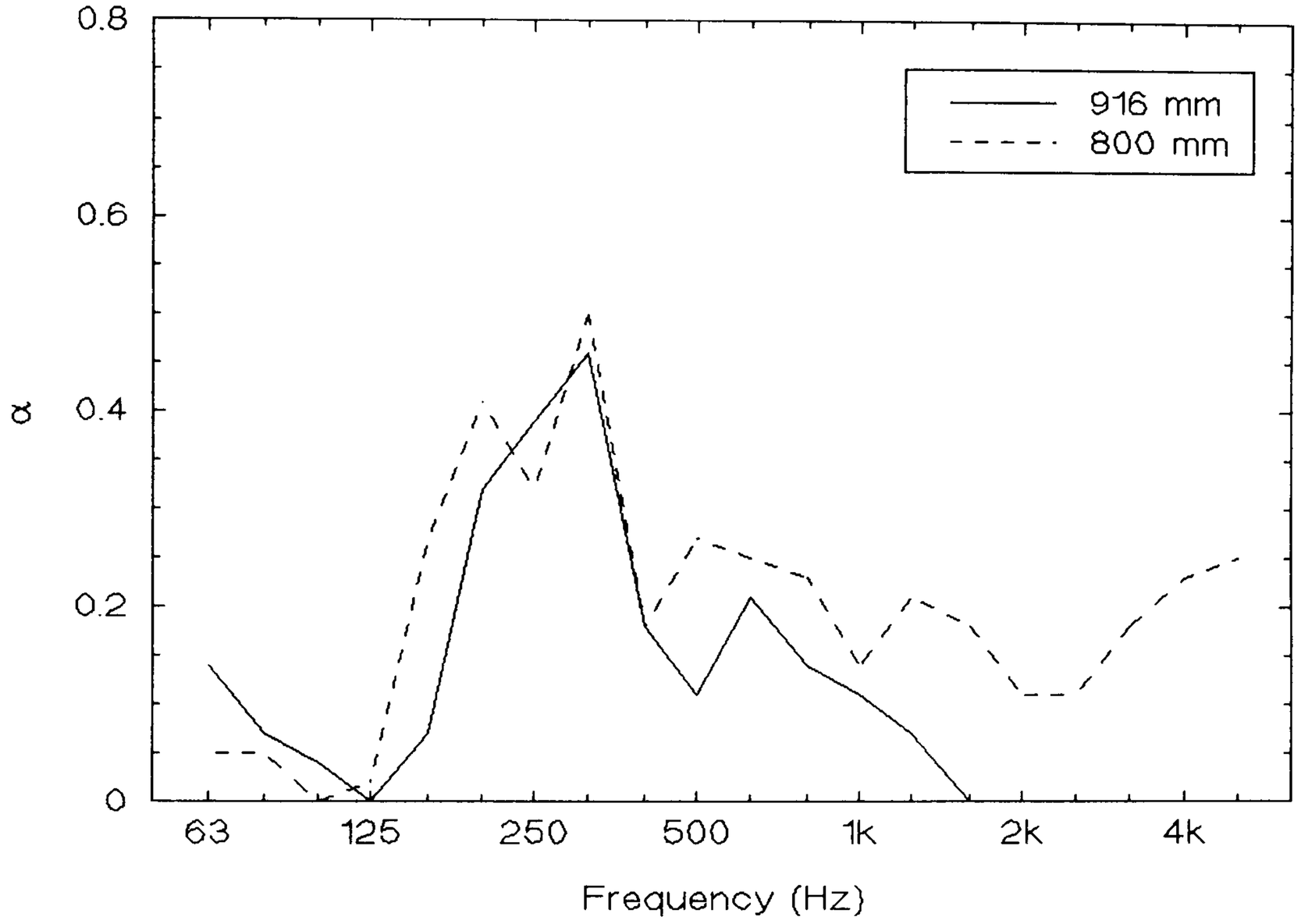

Figure 4.5: Side area absorption coefficient of seat type A at two different row spacings.

It was also found that α_s varies with the row spacing of the test array of seats. This happens in the same manner as the variation of the absorption coefficient of the plan area of the seats, α_p, with row spacing. Increasing the row spacing exposes more absorbing surface due to a decrease in mutual shading by individual chairs. Thus an increase in total absorption is measured, but the area to which the absorption is attributed increases more, so that its absorption coefficient tends to

decrease. Figure 4.5 contains side area absorption data for a well-upholstered theatre seat obtained from measurements at 800 and 900 mm row spacings.

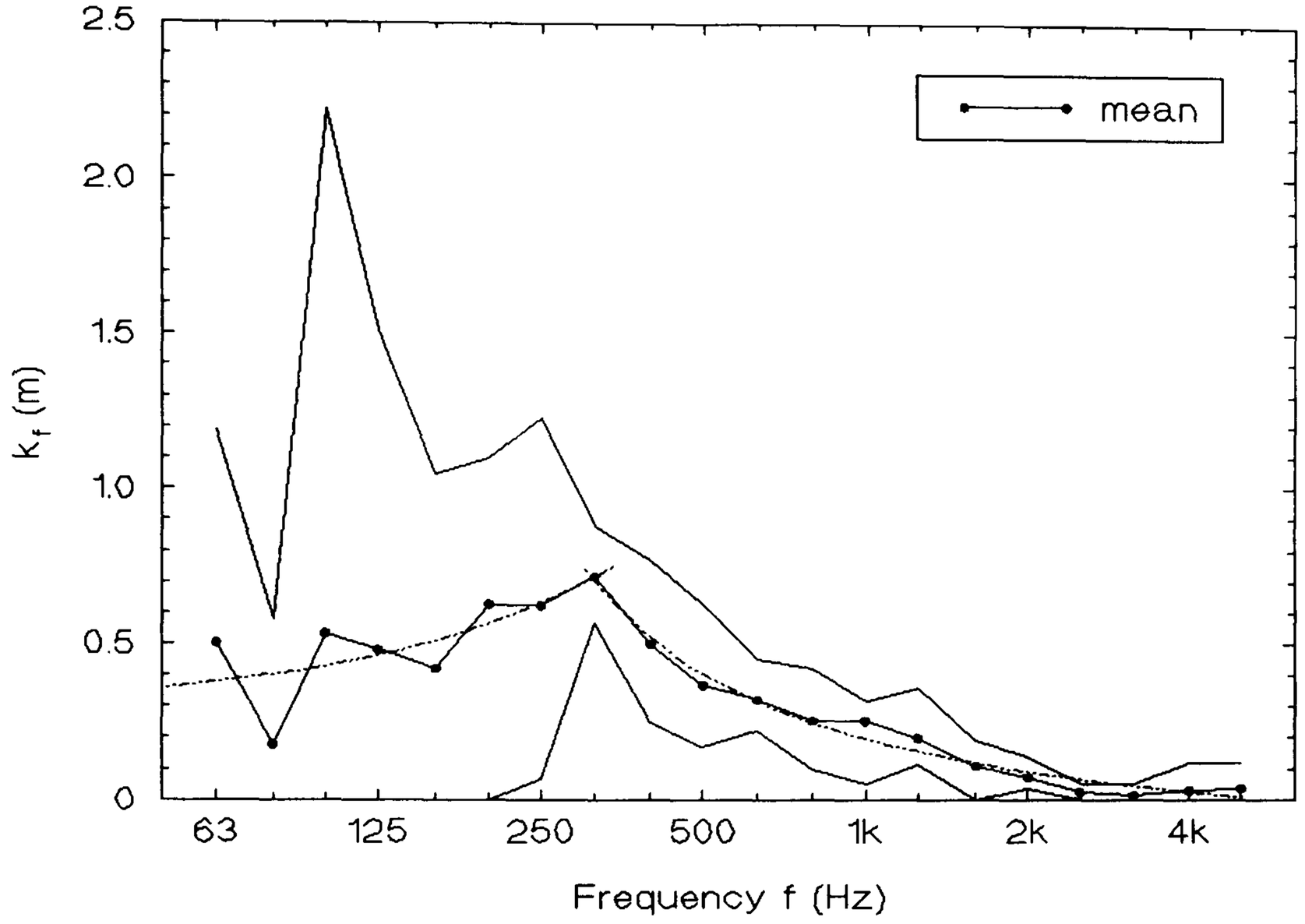

Figure 4.6: Minimum, mean and maximum edge correction strip widths at each frequency for the exposed front row of seven different seat types.

4.2.2 Calculations of Front Row and Side Area Correction Strip Widths, k_f and k_s

The edge correction strip widths corresponding to the data in figures 4.2 and 4.3 have been calculated according to equations (2.12) and (2.13), and they are presented in figures 4.6 and 4.7. It is apparent from figures 4.1 - 4.5 that the typical absorption coefficient of an exposed edge of a seating block is not very similar to the absorption coefficient of its plan area. The strip widths are consequently far from being constant with frequency, in the manner assumed by Beranek.

If an approximation is desired, both k_f and k_s may be estimated by a linear fit at low frequencies, and an inverse logarithmic one at mid and high frequencies, as shown. In figure 4.6 the fitted line is given by

$$k_f = \begin{cases} 0.00136f + 0.291 & (f:\ 63 - 315\ Hz) \\ \dfrac{0.419}{\log(0.0088f)} - 0.247 & (f:\ 315 - 5000\ Hz) \end{cases} \qquad (4.9)$$

and in figure 4.7 by

$$k_s = \begin{cases} 0.00262f + 0.119 & (f:\ 63 - 250\ Hz) \\ \dfrac{0.491}{\log(0.0124f)} - 0.285 & (f:\ 250 - 5000\ Hz) \end{cases} \qquad (4.10)$$

Because of the range of widths in figures 4.6 and 4.7, however, any use of the mean or approximate fits could result in substantial errors for a particular seat type, particularly at low frequencies. If a frequency-constant figure is insisted upon, then 0.5 m seems a better choice than 1 m. We might still expect this to introduce quite large errors into the prediction of auditorium reverberation times, however. Consider the following example: a 2000 seat hall where the seats are divided into 10 blocks, each composed of 10 rows of 20 seats (for simplicity). Each seat is 0.5 m wide and set at 0.9 m row spacing. If the seats are well-upholstered and occupied, then at 5 kHz the absorption coefficient of their plan area can be assumed to be 1.0. The total absorption of all the seating is (20 x 0.5) x (10 x 0.9) x 10 x 1.0 = 900 m^2. Now assume that only one side of each block is exposed to the sound field (a conservative assumption), and that k_s = 0.5 m at all frequencies.

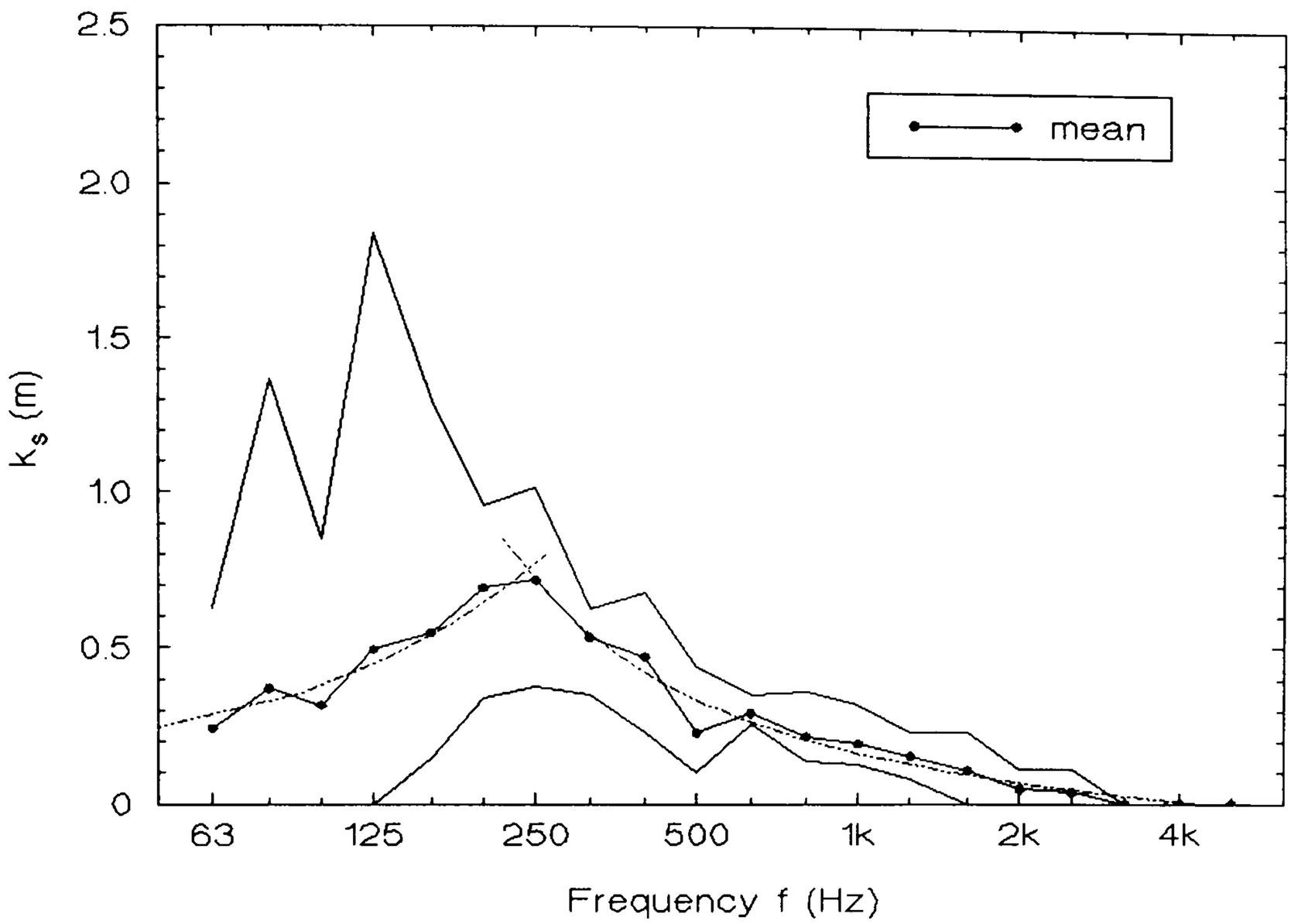

Figure 4.7: Minimum, mean and maximum edge correction strip widths at each frequency for the exposed side area of five different seat types.

Then, at 5 kHz, we would calculate an extra total absorption for all the seat blocks of (10 x 0.9) x 10 x 1.0 x 0.5 = 45 m^2. But, in figure 4.7, the average value of k_s at 5 kHz is 0. Hence, the use of a 0.5 m strip width at all frequencies might well introduce a 5% error into a RT prediction. If a 1 m width were used, the error would be 10%. If this error acted in the same direction as all the other measurement errors involved, then even larger errors might result.

The illustration above is quite conservative. A worst case might be the same auditorium, except that both sides of every seat block are exposed. Seat G2 is used, which produced the k_s = 1.84 m point at 125 Hz in figure 4.7. If the 0.5 m strip

width is again assumed here, then we under-predict the total absorption present by 27%. Of course, the many uncertainties present in an auditorium RT calculation will be quite likely to cancel, and the seat used would probably be closer to the mean. A 5 - 10% error does seem quite plausible, however, so it must be concluded that it is far better to measure the side and front area absorption of a sample of seats rather than rely on a frequency-constant edge correction.

The question of how to treat aisles, as opposed to completely exposed sides, still remains. On the whole, if an aisle is one metre wide, then it seems correct to say that the seats on either side are not fully exposed, due to shading from the seats on the opposite side. If the aisle is carpeted, as it usually is, then sound energy reflected from the floor onto the seats should be less than that encountered in the reverberation chamber. Both these effects would tend to reduce the absorbing power of the aisle seats, but both will probably be frequency-dependent.

Chapter 5

Comparisons between Seating Absorption Measurements in a Reverberation Chamber and in Auditoria

The second part of the exercise to validate the barrier method of measuring seating absorption was a programme of measurements in auditoria. In order that accurate measurements of the *in-situ* absorption coefficient of the seating could be made, it was necessary to measure the RT in the unoccupied hall with all the seats present, and again with as many of the seats removed as possible. This absorption coefficient would then be compared with those from many measurements of a sample of the same seats in the reverberation chamber. Over a 28 month period, it was possible to perform all these measurements for nine halls. Some were multipurpose halls in which a significant portion of the seating could be removed; others were newly built or refurbished. Data was also collected for one of the halls in an occupied condition. Use was also made of data with and without seats present in one hall (C) obtained earlier by Subagio (1986), the author's predecessor in the Department of Applied Acoustics. With new reverberation chamber measurements on the seats from this hall, a data set for one occupied and ten unoccupied halls was available. Figure 5.1 shows photographs of the typical measurement conditions in hall D1.

Figure 5.1: The conditions in hall D1 for RT measurements (top) with the seats installed and (bottom) with them all removed.


EXIT
EXIT

5.1 An Overview of the Ten Halls

Table 5.1 lists the basic geometrical data for the halls, along with their mid-frequency unoccupied RT with all the seats present, T_{mid}. T_{mid} is the average of the RTs in the 500 and 1000 Hz octave bands. Three categories are given for the hall usage: concert, multipurpose or theatre. The halls are sorted according to seating capacity, N_t. N_m is the number of seats that were measured; i.e. the number that could be removed from a hall or the number that were installed if the hall was being built or refurbished. S_{pa} is the total plan area of the N_m seats, with no edge corrections. S_{sa} is the total area of the sides of all the blocks of seats comprising N_m which are exposed to the sound field. For an aisle between two blocks of seats only the exposed area on one side is counted. Similarly, S_{fa} is the total area of the front rows of all the blocks of seats comprising N_m which are exposed to the sound field. If the front row of a balcony block was obscured by a balcony front, then it was not counted for S_{fa}. N_b is the number of balconies.

The table shows that a variety of hall types were used. The only large, modern concert hall was G, which was in the process of construction during this project. The other hall built from new was L, a theatre with a very large flytower which seemed almost fully coupled to the auditorium space (hence the rather large volume per seat in this hall). Several attempts were made to include in the project other halls in the process of construction. However, for economic reasons it is unusual for the seating to be installed in a hall in one short period, with no other substantial construction changes occurring in the meantime. Because this condition was a prerequisite for measuring the absorption of the seating, several *in-situ*

measurements had to be abandoned. Bradley (1992) has complained of the same problem. Arranging half an hour of complete silence was another difficulty. In one project which had a 24 hour construction schedule, this was deemed to be economically unviable.

Hall	Use*	N_t	N_m	V (m^3)	T_{mid} (s)	S_{pa} (m^2)	S_{sa} (m^2)	S_{fa} (m^2)	N_b
G	c	2500	2500	28750	1.97	1386	170	14	1
B1	c/mp	1811	1019	10929	1.65	441	68	40	1
H	c/mp	1150	498	9571	2.02	177	29	25	2
C	mp	≈1000	616	14543	1.98	318	56	17	1
D2	t	900	734	3007	0.88	301	45	5	2
B2	c	702	468	6627	2.13	208	26	25	0
L	t	700	700	12290	2.21	340	50	15	0
O	mp	669	669	8271	1.46	256	44	14	0
M	mp	624	241	1538	0.67	202	15	14	0
D1	t	514	514	2488	0.86	242	62	12	1

Table 5.1: Some geometrical data for the ten halls.

*(c = concert hall, mp = multipurpose hall and t = theatre.)

The second theatre included was D, which underwent an extensive renovation. This involved extending the volume and seating capacity and changing the seating and much of the rest of the interior decor. Four sets of RT measurements were made in this hall, immediately before and after the removal of the old seats, and immediately before and after the installation of the new ones. Because the hall had changed substantially between the two sets, they were counted as separate comparisons, as if they were two different halls D1 and D2. For all the measurements in this hall, the flytower and much of the stage was closed off behind a heavy fire curtain, leaving the single acoustic space of the auditorium.

The halls B1 and H share many similarities, as Victorian designs. Though both these halls are very suitable for the serious classical music sometimes played in them, they are furnished with upholstered free-standing stalls seats to allow a wide range of other uses. Another original Victorian hall, B2, was included but this had been the subject of extensive redesign and refurbishment after being gutted by a fire. Though the stalls seats in this hall were also removable, they were of the heavily-upholstered type often found in dedicated concert halls.

Finally, three modern multipurpose halls were included: C, O and M. O and M were relatively small with quite lightly-upholstered free-standing seats. The seats from hall C were also quite lightly-upholstered, and were fixed to retractable bleachers.

Eight of the halls were rectangular or square in plan. The exceptions were the two new halls, G and L. The plan of the concert hall G was a roughly oval shape made up of eight straight lines. The balcony in this hall extended completely around its plan, so that about one eighth of the total seating capacity was behind the front of the stage. The new theatre, L, is fan-shaped with no balcony and all of the seating is quite steeply raked (at an average 27°).

5.2 The *In-Situ* Measuring System and Absorption Calculation

To make the comparison between reverberation chamber and auditorium as accurate as possible, the same measuring system was used for both. The same type of loudspeakers and microphones (Brüel & Kjær 4165 ½") were used, and a Norwegian Electronics NE830 real-time analyser was also used in the auditorium. The general procedure was to excite the hall with broadband pink noise generated by the NE830 and radiated simultaneously from two loudspeakers placed at the front corners of the stage. The loudspeakers were tilted back to face into the auditorium volume. Five decays were averaged at each of five microphone positions and the analyser fitted straight lines to the decays from -5 to -35 dB to give RTs in octave bands from 63 to 16000 Hz at each position. The positions were spread throughout the hall volume. Every filtered decay curve was stored so that suspect RT values could be checked later. If the results from any one position exhibited significantly less straight decays than the others, it was excluded from the calculation. In most cases, the RTs from each position could be simply averaged in each frequency band to give a mean reverberation time for the whole auditorium.

As with the reverberation chamber measurements, Sabine's equation (equation (2.17)) was used to calculate the *in-situ* seating absorption coefficient. So that reverberation chamber measurements with and without corrections for side and front area absorption could be tested directly against it, the auditorium absorption coefficient was expressed as the total absorption of the seating divided by its plan area. Where the seating was raked, and hence presented a larger area in the hall than its plan, the plan area was divided by $\cos\gamma$, where γ is the rake angle. This adjustment follows a result of Subagio (1986), that the measured total absorption of raked seating increases with $\cos\gamma$. Thus, to correctly incorporate the effects of side and front absorption, the predicted *in-situ* absorption coefficient α_m had to be calculated from reverberation chamber measurements according to equation (2.10) or (2.14). The ratios of exposed side and front area to plan area (adjusted for any rake) in this equation were then given by the values in table 5.1.

Though considerable efforts were made to ensure that each auditorium remained unchanged between the two RT measurements, it was usually necessary to make some allowance for areas of carpet or curtains being changed. The absorption figures for these were taken from reverberation chamber measurements of similar materials. Since temperature and relative humidity measurements were also made at every auditorium, it was also possible to make any necessary corrections for air absorption at high frequencies. This was done using the most recent air absorption data, due to Bass *et al.* (1990). In the case of some of the multipurpose halls, it was possible to make the "full" and "empty" measurements on the same day, so that nothing significant changed apart from the seats.

5.3 The Comparison Procedure

Once an *in-situ* absorption coefficient had been obtained, reverberation chamber measurements were made on a sample of 24 chairs from the auditorium. Part of the validation exercise was to investigate the effect of combinations of several laboratory parameters (row spacing, barrier height, etc., as described in section 2.9), so many reverberation chamber absorption coefficients had to be compared with one auditorium measurement for each hall. Some combinations of parameter values were unlikely to form a basis for a reasonable standard laboratory method. For example, if good agreement was obtained between the *in-situ* data and a measurement at a different row spacing with barriers covering the side of the sample only, then this would most likely be a fluke. Since the number of reverberation chamber data sets was in general quite large, however, a measure of objectivity was brought to the first stage of the comparison process by automating it.

Using a computer, each set of reverberation chamber absorption coefficients for every possible combination of parameters was tested against the auditorium measurement and ranked in order of agreement. The criterion was the sum (over frequency) of the squares of the differences between the two error envelopes. Each error envelope was formed by the absorption coefficient ± one standard error. If this total was zero, then the two envelopes overlapped at all frequencies and could not be distinguished at the level of accuracy of the two measurements. The higher the value of the criterion, the worse the agreement between the two

measurements. Appendix B contains the output of the comparison program for a typical hall.

This automated procedure is quite crude. It does not consider how similar the shapes of the two absorption coefficient versus frequency curves are. Particularly at low frequencies, the auditorium absorption coefficient tends to have a much larger standard error than the reverberation chamber one. This means that it is possible to have several low-frequency absorption coefficient curves of quite different shapes which all overlap the error envelope of the auditorium curve. Because of this, once all the data sets had been ranked for all the halls, more subjective comparisons were made by eye.

5.4 Comparison Results

In the automated ranking, for every hall, the data including the "correct" proportion of front and side absorption (α_m from equation (2.14)) was always ranked better than the data for the plan area absorption only (α_p from equation (2.2)). In turn α_p was always ranked considerably better than the traditional method with the seats in the centre of the chamber with no barriers. In most cases, the data from the traditional measurement was ranked last out of all the absorption coefficients compared - the list in Appendix B is an example.

One of the effects of the larger errors at low frequencies was that the correction for pressure doubling in equation (2.7) did not always improve the rank of a corner measurement. When comparisons of graphs were made by eye, though, the

correction seemed warranted. The same results were also observed for the subtraction of low-frequency barrier absorption.

The data for α_m was not always ranked first for a particular hall. With many measurements being compared, there were sometimes a few parameter combinations coming above α_m. Across all ten halls, though, there was one measurement configuration which consistently produced a better agreement than any other:

> A rectangular array of seats was placed in the corner of the chamber at the auditorium row spacing and surrounded by unabsorbent barriers 0.9 m high for unoccupied seats and 1.2 m high for occupied seats. The absorption of the plan area was measured and corrected for pressure doubling. Two more measurements were made, with the barriers covering the side and front of the array only. A separate measurement of low-frequency barrier absorption was subtracted from all the data. α_m was then calculated from equation (2.14).

The following sections discuss the comparison for each hall in detail. In each graph, "large finite" refers to α_m calculated as described above, "infinite" refers to α_p (this is not α_∞ because it will include diffraction at two edges), and "small" refers to the traditional method with the array in the centre of the chamber with no barriers.

5.4.1 The Concert Halls B2 and G

Figure 5.2 shows the comparison for hall B2. As expected, the auditorium absorption coefficient lies between the reverberation chamber data for the "infinite" configuration (which includes no side area absorption) and the "small" configuration (which includes too much). It is quite well matched by the "large finite" curve.

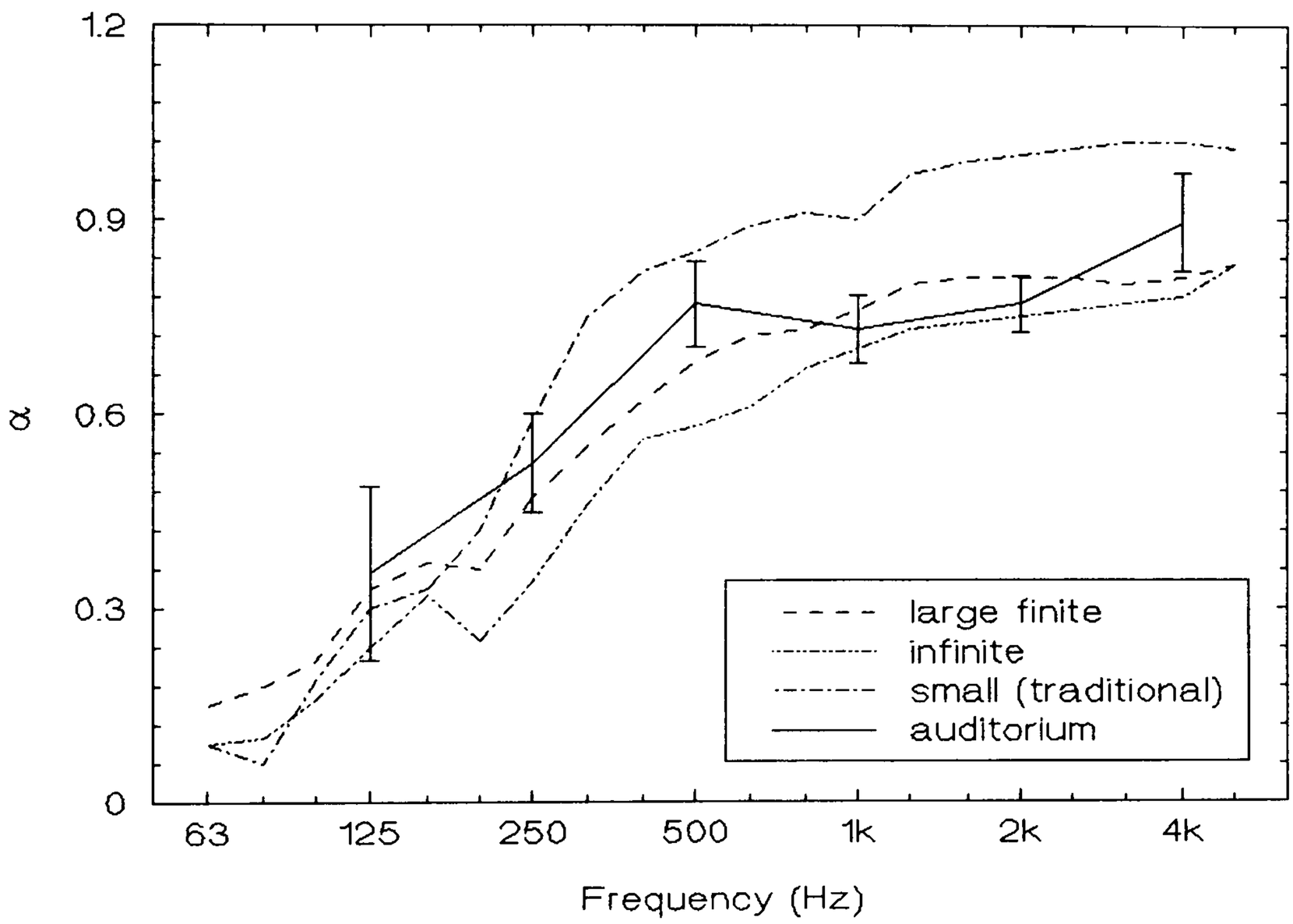

Figure 5.2: Comparison of three reverberation chamber measurements of the absorption coefficient of seats from hall B2 with an *in-situ* auditorium measurement.

The agreement is not perfect, however. Nothing else changed in this hall between RT measurements, so there should be no error in not accounting for other absorption present. The extent of random error is covered by the standard error

shown for the auditorium curve. An envelope of ± one standard error only gives a confidence limit of 67%, so one cannot be certain that the mismatch at 500 Hz is not due to random error. Nevertheless, it is worth investigating. If the difference in absorption coefficients is real, then the most likely cause is a difference between the diffusivity of the sound fields in the reverberation chamber and the auditorium. Such a difference would not be limited to auditoria alone, of course: most "normal" rooms do not achieve the state of diffusion of an ISO chamber. This was one of the reasons why Gomperts (1965) rejected the concept of predicting the absorptive effect of an object in a "normal" room from a sample measured in a diffuse field. Many others on the other hand, notably Kosten (1960), aver that it is better to use a standard sound field for the laboratory method and attempt corrections for non-diffuse conditions.

Kleiner *et al.* (1990) are of the opinion that sound fields in auditoria differ mainly from those in reverberation chambers in having a higher proportion of sound energy travelling laterally, even in the reverberant field, because most of the floor is covered with the highly absorbent audience. If this is so, then the absorbing power of the exposed sides of the seating blocks should be higher in the auditorium. This suggests that in calculating α_m, the absorption coefficient of the front and sides should be increased by some unknown factor, and the absorption coefficient of the plan area reduced by a similar amount. There is some evidence to support this in hall B2 from the graphs of average front row and side area absorption coefficient in figures 4.2 and 4.3. These have a low to mid-frequency peak, so that increasing

the proportion of side area absorption in α_m would tend to raise it at 250 and 500 Hz, thus improving the agreement with the auditorium data.

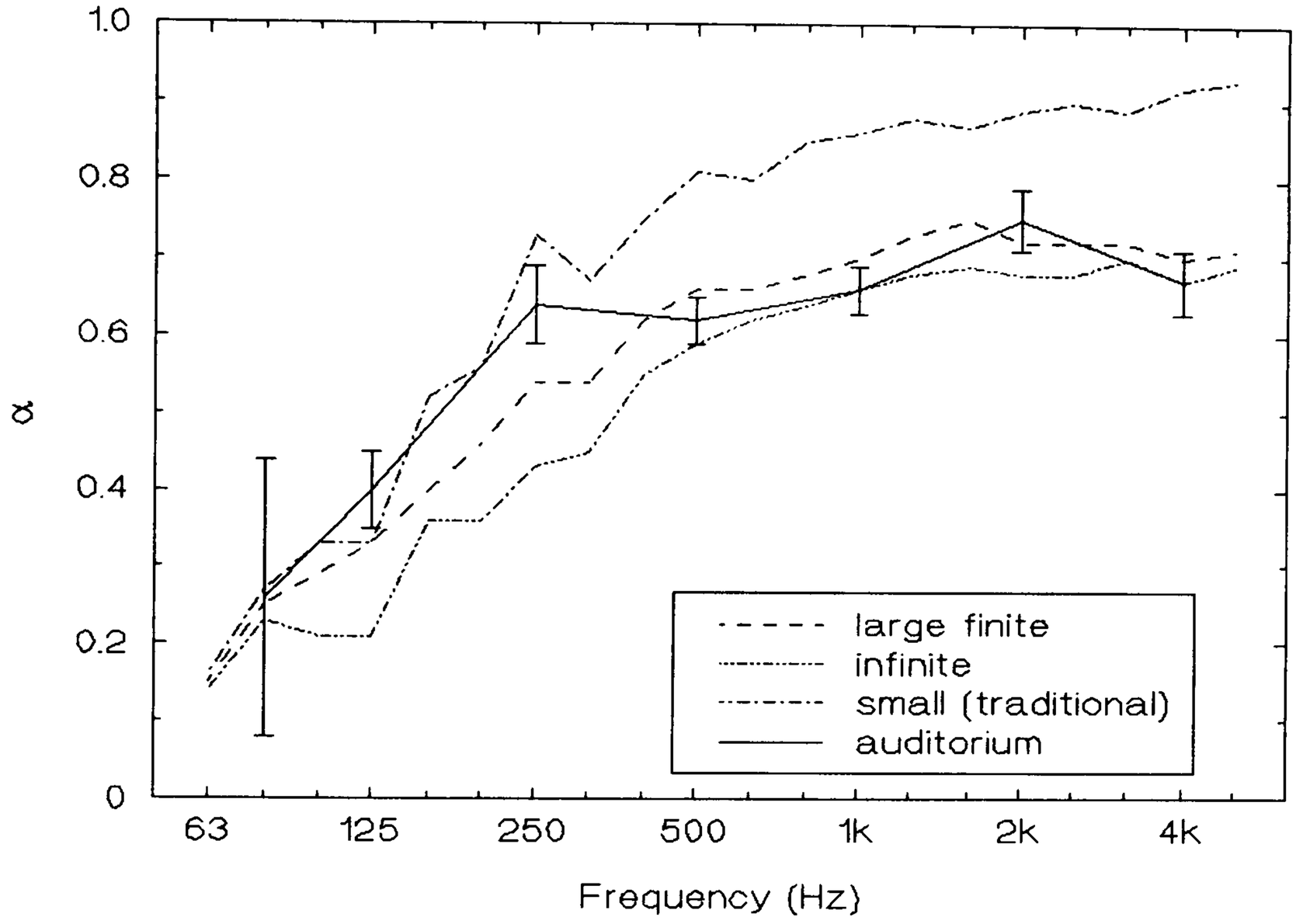

Figure 5.3: Comparison of three reverberation chamber measurements of the absorption coefficient of seats from hall G with an *in-situ* auditorium measurement.

Figure 5.3 shows the comparison for hall G, the large modern concert hall. Again, the auditorium absorption coefficient lies between the "infinite" and "small" measurements. Overall, the "large finite" data is the best match. At high frequencies, the traditional measurement has significantly overestimated the absorption in the hall. The measurement was performed with a 24 seat sample; with the smaller samples suggested in BS 3638: 1987, the excess could be even

greater. At low frequencies, particularly 250 Hz, the "large finite" data is significantly lower than the auditorium data. This might have been caused by a lateral energy emphasis in the auditorium as suggested above. However, in this case the seating area had many aisles bounded on both sides by seats. To test whether these should be counted as two exposed side areas or as one, the amount of side area absorption in the calculation was doubled, and the data compared again with the auditorium measurement. For these seats, the side area absorption coefficient of the seats did not follow the simple peak shape of the average characteristic in figure 4.3. It was found that doubling the proportion of side area absorption made the agreement slightly worse. Instead, the high absorption of the auditorium data at low frequencies may be due to extra absorption being added to the hall during seat installation and being wrongly attributed to the seats. Hall G was one of those measured during construction and the finished auditorium included some large areas of wood panelling. Because of the difficulty of policing the construction schedule completely, it is possible that extra panelling was added or that some other interior feature changed during the seat installation. The large areas of panelling are very likely to have contributed low frequency absorption.

Regarding the putative lateral reverberation emphasis, differences between halls may occur because the geometry of the auditorium should have an effect on the emphasis of lateral reverberation. In hall G, the side walls are broken up into large planes forming the oval shape in plan, and these are further subdivided in section by sloping balcony fronts. Large Quadratic Residue Diffuser panels (see Schroeder (1975)) are suspended from the roof along the sides of the auditorium, tilted to

reflect sound onto the audience. These features were adopted to control the *early* lateral field, but they will also affect the spatial distribution of the reverberant field. In contrast, hall B2 is a classical shoebox shape with no large elements breaking up the continuous plane side walls. This form should encourage a higher proportion of lateral reverberant energy not striking the plan area of the audience than does the shape of hall G. The tentative conclusion is that emphasis of lateral energy in the reverberant field may not exist in all concert halls, and that aisles bounded by seating on both sides should probably be treated in general as one exposed side area so that side absorption is not overemphasised.

5.4.2 An Occupied Measurement in Concert Hall G

In this concert hall it was possible to make RT measurements in the occupied auditorium, and to test a sample of the seats occupied in the reverberation chamber. The auditorium measurement was made at a test concert during the opening of the hall. The "occupied" RT was measured in the hall by the direct impulse method using a gun and five simultaneous tape recording positions distributed throughout the auditorium. An attempt was also made to tape record several maximum length sequences in the occupied hall at a low stimulus level. A description of this method of obtaining impulse responses is given in section 6.1: it can retrieve more information at a low signal-to-noise ratio than other methods. Unfortunately, the recording levels at the microphone positions were set at a very low gain in anticipation of possible overload by the gun, so that synchronising the analysis system to the recorded maximum length sequences was impossible. (It is however thought that this method of obtaining an occupied RT in a hall should be

possible without a paying audience having to be completely silent during the test. In a trial experiment in a small non-standard reverberation chamber, impulse responses were obtained from maximum length sequences with and without a background of uncorrelated pink noise. Without the background noise, the signal-to-noise ratio was 40 dB; with it, the ratio was 0 dB. If the response with background noise was averaged 100 times, then the 4 kHz ⅓ octave decay curves calculated from both conditions were within 0.5 dB over the first 24 dB of decay.)

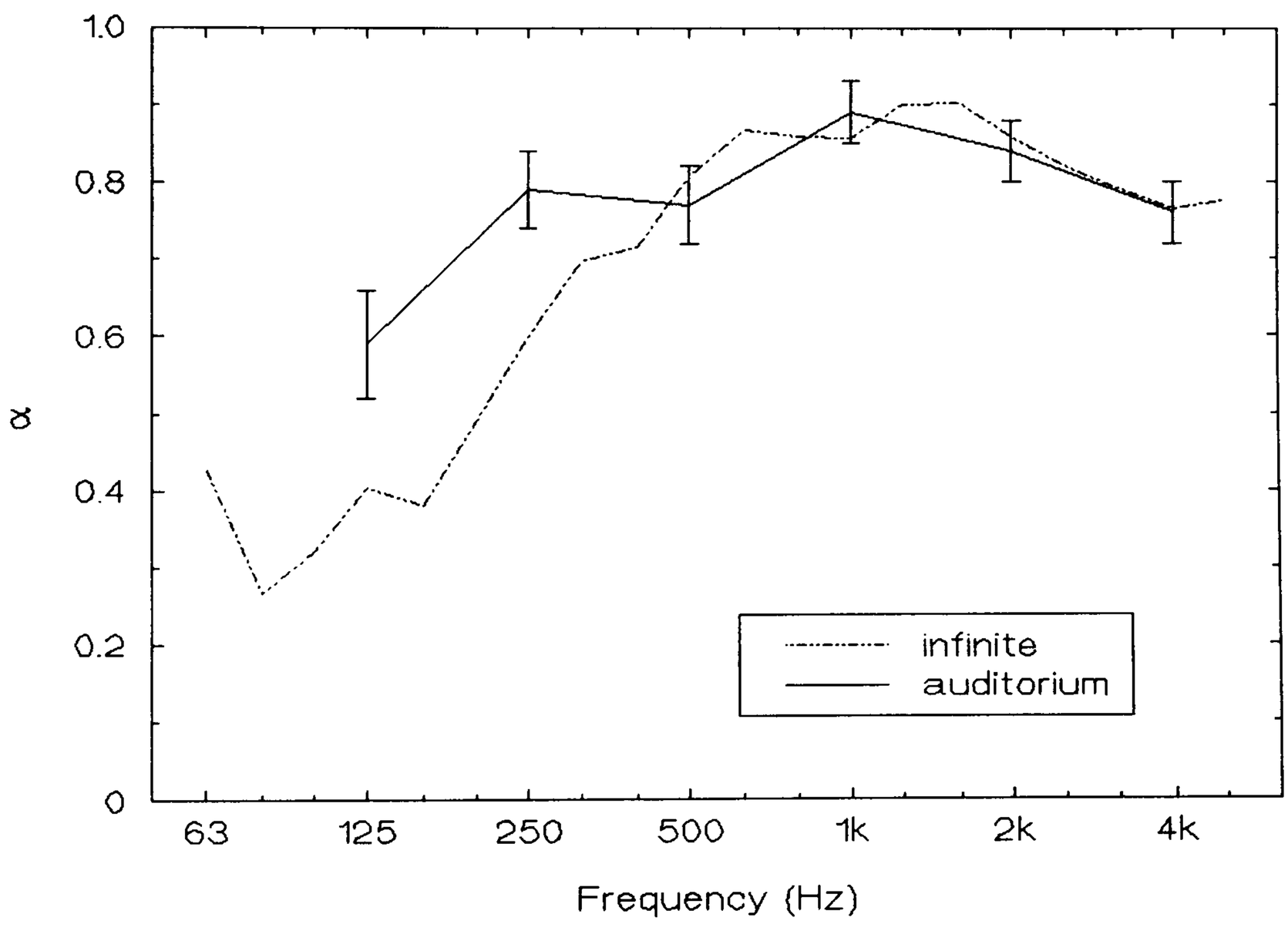

Figure 5.4: Comparison of a reverberation chamber measurement of the absorption coefficient of *occupied* seats from hall G with an *in-situ* auditorium measurement.

The occupied auditorium RT was combined with the RT measured in the hall before any seats were installed to produce the absorption coefficient in figure 5.4. This is compared with a reverberation chamber measurement of 24 occupied seats. Unfortunately, the patience of the 24 test persons in the reverberation chamber was limited to only one measurement. This was done with the sample in the corner of the chamber with both exposed sides covered with 1.2 m high barriers. With only one measurement, corrections for α_f and α_s were not possible. Apart from any diffraction effects, this therefore represents an "infinite" measurement as shown in figure 5.4.

The relationship between the two absorption coefficients in figure 5.4 is very similar to that between the same data for the unoccupied seats in figure 5.3. Because the "infinite" reverberation chamber data does not include any side absorption, it should be below or equal to the auditorium line at all frequencies. In fact, the auditorium absorption seems rather too high at low frequencies, and possibly too low at high frequencies. The extra low frequency absorption will be due to the same problem conjectured for the unoccupied measurement of spurious low-frequency absorption added to the hall. The missing high frequency absorption in the auditorium data is so small it may be due to measurement error. Alternatively, it could be due to a loss of diffusion in the hall when its floor is entirely covered with the highly absorbing audience.

5.4.3 The Concert/Multipurpose Halls B1 and H

The agreement between the "large finite" reverberation chamber data and the auditorium data is very good for hall H, as figure 5.5 shows. As expected, the auditorium line lies between the "infinite" data (which includes no side absorption), and the "small" line (which includes too much side absorption).

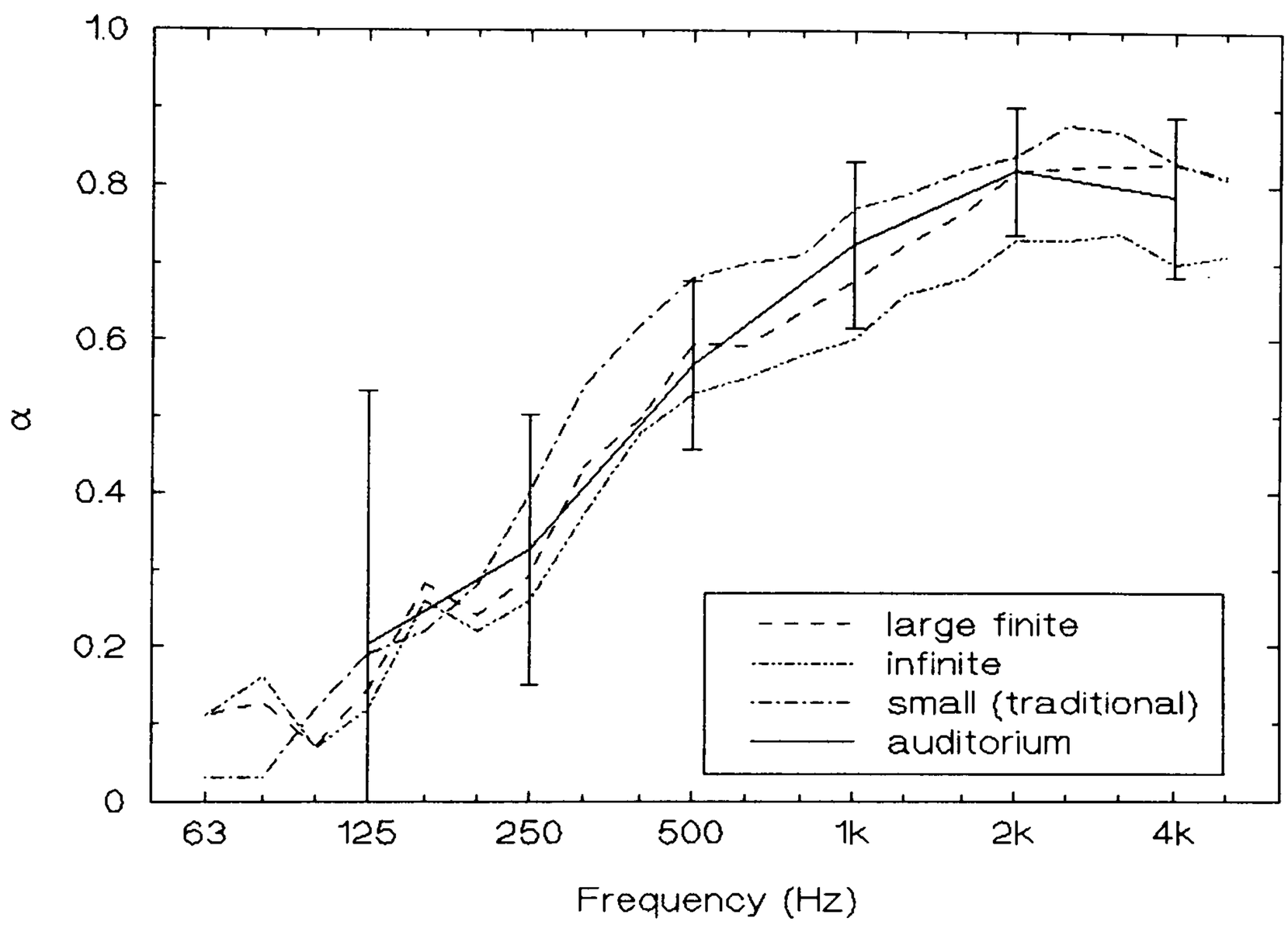

Figure 5.5: Comparison of three reverberation chamber measurements of the absorption coefficient of seats from hall H with an *in-situ* auditorium measurement.

The standard errors estimated for the auditorium data in figure 5.5 are comparatively large. The RTs measured in the hall varied from one microphone position to another considerably. This may be partly due to some of the decays

being corrupted by background noise. The hall is situated in the middle of a town with a busy main road immediately outside. Being Victorian, it does not conform to the high standard of sound insulation found in modern concert halls. Although attempts were made to reject any decays with obvious traffic noise this was not completely possible due to its random and almost continuous nature. The accuracy of the measurement was also compromised by the fact that only 43% of the seats in the hall were removable. Though this still amounted to 498 chairs, less than half the total absorption present would have changed between the two RT measurements. Nevertheless, the reverberation chamber measurement has accurately predicted the average absorption coefficient of the seats in the hall.

For the other large concert/multipurpose auditorium, hall B1, the agreement is good at low and mid frequencies, as shown in figure 5.6. At these frequencies, the auditorium data lies between the extreme reverberation chamber lines, indicating that it is a "sensible" result from a diffuse sound field. At 2 kHz and particularly at 4 kHz, however, the seat absorption in the auditorium is higher than the laboratory measurements. This was one of the measurements made where strips of carpet in the aisles were removed along with the seats. No sample of this carpet was available to measure separately in the reverberation chamber, so a correction was made using a measurement of a typical carpet sample to hand. It may be that this substituted carpet did not absorb high frequency sound as effectively as the material in hall B1.

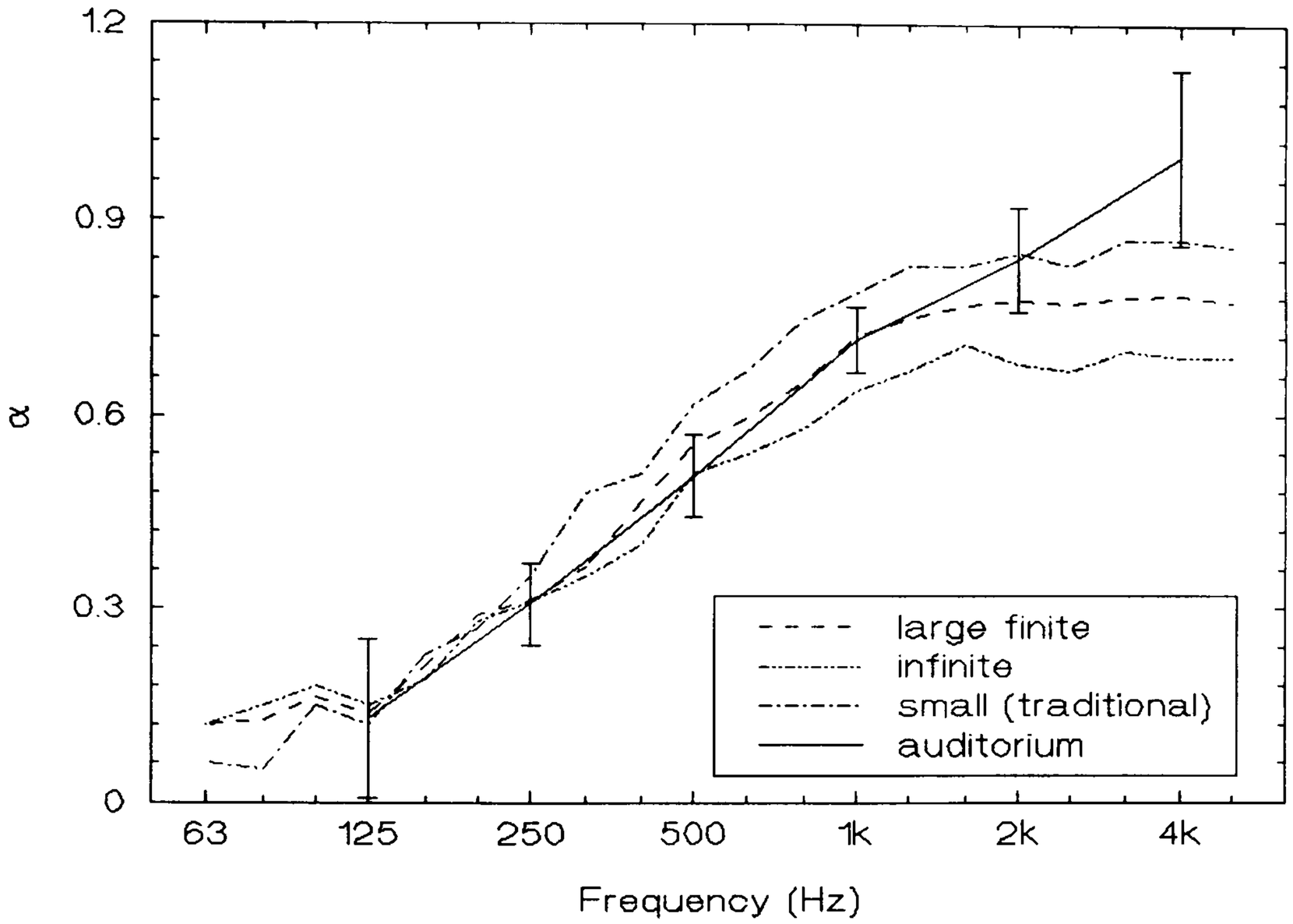

Figure 5.6: Comparison of three reverberation chamber measurements of the absorption coefficient of seats from hall B1 with an *in-situ* auditorium measurement.

5.4.4 The Modern Multipurpose Halls C, O and M

These halls have in common a multipurpose function. As well as, and perhaps partly because of this, they also have in common lightweight chairs and a poor state of diffusion. This has led to problems in predicting the *in-situ* absorption coefficient of the seats in two halls. Nevertheless, in the largest of the three, hall C, the agreement between *in-situ* and reverberation chamber absorption coefficients is quite good up to 2 kHz, as shown in figure 5.7. No reverberation chamber data for the side and front absorption coefficients of these seats was measured, so a "large finite" absorption coefficient cannot be calculated. Because the seats are quite

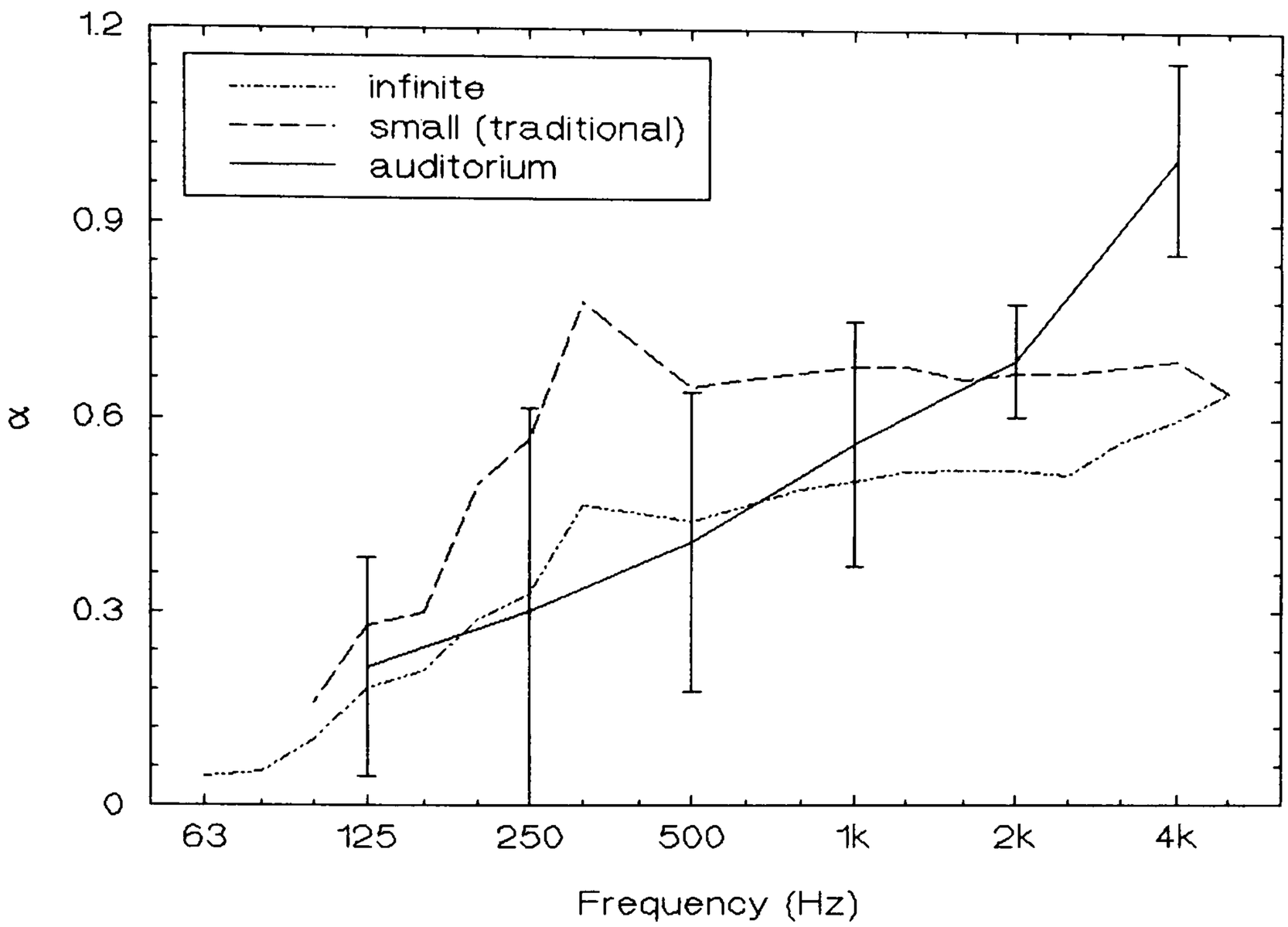

Figure 5.7: Comparison of two reverberation chamber measurements of the absorption coefficient of seats from hall C with an *in-situ* auditorium measurement.

lightly upholstered, and because they are arranged in large blocks in the auditorium, the increase in absorption coefficient due to exposed sides is probably small. Hence a "large finite" line for this hall would not be far above the "infinite" one.

In hall C, the auditorium measurement was complicated by the fact that the folding seats were fixed to retractable bleachers. Since neither could be removed from the hall, the "empty" RT measurement was performed with the seats folded down and the bleachers fully retracted, and the "full" measurement with the bleachers extended and the seats erect. As documented by Subagio (1986), who performed

the auditorium measurements, when the bleachers were extended they were sufficiently far from the side walls to expose an opening at either side leading to the volume under the bleachers. Since these openings were exposed to the reverberant sound field, they were considered totally absorbent at all frequencies. This still leaves a rather high auditorium absorption coefficient at 4 kHz. This is perhaps due to the unfinished surface of the bleachers themselves absorbing energy when extended.

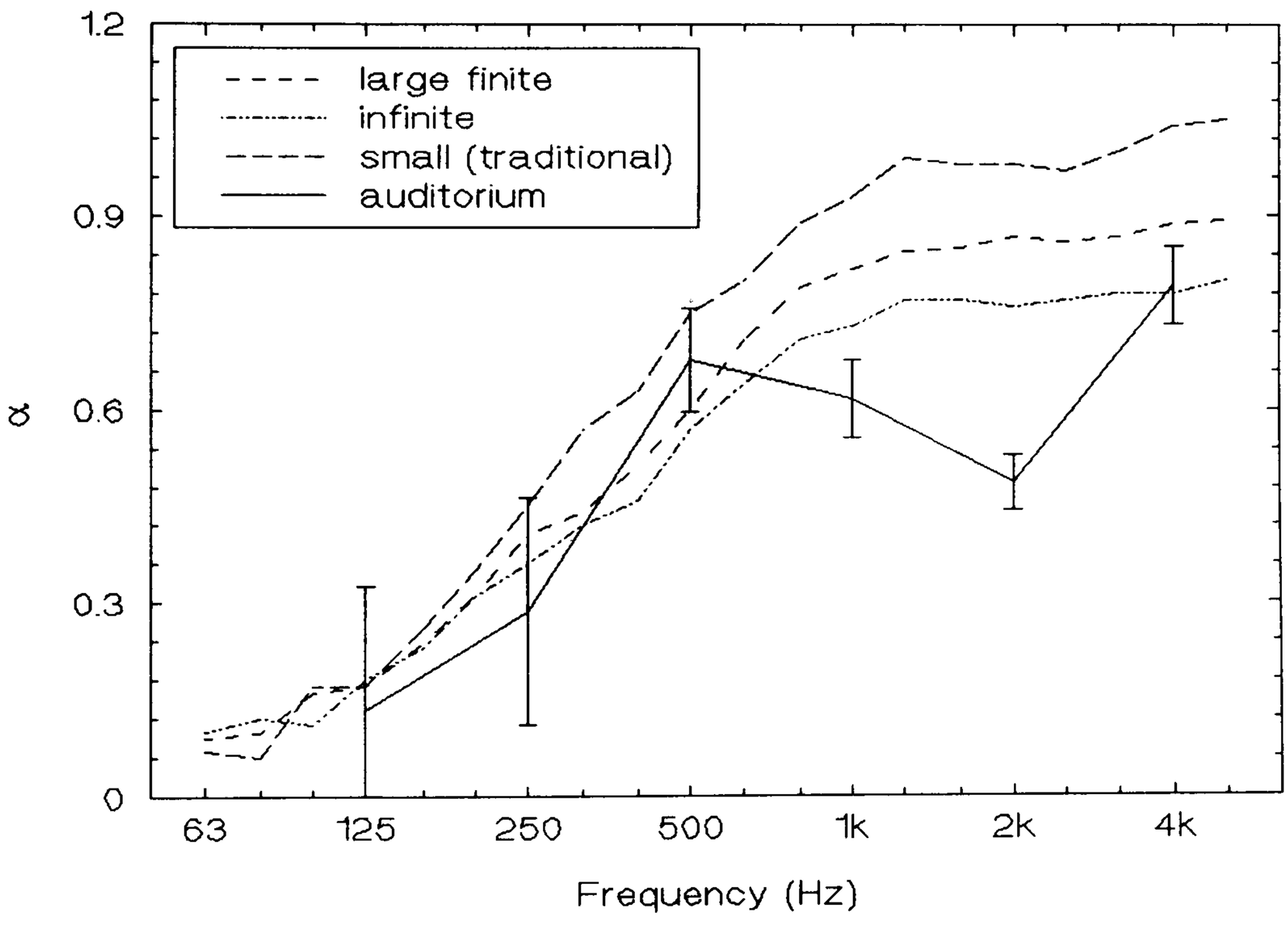

Figure 5.8: Comparison of three reverberation chamber measurements of the absorption coefficient of seats from hall O with an *in-situ* auditorium measurement.

In figure 5.8 the agreement between auditorium and reverberation chamber absorption coefficients for hall O is reasonably good in all frequency bands except 1 and 2 kHz. The same is true of hall M in figure 5.9: in both halls the seats seem to absorb little energy at 2 kHz. Since no reverberation chamber measurements of either seat type exhibit such a dip, it is thought that it must be due to either the auditorium measurement process or some property of both halls. It might be thought that an equipment malfunction was responsible for both cases. This seems unlikely, since the measurements in hall B1 were made between those in M and O, and figure 5.6 shows no such dip in the B1 data. Equally, it is hard to conceive of some spurious absorption present during the "empty" but not the "full" measurements in both halls, which would absorb energy greatly at 2 kHz and not elsewhere.

Instead, it is thought that the dips in figures 5.8 and 5.9 may be due to the sound fields in these halls being so badly diffused at the dip frequency that little sound energy actually strikes the seats. No measurement of the directional distribution of energy in the reverberant field of either hall was made. The evidence for a non-diffuse field comes from the individual decay curves at each measuring position. As can be seen from the mid-frequency curves reproduced in figure 5.10, both halls M and O have some quite badly sagging decays. A way of quantifying the curvature of the decays over the whole auditorium in each frequency band is to examine the difference between the reverberation times T_{15} and T_{30}. These are calculated by fitting the best straight line to the curve between -5 and -20 dB and between -5 and -35 dB respectively. As an index, one might consider the quantity

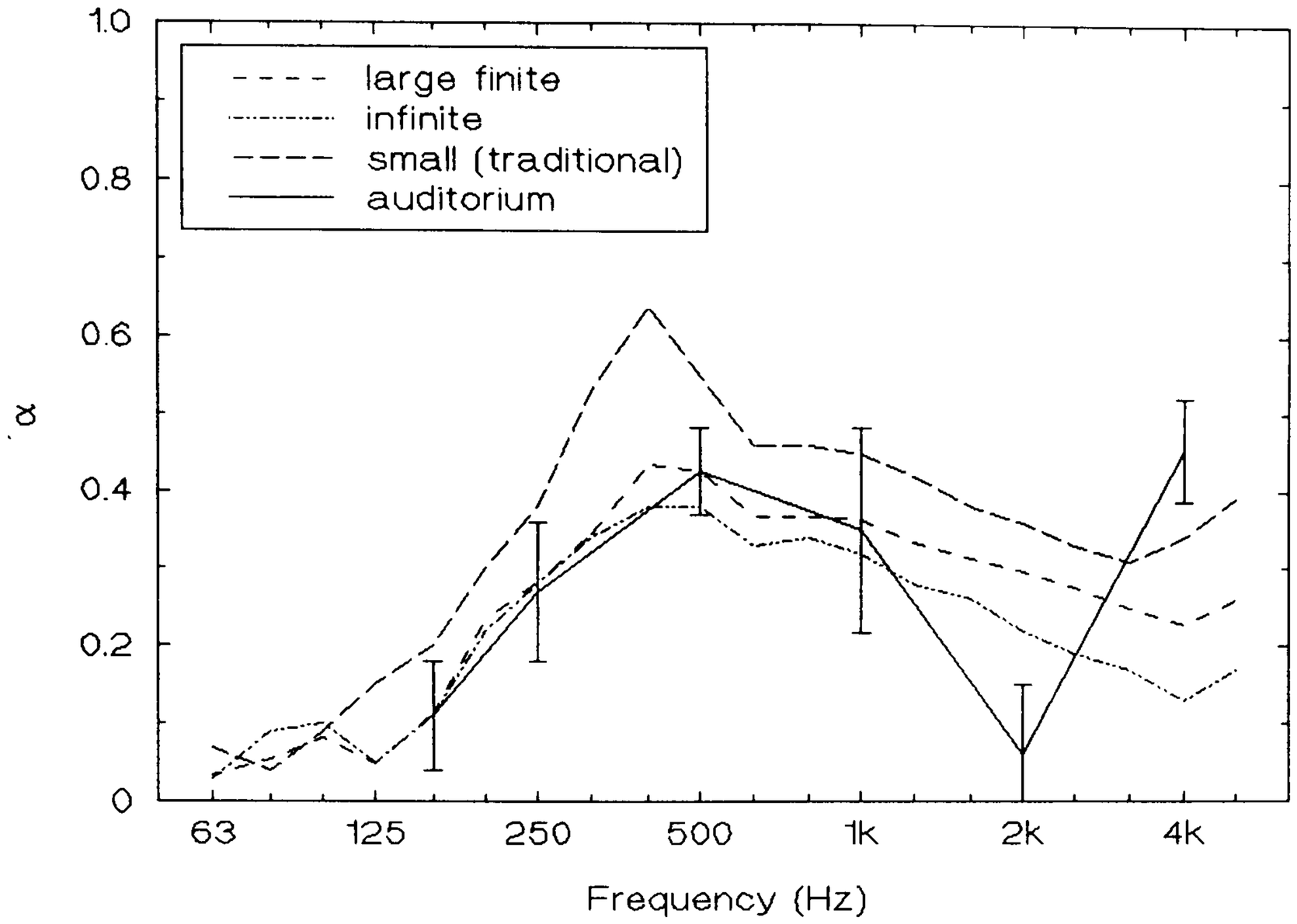

Figure 5.9: Comparison of three reverberation chamber measurements of the absorption coefficient of seats from hall M with an *in-situ* auditorium measurement.

$$\tau = \sum_{i=1}^{m} \frac{100\,(T_{30_i} - T_{15_i})}{m\,T_{30_i}} \qquad (5.1)$$

where m is the number of microphone positions used. τ is thus the percentage decay curve bend averaged across all the measuring positions for a particular frequency band. In a diffuse hall, the decays at some positions might be slightly convex; at others they may be slightly concave; the average bend over all of them (τ) should tend to zero. In a perfectly diffuse space, of course, the decay curves should be perfectly linear. On the other hand, if a hall has badly sagging decay curves, then T_{30} will tend to be longer than T_{15} and τ will be positive.

(a)

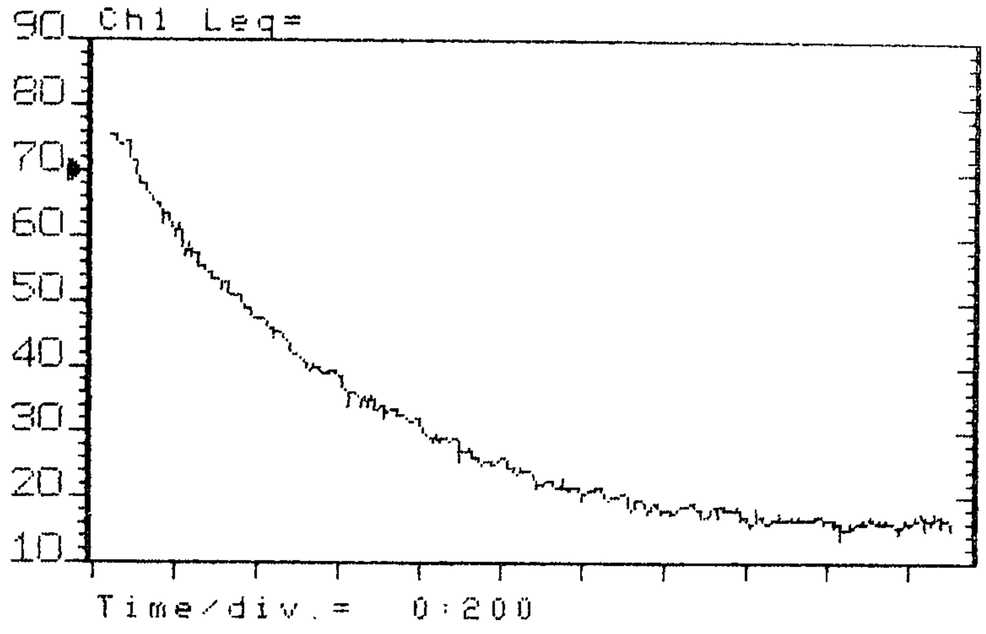

(b)

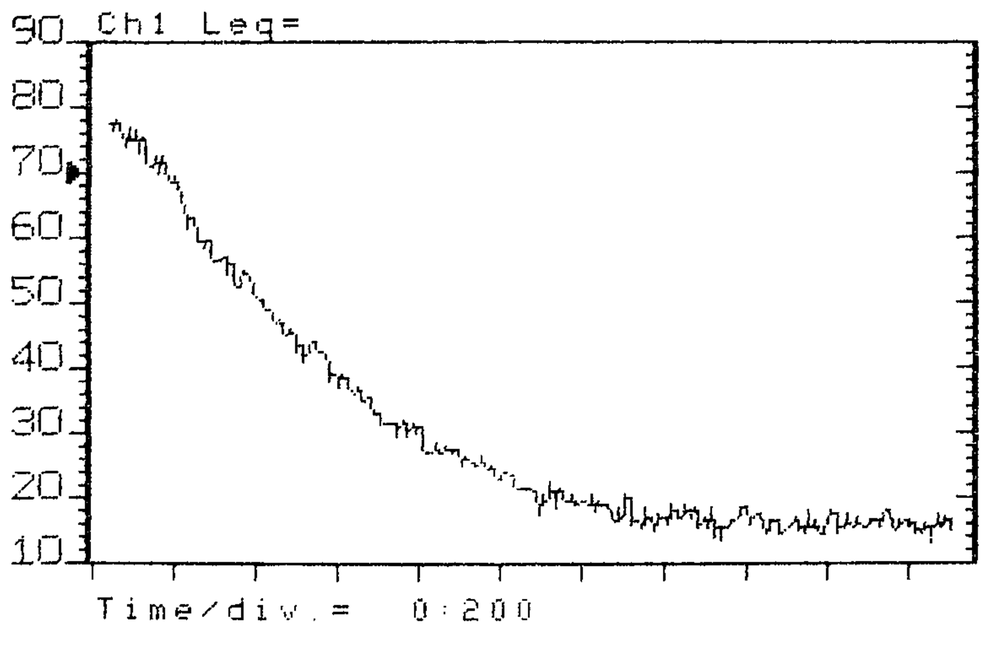

Figure 5.10: Sagging decay curves from (a) hall M in the 2 kHz octave band with the seats removed and (b) hall O in the 1 kHz octave with the seats present.

Figure 5.11 shows that the average bend in the decay curves of hall M is large and positive from 1 - 2 kHz compared with the average bend for the modern concert hall G. This is in the same frequency range as the dip in auditorium absorption coefficient for hall M in figure 5.9. However, the value of τ for hall O is not much larger than that of hall G over the same range, although individual decay curves have strongly non-linear decay patterns.

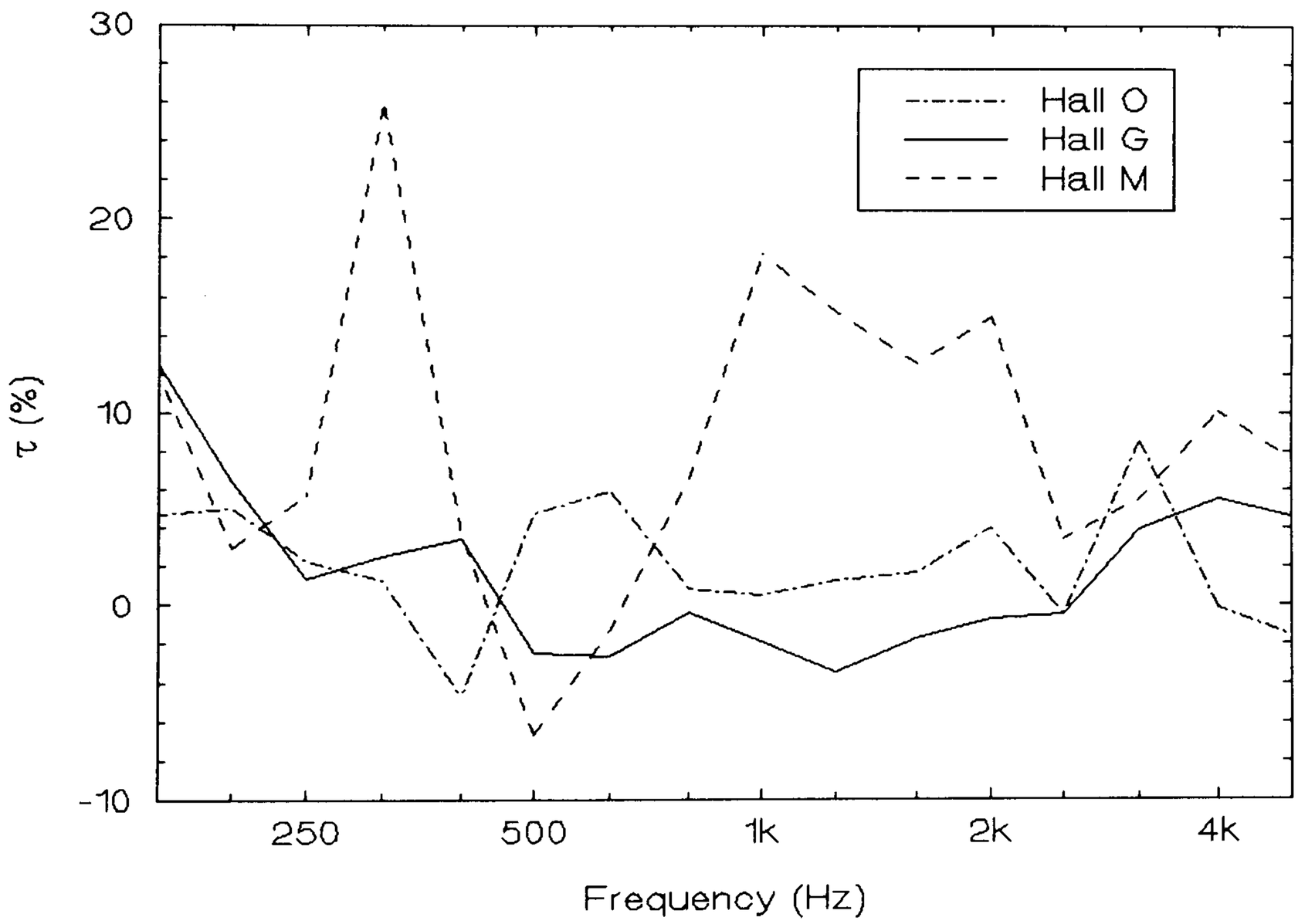

Figure 5.11: Percentage bend τ in decay curves averaged across all measuring positions in three auditoria.

5.4.5 The Theatres D1, D2 and L

In the last group of halls to be investigated, the auditorium calculation is slightly complicated by the problem of the volume of the stagehouse or flytower. Being

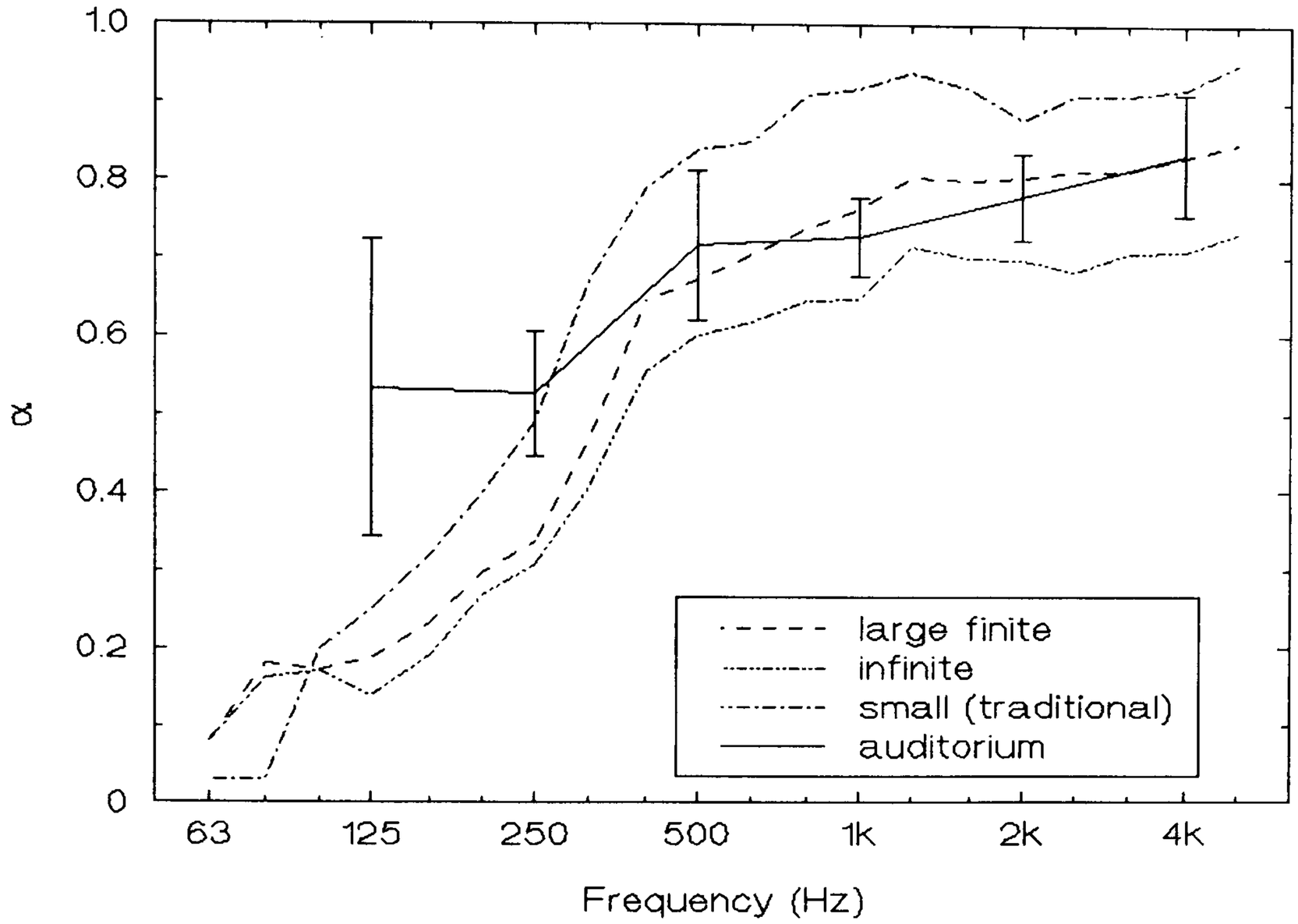

Figure 5.12: Comparison of three reverberation chamber measurements of the absorption coefficient of seats from theatre L with an *in-situ* auditorium measurement.

theatres, all three of these halls have a proscenium arch coupling the volume of the flytower over the stage to the volume of the auditorium where all the seats are installed. The problem was minimised in hall D both before (D1) and after (D2) refurbishment, since the area under the proscenium arch was fairly small and it was covered by a heavy fire curtain during all measurements. It was therefore assumed that the volume of the stagehouse did not play a part in the sound field in the auditorium of hall D. In hall L, conversely, the RT measurements were made during construction. In this theatre, a very large flytower was coupled to the auditorium by a large opening. Since there was no evidence of a dual decay rate

in the recorded decay curves, it was assumed that the coupling between the two spaces was perfect, and the volume of the flytower was included in the absorption calculation. Figure 5.12 shows that this has resulted in the auditorium absorption coefficient calculated for hall L being predicted well by the "large finite" reverberation chamber data for mid and high frequencies. At low frequencies, the auditorium data is well above the reverberation chamber lines. This discrepancy is similar to the one found for hall G, which was also under construction. It is likely that the reason is the same in both cases: additional low-frequency absorption in the form of interior wall panelling being added or changed during seat installation. It is not therefore thought that this discrepancy represents any failure of the reverberation chamber method, but a problem in the validation process.

A very similar comparison graph is found for hall D1 in figure 5.13. Again, the match between the *in-situ* measurement and the "large finite" prediction is very good, except at low frequencies. Since this hall was being extensively renovated during the measurements, this low-frequency discrepancy is also likely to extra absorption being wrongly attributed to the seats. This time, measurements were made before and after all the seats were removed from the theatre for extensive renovation, and it may well be that some interior panelling was removed at the same time.

The final hall comparison is for theatre D2 (D1 after refurbishment) and it appears in figure 5.14. This time, the agreement between the "large finite" data and the *in-situ* measurement is not quite so good. The match is best at mid frequencies; at

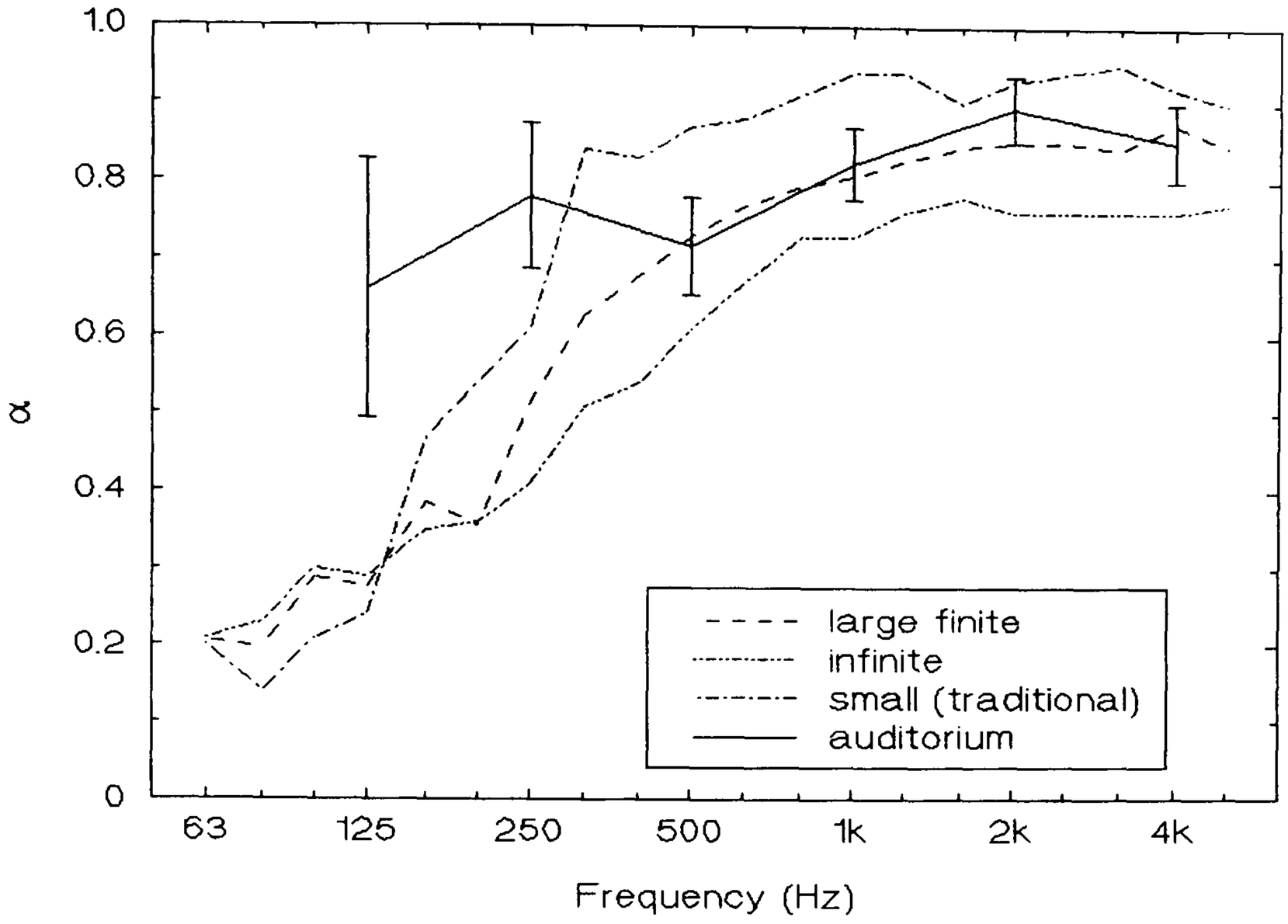

Figure 5.13: Comparison of three reverberation chamber measurements of the absorption coefficient of seats from theatre D1 with an *in-situ* auditorium measurement.

low and high frequencies, the reverberation chamber coefficient is too high. The seats for this theatre were unusual in the large low-frequency absorption coefficient they exhibited in the reverberation chamber. In chapter 3 they were used to investigate low-frequency barrier absorption problems, and their high absorption was attributed to a hollow squab acting as a panel absorber. It was conjectured in chapter 3 that as well as providing low-frequency absorption themselves, the barriers used in the reverberation chamber measurements might also tend to increase the low-frequency absorption of the chairs inside them. Normally, this would not be very noticeable as most types of unoccupied seating do not absorb

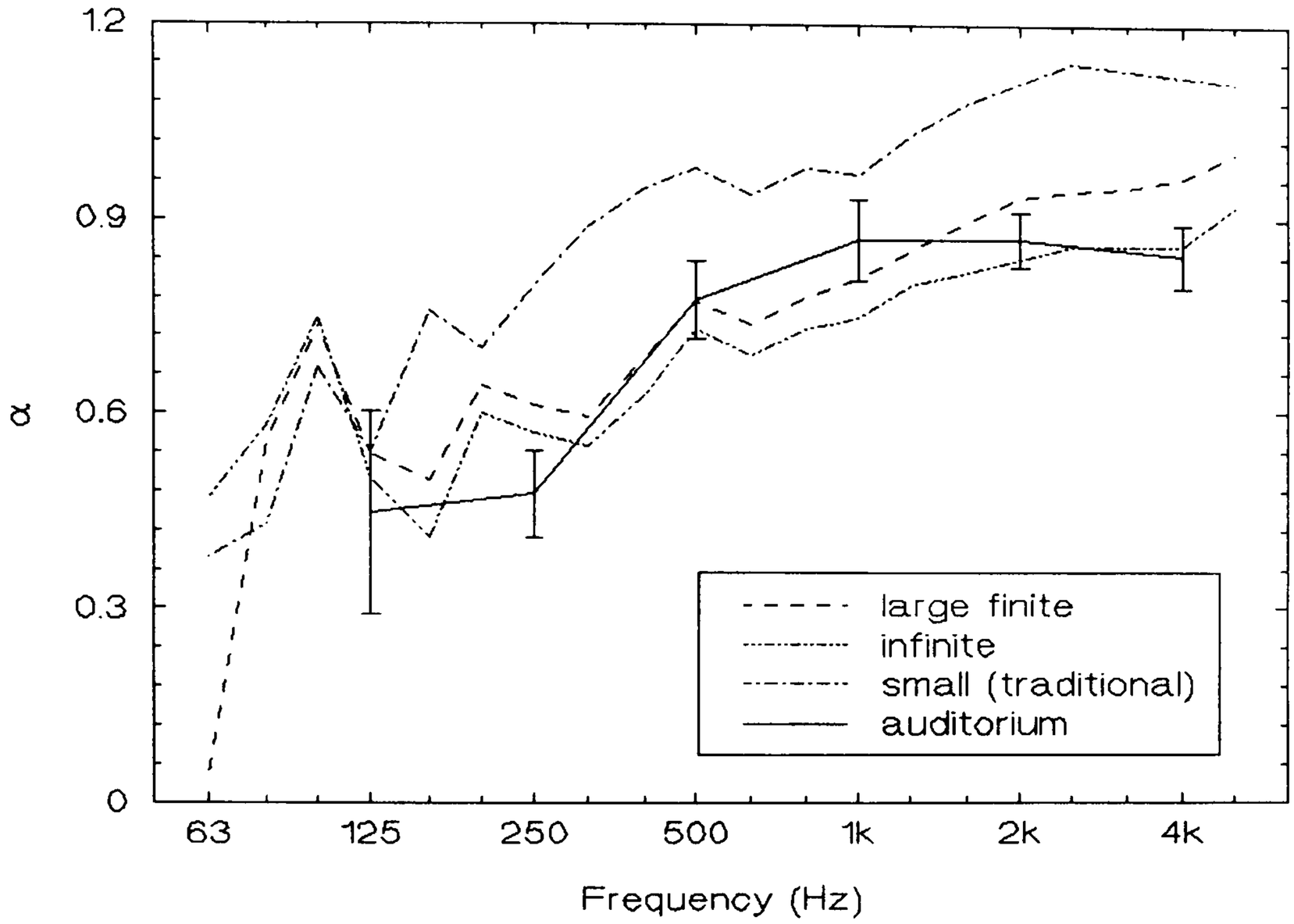

Figure 5.14: Comparison of three reverberation chamber measurements of the absorption coefficient of seats from theatre D2 with an *in-situ* auditorium measurement.

well at low frequencies. In the case of seat D2, however, it may be that even after the reverberation chamber data has had a measurement of the spurious barrier absorption subtracted it still overemphasises the low-frequency absorption of the seats themselves.

At high frequencies, the *in-situ* absorption coefficient is slightly lower than the "large finite" calculation, and this may be due to the auditorium field being less diffuse at high frequencies then that in the reverberation chamber. From table 5.1 it can be seen that after refurbishment, the volume per seat of D2 stood at only 3.3

m^3. This is rather less than the 8 - 10 m^3 commonly used as a rule of thumb for concert halls. It might be thought that theatre D2 was just too full of highly absorbing seats to achieve a diffuse field at high frequencies.

5.5 Conclusion

After validating the optimised barrier method for measuring seating absorption in ten auditoria, it can be concluded that it gave close predictions in eight of them. In all ten halls, ranging from a large modern concert hall to a small theatre, any deviations from a good prediction not attributable to random error can be explained by problems in the validation process or hall measurements themselves. These mostly take the form of uncertainties due to the presence of extra absorbing material in the auditorium during the validation. In two halls, a large dip in the auditorium seat absorption coefficient was found which was not predicted by any reverberation chamber measurement. There is evidence that very poor diffusion was the cause for this in at least one of the halls.

In all ten halls, the traditional reverberation chamber measurement method overestimated the *in-situ* absorption coefficient. This means that a reverberation time calculation for a new hall based on such a measurement is very likely to give too low a value. Because the overprediction of the traditional measurement is quite large, and the seating is the major absorber in a hall, the deviation from the design value of RT would probably be greater then the subjective difference limen of 3 - 4% quoted in section 2.3. The new method will also give more accurate results than the use of either Beranek's or Kosten's average absorption data will allow in

almost all cases. Finally, the present method achieves an accuracy at least equal to the more lengthy one proposed by Bradley (1992). It is therefore proposed that the optimised barrier method of measuring seating absorption should be adopted for all designs where accurate RT prediction is desired.

Part II

Chapter 6

Seat Dip Attenuation in a Typical Concert Hall

This chapter commences the second section of the thesis, on seat dip attenuation, with measurements of the phenomen in an unoccupied concert hall, the Free Trade Hall, in Manchester. This auditorium has a seating capacity of 2500, of which 1122 are on a stalls floor which is nearly flat. A decision was made early on to concentrate on unoccupied measurements for three reasons: firstly, early measurements of the phenomenon by Schultz and Watters (1964) and Sessler and West (1964) showed little difference in the form of attenuation with and without an audience. It is thought that the present results will apply at least qualitatively to the occupied condition. Secondly, because the mechanism of the attenuation is not exactly understood, it seemed best to restrict the complexity of the experimental conditions. Finally, obtaining a sufficient number of subjects for occupied measurements in concert halls is usually difficult, and in this case it would have considerably reduced the number of measurements which could be made in the time available.

6.1 Measurement System Using Maximum-Length Sequences

In the early studies of sound propagation in auditoria by Schultz and Watters (1964) and Sessler and West (1964), methods based on a measurement of the attenuation

of tone-bursts or single-cycle sine waves were used. Greater repeatability and detail can be obtained by measuring the impulse response across the seats. The desired transfer function is generated by a Fast Fourier Transform (FFT) of the early part of the impulse response. The impulse response can of course be measured directly with a pulse source as Ishida et al. (1989) did. However, vastly improved signal-to-noise ratios may be obtained by using pseudo-random noise, in the form of a maximum-length sequence (mls), as a stimulus. MLS methods were introduced into acoustics by Schroeder (1979), and are comprehensively described by Rife and Vanderkooy (1989).

A binary mls is a two-valued periodic sequence of length 2^N-1, where N is an integer, whose autocorrelation is an impulse (Golomb, 1967). When the output of a system subjected to a mls is correlated with the input mls, the system impulse response is recovered. This can also be done with white noise as a stimulus, but, unlike white noise, a mls is deterministic, and so a system's response to a mls can be picked out from background noise easily. In theory, no time averaging of the system output is needed to determine the response precisely in the presence of completely random background noise. In practice, a small number of averages may be necessary. In common with white noise, however, a mls has a flat power spectrum, which enables the experimenter to supply far more energy to the system than with a single pulse. The necessary cross-correlation is quickly achieved by the fast Hadamard algorithm described by Alrutz and Schroeder (1983) and Borish and Angell (1983).

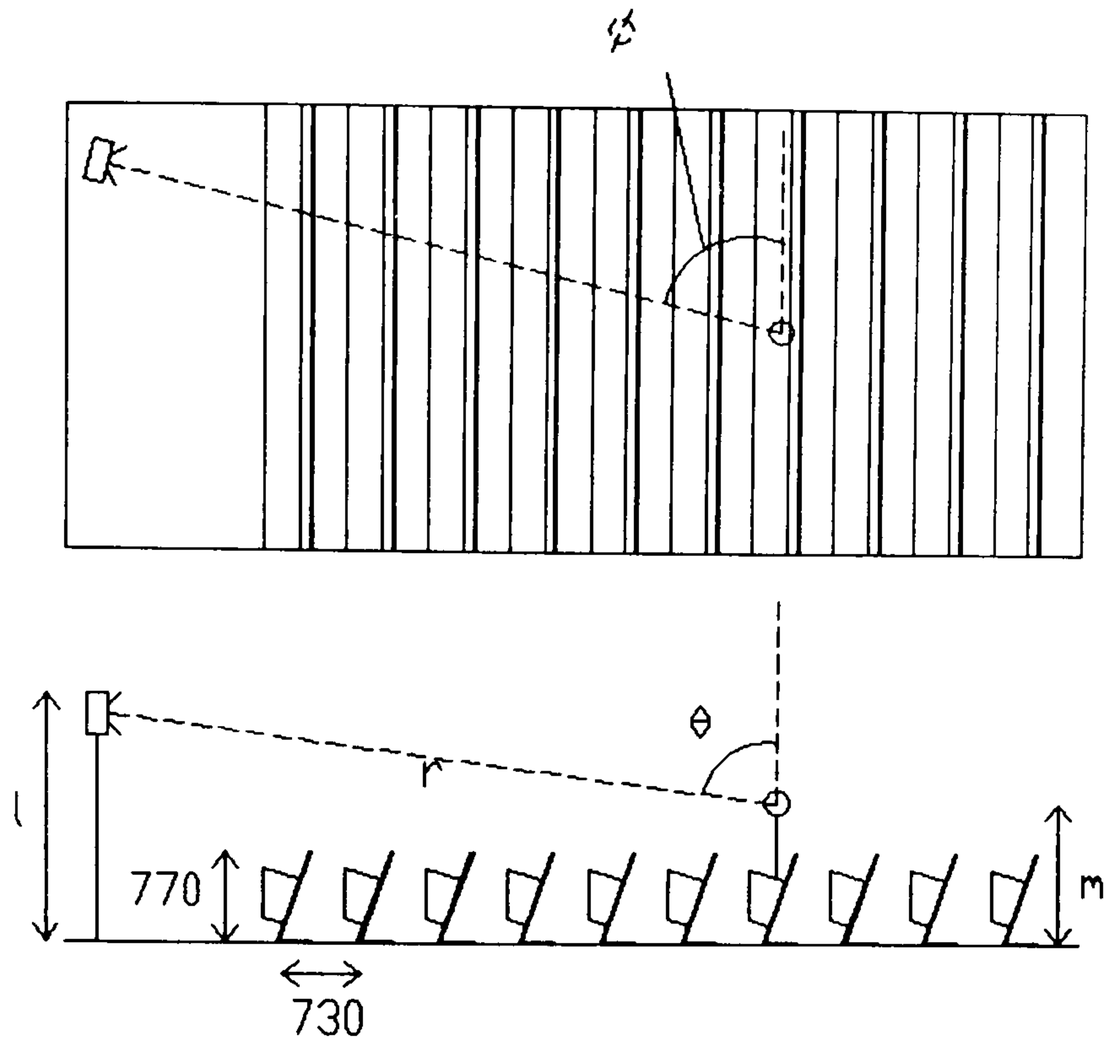

Figure 6.1: Arrangement for measuring seat dip attenuation in concert hall.

All the measurements described in this chapter were made using a PC-based commercially-available mls system, called MLSSA (see Rife, 1987). The basic experimental set-up was as shown in figure 6.1. The pseudo-random noise was radiated by a loudspeaker in front of the seating and sampled at a microphone in the seating. The impulse response was automatically obtained and then the transfer function was found by applying a FFT to a section of the response selected by the operator. This spectrum was normalised to an anechoic calibration of the whole measuring system, so that the influence of the loudspeaker, microphone, etc., was removed. The MLSSA measuring hardware, including a 12-bit A/D convertor (allowing 72 dB dynamic range), was installed in a portable 286-based PC, for convenience in field measurements. Because the main thrust of the experiments

was to be towards the attenuation suffered by the direct sound, it was not thought important that an omnidirectional loudspeaker be used.

6.2 The Effect of Parameters r, m, θ, and ϕ on the Direct Sound Seat Dip Attenuation

To judge from the experimental data already in the literature, the most important parameters affecting seat dip attenuation in a given hall are: the number of seat rows between source and receiver, or the source-receiver distance r; the microphone height m; the angle of elevation θ of the sound path; and the angle of azimuth ϕ of the path (these quantities are defined in figure 6.1). For the present study, the values of r were limited by the position of the balcony overhang in the Free Trade Hall. The overhang provides strong reflections to all seats under it, giving them untypical transfer functions. The length of impulse response chosen to create the transfer function is also governed by the arrival time of this first room boundary (ie non-seat-floor) reflection. Hence only the first 10 ms of impulse response, after the arrival of the direct sound, is used in the following graphs. This section of the impulse response was multiplied by a half-Hamming window before applying the FFT. The window minimises the spectrum leakage that occurs when the impulse response has not died away to zero at 10 ms.

Of course, there are many hundreds of reflections due to arrive at a listener's ears after 10 ms, so that the transfer function from the stage to a given seat will change over time. Eventually, the seat dip attenuation will diminish. The first lateral

reflections from the walls of an auditorium will usually arrive at grazing incidence, though, so the attenuation should persist for them. In addition, even before the arrival of these first geometric early reflections, the transfer function will vary with time, due to the arrival of the diffracted sound from all the seat-floor surfaces. This development over time is dealt with in section 6.3; the following graphs show only the attenuation experienced by the direct sound in a 10 ms time window.

Researchers	r (metres)	m (metres)	θ°	φ°	scale
Schultz and Watters (1964)	10.7 - 34.1	0.914 - 3.353	34 - 87	0, 45, 90	1:1 & 1:10
Sessler and West (1964)	7 - 31	1.2 & 5.5	?	0, 45, 90	1:1 & 1:10
Ando et al. (1982)	∞	0.90 - 1.70	70 - 89	90	calc only
Iida and Ando (1986)	1.9 - 12.3	?	80, 85, 89	45 - 90	1:1
Ishida et al. (1989)	?	1.4	78 - 87	70, 83, 90	1:10
Bradley (1991)	?	0.9 - 3.0	62 - 89	36, 61, 90	1:1
present	2.87 - 19.30	1.14 - 2.38	61 - 89	45, 90	1:1 & 1:10

Table 6.1: The range of seat dip measurement parameters in the literature.

Table 6.1 gives the ranges of parameters used, and shows how they compare with those in the literature. The value of m = 1.14 metres, at which most of the present measurements were made, represents a typical auditor ear height. All following the transfer function graphs have been normalised to an anechoic measurement of the direct sound at r = 1 metre. $20\log_{10}r$ has also been added to all the spectra to remove the excess attenuation due to spherical spreading.

6.2.1 Number of Seat Rows Propagated Over (r)

Figure 6.2 demonstrates that a large attenuation of 18.5 dB at 192 Hz has been established when sound has propagated over only three rows of stalls seats. The shape of the transfer function remains very similar six rows back, with the maximum attenuation increasing to 23.8 dB at 178 Hz. After nine rows, the maximum attenuation has increased by another 2.3 dB and its frequency decreased further to 163 Hz.

This result agrees with most of the data in the literature for the effect of r on full-size measurements. Sessler and West (1964) measured increases in seat dip attenuation and decreases of dip frequency as r was increased up to 19 metres (15 rows back) in the New York Philharmonic Hall. Further increases in r did not change the attenuation much. Schultz and Watters (1964) found that the attenuation in Boston Symphony Hall worsened slightly for r = 10.7 - 19.5 metres and then stayed nearly constant up to 34 metres. They also made measurements in La Grande Salle, Montreal, and found little change in attenuation at three positions for which r = 14.6 - 28 metres. Finally, Iida and Ando (1986) measured

increasing seat dip attenuation at decreasing frequencies up to 5 metres back and no difference thereafter.

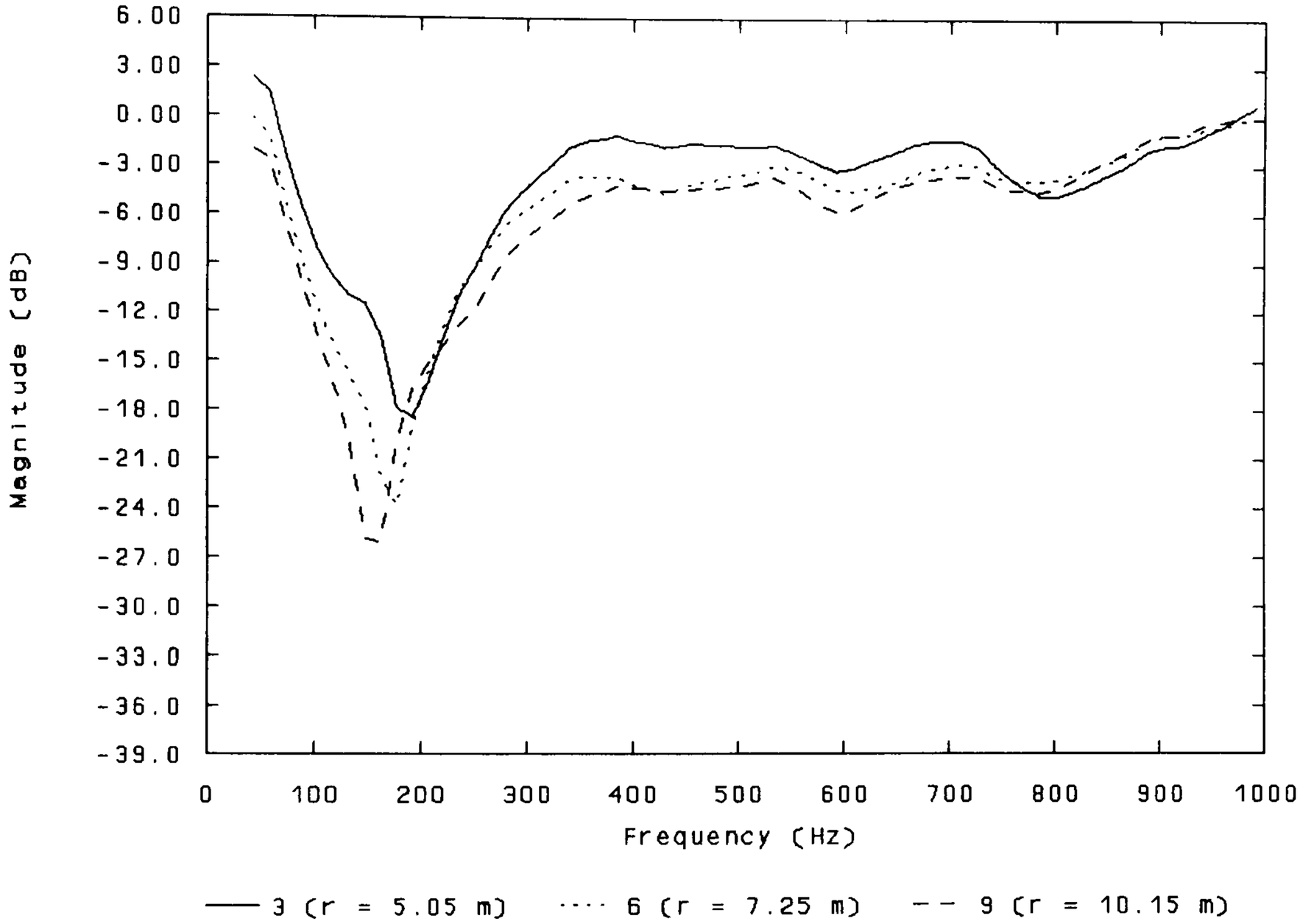

Figure 6.2: Transfer function (first 10 ms after direct sound) across stalls seats. Parameter: number of rows propagated over (m=1.14 metres, $\theta=87°$, $\phi=90°$).

All of this data seems to agree with the statement that seat dip attenuation increases with the number of seat rows travelled over, up to a maximum governed by other parameters, including m, θ, ϕ and perhaps the seat and floor design. This may happen because of the continual arrival of diffracted sound from successive seat rows as the direct impulse propagates over them. The diffracted sound is shifted in phase with respect to the direct sound and so the interference of the two

results in cancellation at a particular frequency. The cancellation is never perfect (and hence the attenuation total) perhaps because the amplitude of the diffracted sound is modified by the floor and seat surfaces.

In this interpretation, most of Schultz and Watters measurements were made at positions far enough back to be in the region of maximum attenuation for their particular values of m, θ and ϕ. The position of the front of the balcony in the Free Trade Hall meant that it was not possible to make measurements of seat dip attenuation on the direct sound only very much further back than those in figure 6.2. The data in the literature indicates that, had this been possible, the attenuation would probably not have worsened very much from that shown in figure 6.2 for nine rows back. It is important to emphasise, however, that quite severe attenuation can occur as close as three rows back from the stage, with a low source.

6.2.2 Microphone Height (m)

When the microphone height, m, is increased from 1.14 metres (ear height) through 1.56 metres to 2.38 metres, both the frequency of the dip and the maximum attenuation decrease, as shown in figure 6.3. (For these measurements, loudspeaker height l was held constant, so θ varies.) These results are in good agreement with those in the literature. They also accord with subjective impression: if the mls signal, which sounds like white noise, is radiated towards a seated listener in the stalls, a distinct increase in bass level can be heard on standing up. (The author was never brave enough to try this during a classical concert!)

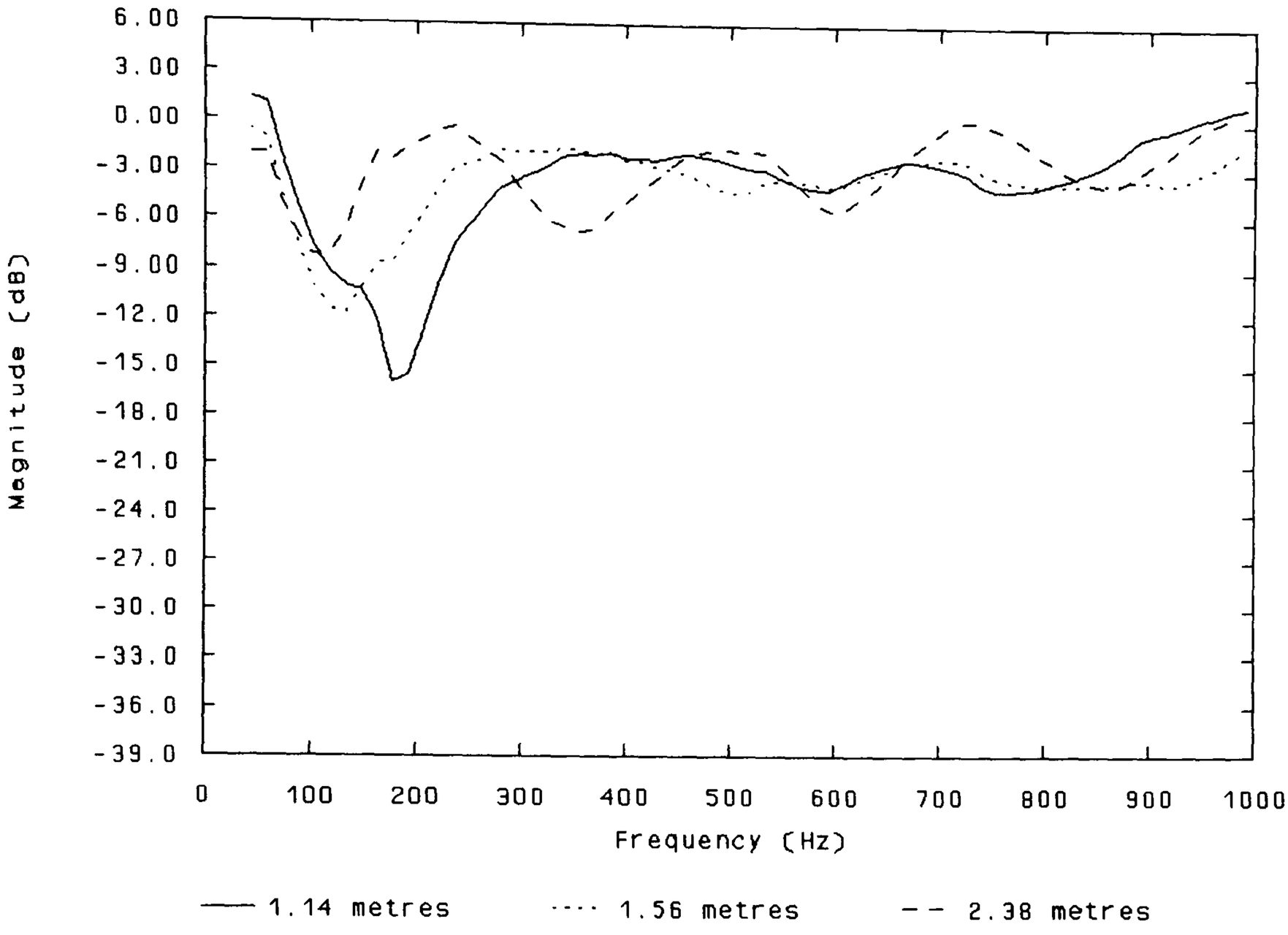

Figure 6.3: Transfer function (first 10 ms) across stalls. Parameter: microphone height, m (3 rows back, l=1.77 metres, ϕ=90°).

When m = 2.38 metres, the transfer function is that of a comb filter. This suggests that here the impulse response is dominated by a single reflection. Cremer and Müller (1982b, pp. 108-113) proposed that a rough approximation of seat dip attenuation could be found from considering a reflection from a locally-reacting surface at the height of the tops of the seat backs. In fact, the right pathlength difference seems to be found with a single reflection striking the *floor* between loudspeaker and microphone. This crude artificial impulse response and its spectrum is shown in figure 6.4. For such a high receiving position, the vertical angle of incidence is not near grazing, and so the floor reflection is positive. The success of this explanation begged the question: could seat dip attenuation in

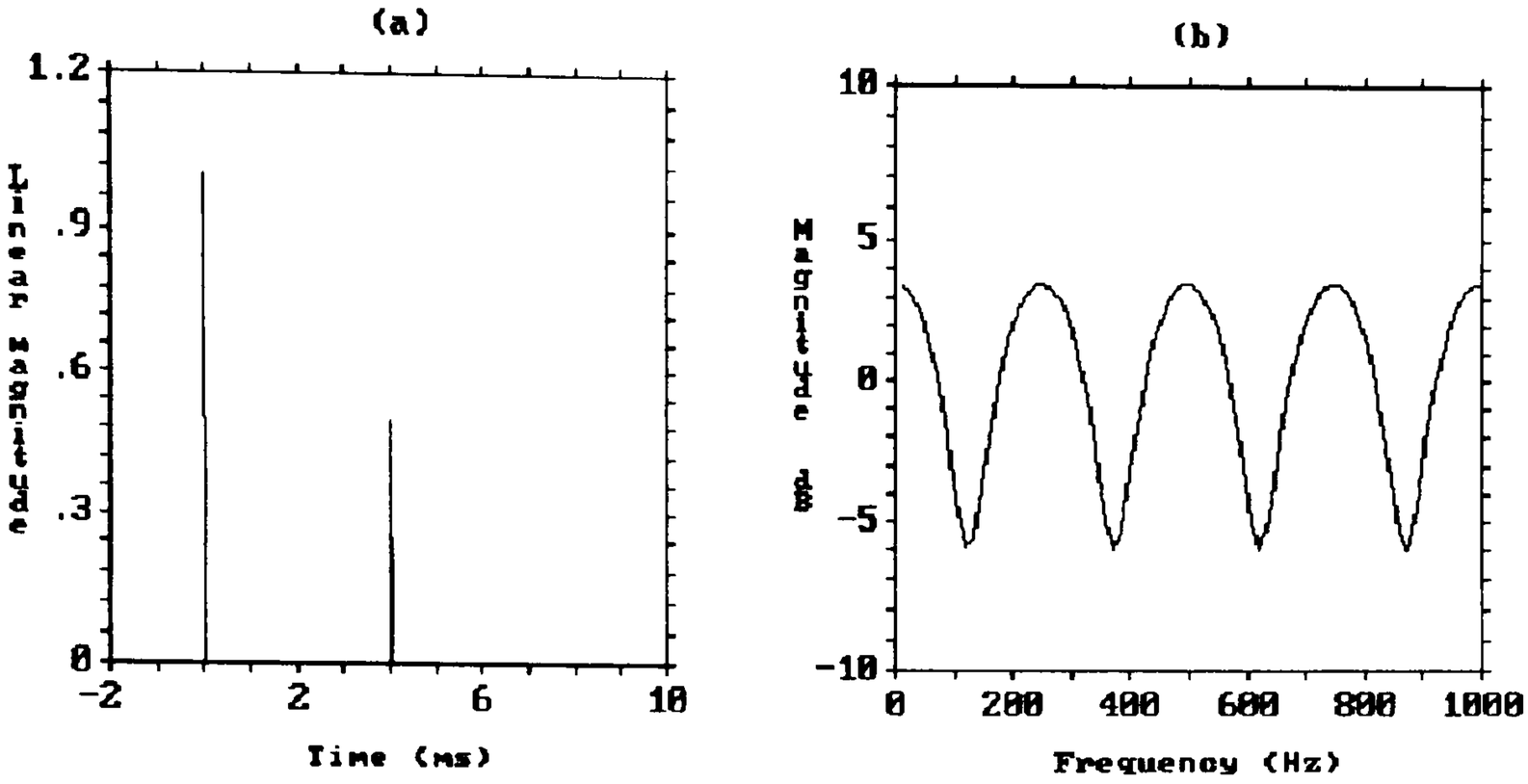

Figure 6.4: Synthesised (a) impulse response and (b) spectrum of direct sound plus a single reflection from stalls floor.

general be modelled in this way, perhaps with negative reflections from the seat tops for measuring positions nearer grazing incidence? Would it be better to try to model the impulse response rather than to think of resonances between seat rows or try to solve the Helmholtz equation over the seats, as had been attempted in the past? Chapter 9 describes a computer program which was the outcome of this line of thought.

6.2.3 Vertical Angle of Incidence (θ)

At a fixed receiving position, as θ is increased, the frequency of maximum attenuation increases from 118 Hz to 178 Hz and the dip attenuation increases significantly - from 20.5 dB for $\theta = 82.0°$ to 36.0 dB for $\theta = 88.8°$. This is demonstrated in figure 6.5. These effects agree qualitatively with previous 1:10 scale model tests by Ishida et al. (1989) and Schultz and Watters (1964).

A slight increase in broadband attenuation is also seen for increasing θ in figure 6.5. This is the only effect of θ predicted by the theoretical model of Ando et al. (1982), which exhibits a broadband increase in attenuation from 0 to 400 Hz and no change in the dip frequency, with θ increasing.

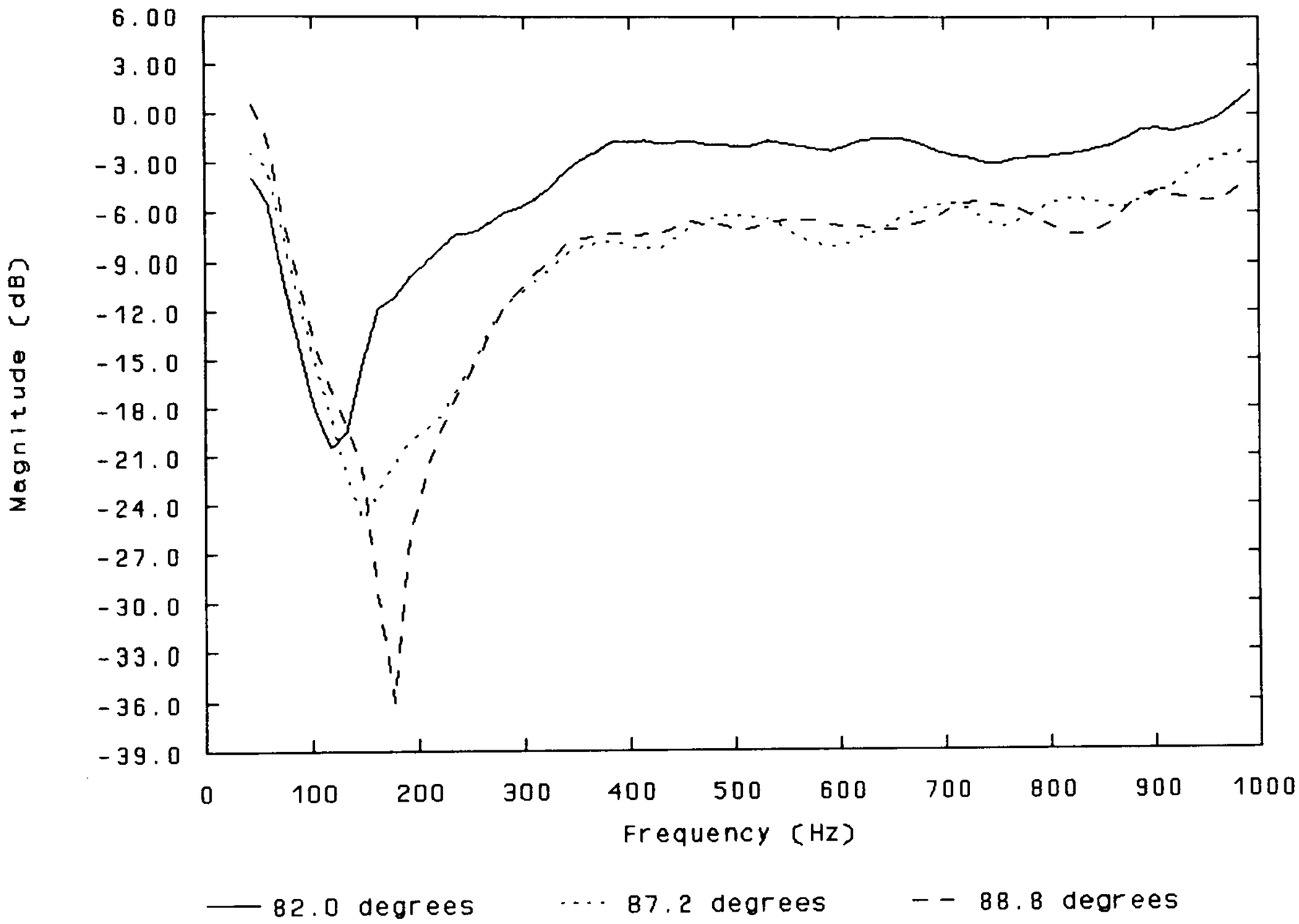

Figure 6.5: Transfer function (first 10 ms) across stalls. Parameter: θ (12 rows back, m = 1.14 metres, $\phi = 90°$).

6.2.4 Horizontal Angle of Incidence (ϕ)

Two values of ϕ were considered. Figure 6.6 shows that, when ϕ is changed from $90°$ to $45°$, the dip is shifted upwards in frequency from 178 to 252 Hz. This effect is described in previous 1:10 scale model measurements by Sessler and West (1964).

Schultz and Watters (1964) and Ishida et al. (1989) found an increase in attenuation as well as a dip frequency increase.

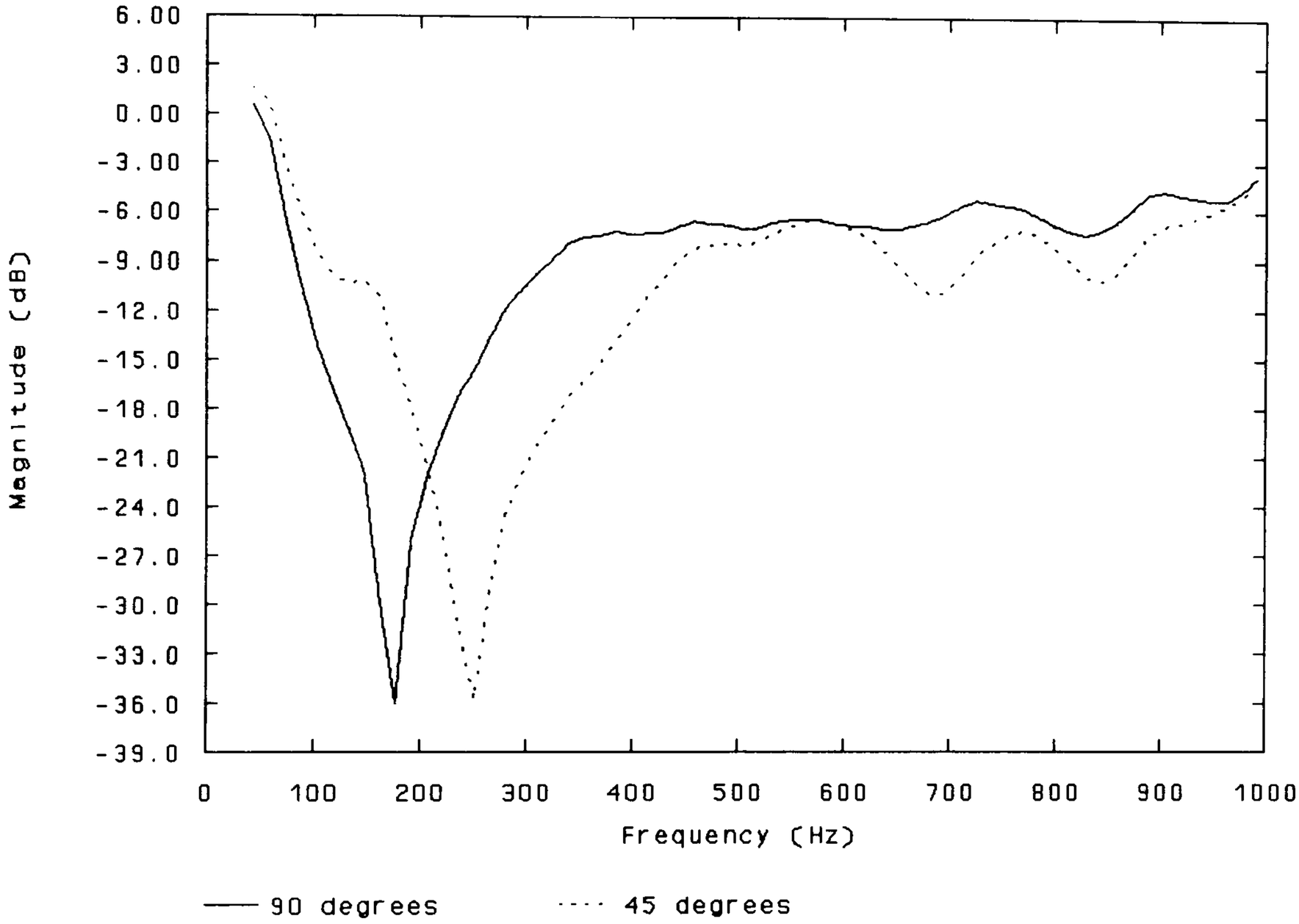

Figure 6.6: Transfer function (first 10 ms) across stalls. Parameter: ϕ (12 rows back, m = 1.14 metres, $\theta = 89°$).

The fact that its frequency varies with ϕ adds to the possible subjective significance of the attenuation. The direct path and early lateral reflections should have a variety of different azimuth angles. This means that, for a given bass note, there is an increased likelihood that one or more sound paths will attenuate that note maximally. Although other authors - Schultz and Watters (1964) - have shown that a small attenuation even exists for $\phi = 0°$, such an extreme angle is unlikely to

occur for a lateral reflection in real halls, except perhaps at seats close to the front of the stalls in a reverse-fan shaped hall.

6.3 Changes in Seat Dip Attenuation Over Time

The graphs above demonstrate how seat dip attenuation depends on four parameters. The seat dip spectrum also varies over time, at a given seat with fixed measurement parameters. Figure 6.7 shows spectra for sound passing over three rows of seats, with m = 1.14 metres, $\theta = 83°$, and $\phi = 90°$. The time window for these spectra always starts at the direct sound arrival. The impulse response corresponding to these spectra is shown in figure 6.9. Note that the later spectra in figure 6.7 will include not just the direct impulse and diffracted sound from the seats and floor, but also geometrical room reflections from the side walls and ceiling of the auditorium.

Some attenuation is present only 5 ms after the arrival of the direct sound, though the dip is quite shallow and broad: the largest attenuation is only 18 dB at 178 Hz. At 10 ms, this dip has both sharpened and deepened. A little later, at 15 ms, the spectrum is a very similar shape, but the bottom of the dip has risen. At 20 ms, it begins to go down again, reaching a nadir of 37 dB at 25 ms after the direct sound arrival. From 25 to 40 ms, the main dip gets smaller, but at 40 ms, a second dip at a higher frequency (207 Hz) has been established. From 40 to 50 ms, both of these main dips then increase again. Over the same 50 ms, a few lesser dips higher up the frequency range also grow, but the spectrum above 250 Hz stays substantially the same shape.

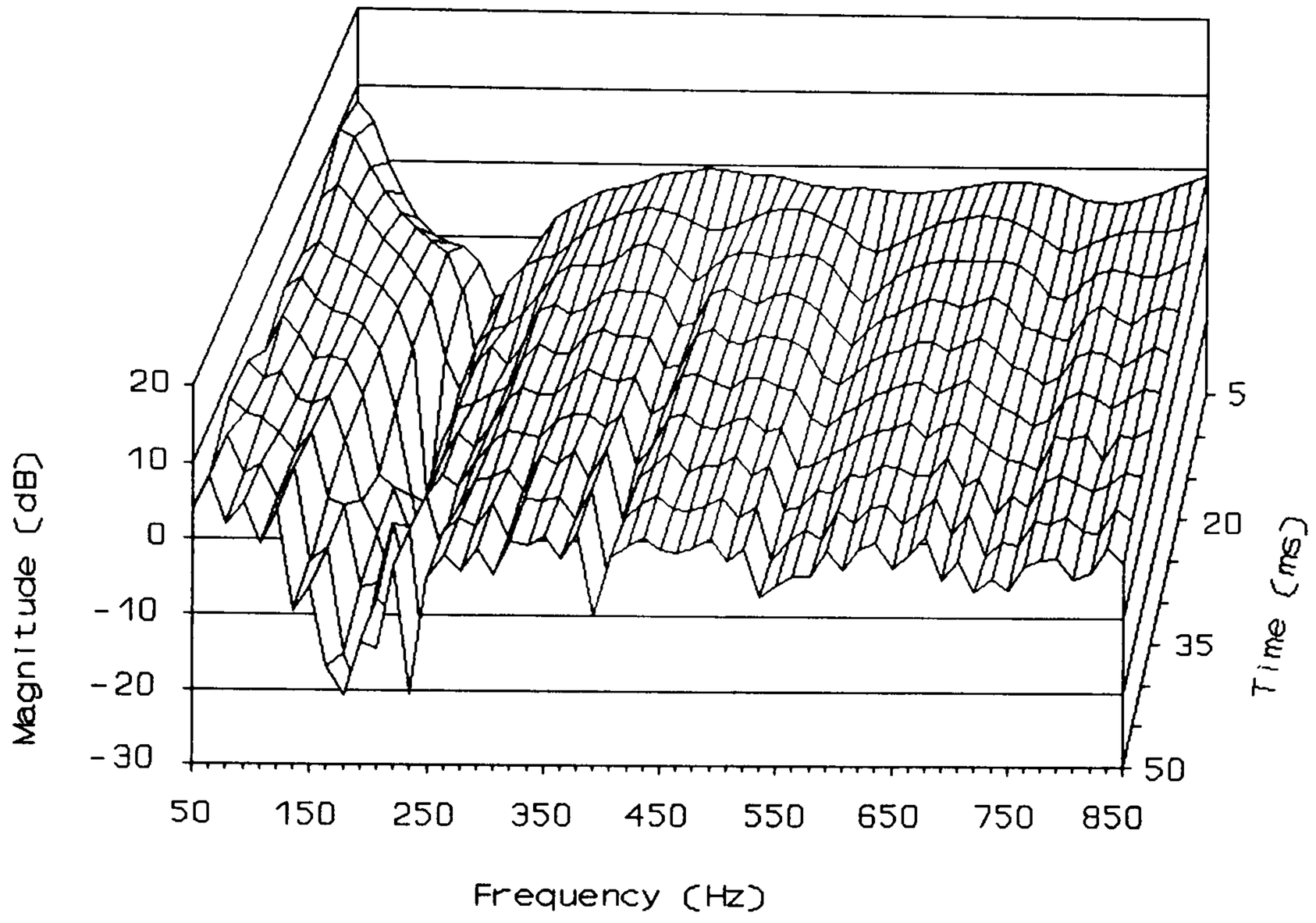

Figure 6.7: Seat dip spectra at several points in time after the direct sound arrival. (3 rows back, m=1.14 metres, θ=83° , ϕ=90° .)

This change over time means that early reflections from the auditorium boundaries influence the low frequency level at a seat considerably. The increase in attenuation around 20 ms is probably caused by the arrival of a grazing reflection from the nearest side wall. This will have a larger θ than the direct sound and so we might expect it to suffer greater attenuation (see figure 6.5). By 40 ms, the first non-grazing room boundary reflection will have arrived, from the ceiling. Because this cannot have suffered seat dip attenuation, the overall low-frequency level at the microphone increases. The appearance of the double dip towards 50 ms may also be caused by room boundary reflections. As some of these will be lateral reflections propagating at values of ϕ less than 90° , they might experience seat dip attenuation at a higher frequency than the direct sound, which is at 90° (see figure

6.6). These reflections may thus partially cancel the main low-frequency dip and start a new one at a slightly higher frequency.

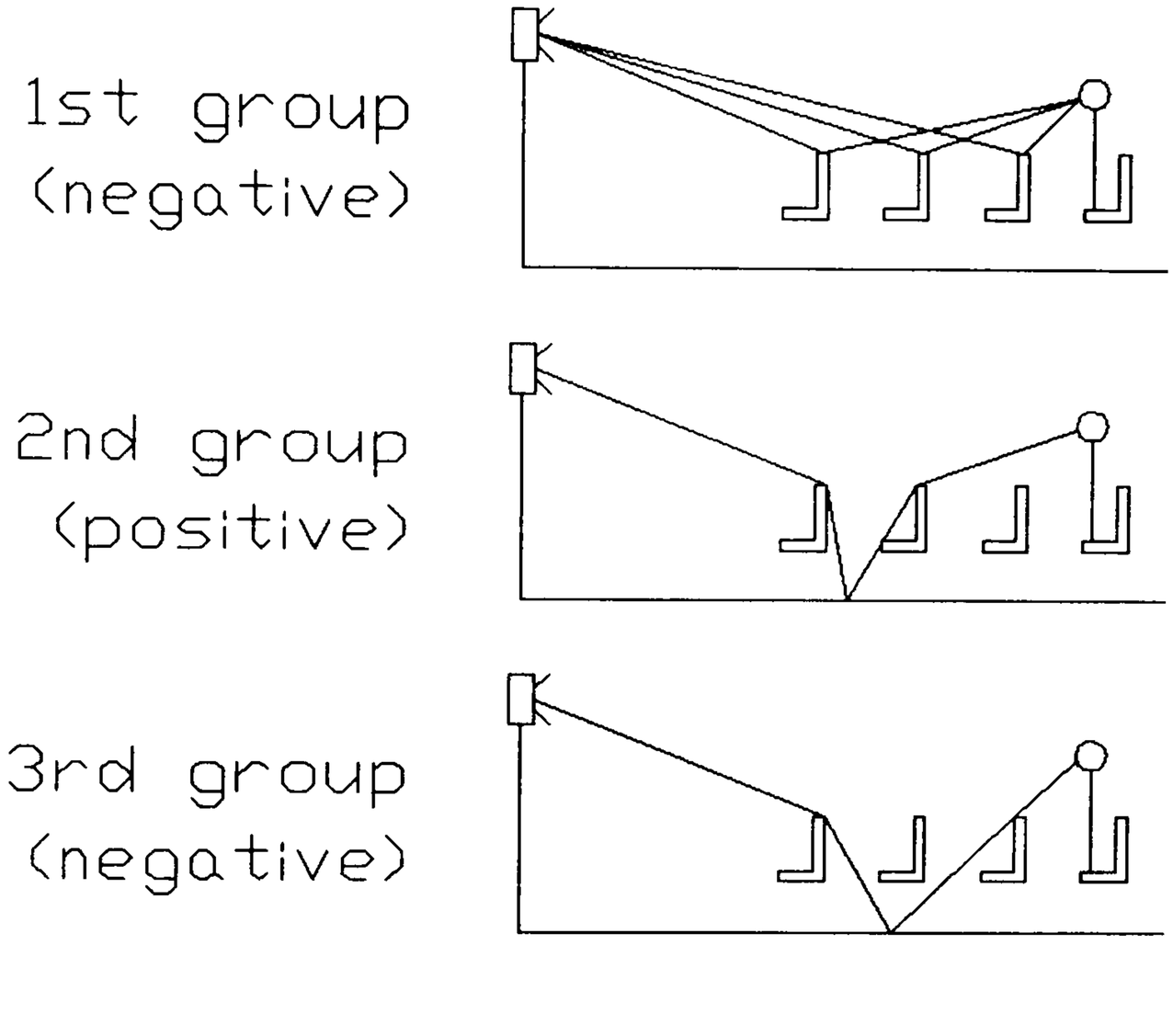

Figure 6.8: Examples of the three different groups of reflections causing seat dip attenuation, according to Ishida *et al* (1989).

What is also apparent from figure 6.7 is that the spectrum changes before any sound could arrive from the room boundary, that is, before 20 ms. This hints at the influence of different groups of reflections from the seats and floor. A description of a seat dip impulse response in this way was first given by Ishida et al. (1989). They split the early impulse response into three parts. An example of each part is shown in figure 6.8. First, large negative reflections from the seat tops arrived immediately after the direct sound. Secondly, small positive reflections from the lower parts of the seats and the floor arrived at 2 - 8 ms, they said. Finally, small

negative reflections arrived via the underpass of the seats over 8 - 14 ms in their experiments. This seems to be a broadly plausible scenario, though one part of it is contradicted by figure 6.7. Ishida et al thought that the last group of reflections, arriving after 8 ms, were responsible for an increase in level around 50 Hz. In the above measurement, though, the level at 50 Hz is already 8 dB at 5 ms after the direct sound, and the peak dies away somewhat after 10 ms. If these groups of reflections are present, then the very low-frequency increase in level must be caused at least partially by the earliest arrivals.

6.3.1 Tracking the Seat Dip Minimum

Since it was felt that the change in the main dip over time offered some clues for the temporal causes of seat dip attenuation, a computer program was written to track this for a given impulse response. Called "Longfft", it applies a window to the impulse response. The start of the window is always just before the direct sound arrival, and, to start with, the end of the window is close afterwards, say at 1 ms. The rest of the impulse response is set to zero. A FFT is then taken of this time series, and the resulting magnitude spectrum scanned for its minimum over a fixed frequency range (usually 20 - 1000 Hz). This magnitude, in dB, is plotted against the time at which the window ended. The end of the window is then moved forward by a small increment, and the process repeated. This continues to the end of the impulse response, giving a plot of how the narrowband spectrum minimum changes over time.

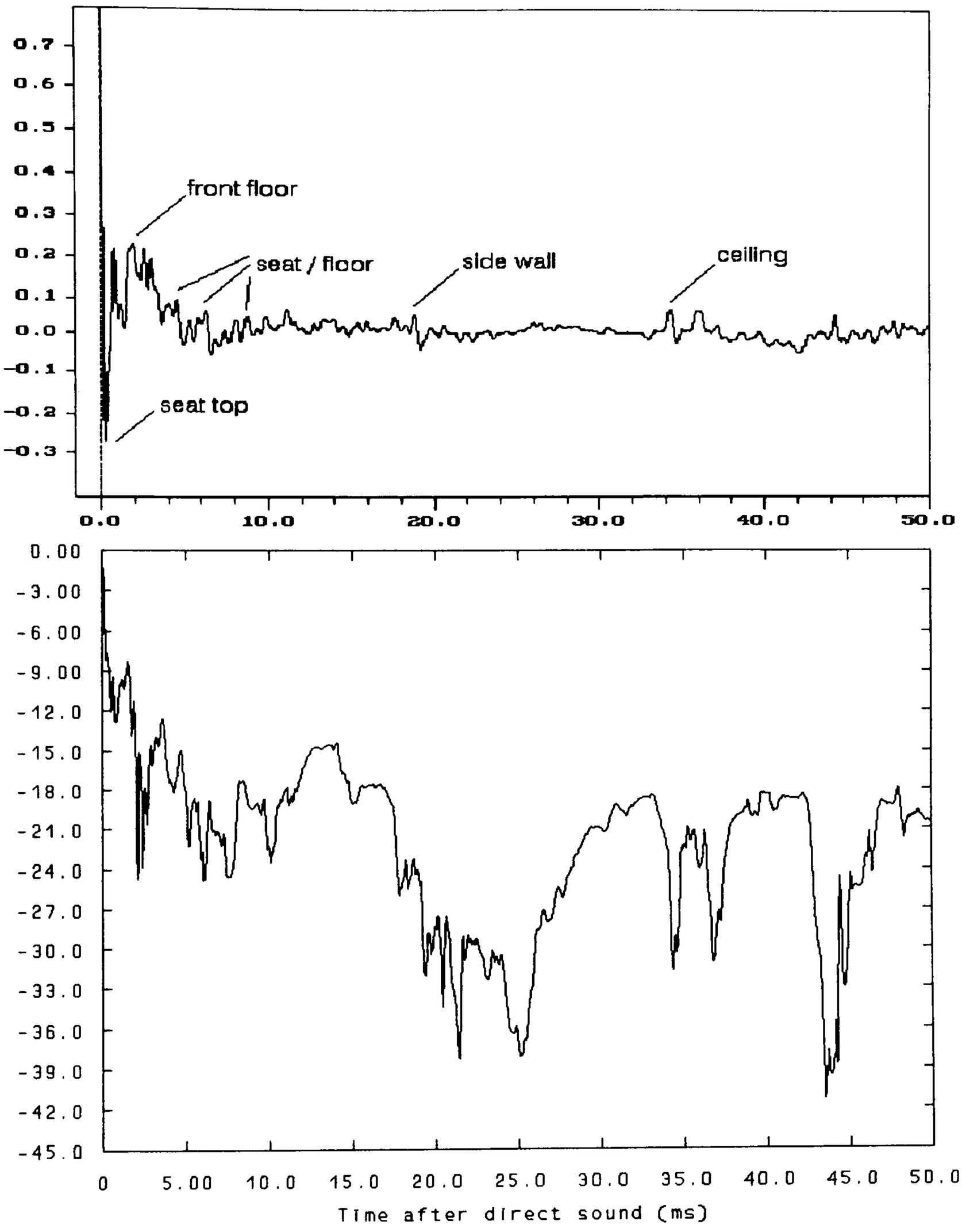

Figure 6.9: Narrowband minimum of seat dip spectrum versus end time of FFT window, plotted below the low-pass-filtered impulse response. (3 rows back, m = 1.14 metres, $\theta = 83°$, $\phi = 90°$.)

Figure 6.9 is a result from the same measurement used for the spectra in figure 6.7. That is, for a spectrum at a given point in time in figure 6.7, the minimum will appear against that time in figure 6.9. The impulse response for the measurement is also shown above the Longfft graph. Because this impulse response is deconvolved to remove the loudspeaker influence, it had to be low-pass filtered at 2 kHz to avoid time-domain ringing. This means that individual reflections are somewhat less sharp than in a broadband response. The room boundary reflections are also a little small, due to the use of a non-omnidirectional loudspeaker. Possible paths for the reflections identified in the impulse response in figure 6.9 are shown schematically in figure 6.10.

Most of the major variations of the dip depth in figure 6.9 correspond to features in the impulse response. The correspondence is particularly good for the period 0 - 15 ms after the direct sound arrival, during which Ishida et al thought the seat dip reflections arrived. Starting from the left-hand side, a large negative reflection appears in the impulse response at 0.5 ms. This could have come from the top of a seat back, and it corresponds to the dip appearing in the spectrum after only 0.5 ms. The spectrum minimum then drops further around 2.7 ms, as the next group of reflections in the impulse response arrive. The dip recovers briefly, and then drops again from 3.5 to 10 ms, with many small rises and falls corresponding to the small positive reflections in the impulse response. The effect of any further seat reflections are probably then obliterated by the arrival of diffracted energy from the front of the side balcony at 11 ms.

That these early features of the impulse response are probably reflections from the seats and floor can be demonstrated by constructing ray diagrams in which the rays are allowed to diffract over the tops of the seat backs. Figure 6.10 shows some constructions for this measurement configuration. It can be seen that the timing of the front floor ray at 2.8 ms matches up well with the broadband impulse response and with the effect on dip depth. The multiple seat/floor ray is one of several which can be constructed with arrival times of 3.3 - 12.2 ms.

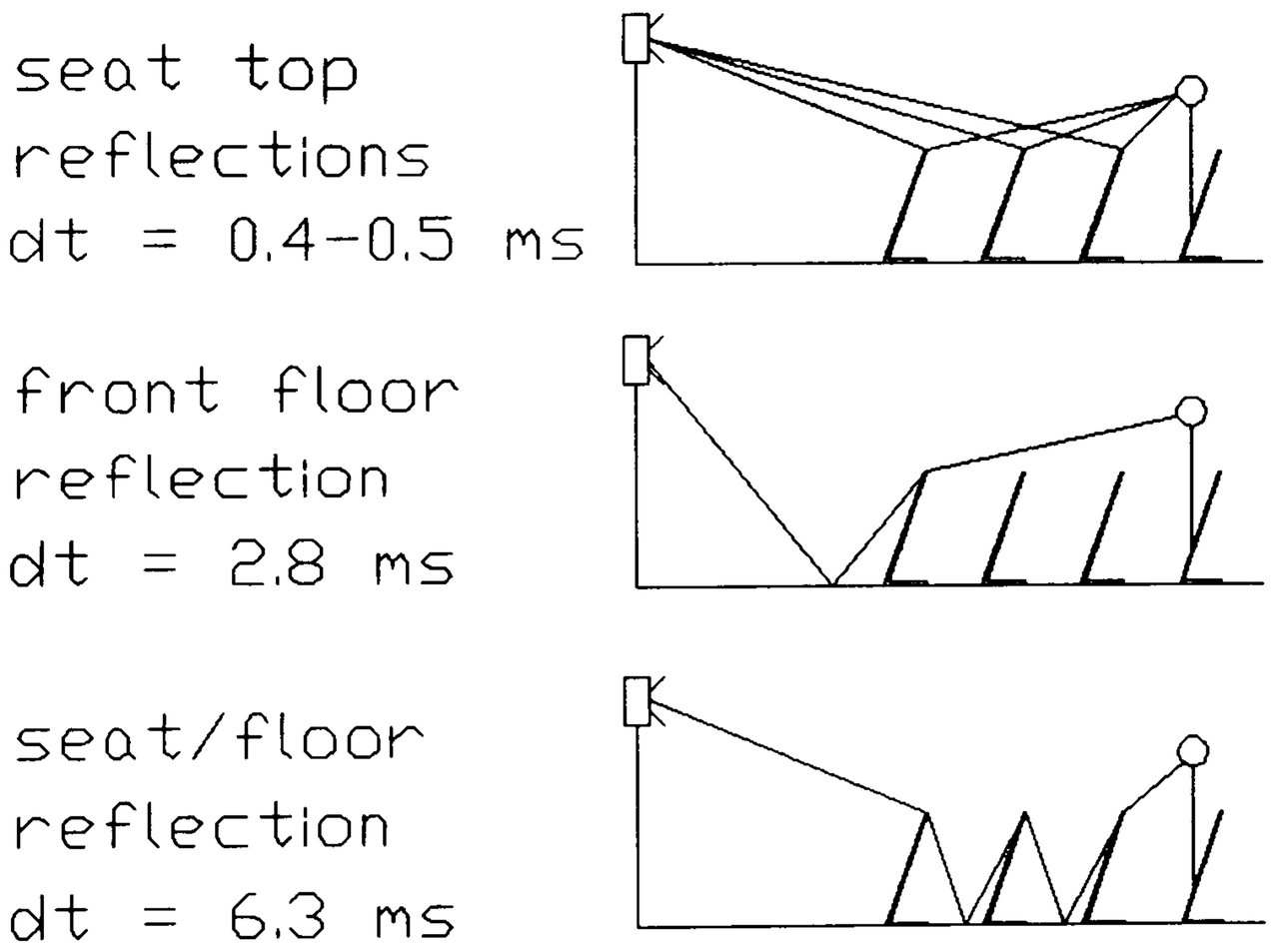

Figure 6.10: Seat dip ray constructions (m = 1.14 metres, $\theta = 83°$, $\phi = 90°$).

It appeared from this initial analysis that seat dip attenuation could be thought of in the time domain as a series of rays, each producing a small impulse at the microphone. Each of these impulses, when combined with the direct sound, will produce a comb filter spectrum similar to that in figure 6.4(b), above. If the

reflection has a negative amplitude instead of a positive one then the spacing of maxima and minima will be the same, but 0 Hz will be at a minimum instead of a maximum; that is, the spectrum will be "phase-shifted" by 180° in the frequency domain. Because these reflections arrive at different times, each will produce a different spacing of minima and maxima in the spectrum. If several of these reflections are superimposed in the time domain, then their spectra will also be superimposed. At some frequencies, therefore, it is likely that several minima will coincide, giving a very low level. This is the main dip. At other frequencies, maxima and minima will tend to cancel out, leaving a roughly flat frequency response elsewhere.

Two things were apparent straightaway from this description of seat dip attenuation. Firstly, that it accords with the idea of Ando *et al.* (1982) to reduce the attenuation by installing resonant absorbers into the floor between the seat rows. These absorbers would tend to remove the multiple seat/floor rays, thus reducing the number of comb-filter minima in the frequency domain. A practical trial of the absorber scheme is described in chapter 7. The second ramification is that this ray construction process is very amenable to computer calculation. Chapter 9 describes a program which simulates seat dip impulse responses along the lines described above.

6.3.2 The Persistence of Seat Dip Attenuation

It has been seen above that there is a significant narrowband low-frequency attenuation in the spectrum of a typical seat 50 ms after the direct sound arrives.

This prompts the question: does the low-frequency attenuation ever disappear later on? This is most sensibly answered by looking not at the lowest narrowband level over time, but at the average level over an octave. This is because the continual arrival of reflections leads to a very spiky narrowband FFT spectrum, so that it is often possible to find at, say, 200 ms, a very deep attenuation at one discrete frequency point only.

The program Longfft mentioned above was therefore adapted to provide also the level in a fixed octave band as a function of the end time of its FFT window. It should be mentioned that this was not done simply by summing all the discrete spectrum points which fell inside the octave. This is because the octave is on a logarithmically spaced frequency scale, and the spectrum points are on a linear one. If the discrete spectrum is plotted with a logarithmic frequency axis, then there are more points in the upper half of the octave than in the lower. In other words, the lowest-frequency discrete point falling inside the octave stands for more of that band than does the highest-frequency one. For an accurate average level across the octave, each point should therefore be weighted according to how much of the band it represents. Of course, this only makes much of a difference where the spectrum level changes greatly across an octave band, as it often does in a seat dip spectrum.

A plot of these average levels is shown in figure 6.11, for the 100, 200 and 400 Hz octaves. The non-standard octaves were dictated by the choice of the 200 Hz band as that suffering the greatest attenuation. (Note that though this is also a typical measuring position, it is different from the one considered above.) It seems that

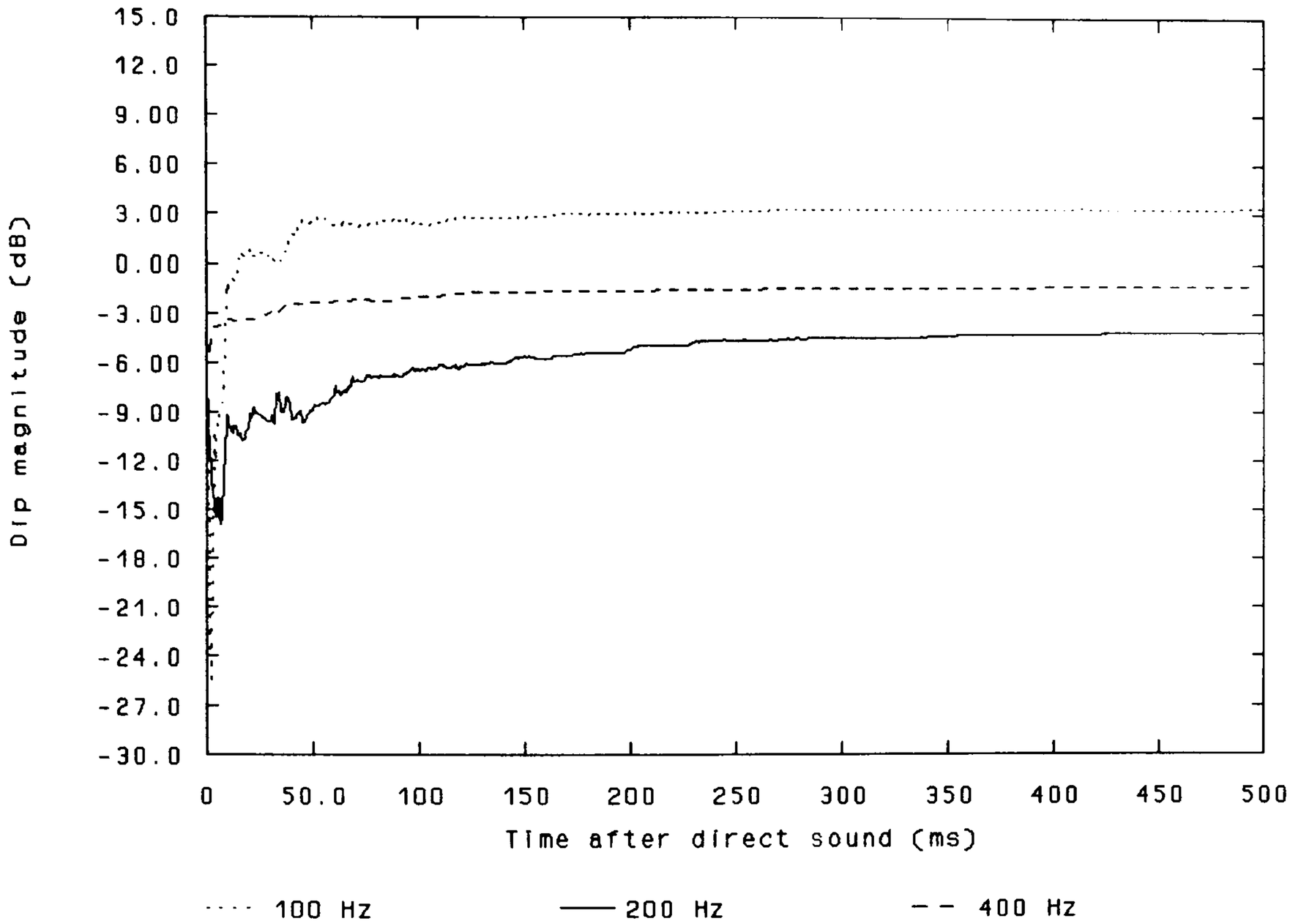

Figure 6.11: Fixed-frequency octave band level of seat dip spectrum versus end time of FFT window. (9 rows back, m=1.14 metres, θ=87° , ϕ=90° .)

the bass level never fully recovers from the seat dip attenuation suffered by the direct sound and early reflections. After 400 ms, the 200 Hz octave level has flattened out at -4.2 dB. The 400 Hz octave has suffered less attenuation, while the 100 Hz octave is above 0 dB after 50 ms. The higher octaves are also close to 0 dB.

Though the 200 Hz octave is still lacking at 500 ms, non-grazing reverberant energy has raised its level from -6.4 at 100 ms to -4.2 dB. So far then, the evidence does not contradict the idea of Schultz and Watters (1964) that a "sufficiently strong"

reverberant field might compensate for the seat dip effect. Significant further increases in the strength of non-grazing reverberation may be mitigated against by the nature of the reverberant field in an auditorium, though. This is because it cannot be truly diffuse, due to the concentration of absorption onto one surface of the room (i.e. the audience). Sound which strikes this surface will be absorbed, leaving a greater proportion of sound paths nearly horizontal to the seating, than would otherwise exist. There will thus always tend to be a greater proportion of grazing paths in an auditorium reverberant field than in a truly diffuse one. This problem has long been an area of interest in the method for measuring absorption in a reverberation chamber, as is described by Cremer and Müller (1982a, p. 335). The subjective effects of increasing reverberation in a sound field with seat dip attenuation are discussed in section 11.3.

6.4 Effect of Seat Dip Attenuation on Room Acoustic Parameters

Seat dip attenuation has a marked effect at a typical stalls seat on parameters sensitive to the early energy field. Figure 6.12(a) shows a decrease in C_{80} of 5 dB from mid to low frequencies, and a corresponding increase (b) in T_s of 45 ms. The most affected octave band is 200 Hz, where seat dip attenuation was shown to be greatest in figure 6.11. That these effects are caused by seat dip attenuation can be shown by comparison with figures 10.5 - 10.8. These show similar peaks or dips in early energy measures appearing when seat dip attenuation is gradually introduced in a concert hall simulator. The simulator is described in full in chapter 10. The forms of figure 6.12(a) and (b) are as expected, because seat dip attenuation will remove more early energy than late energy in the 200 Hz band.

A parameter which looks only at the early energy, is G_{40}, the energy of the first 40 ms of impulse response referenced to the source measured anechoically at 10 metres. This has been used by Bradley (1991) to study the seat dip effect, and figure 6.12(e) looks very like his figure 6(a) showing G_{40} for Boston Symphony Hall, Amsterdam Concertgebouw and Vienna Musikvereinssaal.

The decay parameters are less affected by seat dip attenuation. There is a slight peak in the graph for EDT, figure 6.12(c), at 200 Hz. The early decay curve here may have a shallower gradient due to early energy being lost. The more global parameter of RT, measured over 30 dB of decay, shows no sign of being affected in figure 6.12(d).

Unfortunately, no measurement of the Early Lateral Energy Fraction, L_f, was made in the Free Trade Hall. A measurement in the simulator described in chapter 10 was made, and in figure 10.9 it shows almost no change with varying seat dip attenuation. This is because attenuation was applied to both frontal and lateral sound paths and thus the relative magnitude of lateral to frontal early energy does not change. This is likely to be the case in the real concert hall, though the shift in dip frequency caused by varying ϕ in the hall might have some effect on L_f.

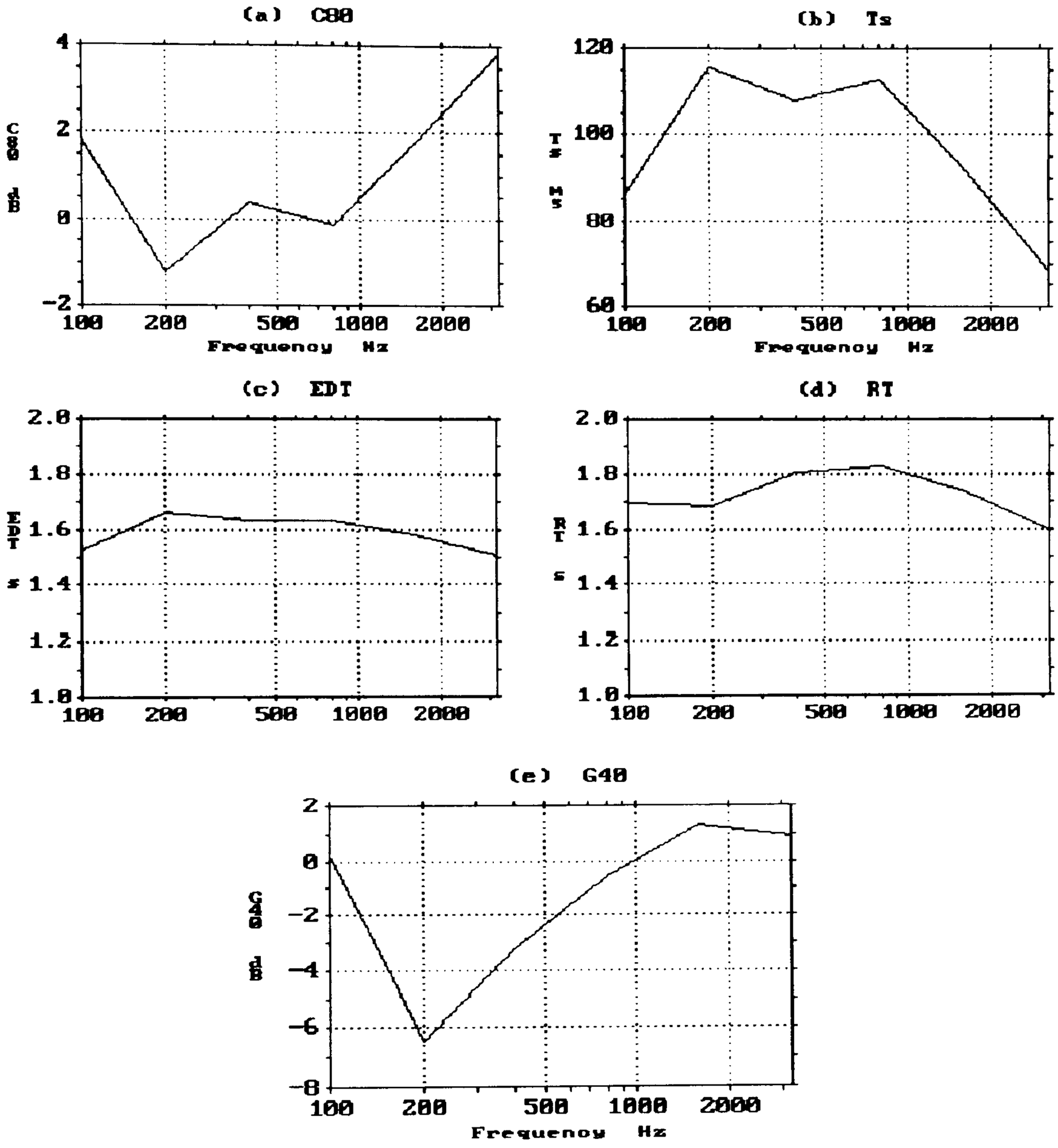

Figure 6.12: (a) Clarity, (b) Centre Time, (c) Early Decay Time, (d) Reverberation Time and (e) Strength at a stalls seat in the Free Trade Hall. (9 rows back, m = 1.14 metres, $\theta = 87°$, $\phi = 90°$.)

6.5 Conclusion

It can be concluded that seat dip attenuation has a dramatic effect on the early energy spectrum in a typical concert hall, leaving a measurable impression on a spectrum at 500 ms after the direct sound arrival. This also shows up clearly in graphs of C_{80}, T_s and G_{40} versus frequency. Details of the early spectrum dip are affected by the number of rows over which the direct sound propagates, its angles of incidence, and the height of the receiver above the seats. The shape of the attenuation evolves considerably over time, in a way which seems to be governed by the arrival of discrete reflections from the seats and floor. This mechanism agrees with a previous suggestion for a remedy for the attenuation and points the way to a new numerical simulation of it. Further chapters deal with these aspects in more detail.

Chapter 7

Seat Dip Attenuation and Floor Absorbers

The idea of using resonant absorbers mounted in the floor between seat rows to ameliorate seat dip attenuation was first suggested by Ando *et al.* (1982). Their results were theoretical only, based on solutions of the wave equation above a two-dimensional profile representing seats and floor. While their model does not reflect some of the real behaviour of seat dip attenuation (the variation with θ, for example), the resonant absorber scheme seemed promising in a pilot experiment with real seats performed by Subagio (1986, p. 93). Accordingly, extensive measurements were made in the Free Trade Hall with three types of resonant absorber, whose absorption coefficients measured in a reverberation chamber are given in figure 7.1. A photograph of a typical measurement with absorbers in the Free Trade Hall is shown in figure 7.2.

One of the absorbers is interesting for its design implications. It is an outlet diffusing box from an underfloor ventilation system for auditoria. This raises the possibility of incorporating a method for reducing seat dip attenuation into vital building services. The box, shown in figure 7.3, is meant to be mounted flush with the floor. It is made up of a steel box with two perforated metal sheets placed on top. The sheets are spaced 42 mm apart, and have a further removable grill placed on top. The grill was found not to change the absorption. The mechanism for the

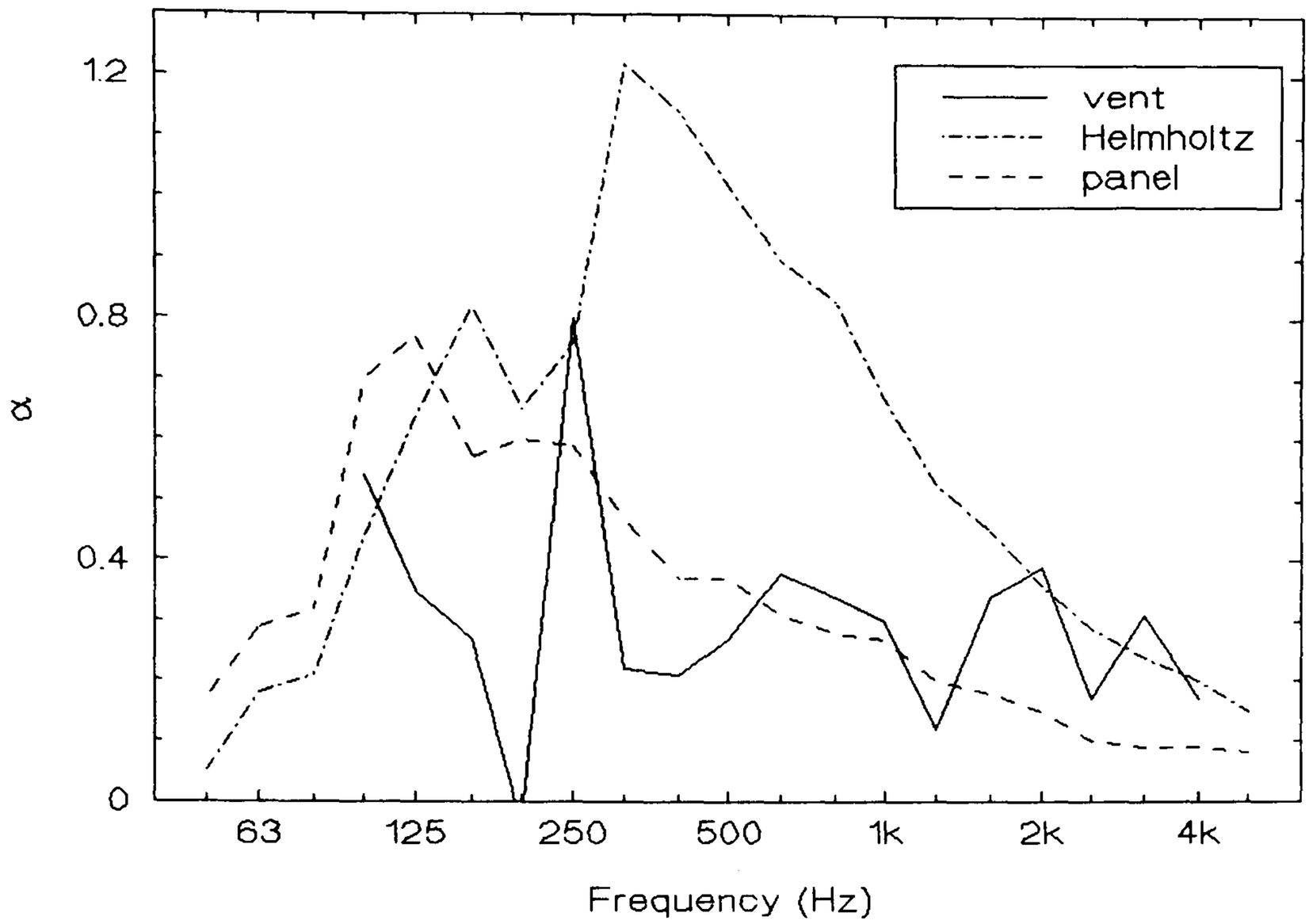

Figure 7.1: Random incidence absorption coefficient α of three absorbers used in seat dip experiments.

vent box's absorption is the usual Helmholtz resonator, with plugs of air between the perforated sheets moving on a long air spring behind them. The theoretical resonance frequency is (from Cremer and Müller (1982a, p. 396))

$$f_{res} = \frac{c}{2\pi}\sqrt{\frac{\pi a^2}{l'V}}\,; \qquad l' = l + \frac{16a}{3\pi} \tag{7.1}$$

where V = volume of cavity (spring)

a = hole radius

l = length of air plug

Figure 7.2: A seat dip attenuation measurement in the Free Trade Hall with floor absorbers between the seat rows.

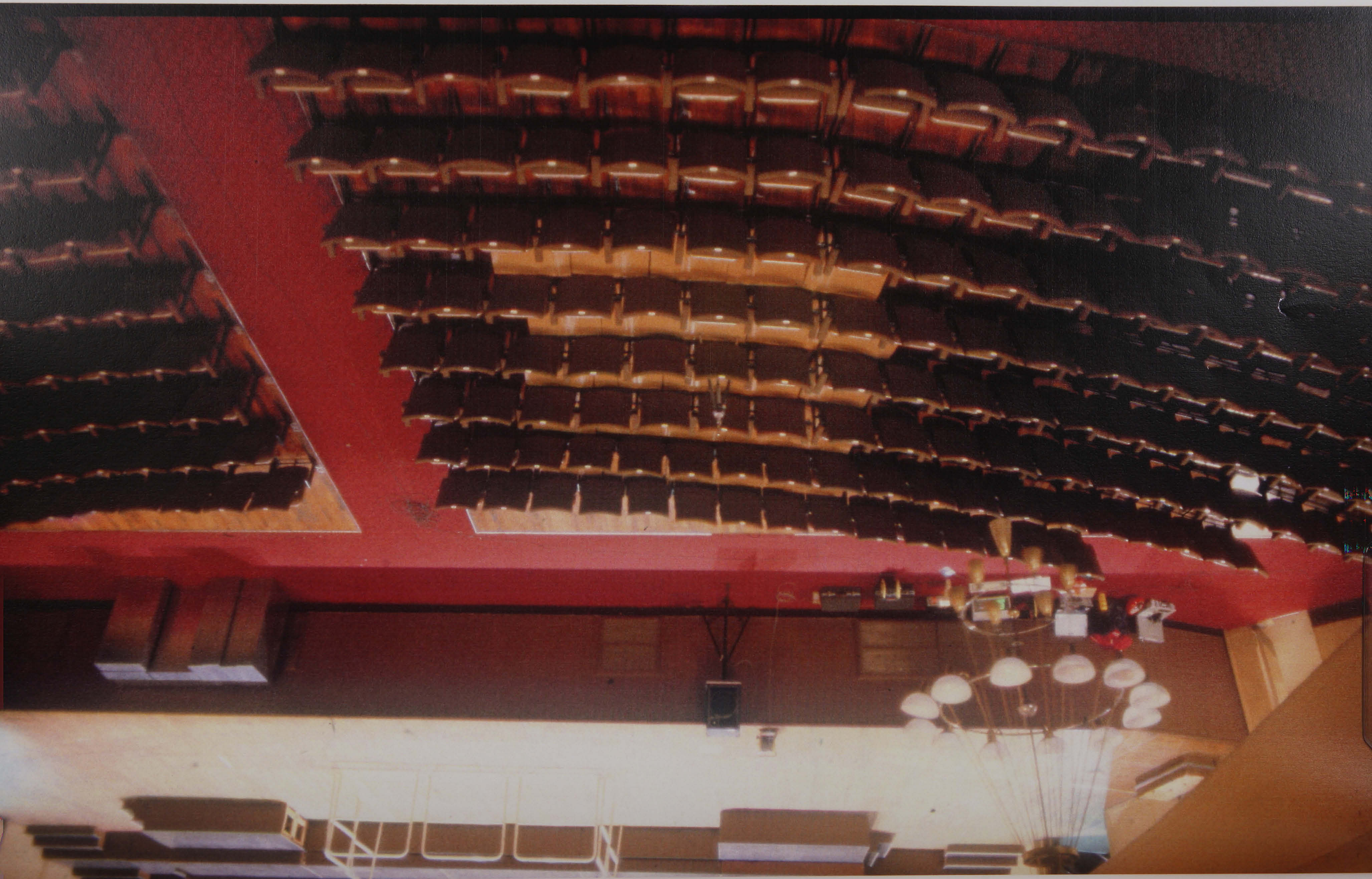

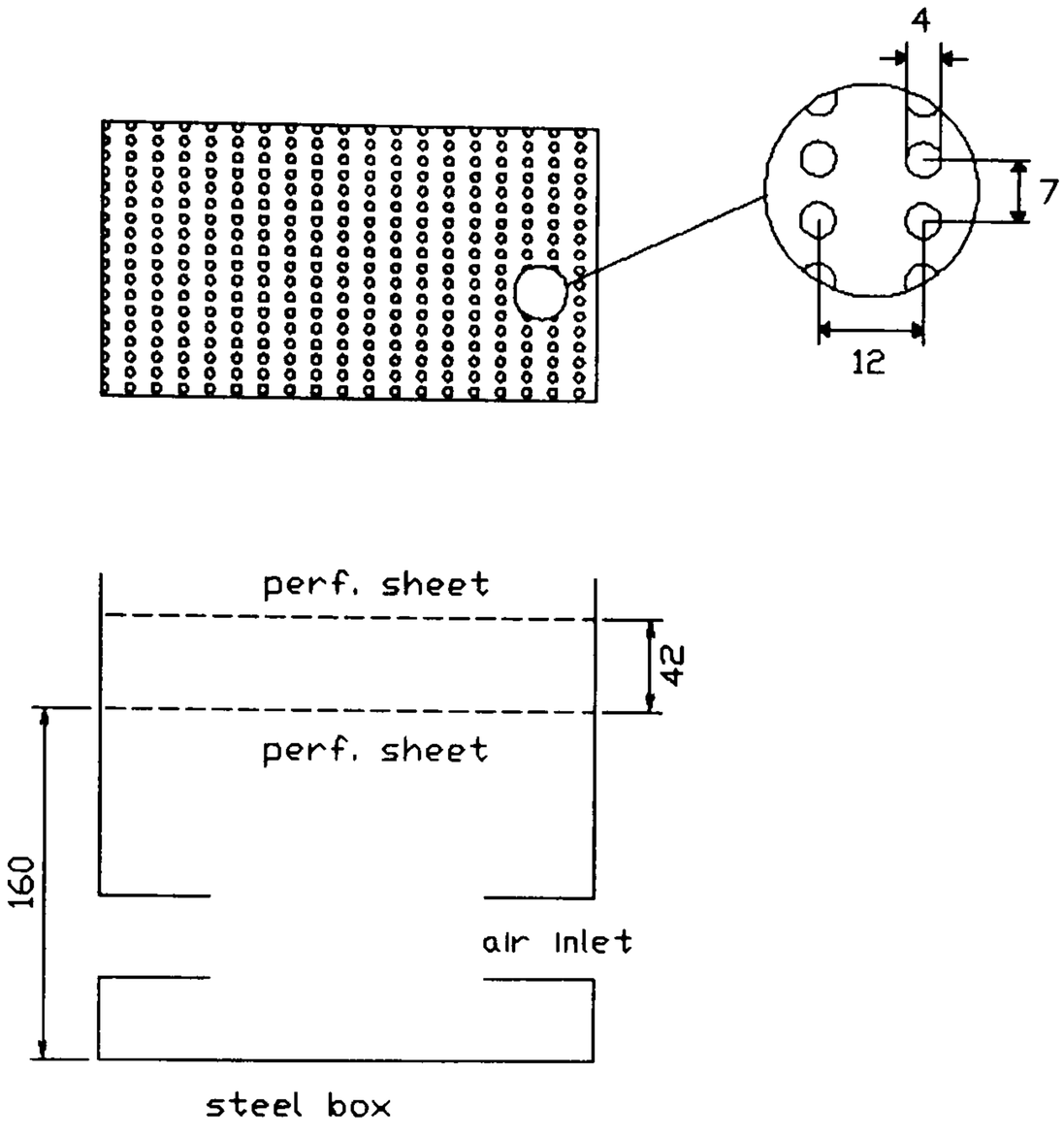

Figure 7.3: An under-floor ventilation outlet box, used as a resonant absorber.

For the dimensions in figure 7.3, this yields a resonance at 249 Hz, the same as that measured in the reverberation chamber. The absorption peak is so narrow because the box contained hardly any damping material. The rise in the absorption coefficient of the vent boxes at the lowest frequencies is dubious: this measurement was made in a non-standard chamber which was not very diffuse at these frequencies. In particular, the area of diffusing panels, their orientation, and the number of microphone positions used in the automated measurement procedure was unsatisfactory. Unfortunately, it was only possible to adjust the orientation of the diffusors. This was because the measurements had to be made at the site of the

manufacturer in Finland and very little time was available for making the reverberation chamber there more diffuse.

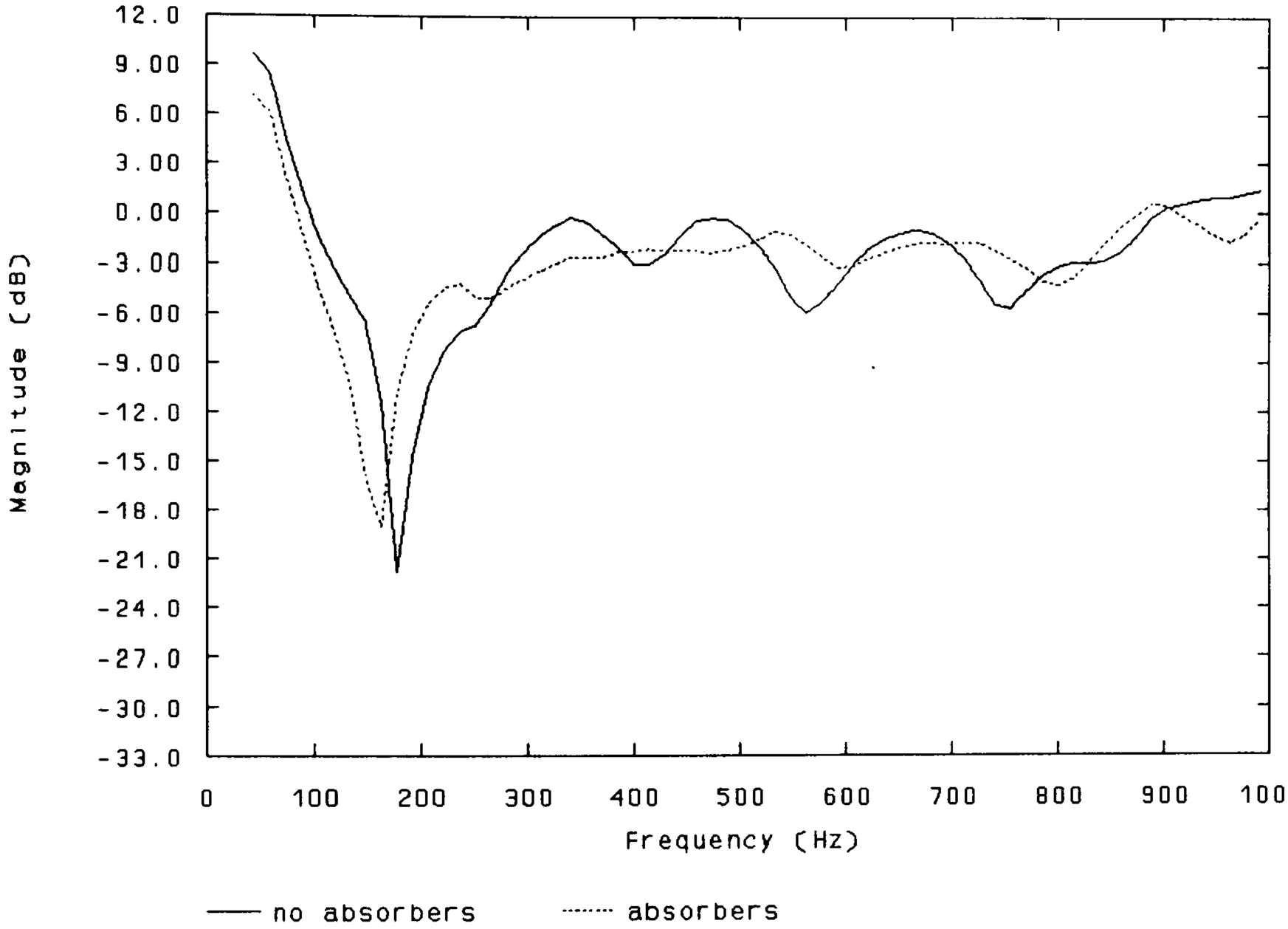

Figure 7.4: Transfer function (first 10 ms) across Free Trade Hall stalls. Parameter: 3 rows of 5 modular Helmholtz absorbers (3 rows back, m=1.14 metres, $\theta=83°$, $\phi=90°$).

The other two resonant absorbers were more conventional types, and they were measured in an ISO chamber. The difference in magnitude in figure 7.1 between absorbers at the absorption peak is due mainly to the measurement arrangement. The vent boxes were fixed into a plenum chamber on a 1 x 0.5 metre grid to represent auditorium seat spacing, while the other two absorbers were measured in a homogeneous block. The panel absorbers were 9 sheet steel boxes, each 1175 x

574 x 200 mm, filled with fibreglass. The top of each steel box was drilled with 3 mm diameter holes at 41 mm intervals. The modular Helmholtz absorbers were 25 plywood boxes, each 600 x 600 x 134 mm. These were filled with layers (from the bottom) of 51 mm air gap, 18 mm chipboard, and 53 mm fibreglass. Each Helmholtz box was faced with 6 mm fibreboard drilled with 6 mm diameter holes at 25 mm intervals. Both these absorbers behave at least partially according to equation 7.1.

An example of the effect of floor absorbers on a seat dip spectrum for the direct sound is given in figure 7.4. Here, five of the modular Helmholtz absorbers have been placed on the floor between each of the seat rows in front of the microphone. 10 ms after the direct sound arrives, the main attenuation has been reduced by 3.4 dB and shifted slightly downwards in frequency. The absorbers have also smoothed out some of the higher frequency ripples.

7.1 Floor Absorbers and Discrete Seat Dip Reflections

It was found that the effect of the absorbers changes over time. Figure 7.5 is a repeat of figure 6.9, this time with and without floor absorbers. The narrowband spectrum minimum is plotted against the time after the direct sound arrival at which the spectrum was formed. Again, the impulse responses shown as well have been low-pass filtered at 2 kHz to avoid time-domain ringing.

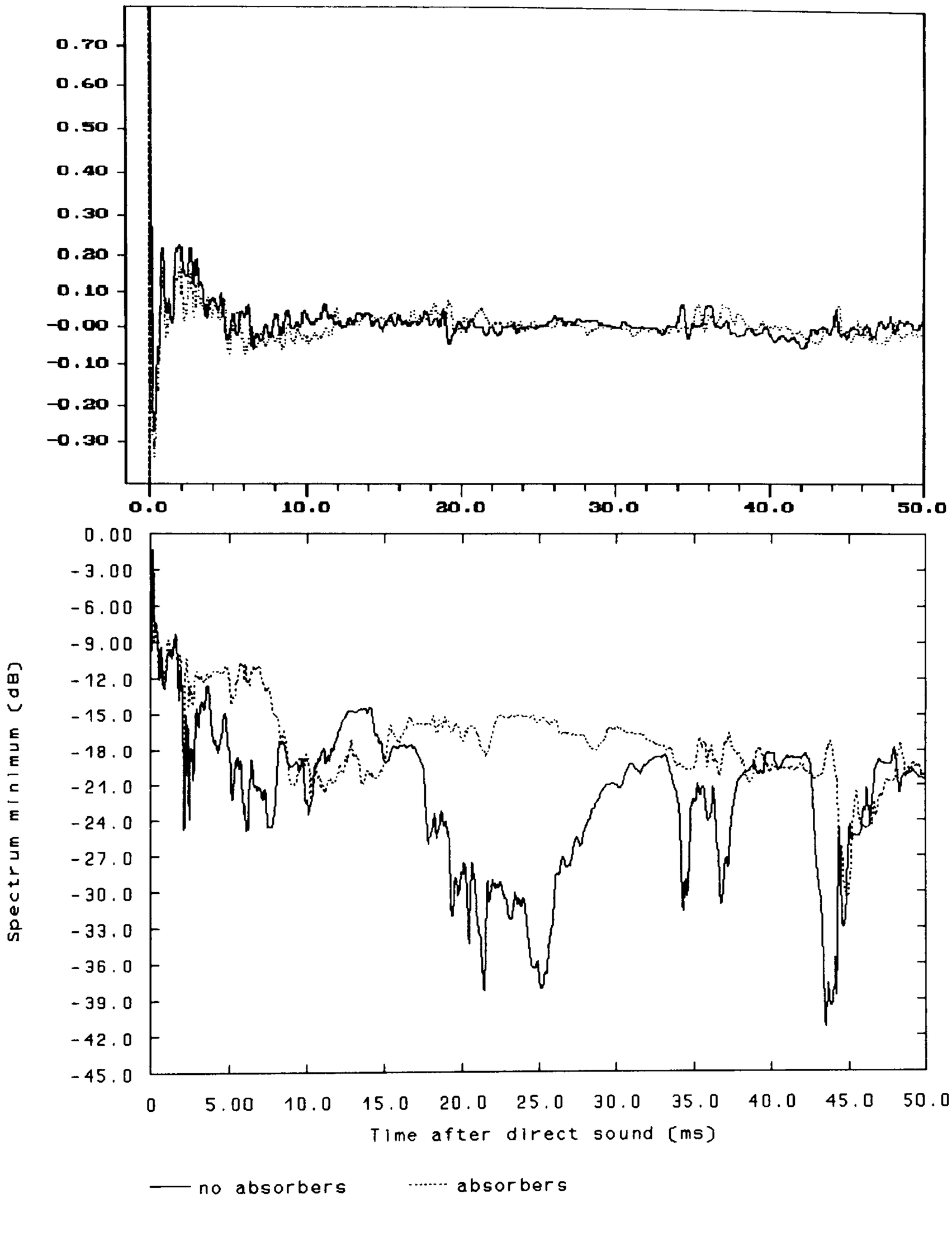

Figure 7.5: Effect of floor absorbers on narrowband seat dip minimum over time, plotted below the low-pass filtered impulse response (3 rows back, m = 1.14 metres, $\theta = 83°$, $\phi = 90°$).

These graphs give further support for the conception of seat dip attenuation as the spectral effect of discrete reflections from the seats and floor. The absorbers seem to have substantially attenuated the early seat-floor reflections, in the region 2.5 - 8 ms. This can be seen in the impulse response, but is more clear in the spectrum minimum graph. The worst period of attenuation, after the side wall reflection arrival, has also been dramatically affected by the absorbers. Around 12 ms, however, the absorbers have made the attenuation deeper. This is perhaps due to their effect on sound which reflects between the floor and underside of the seats many times. These waves would tend to strike the absorbers themselves near grazing incidence, and thus be reflected with negative amplitudes. This is according to the simple law of specular reflection:

$$R = \frac{z\cos\theta - 1}{z\cos\theta + 1} \qquad (7.2)$$

where R = complex reflection coefficient

z = impedance of the absorber in $\rho_0 c$ units

θ = angle to the normal

As θ approaches 90° , then $|R| \rightarrow -1$. Although this is probably a crude simplification for some complex wave behaviour in this region, some small negative reflections do appear in the impulse response with absorbers in the right time region.

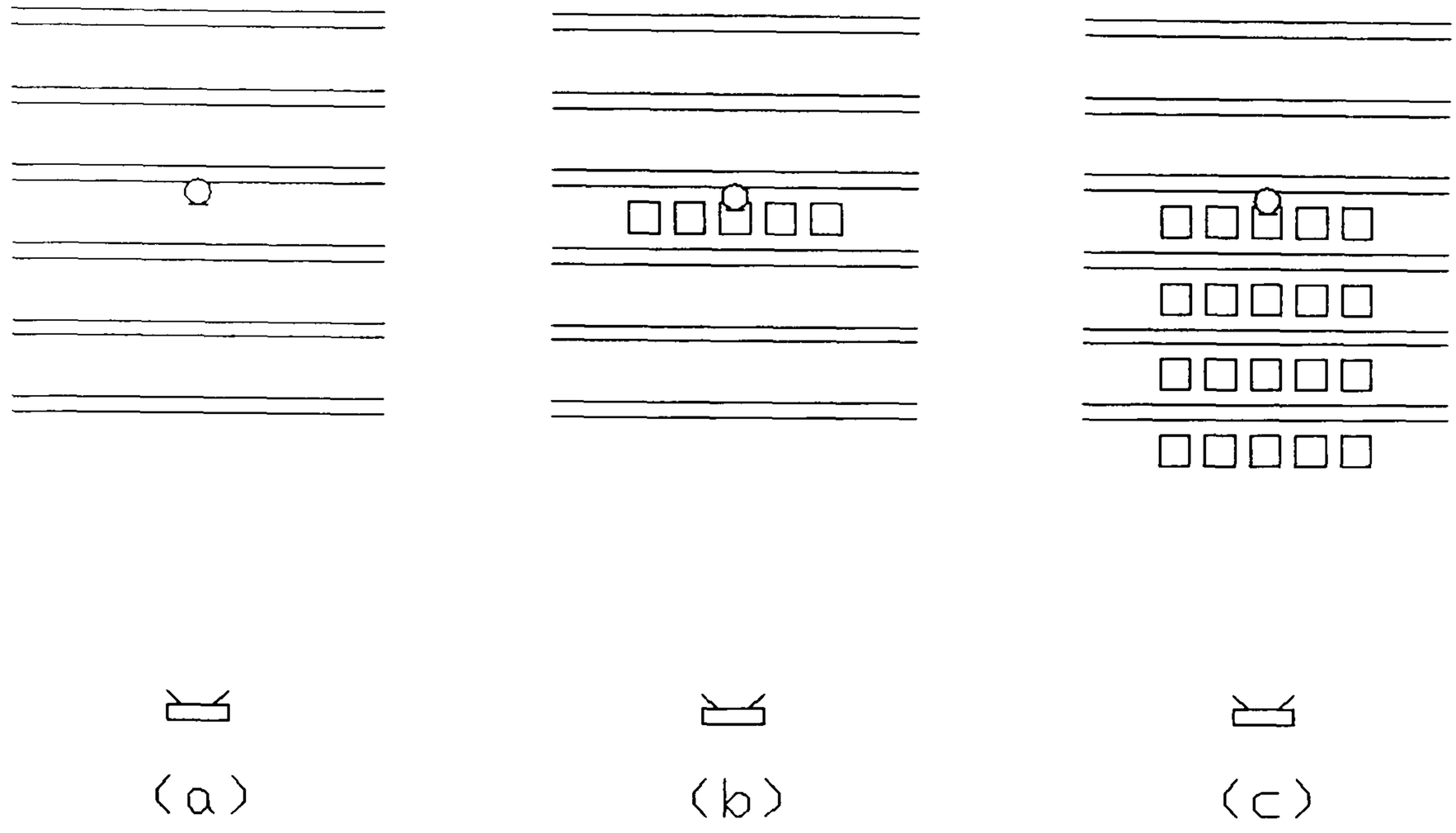

Figure 7.6: Plan views of arrangement for experiment with different rows of absorbers: (a) no absorbers; (b) absorbers in microphone row only; (c) absorbers in all rows in front of microphone.

7.2 The Effect of Each Row of Absorbers on Discrete Reflections

If seat dip attenuation is indeed caused by groups of discrete reflections, then this should be evident if one, then two, then three rows of absorbers are used. An experiment was conducted with the microphone three rows of seats back, as shown in figure 7.6(a). After measuring the transfer function with no absorbers, five modular Helmholtz absorbers were placed on the floor in the row containing the microphone, and the measurement repeated (figure 7.6(b)). The rows in front were then similarly filled one by one with absorbers and the measurement made again each time.

Figure 7.7 shows the effect that this has on the magnitude of the dip over time. This effect is typical of all three types of absorber. One row of absorbers lessens the attenuation in the period 3 - 7 ms, which agrees well with the sample ray constructions outlined in figure 6.9. Some seat/floor ray paths do not reflect from the floor in this row, though, so filling all the rows in front of the microphone further lessens the attenuation in this interval. In particular, putting absorbers at the very front lessens the early attenuation at 2.2 ms. This is when the first "front floor" reflection (see figure 6.9) would arrive for this measuring arrangement. This very early attenuation could presumably have been further ameliorated by spreading the absorbers further over the floor area in front of the seating. It is, however, the single row of absorbers nearest the microphone which has the greatest effect, as might be expected.

As in figure 7.5, the floor absorbers in figure 7.7 have had a deleterious effect on the attenuation minimum when more complicated reflections might be arriving. Further evidence for complicated paths after 10 ms appears when absorbers are added, one row at a time, to the two rows behind the microphone. Figure 7.8 plots what happens to the attenuation minimum in this case. When the rows in front of the microphone are already filled with absorbers, adding absorbers to the rows behind has a negligible effect on the maximum attenuation for the first 8 ms. After this, it seems that scattered sound from seats and floor behind the microphone must have an effect on the attenuation at the microphone. Again, the effect of the absorbers is not always beneficial in this interval. This back-scattered sound must be following a complicated path if its delay is at least 8 ms, and it comes from the

Figure 7.7: Early seat dip spectrum minimum over time, with different numbers of seat rows filled with absorbers. (3 rows back, m = 1.14 metres, $\theta = 87°$, $\phi = 90°$.)

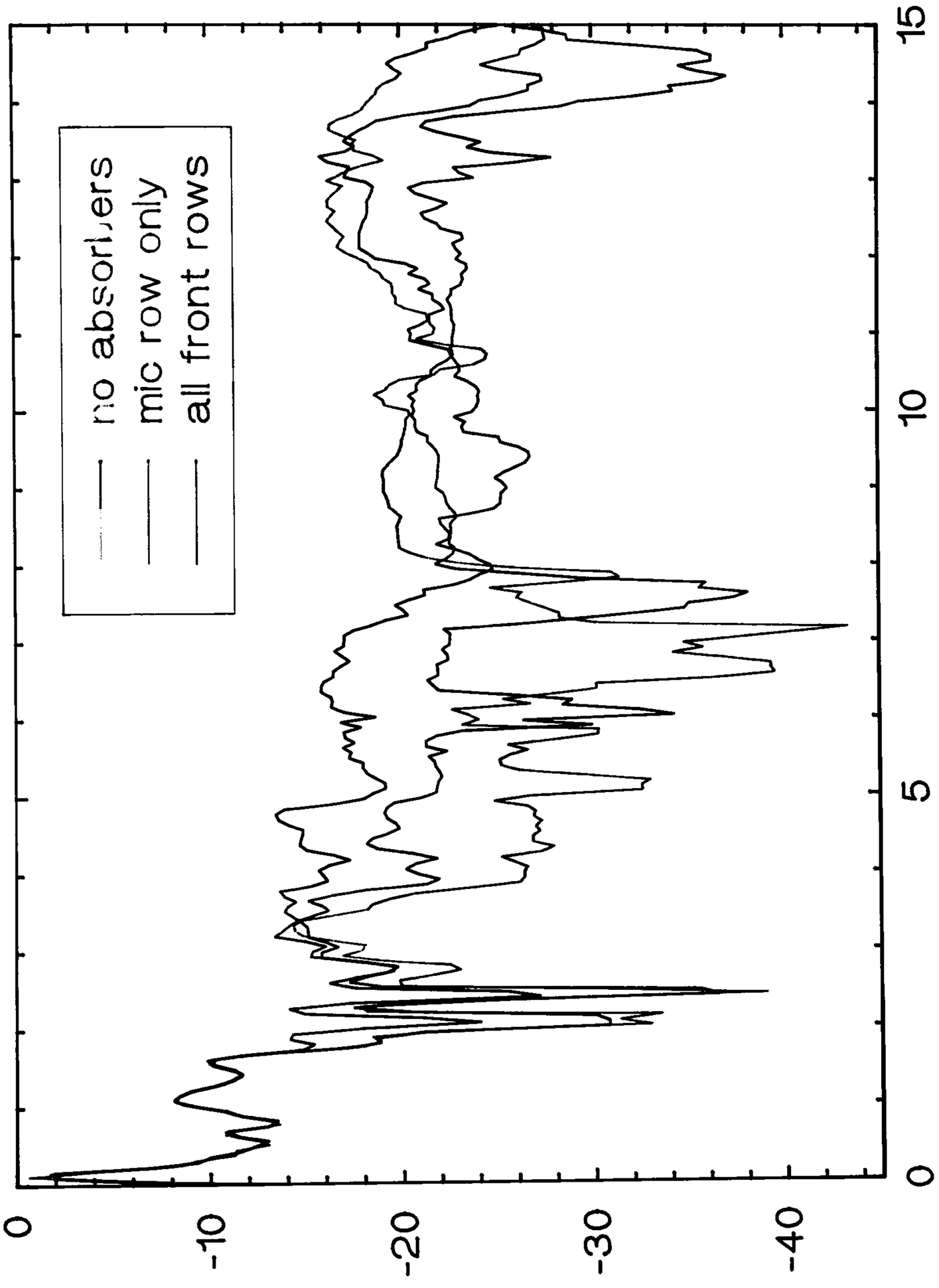

Figure 7.8: The effect of filling seat rows behind the microphone with floor absorbers, on the seat dip minimum of the early spectrum. (3 rows back, m=1.14 metres, θ=87° , ϕ=90° .)

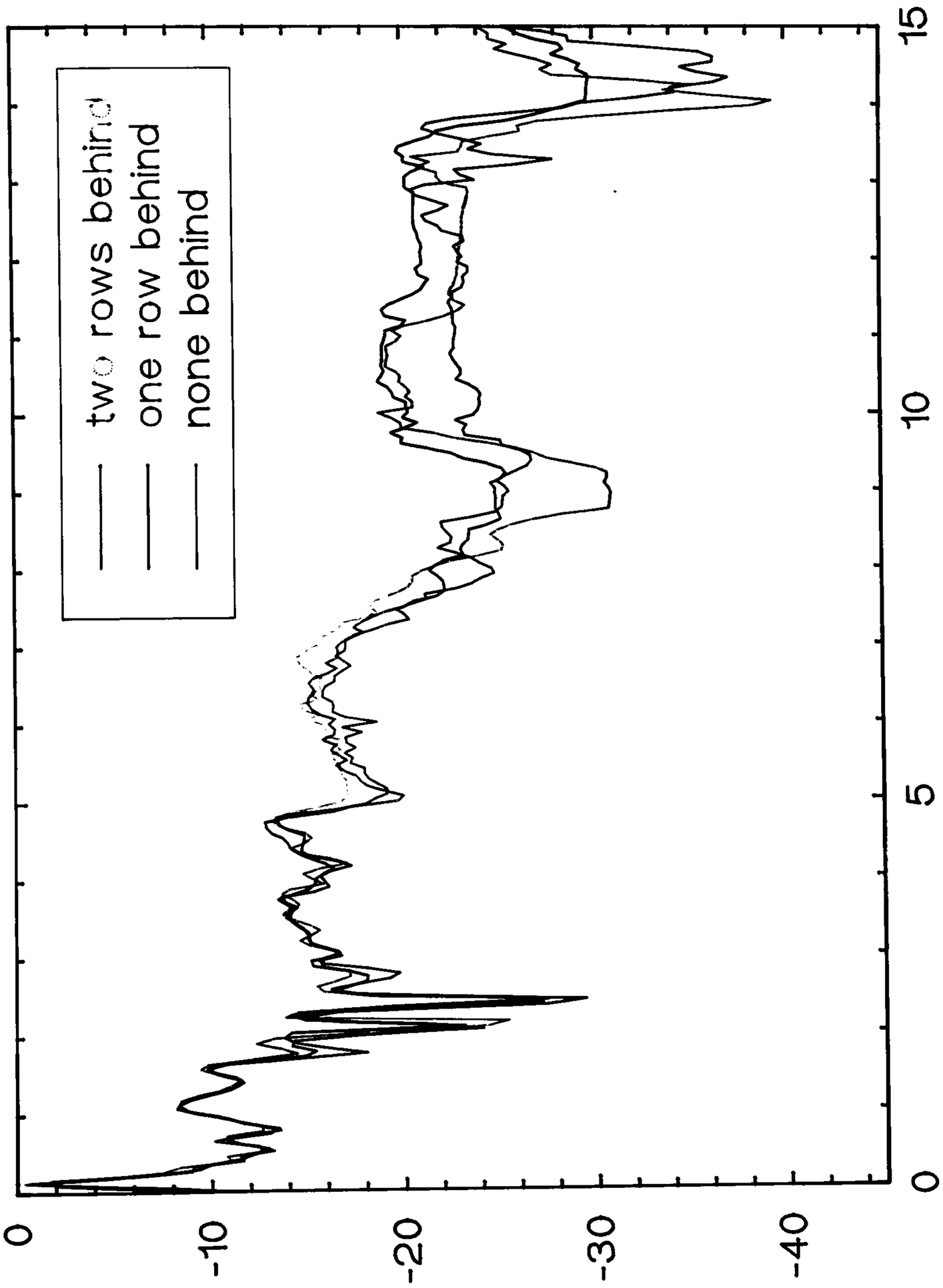

seats and floor immediately behind the microphone. Note that this delay is too short for another room boundary reflection to have arrived.

In general, although the floor absorbers do not raise the dip minimum at all points in time, they do keep it at a more constant level over the first 50 ms. This stabilisation may be of some use in itself to hall designers. The stabilisation phenomenon, and the absorbers' effect on the early seat-floor reflections are common to all measuring positions.

7.3 Classifying Absorber Performance by θ and r

The effect of the absorbers on the maximum narrowband attenuation has proved useful in providing further evidence for the nature of the attenuation process. However, a reduction in narrowband attenuation is probably not as subjectively significant as the effect on octave bands. Hence, the factors governing absorber performance were sought by looking at their effect on 100, 200 and 400 Hz octave band levels over time for 128 measurements. The three clearest factors were found to be θ, r, and absorber type. Four groups of absorber effect were identified, differing mostly in θ.

At low values of θ (72° , 77° & 80°), the absorbers make little difference. For 77° (figure 7.9), the early attenuation is mostly in the 100 Hz band, but after 20 ms the octave band attenuation is never greater than 5 dB in any of the 100, 200 or 400 Hz bands.

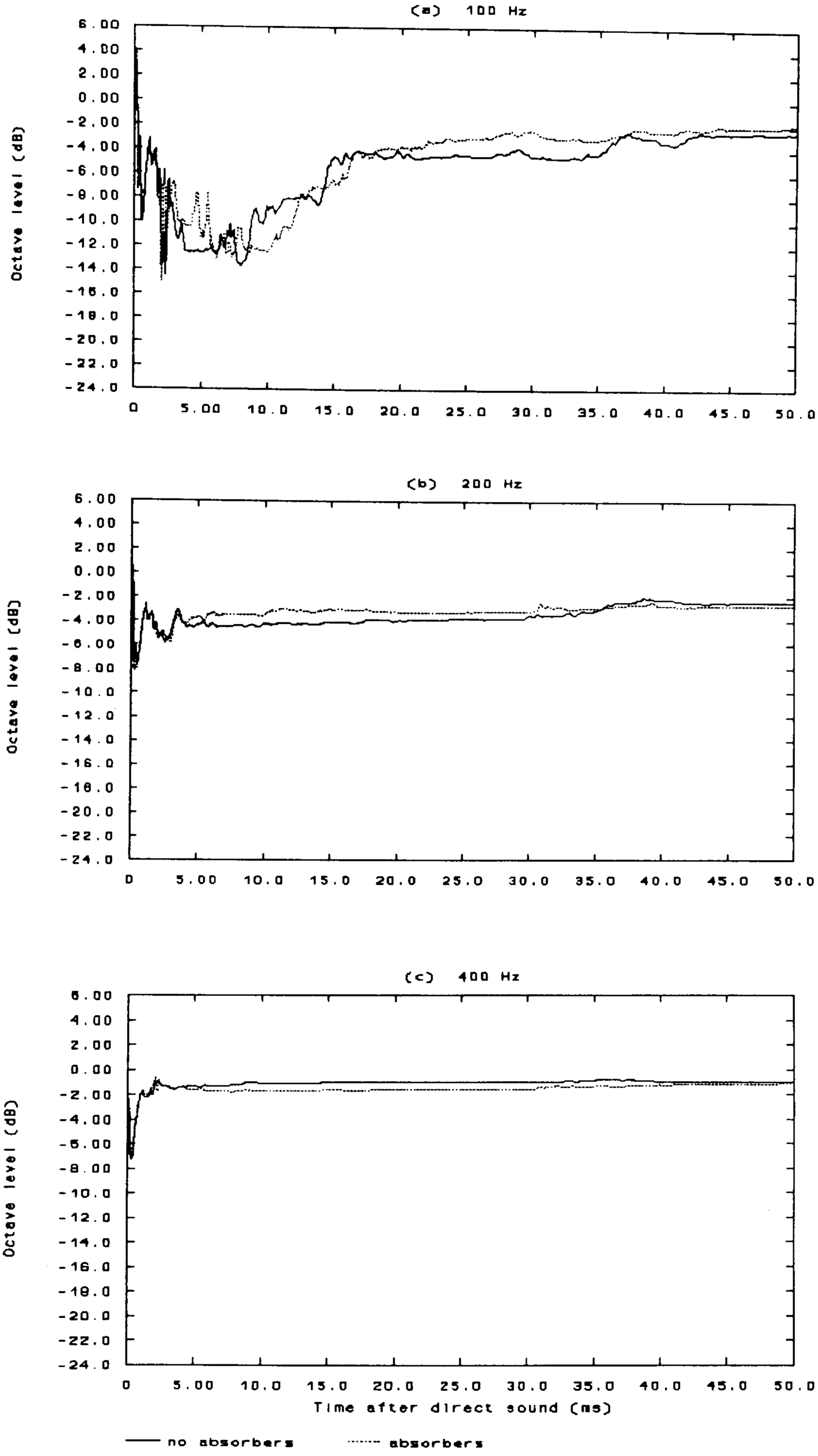

Figure 7.9: Low θ and the effect of Helmholtz absorbers on (a) 100 Hz, (b) 200 Hz and (c) 400 Hz octave band levels in a seat dip spectrum over time. (6 rows back, m = 1.14 metres, $\theta = 77°$, $\phi = 90°$.)

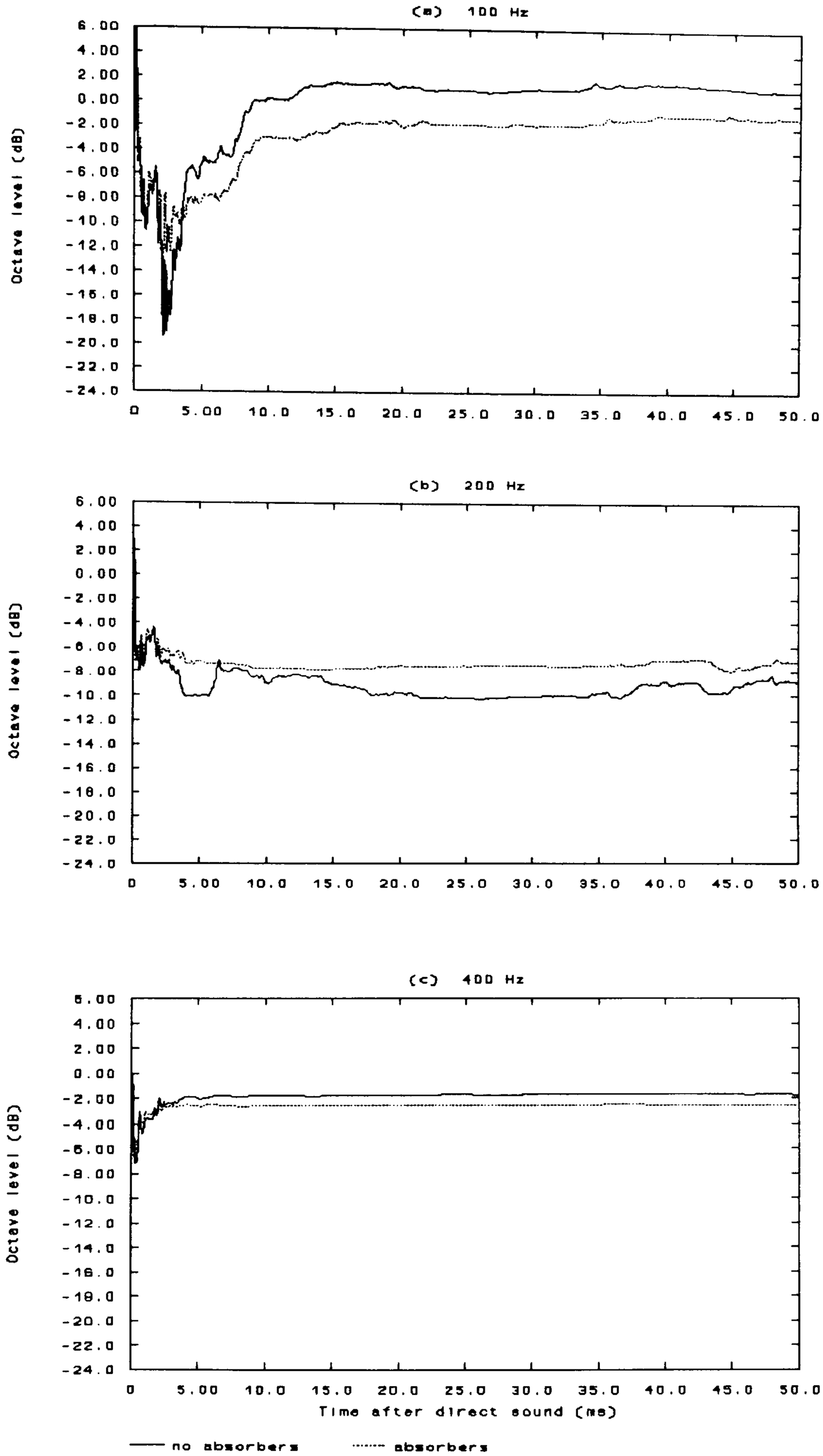

Figure 7.10: Medium θ and the effect of Helmholtz absorbers on (a) 100 Hz, (b) 200 Hz and (c) 400 Hz octave band levels in a seat dip spectrum over time. (3 rows back, m = 1.14 metres, $\theta = 83°$, $\phi = 90°$.)

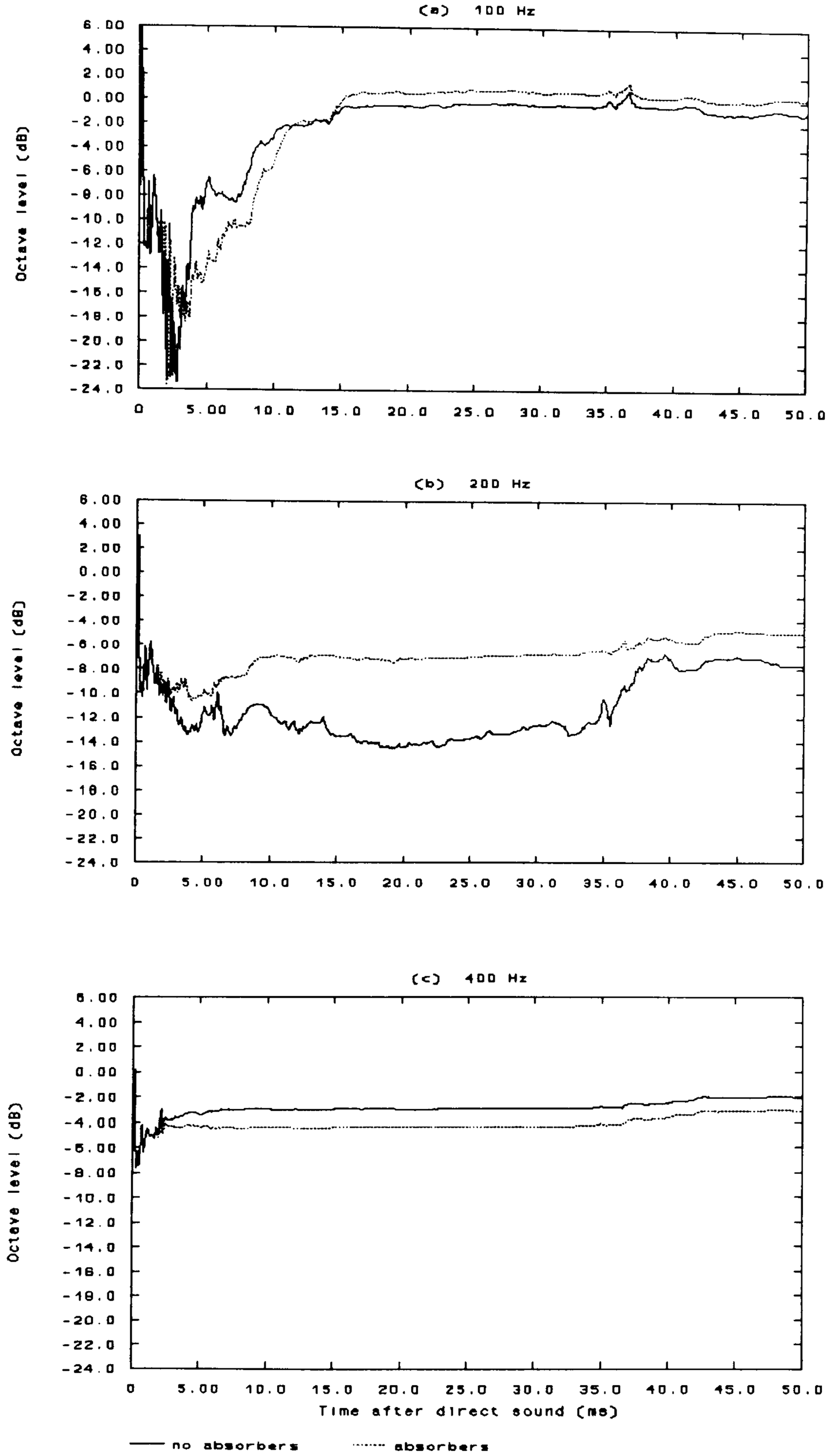

Figure 7.11: The best case: medium θ and the effect of vent absorbers on (a) 100 Hz, (b) 200 Hz and (c) 400 Hz octave band levels in a seat dip spectrum over time. (6 rows back, m=1.14 metres, θ=87° , ϕ=90° .)

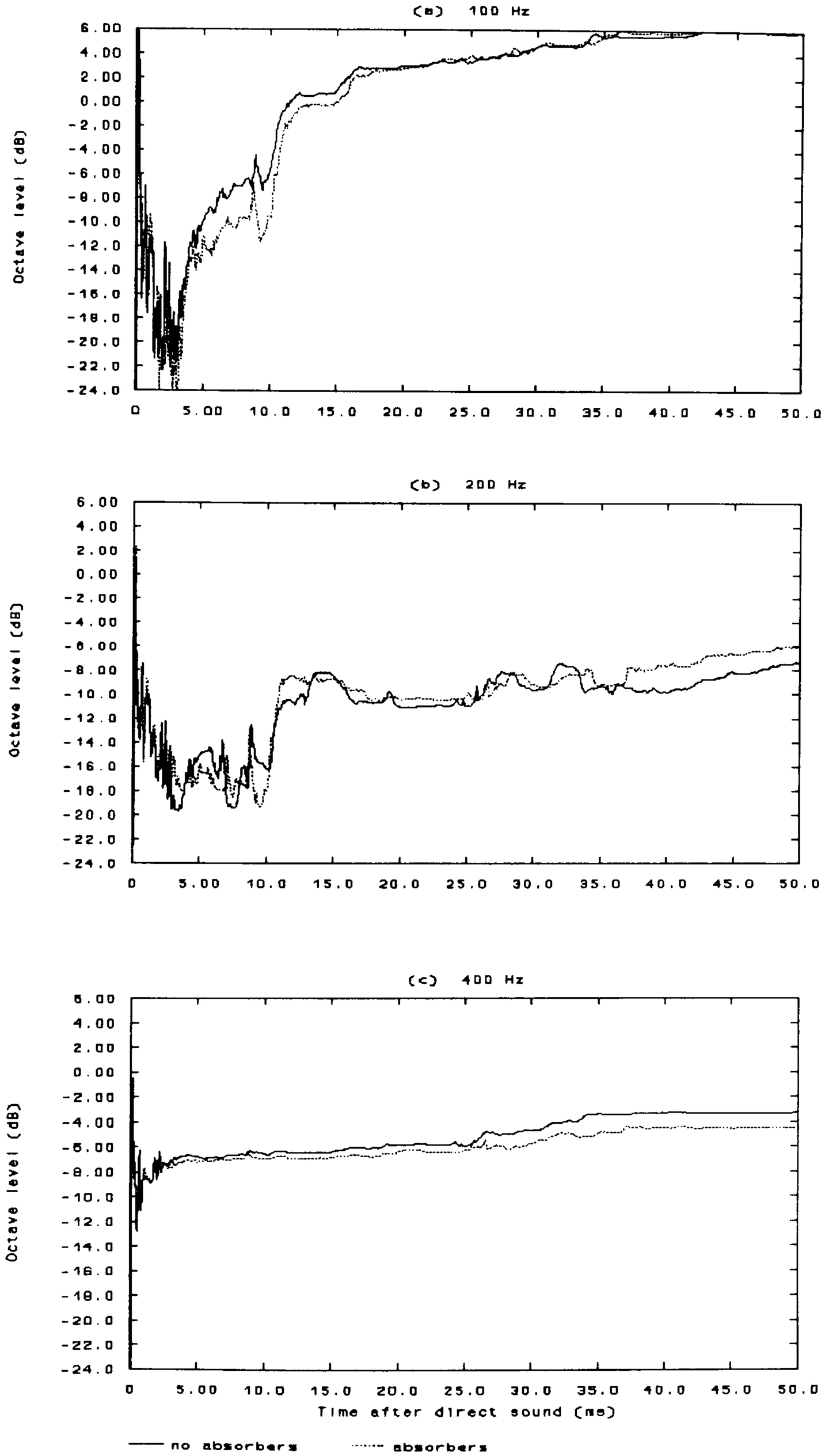

Figure 7.12: High θ and the effect of Helmholtz absorbers on (a) 100 Hz, (b) 200 Hz and (c) 400 Hz octave band levels in a seat dip spectrum over time. (12 rows back, m=1.14 metres, $\theta=89°$, $\phi=90°$.)

At higher values of θ, 83° - 87° , the early deep attenuation in the 100 Hz octave does not last long. After around 5 ms, the 200 Hz band is the worst affected. In most of the measurements in this range, floor absorbers raised the 200 Hz band level at the expense of the 100 Hz level, for most of the 5 - 50 ms period. Figure 7.10 shows a typical measurement, made at 83° . Thus, in the octave spectrum over this period, the dip becomes broader and shallower. This may be considered an improvement. There is some evidence that, within this range of θ, the absorbers make a greater difference at a greater source-receiver distance. This is not surprising; at a position nine rows back, the microphone would receive many more reflections which have hit the floor between rows, than at a position three rows back. There is therefore more scope for the absorbers to be effective.

The third group of results is composed of a few exceptions to the general behaviour of the 83° - 87° group. Figure 7.11 plots one of these: the floor absorbers make a large improvement in the 200 Hz band, with little, or no, deleterious effect in the adjoining bands. Though repeatable, these were not confined to any one absorber type or exact measuring position. Factors other than floor absorption may be at work in producing this almost ideal behaviour. For the case in figure 7.11, for example, the vent boxes used were tall enough to partially block any sound paths via the seat underpass. Other experimenters - Ishida *et al.* (1989) and Sessler and West (1964) - have shown that blocking the underpass can reduce attenuation. One of the other measuring positions in this group was also close enough to two balcony fronts to receive significant early unattenuated energy from them. (This was

estimated using a computer model by Lam and Hodgson (1990) available at Salford which can calculate the integrated sound field around an arbitrary object.)

The fourth group of results is taken from measurements made at the most extreme values of θ: 88° and 89° . As figure 7.12 shows, at these positions, the 400 Hz octave is badly attenuated as well as the 200 Hz one. The floor absorbers have little effect. It therefore seems that at angles very close to 90° , any reflections via the floor are little affected by floor absorbers. These angles are, though, rather closer to grazing than those one would expect to find in an auditorium.

7.4 Differences between Absorbers

In general, the Helmholtz modular absorbers were found to be the most effective in raising the 200 Hz octave band level, and figure 7.13 shows a typical comparison. This is probably because they were found to have a higher random incidence absorption coefficient than the others: see figure 7.1. The panel absorber seems to act at too low a frequency to be of much help. The vent boxes were almost as effective as the Helmholtz absorbers in the 200 Hz octave, and they typically reduced the 100 Hz octave levels less (it should be noted that the range of the level axis in figure 7.13(a) is twice that in (b)). This greater focusing of effect is probably due to the sharpness of the resonant absorption peak of the vent boxes in figure 7.1. All the absorbers had a very similar effect on the 400 Hz octave (a very small reduction in level for most measurements), so this is not shown in figure 7.13.

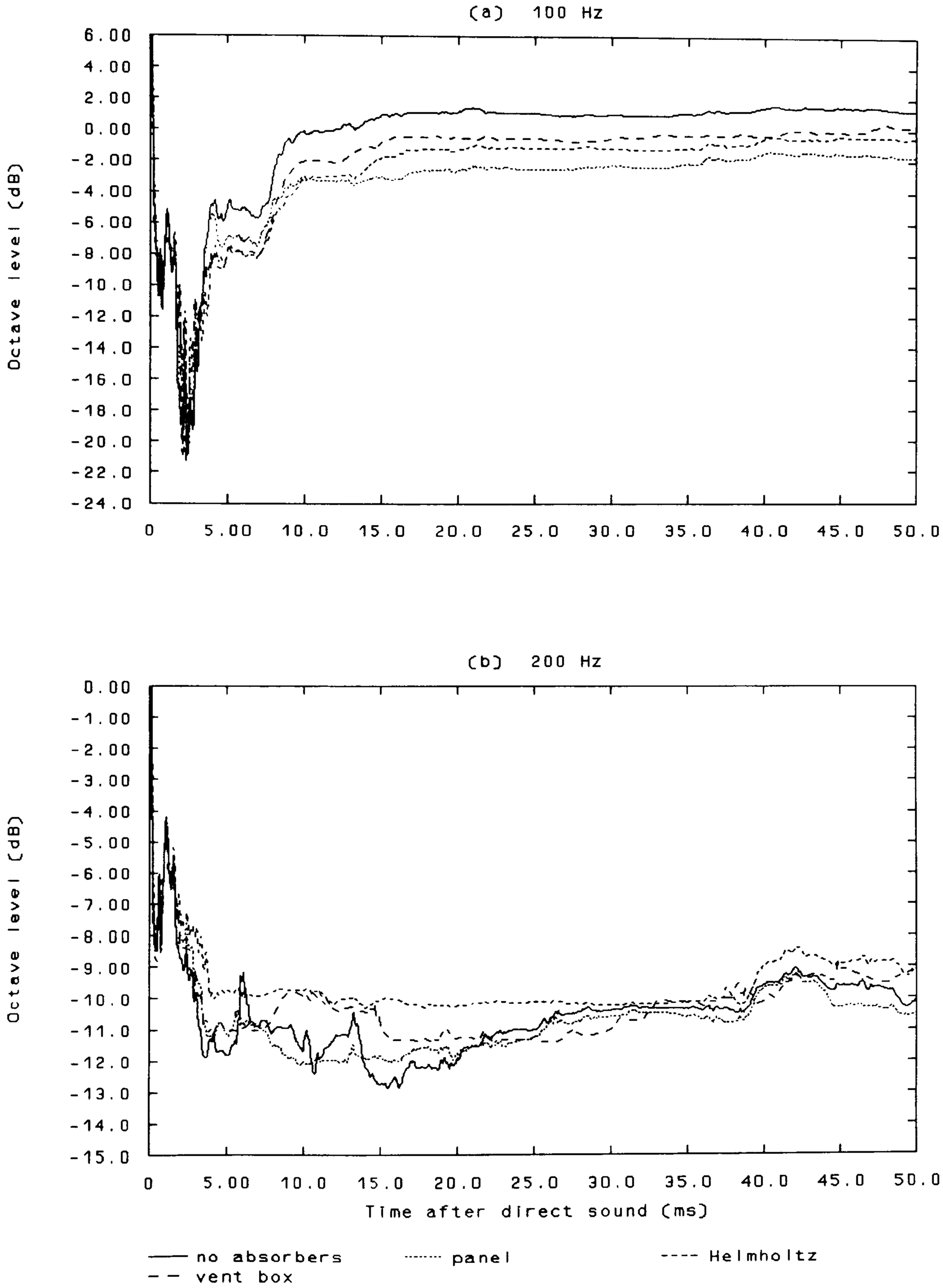

Figure 7.13: Differences in performance of floor absorbers over time in reducing (a) 100 Hz and (b) 200 Hz octave band seat dip attenuation. (3 rows back, m=1.14 metres, θ=87° , ϕ=90° .)

Of the three types of absorber studied, then, the floor ventilation outlet boxes are probably the best choice for attempting to improve seat dip attenuation without interfering too greatly with lower frequency octave levels in the early sound. These absorbers are also the best from a practical point of view, since they can be more easily incorporated into the building of a new hall as part of the ventilation system, than could either of the other two types.

7.5 Other Effects of Floor Absorbers

Bradley (1991) used the strength of the first 40 ms of sound, G_{40}, to investigate the beneficial effects of overhead reflectors on reducing seat dip attenuation. Maximum improvements of 2 dB at 125 Hz and 3 dB at 250 Hz were obtained. Maximum effects of a similar order were found in the present study on floor absorbers, as figure 7.14 shows.

The floor absorbers, though, are more selective than overhead reflectors. Figure 7.14 shows that they only effect low-frequency G_{40} values. Bradley's figure 10 shows that the reflectors increase G_{40} values from 125 to 4000 Hz. Because such plane reflectors provide significant early energy at mid and high frequencies from overhead, they may cause serious image shift and tonal coloration via the comb filter effect Barron (1974, p. 32).

The most important disadvantage of floor absorbers is that they will tend to increase the random incidence absorption coefficient of auditorium seating at low frequencies. Figure 7.15 presents a measurement made on seating with and without

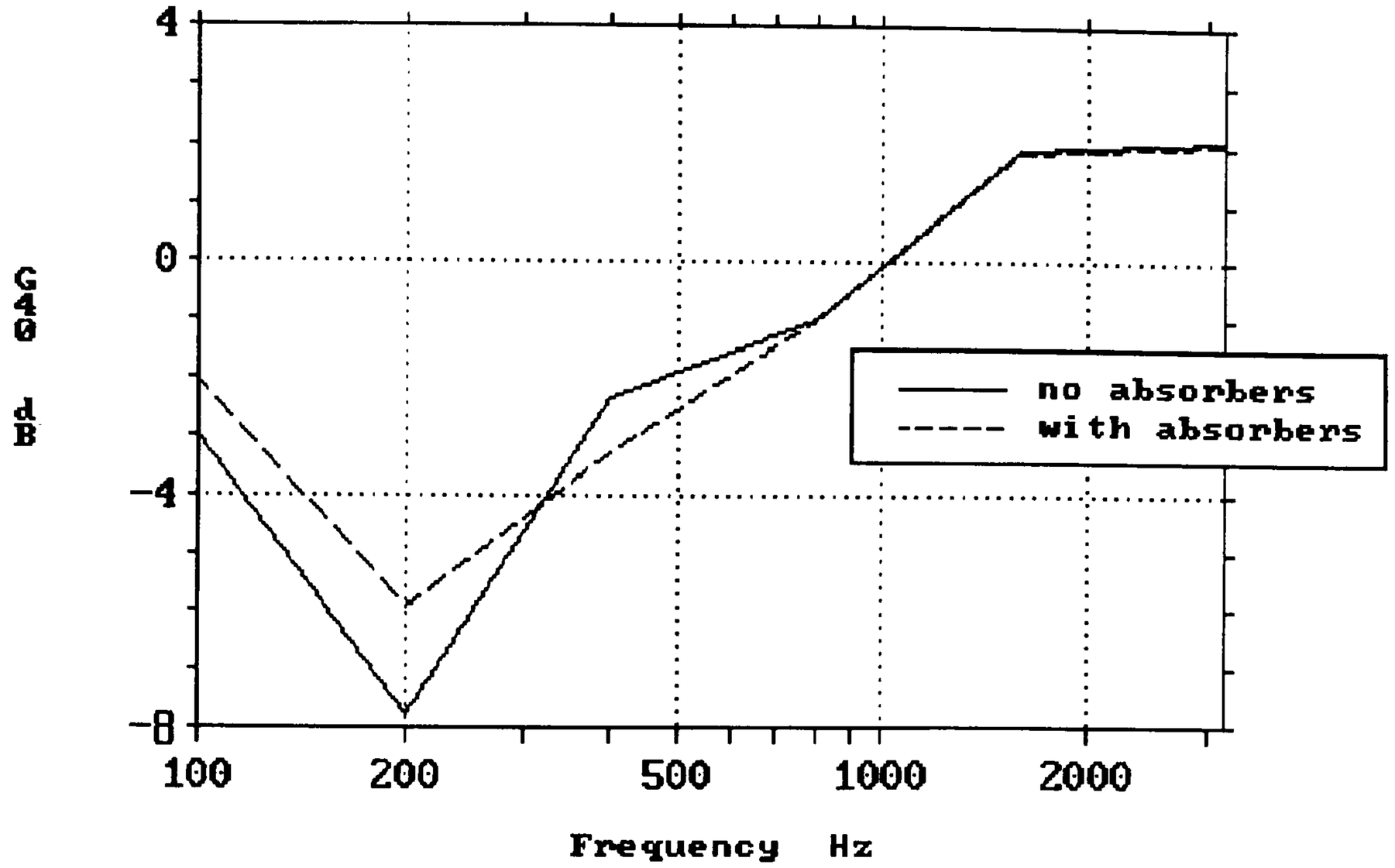

Figure 7.14: Effect of floor absorbers on strength (G_{40}). (6 rows back, m=1.14 metres, θ=87° , ϕ=90° , vent boxes used.)

vent outlet boxes exposed. This measurement was made in the rather non-diffuse reverberation chamber mentioned above. The measurement configuration was three rows of six seats, at a 1 metre row spacing, with one vent outlet under each chair. The seats were placed in the corner of the chamber, following the method investigated in chapter 2, but barriers were not available to obscure the front and side of the seating array. (Again, due to time constraints, this measurement in the Finnish reverberation room was not ideal.) Consequently, the absolute absorption coefficients are unrealistically high. Nevertheless, the magnitude of the increase shown probably is realistic. Although these absorbers have little damping, and a sharp absorption peak at 250 Hz, they have affected most of the low-frequency

range considerably. The two other types of floor absorber used have broader resonance peaks, and so would be likely to affect seating absorption even more. It should be noted that this measurement was made on unoccupied seats. Occupied seats would have a higher absorption coefficient to start with (see figure 2.13, above), and so would perhaps not be affected so greatly.

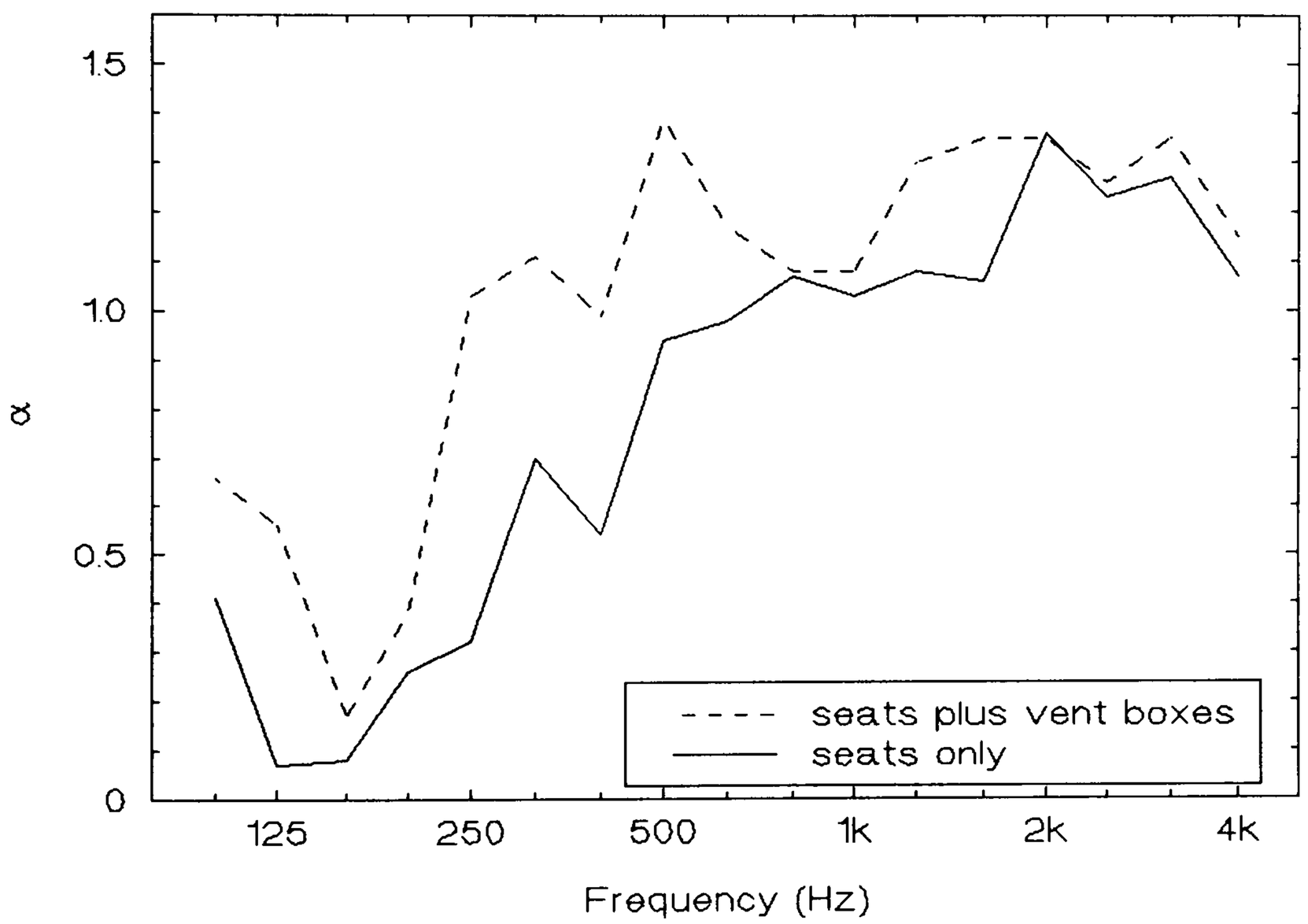

Figure 7.15: Increase in random incidence absorption of well-upholstered auditorium seating caused by vent box floor absorbers.

Chapter 8

The Third Dimension of Seat Dip Attenuation

So far, the seat dip effect has been treated mostly as a two-dimensional one. This is a simplification: the width of seating plane over which the direct sound propagates significantly affects the attenuation at the microphone. To investigate this, first of all some 1:10 scale model seats were developed.

8.1 1:10 Scale Model Seat Experiment: Variation of Attenuation with Seat Plane Width

Though the seats are limited in detail they have the principal dimensions of a particular well-upholstered concert hall seat including that of the underpass height, as shown in figure 8.1. This real seat was a standard model from a large manufacturer. The models are constructed from 20 ga. aluminium and 30 kg/m^3 CMHR foam. The random incidence absorption coefficient of the model seats is accurately scaled, as shown in figure 8.2. The absorption coefficient of the seats was measured in an exact 1:10 scale model of the standard ISO reverberation chamber used for the full-scale measurement. Though the arrangement of stationary diffusers and microphone positions was different in the model, it complied with appropriately scaled values of all the B.S. criteria.

Because the seats are physically accurate, it means that the absorption is probably realistically distributed over the seats, and this distribution is important for the

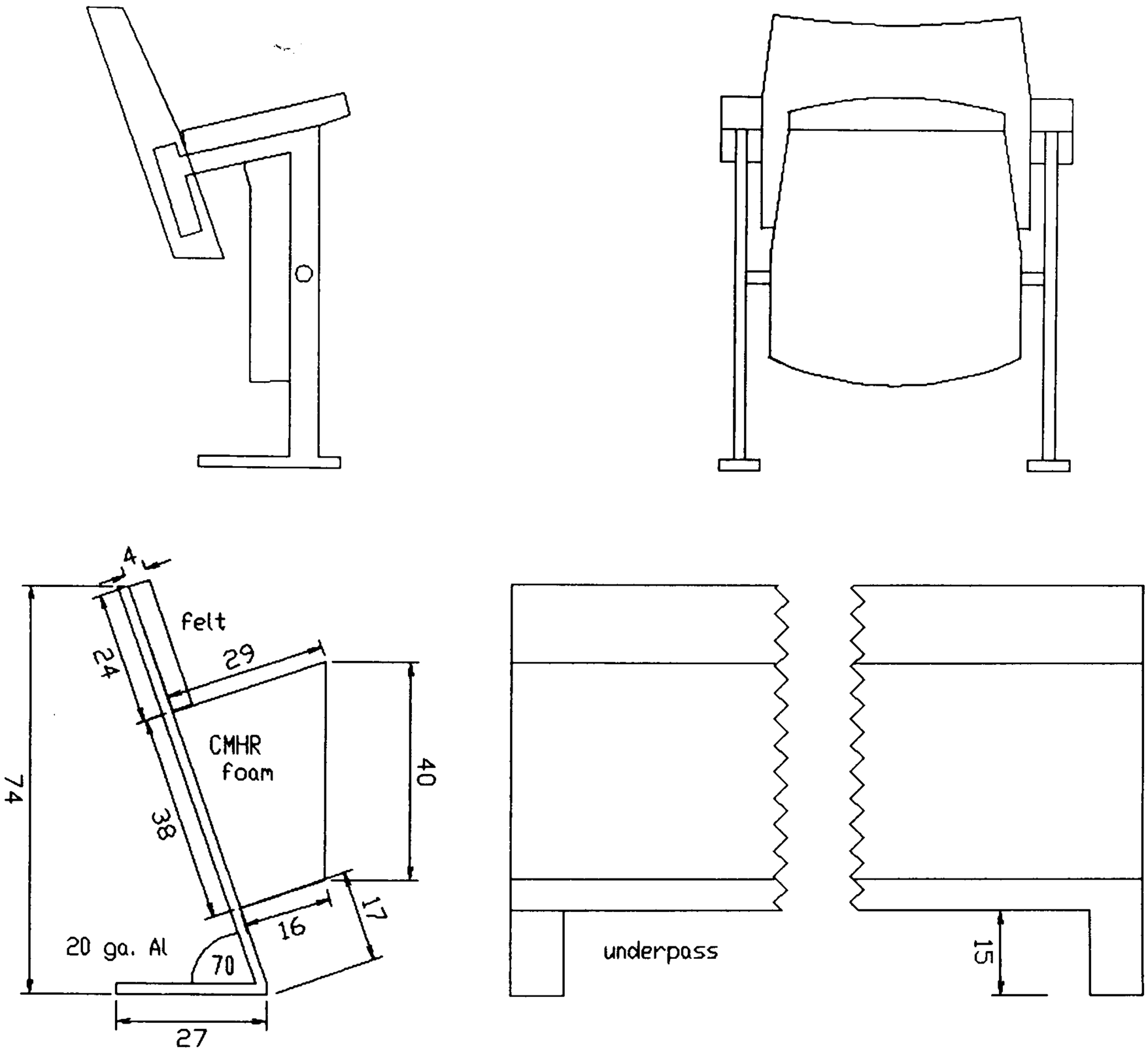

Figure 8.1: The 1:10 scale model bench seat below the standard full-size auditorium chair on which it is based.

investigation of seat dip attenuation. (In particular, as section 9.3.5 will show, the impedance of the top of the seat back is probably important.) It is expected that measurements performed on these seats will have relevance at full scale. The floor was a 2 mm lead sheet bonded to 10 mm plywood (placed lead uppermost).

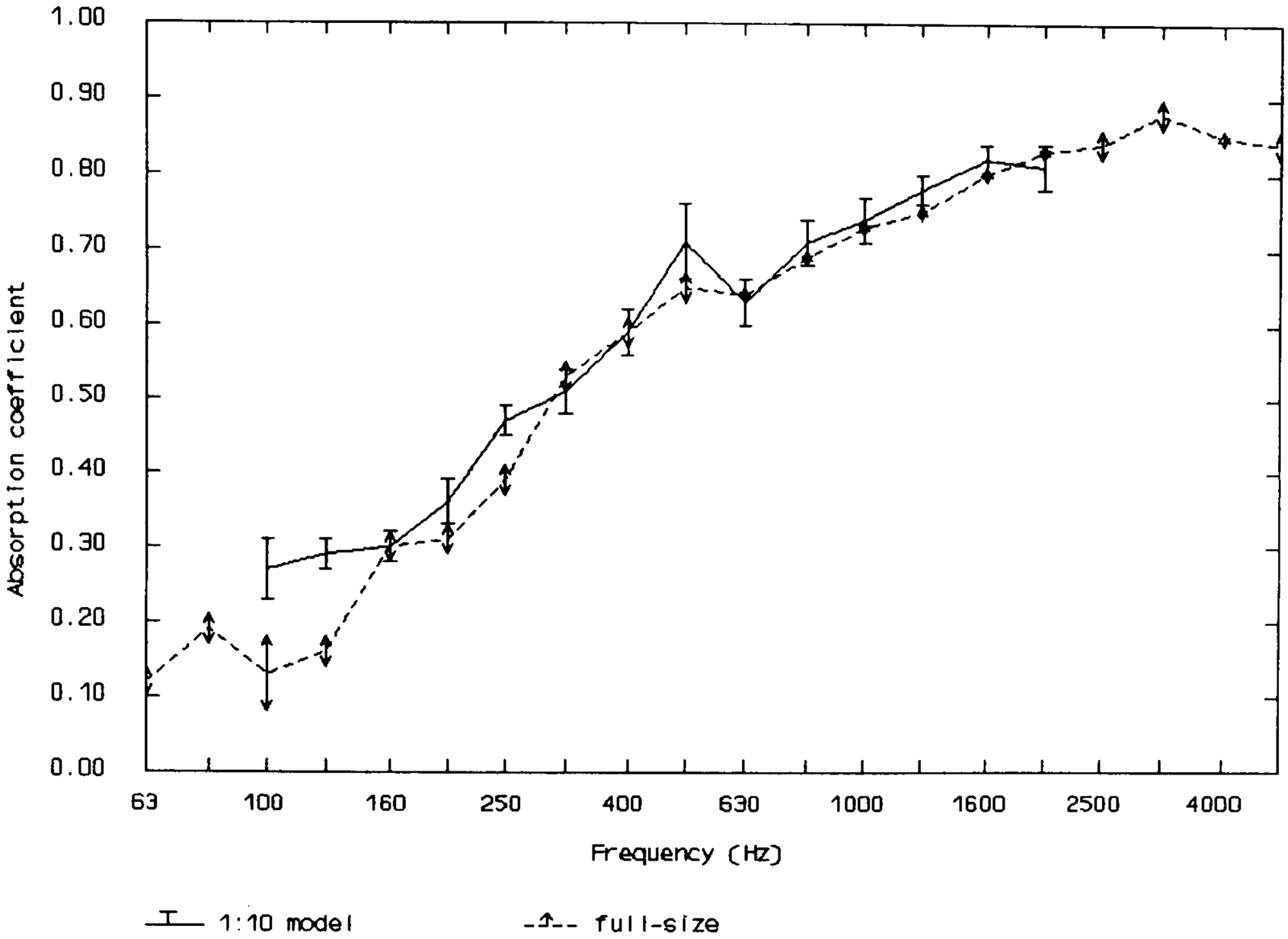

Figure 8.2: Absorption coefficient of 1:10 scale model seats and full-size well-upholstered seats. The bars represent ± one standard error.

The seat dip measurements were performed in an anechoic chamber. 10 rows of bench seats were arranged as in figure 6.1. The frequency response function across six rows of seats was determined for three different widths of seat-floor plane, corresponding to five, ten and twenty seats wide. For all the measurements, l = 143 mm, m = 114 mm, r = 836 mm, θ = 88°, ϕ = 90°. The microphone was always at the midpoint of the width of the plane and, this time, the row spacing was 90 mm. In each case the floor was the same width as the seats. As before, the measured spectra were normalised to one of just the loudspeaker and microphone under anechoic conditions. A photograph of a measurement over the narrowest plane appears in figure 8.3.

Figure 8.3: Seat dip attenuation measurements on 1:10 scale model seats in an anechoic chamber.

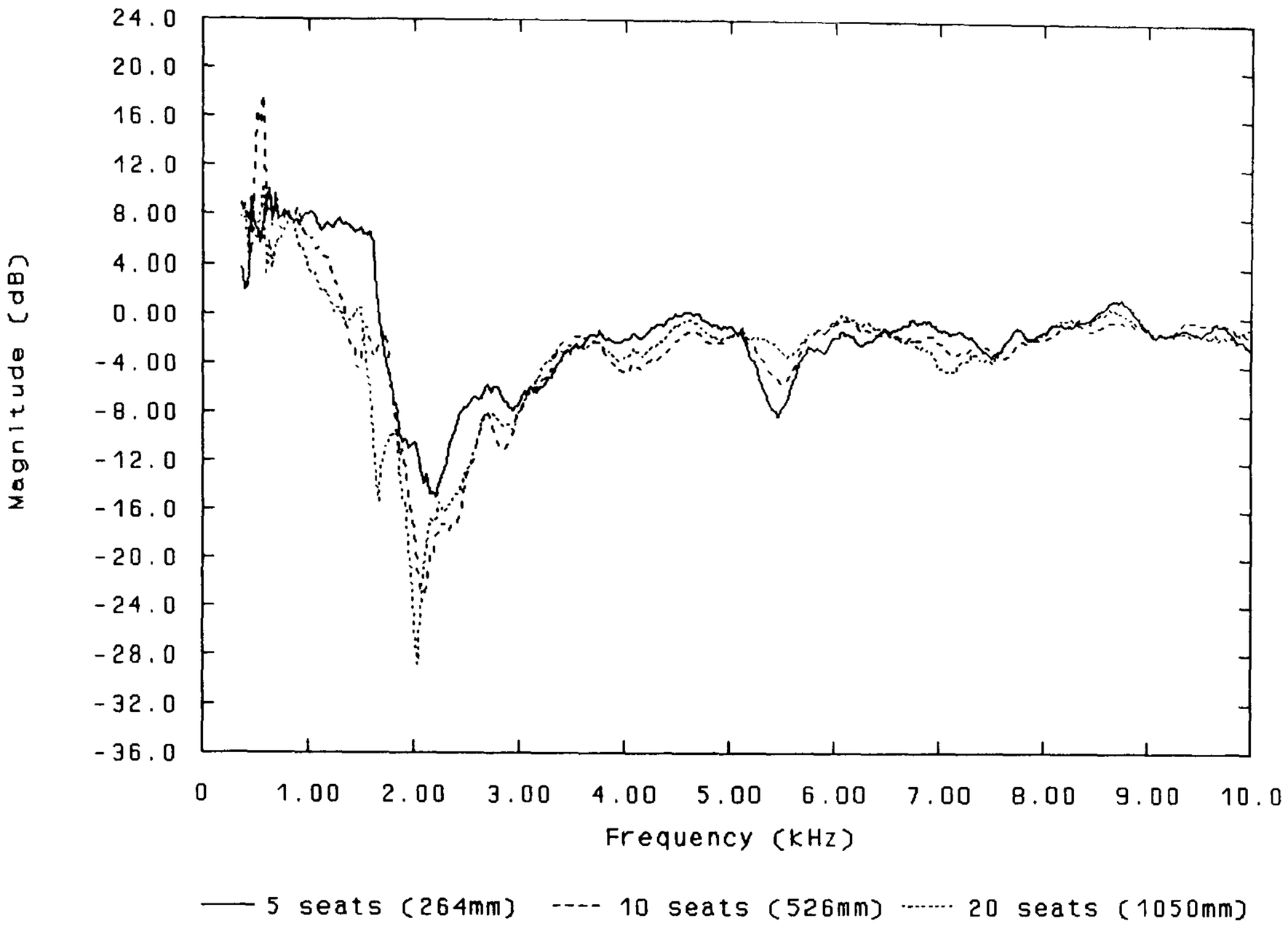

Figure 8.4: Transfer function across 1:10 scale model seats. Parameter: width of seating plane (6 rows back, m=114 mm, θ=88° , ϕ=90°).

The results in figure 8.4 are obtained by Fourier Transforming the full 35 ms impulse responses. They show that the main effect of widening the seat-floor system is to deepen the attenuation dip. The maximum attenuation is increased from 15 to 23 to 29 dB, whilst the frequencies of maximum attenuation are almost identical.

A second effect of widening the seat-floor plane is to lessen the strength at the microphone of sound diffracted from the edges of the floor. This is probably what has caused the small dip at 5.5 kHz in figure 8.4 to decrease in size as the plane is widened. Because the stalls floor extends much further than a width of ten seats

in a typical real concert hall, one would not expect this phenomenon to occur in such a hall. No evidence of it was found in the Free Trade Hall measurements in chapters 6 and 7. At a width of twenty seats, this second dip is negligible.

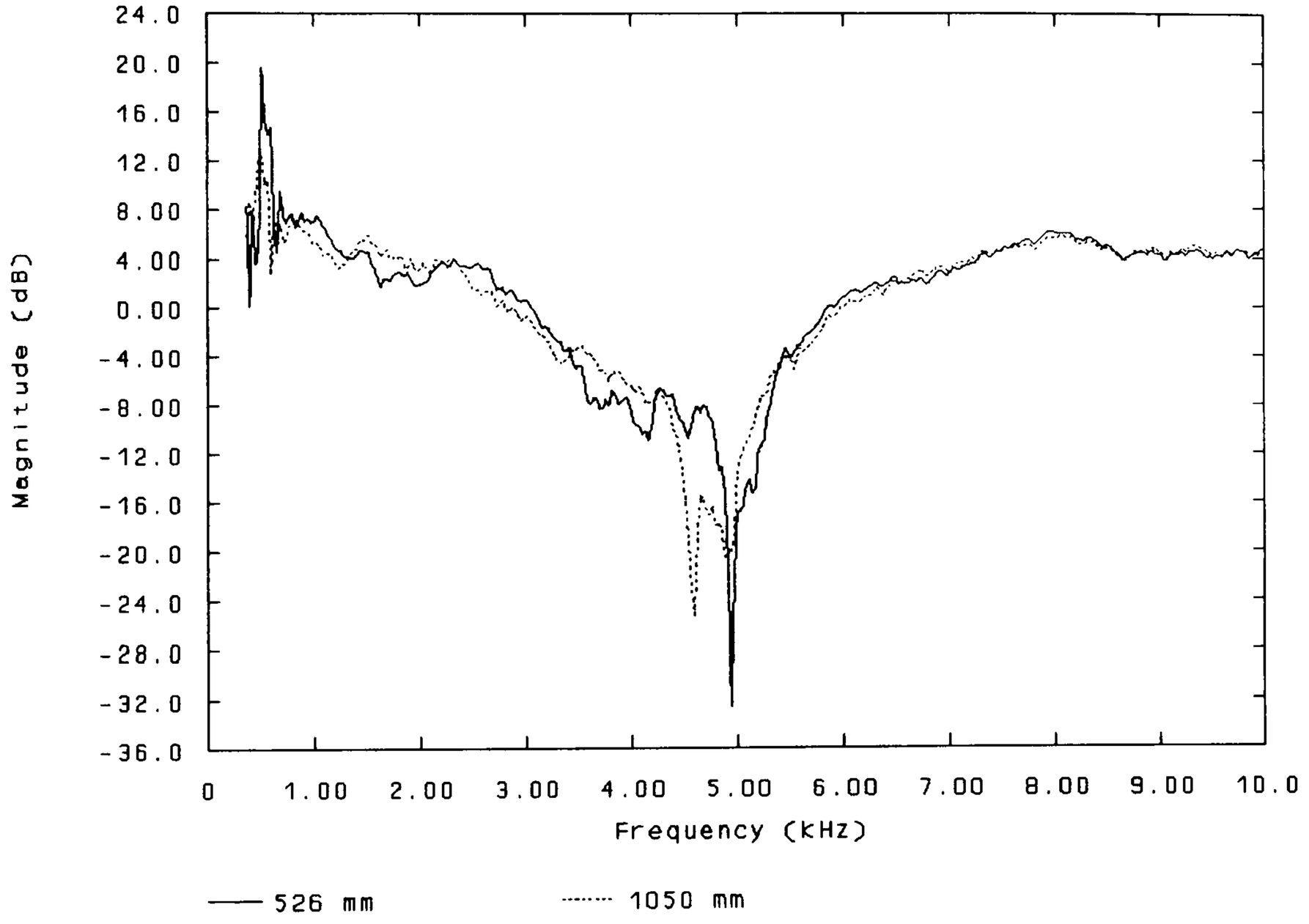

Figure 8.5: Transfer function across centre of 1:10 scale model floor plane only. Parameter: width of floor plane (r=835 mm, m=114 mm, θ=88° , ϕ=90°).

To provide further evidence for floor edge diffraction, measurements over two of the different floor widths were repeated with the model seating removed. Figure 8.5 shows that there is now no seat dip at 2 kHz and that the diffraction dip around 5 kHz is much larger.

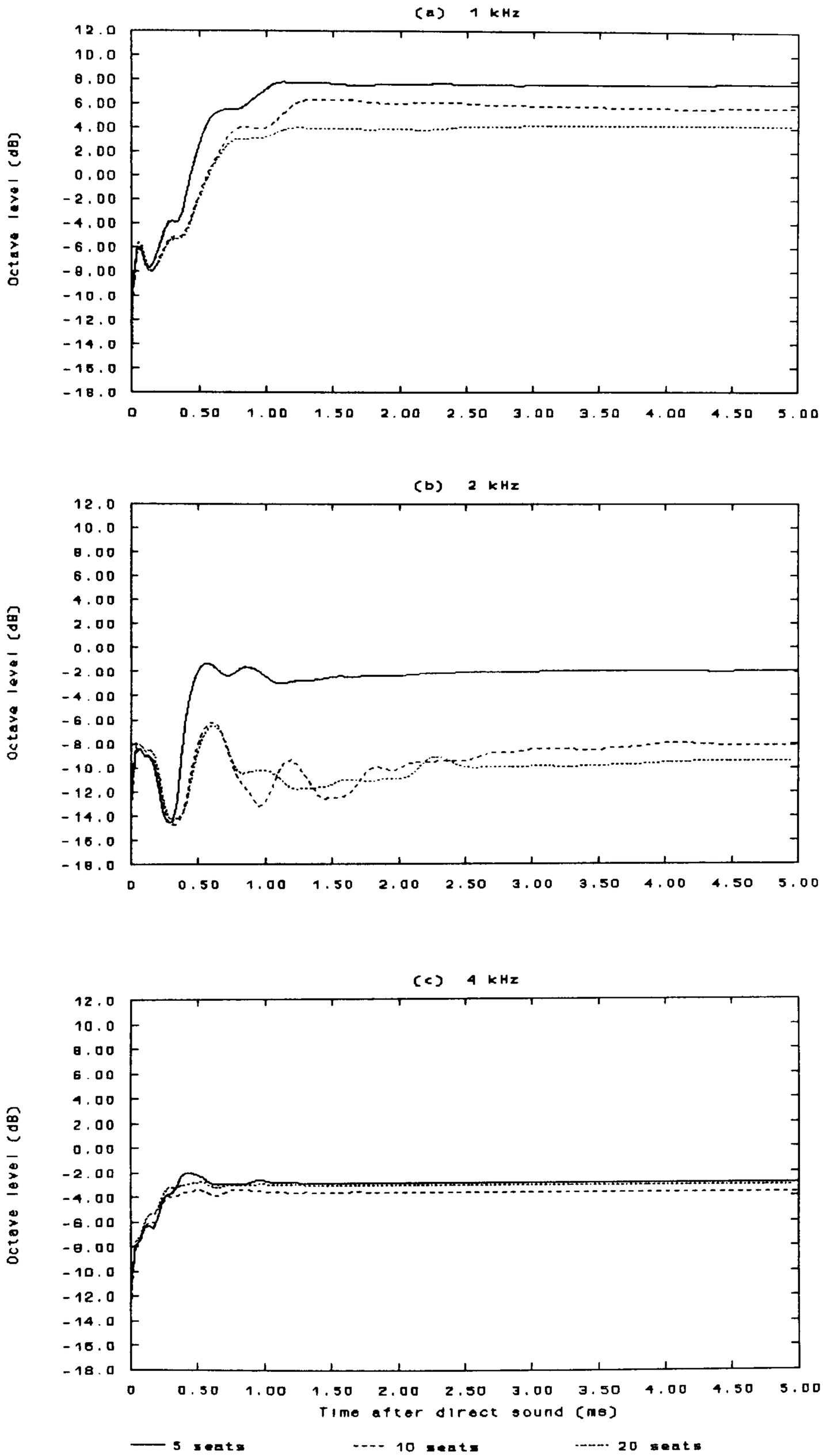

Figure 8.6: The effect of 1:10 scale model seating plane width on (a) 1 kHz, (b) 2 kHz, and (c) 4 kHz octave band levels over time. (6 rows back, $m = 114$ mm, $\theta = 88°$, $\phi = 90°$.)

Further analyses of the model seat transfer functions in figure 8.4 were made using program Longfft. The level received at the microphone in octave bands, as a function of time, is plotted in figure 8.6. (These graphs show a good qualitative agreement with results for the corresponding geometry in the Free Trade Hall.) Figure 8.6(b) shows that a considerable increase in 2 kHz octave band attenuation occurs when the seat-floor plane is widened from 5 to 10 seats. At most points in time, increasing the width further to 20 seats has little effect on the 2 kHz octave band attenuation, and only a slight one on the 1 kHz band attenuation. Hence, it seems that there is a limiting width of seat-floor plane for significant seat dip attenuation to take place. For the above measurement geometry, the subjective threshold for seat dip attenuation of 7.1 dB (see chapter 11) occurs at a width between 5 and 10 seats. The behaviour may be different at other values of θ or r. Though this is significant, it is probably of limited value to a hall designer, as restricting seat block widths to 5 seats is not usually possible.

Another interesting feature of figure 8.6(b) is the variation of 2 kHz octave band attenuation up to 2 ms after the arrival of the direct sound. (Because these are 1:10 scale measurements, this is equivalent to a full-size period of 20 ms.) We have already seen above in figure 8.4 that seating outside the direct line of propagation from loudspeaker to microphone has an effect on the attenuation perceived at the microphone. However, the minimum path length difference between the direct sound and sound which travels to the microphone via the edge of the seat-floor plane is only 0.44 ms, for 10 seats wide. This, then, is more evidence for sound reflecting back and forth between seat rows many times, perhaps across the full

width of the seat-floor plane, before arriving at the microphone. In a real hall, the picture would be even more complex, with 20 ms of multiple "late seat dip" reflections occurring for each main impulse arriving, in the form of the direct sound and then side wall reflections, etc.

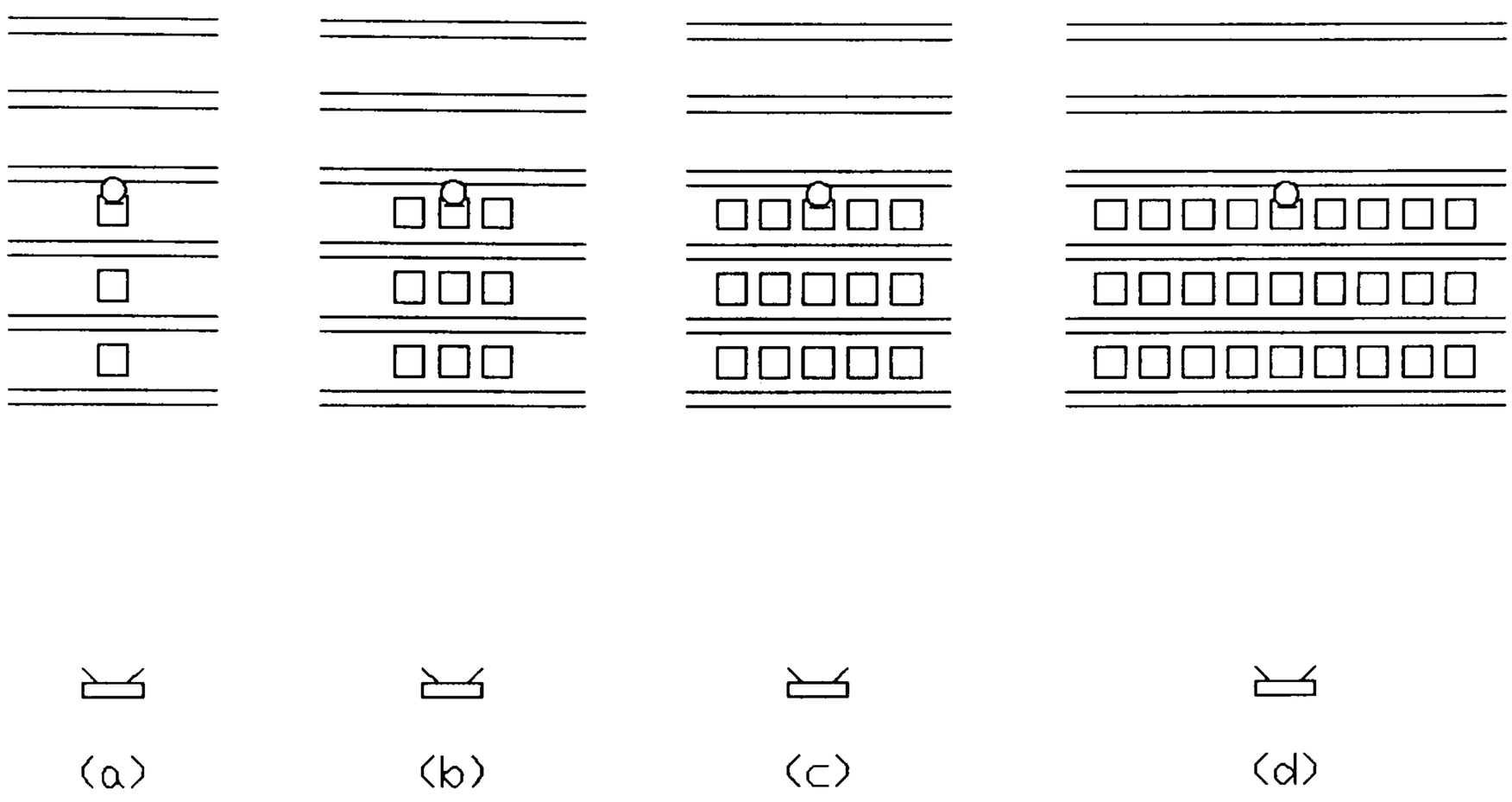

Figure 8.7: Varying the width of the floor absorber layout between loudspeaker and microphone in the Free Trade Hall: (a) one absorber wide, (b) three, (c) five and (d) nine.

8.2 Full-Size Experiments: Variation of Attenuation with Geometry of Floor Absorber Patch

There is some evidence from the Free Trade Hall measurements that the "late seat dip" reflections postulated above come not just from the seats themselves, but at least partly from the floor between them. In one experiment, a fixed receiver

position was chosen in the middle (width) of a large block of seats, and the layout of floor absorbers between the source and microphone was varied. Blocks one absorber wide, then three, five and nine were tried, as shown in figure 8.7. Figures 8.8 and 8.9 show the results for the effects over time in the 100 and 200 Hz octave bands.

In figure 8.8, treating only the seats along the line of direct propagation has made little difference. Increasing the width to a 3x3 and then a 3x5 absorber configuration, in figure 8.9, progressively reduces the seat dip attenuation in the 200 Hz band, for 7 to 20 ms, and makes the attenuation worse in the 100 Hz band. Increasing the absorber width further to 3x9 seems to make the 200 Hz attenuation worse again. It is interesting that this worsening of attenuation happens in the period 10 - 15 ms, because floor absorbers were also found to make the attenuation worse in this time period in figure 7.5. In section 7.1, this was tentatively attributed to waves striking the floor absorbers themselves near grazing incidence and thus returning with negative amplitudes. It is perhaps the case that widening the patch of floor absorbers sufficiently (i.e. to nine blocks wide) allows an incident angle near grazing for sound which is diffracted back to the microphone.

This implies that, like the model seats, the Free Trade Hall seats exhibit a sort of extended reaction. "Late seat dip" reflections which arrive via the floor some distance from the direct propagation line can influence the attenuation at the microphone. Hence the most effective floor absorber treatment is probably one which also covers seating to either side of the direct sightline. Although the widest

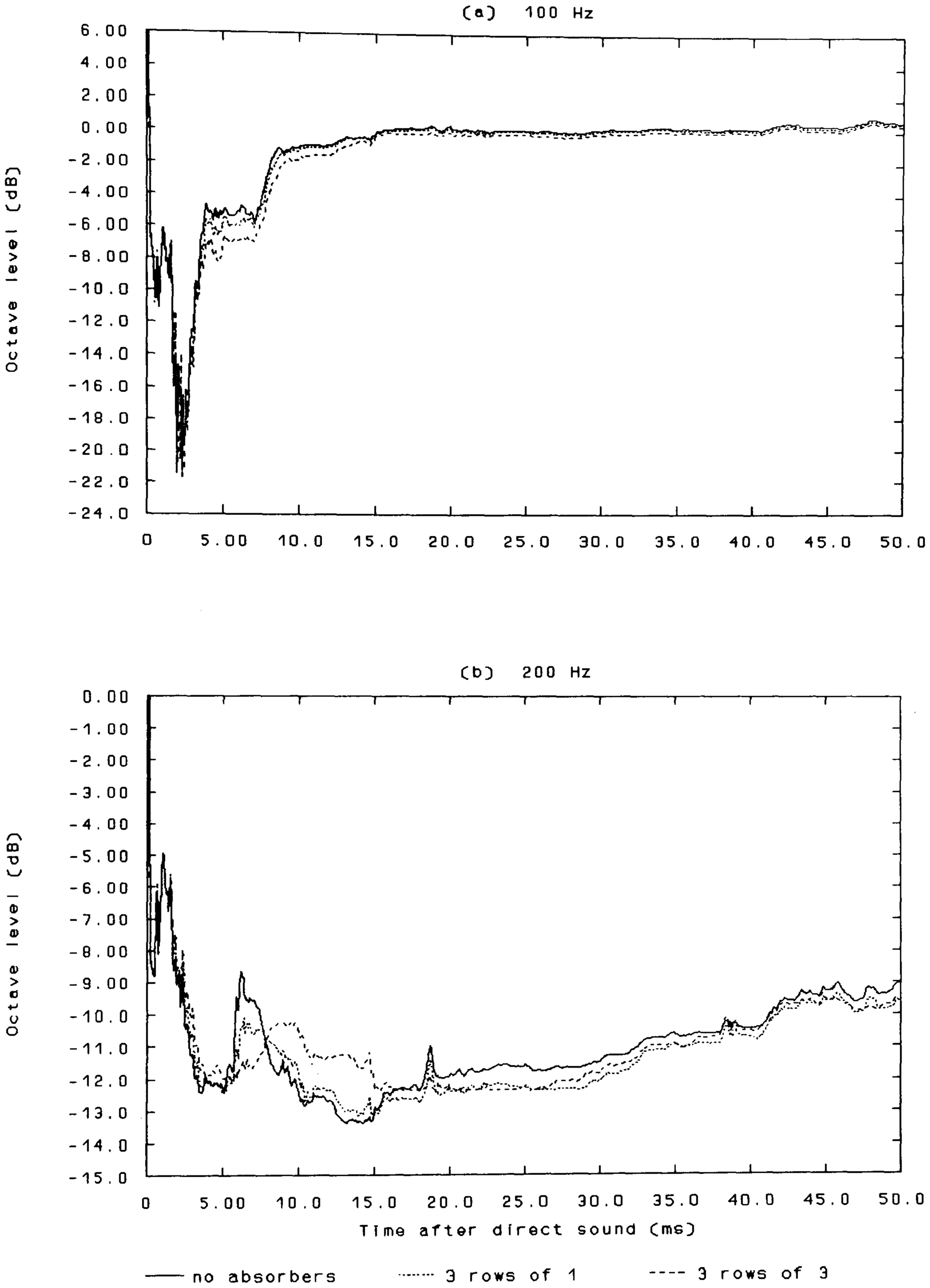

Figure 8.8: The effect of full scale absorber layout on (a) 100 Hz and (b) 200 Hz octave band levels. (3 rows back, m=1.14 metres, θ=87° , ϕ=90°; 0, 1 or 3 absorbers wide.)

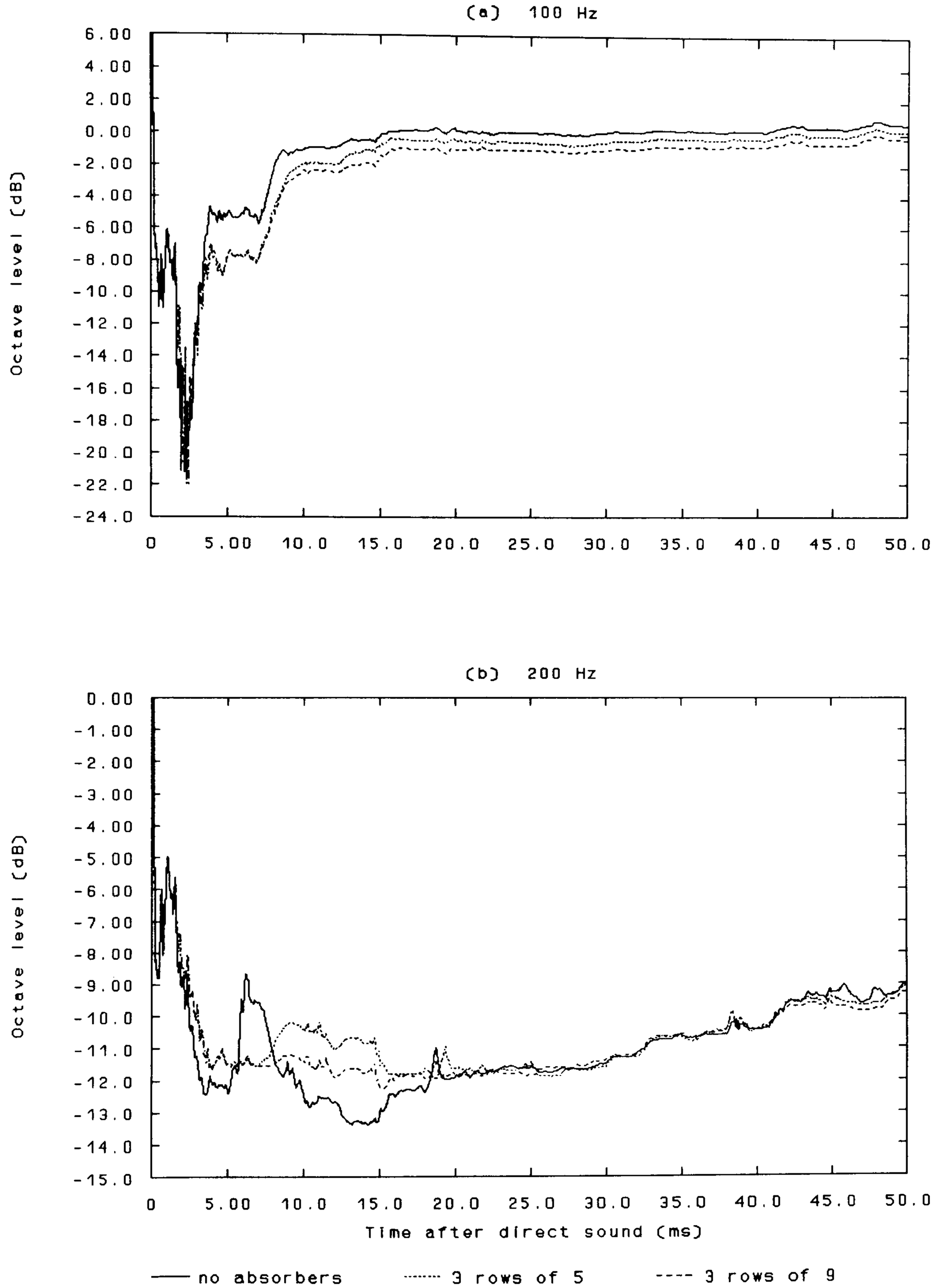

Figure 8.9: The effect of full scale absorber layout on (a) 100 Hz and (b) 200 Hz octave levels over time. (3 rows back, m=1.14 metres, θ=87° , ϕ=90° ; 0, 5 or 9 absorbers wide.)

block of absorbers tried was not the most effective, leaving some seats untreated with floor absorbers would probably be detrimental overall. In section 7.2 it was found that the most important absorbers were those closest to the microphone, so restricting the width of a patch of absorbers to five would cause a bigger problem at another seat than it would solve at the measuring position. Of course, in a real auditorium, if floor absorbers were to be tried, it is unlikely that only some seats would be treated.

These results do have implications for the development of computer models. For a model which specifically addresses seat dip attenuation, like the one in chapter 9, it seems that three-dimensional (not just two-dimensional) surface modelling will be needed for quantitatively accurate results. This then implies that, for general auditorium ray-tracing programs, the many multiple reflections going to make up seat dip attenuation would make it too complex and slow to model exactly for each ray passing close to seating. In this case, a more approximate two-dimensional method or a look-up table of experimentally-obtained attenuation magnitudes and frequencies as suggested by Iida and Ando (1986) might be best.

Chapter 9

A Simple Theoretical Model of Seat Dip Attenuation

9.1 Background

With the recent renewed research interest in seat dip attenuation, attention has been paid to the goal of obtaining an accurate theoretical model. Although quantitative predictions for a given hall before it is built must be the final goal of such work, theoretical models may also offer useful explanations of the effect through qualitative results. There are currently two models in the literature, due to Ando *et al.* (1982) and Kawai and Terai (1991).

9.1.1 Ando et al.'s Theoretical Model

Ando *et al.*'s work is based on the application of the Helmholtz equation to a plane wave incident on an infinite periodic rectangular profile. For an arbitrary profile, Ando and Kato (1976) show that the problem reduces to solving:

$$\frac{\partial^2 \Phi_n}{\partial x^2} + \frac{\partial^2 \Phi_n}{\partial y^2} + k^2(1 - \sin^2\theta\cos^2\phi)\Phi_n = 0 \qquad (9.1)$$

where Φ_n is the velocity potential in the nth horizontal subdivision of the profile

k is the wavenumber

θ and ϕ are the vertical and horizontal angles of incidence, as used previously and defined in figure 6.1

When equation (9.1) is combined with several boundary conditions dictated by the form of the seating profile, a system of complex linear equations is found. These may be solved by computer for each frequency of interest to find the steady-state sound level at a receiver. Ando *et al.*'s paper concentrated on the simplest representation of seats as parallel barriers, and they investigated the effects of letting a slit resonator into the floor, as shown in figure 9.1.

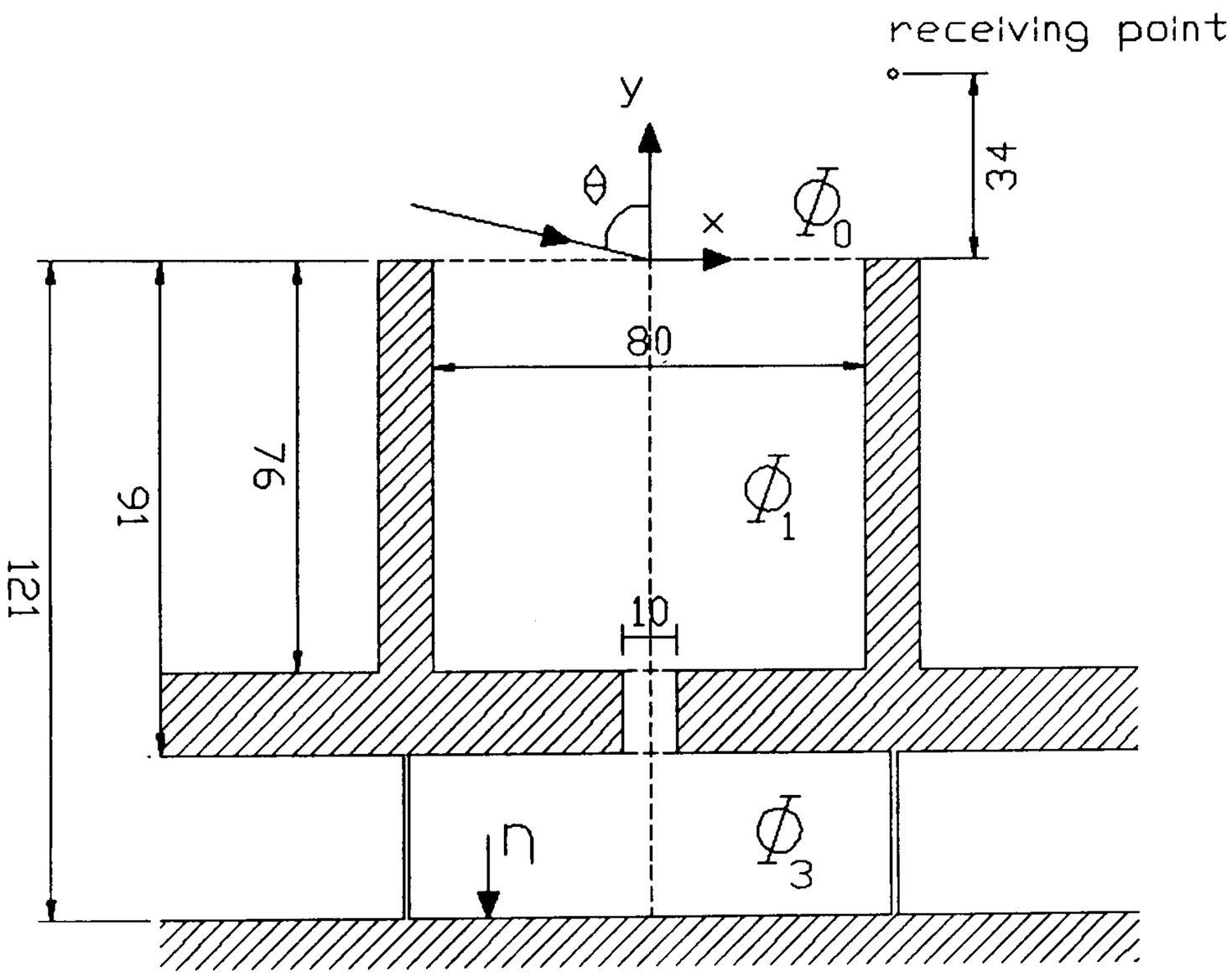

Figure 9.1: Profile of seats and slit resonator in floor used in Ando et al.'s theoretical model. (The dimensions are in cm.) After Ando *et al.* (1982).

One of Ando *et al.*'s spectra was in good agreement with the model measurements of Sessler and West (1964), and the computational model also gave a reasonable qualitative prediction for the effect of varying the receiver height. However, the

crucial effect of varying the vertical angle of incidence θ is not well predicted. The theory produces a uniform broadband increase in attenuation with increasing θ, instead of the selective increase in dip attenuation and increase in dip frequency exhibited by all the measurements in the literature (see figure 6.5, for example). Though this model cannot produce good quantitative predictions for concert hall design, it does offer the possibility that seat dip attenuation can be reduced by changing the specific admittance η of the floor between the seats. In particular, large improvements were predicted when η was changed from (0.01, 0.0) to (0.6, 0.0), whether this applied to a profile with an intact floor or to the bottom of a slit resonator let into the floor, as in figure 9.1. The prediction of this effect of resonant floor absorbers was the primary contribution of Ando *et al.*'s work.

9.1.2 Kawai and Terai's Theoretical Model

Kawai and Terai (1991) use a form of Helmholtz-Kirchhoff integral equation in their theory, a common approach to acoustic scattering problems. As in Ando *et al.*'s theory, this results in an algorithm which obtains a velocity potential at a receiver due to contributions from many parts of an arbitrary surface. This method is less restricted than Ando *et al.*'s in that it only requires that the surface is composed of thin rigid plates which can be covered with uniformly sized elements. As Kawai and Terai emphasise in their paper, there is no need for the seat/floor surface to be periodic or infinite in any direction. They therefore present results for both two- and three-dimensional surfaces. They report that calculating a whole spectrum from the many elements covering a three-dimensional seating surface takes considerable computing resources.

Kawai and Terai demonstrate some results that are in good agreement with scale model measurements. However, their theory makes unrealistic predictions of the effect of varying θ. Though their calculated spectra have many minima and maxima, raking the seats (and thus decreasing θ) in general moves most of the seat dip attenuation to higher frequencies. This contradicts the measured data in Ishida *et al.* (1989), Schultz and Watters (1964) and Bradley (1991). Another criticism of the results in Kawai and Terai's 1991 paper is that they make no provision for either floor or seating having absorptive surfaces. As Ando *et al.*'s calculations and the measurements with floor absorbers in chapter 7 have shown, this can be important. However, in a more general paper which includes a description of the transient form of the theory, Terai and Kawai (1989) introduced the novel concept of "impulse admittance" which is a way of representing absorption in the time domain. Though this was not used in their seat dip calculations, it seems that it could be.

In some respects, Kawai and Terai's calculations do give realistic results. The effect of increasing r is generally to deepen the main attenuation dip and move it to a slightly lower frequency, as was found in the Free Trade Hall in figure 6.2. Also, one of their graphs for propagation over a three-dimensional surface shows that one effect of increasing the width of the seat rows from three to six metres is to deepen the main dip from 13 to 20 dB and increase its frequency slightly. This is in good agreement with the 1:10 scale model results presented above in figure 8.3, where similar configurations result in dips of 15 and 23 dB.

9.2 A Time Domain Approach

The two models described above are both constant-frequency methods: they produce a solution at one discrete frequency. The procedure for each has to be repeated many times to obtain a spectrum. The new method differs in that it operates in the time domain, producing a synthetic impulse response of sound passing over seating which then has to be Fourier Transformed to obtain a spectrum. It is also computationally and conceptually far simpler than the two existing methods, yet it produces qualitative predictions of equal merit.

The new method is based on the ray-drawing procedure described in part 6.3.1. Sound is assumed to travel from a loudspeaker to a microphone over some parallel vertical barriers representing rows of seats. The construction, as shown in figure 9.2, is two-dimensional. The sound can undergo geometric reflections at the floor between the barriers, and it can also diffract over the tops of the barriers. A particular arrangement of loudspeaker, microphone and barriers is described as a set of nodes at which sound will either reflect or diffract. The nodes are at the loudspeaker, the microphone, the tops of the barriers, and on the floor at the positions of geometric reflection, as in figure 9.2. Each node has a position (x,y) and a complex specific impedance, z_n. Every possible path from source to receiver via the nodes is then found, excluding obscured combinations such as 6-3 in figure 9.2. For each path constructed an impulse starts out from the loudspeaker at time $t = 0$. When "reflecting" from a node the magnitude of the impulse is multiplied by the modulus of the geometric reflection coefficient,

$$R = \frac{Z_n \cos\alpha - 1}{Z_n \cos\alpha + 1} \qquad (9.2)$$

where α is the angle to the normal at the node.

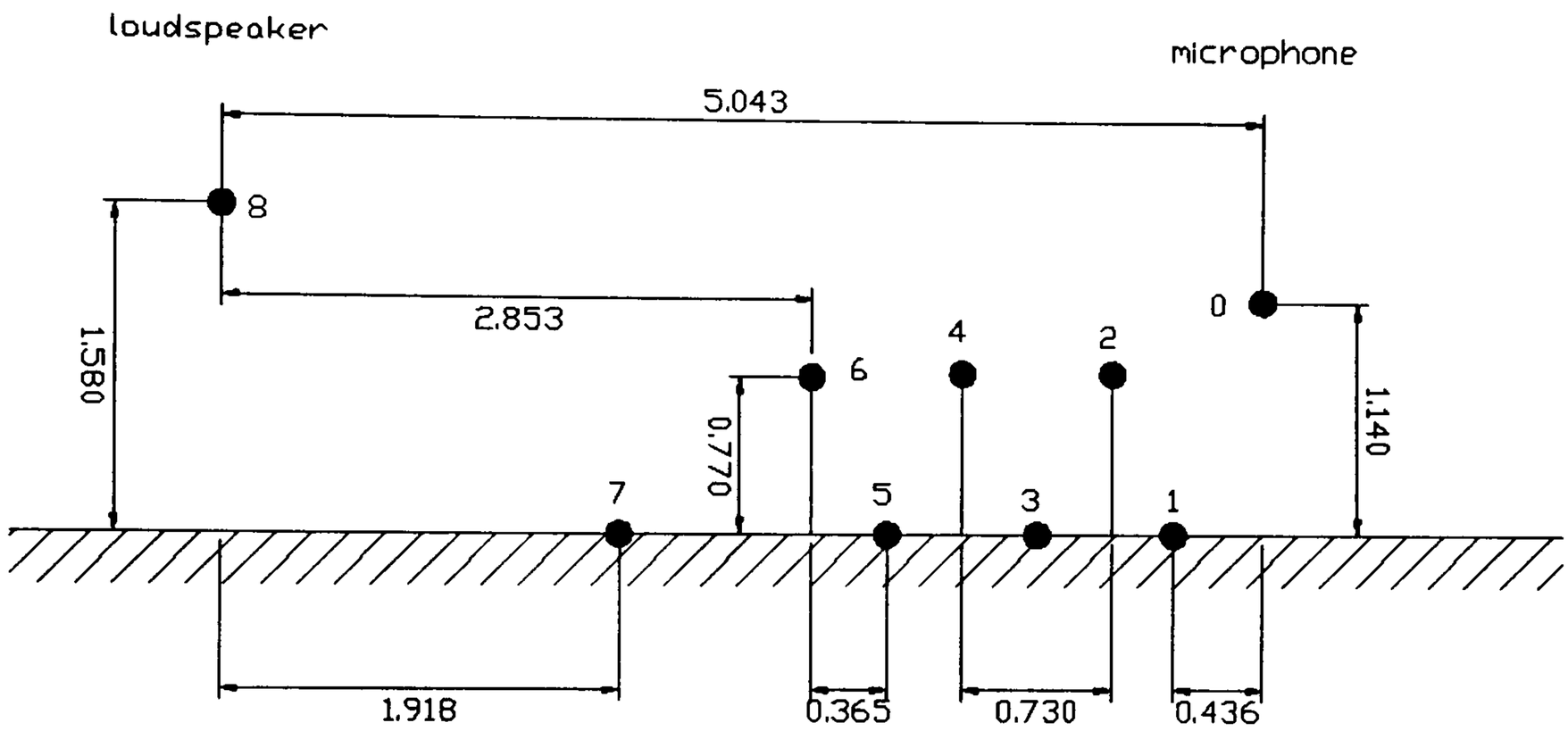

Figure 9.2: Typical node diagram representing sound passing over three rows of "seat" barriers in simple theoretical model (l=1.58 metres, m=1.14 metres, s=0.73 metres, h=0.77 metres, θ=85° , ϕ=90°).

To allow for the negative reflections apparent in real seat dip impulse responses, the sign of the real part of R is used in the multiplication. For want of anything better, the same operation occurs without the sign when an impulse "diffracts" at a node. When an impulse reaches the microphone its magnitude is divided by the pathlength to account for spherical spreading. The pathlength also dictates the position in time of the impulse in the total impulse response. Once this procedure has been followed for all possible paths, the total impulse response is Fourier

Transformed to yield the seat dip spectrum. An implementation in FORTRAN 77 of the algorithm for producing the impulse response is listed in Appendix C.

The main weakness of this model is its extremely simple treatment of diffraction. It was felt that sufficient time was not available to produce a more realistic treatment. The problem of representing diffracting waves in a geometrical computer model is not a simple one and considerable research effort is currently focused on it by, amongst others, Asayama *et al.* (1989), Jaroch *et al.* (1990), Sekiguchi and Kimura (1991), Stephenson (1990a) and Stephenson (1990b). A second weakness is that equation (9.2) describes reflection from an infinite surface. In practice, the finite surfaces represented by nodes in the model will have a radiation impedance different from $1/\cos\alpha$. Recent work by Rindel (1991) suggests a way in which the radiation impedance of a finite surface might be easily approximated - unfortunately there was not time to incorporate it into the results discussed here. The third shortcoming of the model is that the value of impedance used for z_n in equation (9.2) cannot be frequency-dependent. Obviously, this is an approximation of the real situation, though one which was also used in Ando *et al.*'s 1982 work. It might be possible to incorporate a frequency-dependant impedance by making many runs of the model for a given geometry and changing z_n each time to have values appropriate to a discrete frequency. The total level in each of these frequency-constant impulse responses could then be summed to produce a spectrum of discrete points. Because it was desired to present only a simple model here, a trial of this adaptation is left for future work.

9.3 Results from the New Prediction Method

Simple though it is, the new method has produced reasonable qualitative predictions of most of the main parameters affecting seat dip attenuation. In examining these, the notation introduced in chapter 6 is used with the following additions: s, the inter-row spacing; h, the "seat" barrier height; z_f, the specific impedance of the floor; and z_s, the specific impedance of the "seat" tops. In any particular impulse response calculation, z_f was the same for all nodes on the floor and z_s was the same for all nodes on the "seat" tops.

9.3.1 Number of Seat Rows Propagated Over (r)

For these calculations, the values for z_f and z_s were taken from low-frequency normal impedance measurements on thick carpet with underlay and 50 mm thick seating foam respectively. As r was increased, so was l so that θ was held constant at 85° . Figure 9.3 shows that when the number of barriers between source and receiver is increased from three, through four and five, to six, the dip at 400 Hz becomes deeper and moves down in frequency. This agrees qualitatively with the comparable graph for the Free Trade Hall Measurements in figure 6.2.

The agreement is qualitative only, since the main dip frequencies here are round 400 Hz, and those in the Free Trade Hall are round 200 Hz. In the literature, the range of dip frequencies recorded in real halls is about 100 - 300 Hz. There is no obvious factor of two to change in the model to retify this, though perhaps a more sophisticated treatment of diffraction might help. If diffracted impulses from the seat-floor system are smeared in time, then their counterparts in the frequency

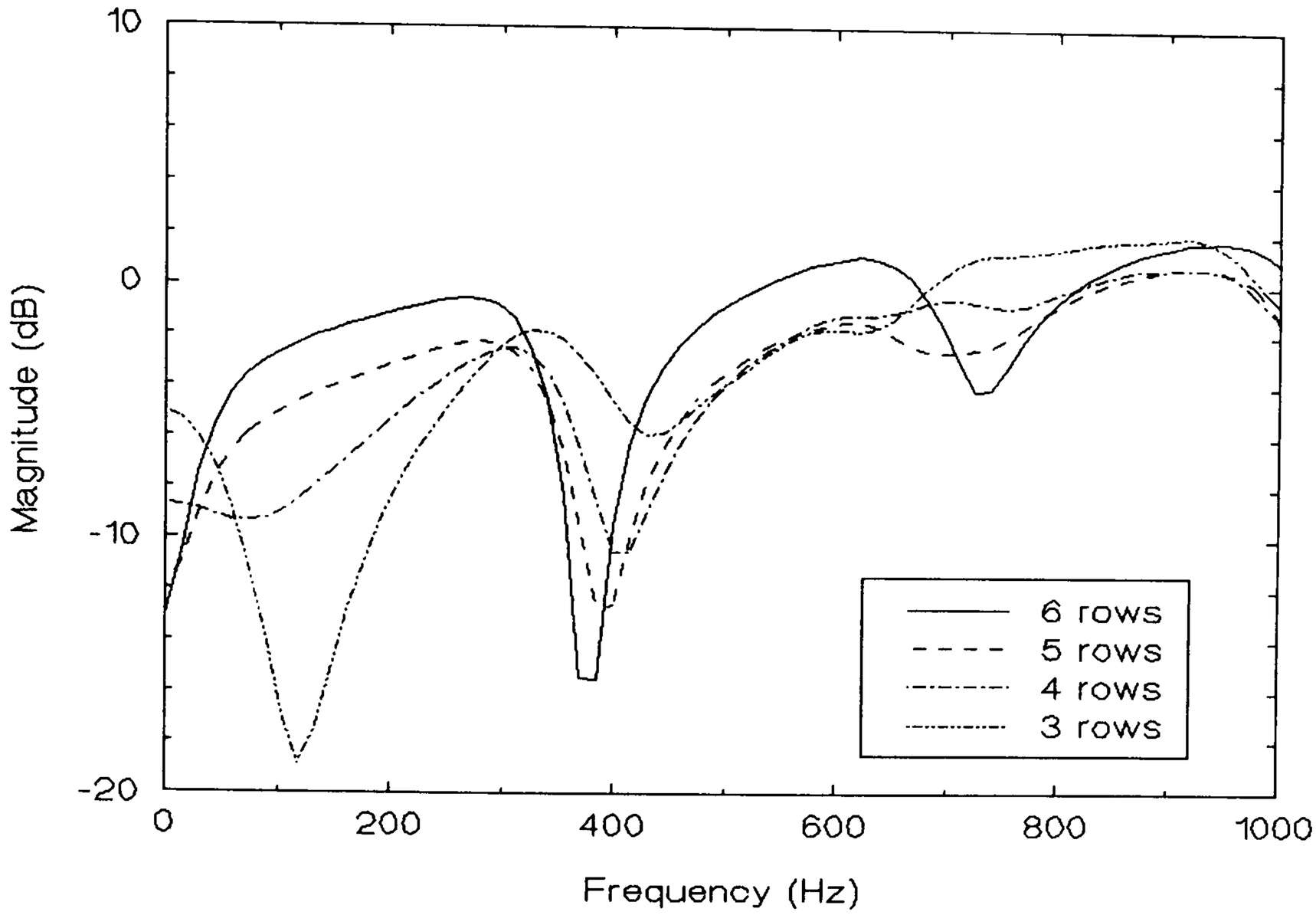

Figure 9.3: Prediction of effect of number of seat rows on seat dip attenuation (m=1.14 metres, θ=85° , z_s=(2.5, -2.0), z_f=(2.0, -10.0), s=0.73 metres, h=0.77 metres).

domain may combine to give a cancellation at a different frequency from that produced with no smearing. Time smearing would effectively lengthen the delay of some of the energy arriving at the microphone. If an impulse is delayed then the first minimum it produces in the frequency domain (like that in figure 6.4) will be at a lower frequency.

9.3.2 Vertical Angle of Incidence (θ)

Increasing θ makes the attenuation dip worse around 400 Hz, as shown in figure 9.4. This is in good qualitative agreement with the measured data in figure 6.5.

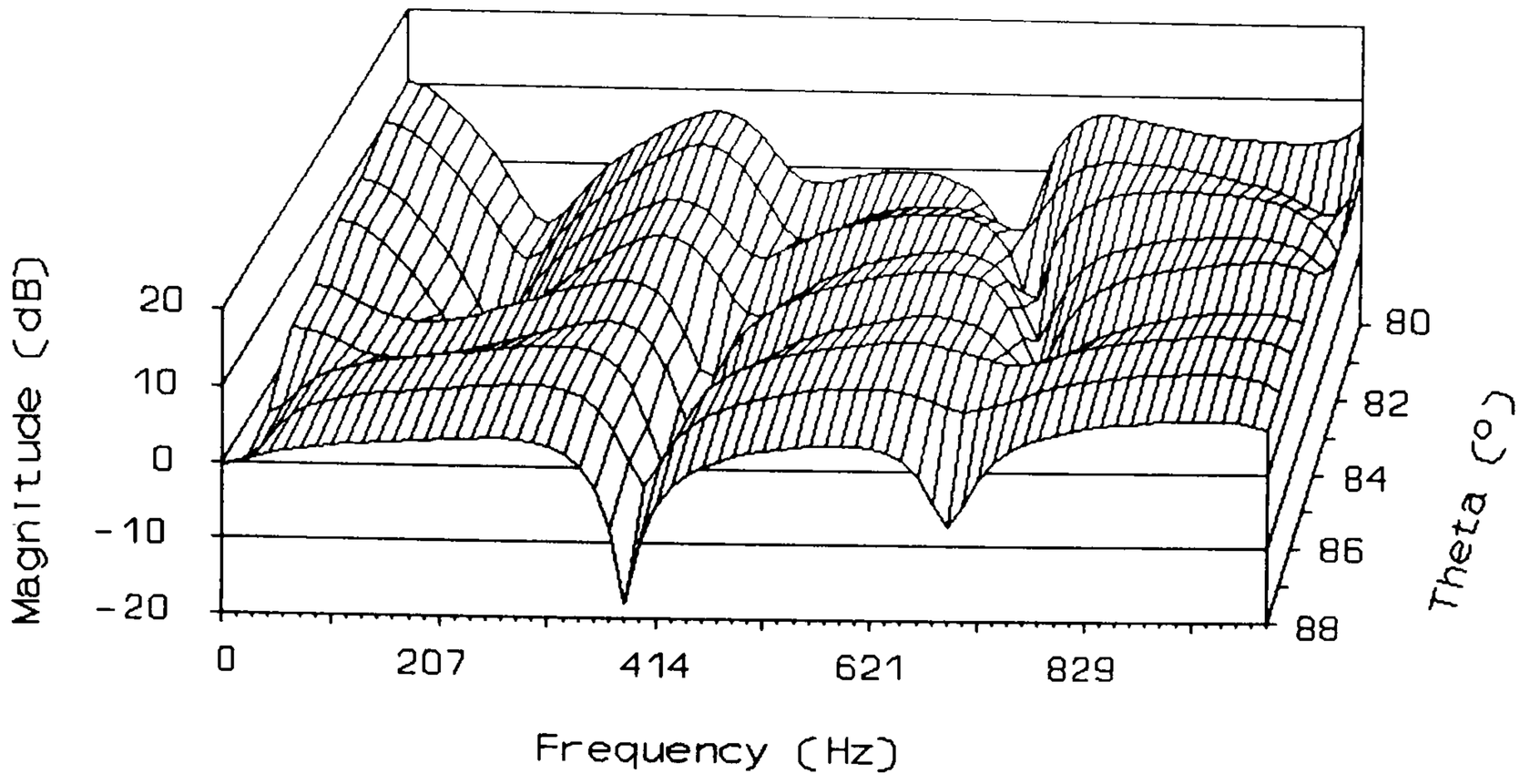

Figure 9.4: Prediction of effect of θ on seat dip attenuation (6 rows back, m=1.14 metres, z_s=(2.5, -2.0), z_f=(2.0, -10.0), s=0.73 metres, h=0.77 metres).

The dip around 400 Hz is the only one which is consistent across the range of θ in figure 9.4. Other dips and peaks appear and disappear, sometimes suddenly, as θ changes. These sharp differences are probably due to the sudden cut-off between reflection and diffraction behaviour in the model. More realistic predictions might result from an algorithm which allowed reflection and diffraction simultaneously, with a gradual change between the proportions of either.

9.3.3 Microphone Height (m)

In figure 9.5, increasing the microphone height from 1.14 metres (representing head height) decreases the magnitude of the attenuation and its frequency. Both these effects are again in qualitative agreement with the corresponding Free Trade Hall measurements of figure 6.3. Either side of the main dip around 400 Hz, though, the

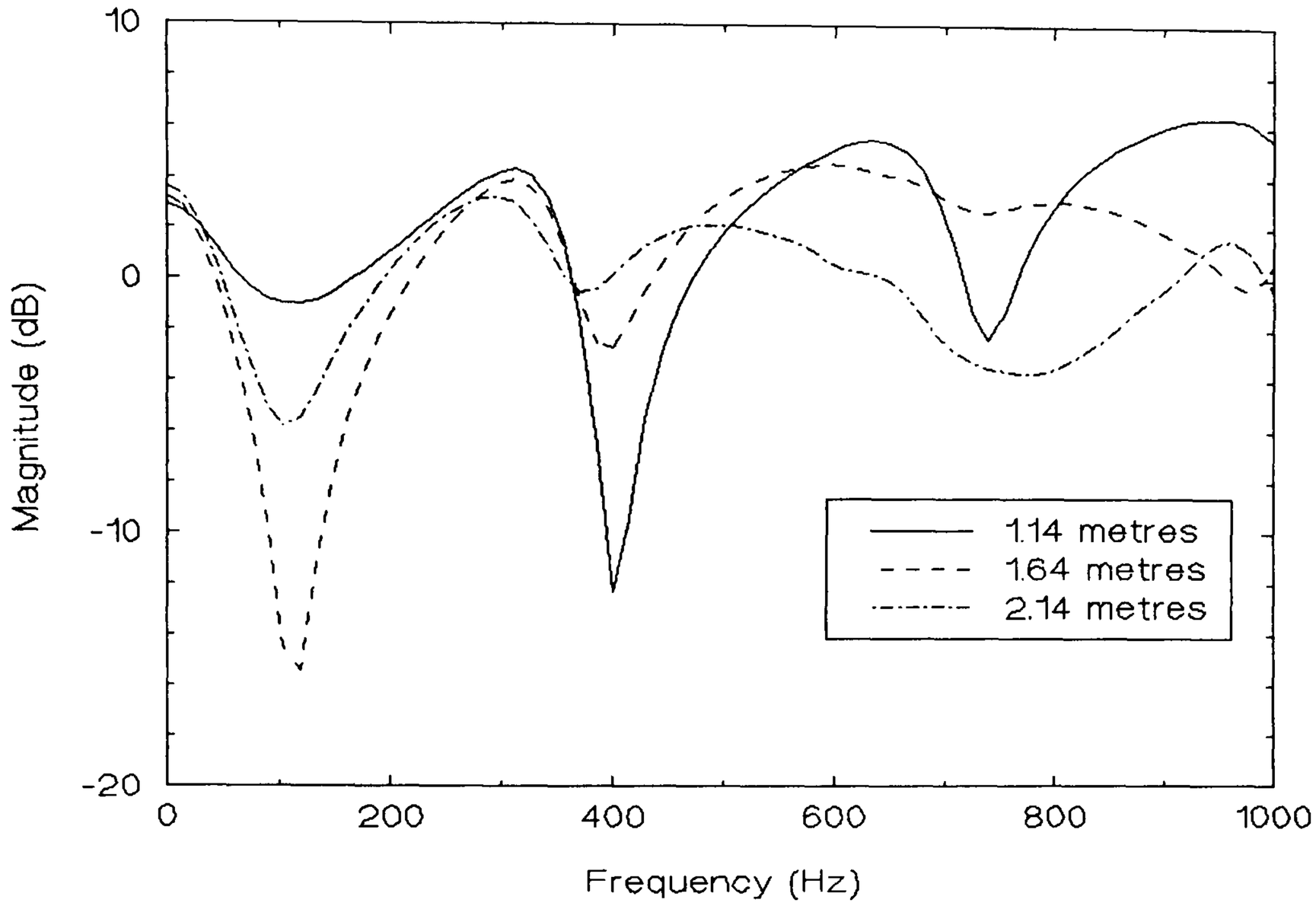

Figure 9.5: Prediction of effect of m on seat dip attenuation (6 rows back, l=1.77 metres, z_s=(2.5, -2.0), z_t=(2.0, -10.0), s=0.73 metres, h=0.77 metres).

predicted spectra are not always in good agreement with the measured ones. This is ironic, since it was the simple case of a receiving point high above the seats which first gave rise to the idea, in figure 6.4, that seat dip attenuation might be predicted by one or more discrete reflections in an impulse response. This idea led to the development of the present simple model.

Unfortunately, the model seems to supply too many separate strong reflections for the case of a high microphone. That is, it does not tend naturally to only one reflection node for a high receiver thus producing a comb filter spectrum , as in

figure 6.3. Again, it is possible that the unrealistic diffraction simulation is to blame here: as the microphone is raised, the path length differences between individual reflections will get smaller. Without time smearing of the individual impulses, they do not overlap closely enough for a high receiving point to see a single large impulse. This would produce the required comb filter spectrum. If the diffracted impulses were smeared in time, then it is possible that they would overlap enough to give a comb filter spectrum.

9.3.4 Floor Impedance (z_f)

Figure 9.6 demonstrates the effect of simultaneously varying the specific impedance of all the floor nodes in the model. Using (10.0, 0.0) to represent a hard floor gives a very sharp and deep attenuation dip at 400 Hz. Replacing this with the typical carpet figure of (2.0, -10.0) reduces the dip dramatically from 35 to 13 dB. The floor impedance is then further reduced to be the same as the value used for z_s, (2.5, -2.0). This results in hardly any improvement in the main attenuation dip and a considerable worsening in low-frequency levels. Finally, making the floor totally absorbent with z_f=(1.0, 0.0) removes the main attenuation dip entirely, but further worsens the level from 0 to 350 Hz. This case represents the effect of the direct sound and reflections from the seat tops only.

These results are similar to those obtained by Ando *et al.* (1982). They imply that the improvements offered by floor absorption follow a law of diminishing returns. The biggest improvement is seen when putting some absorption on a hard floor, and gains are small thereafter. This may explain why the measurements with absorbers

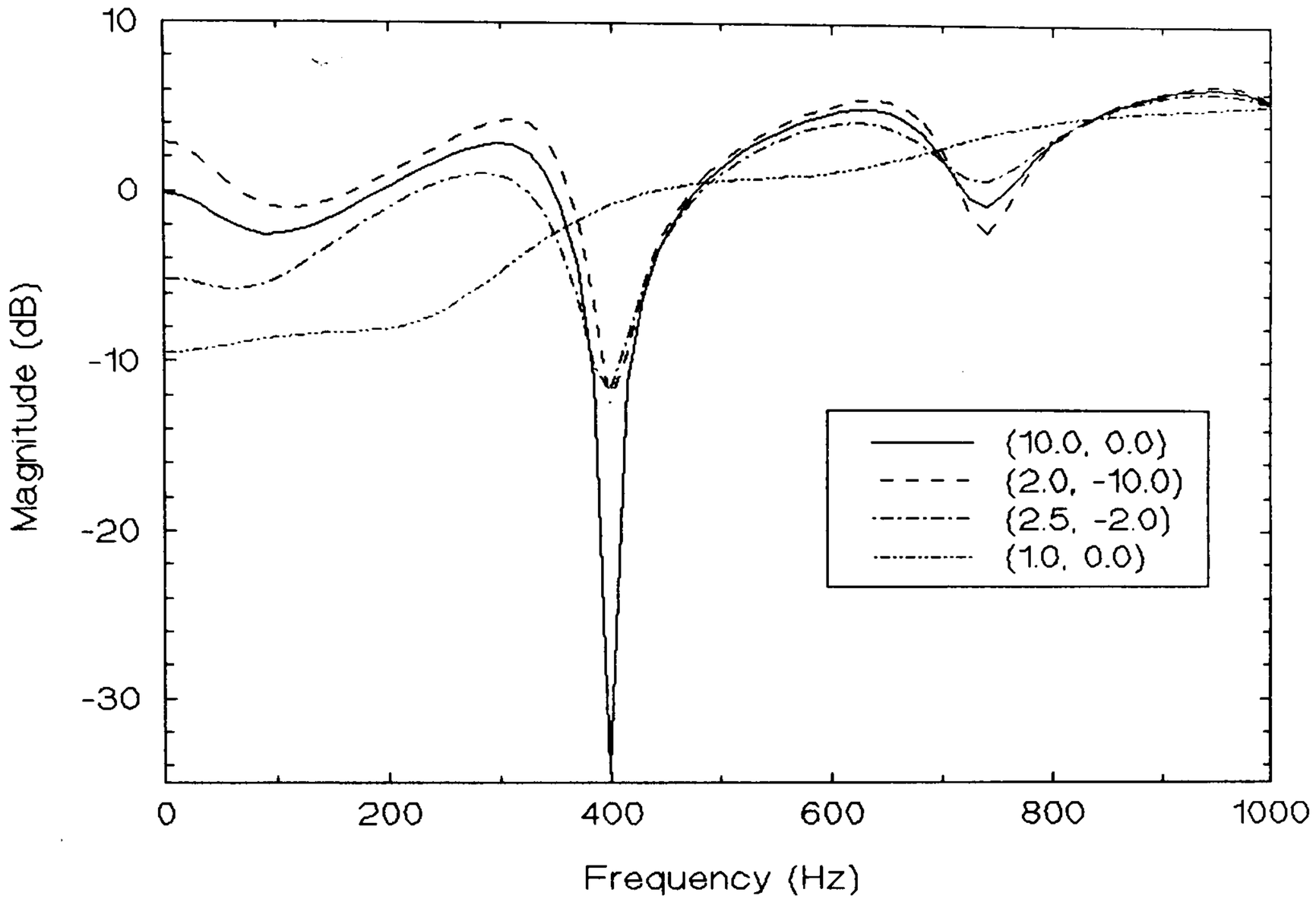

Figure 9.6: Prediction of effect of z_f (in $\rho_0 c$ units) on seat dip attenuation (6 rows back, m=1.14 metres, θ=85° , z_s=(2.5, -2.0), s=0.73 metres, h=0.77 metres).

in a real concert hall detailed in chapter 7 revealed smaller improvements than those predicted in Ando *et al.*'s paper.

9.3.5 Seat Top Impedance (z_s)

Figure 9.7 shows how making comparatively small reductions in the real part of the seat top impedance reduces the attenuation dip considerably. All four values considered are realistic low-frequency normal specific impedances for seating foams. This result implies that, as well as using resonant floor absorbers, it may be possible to reduce seat dip attenuation by increasing the low-frequency absorption of the

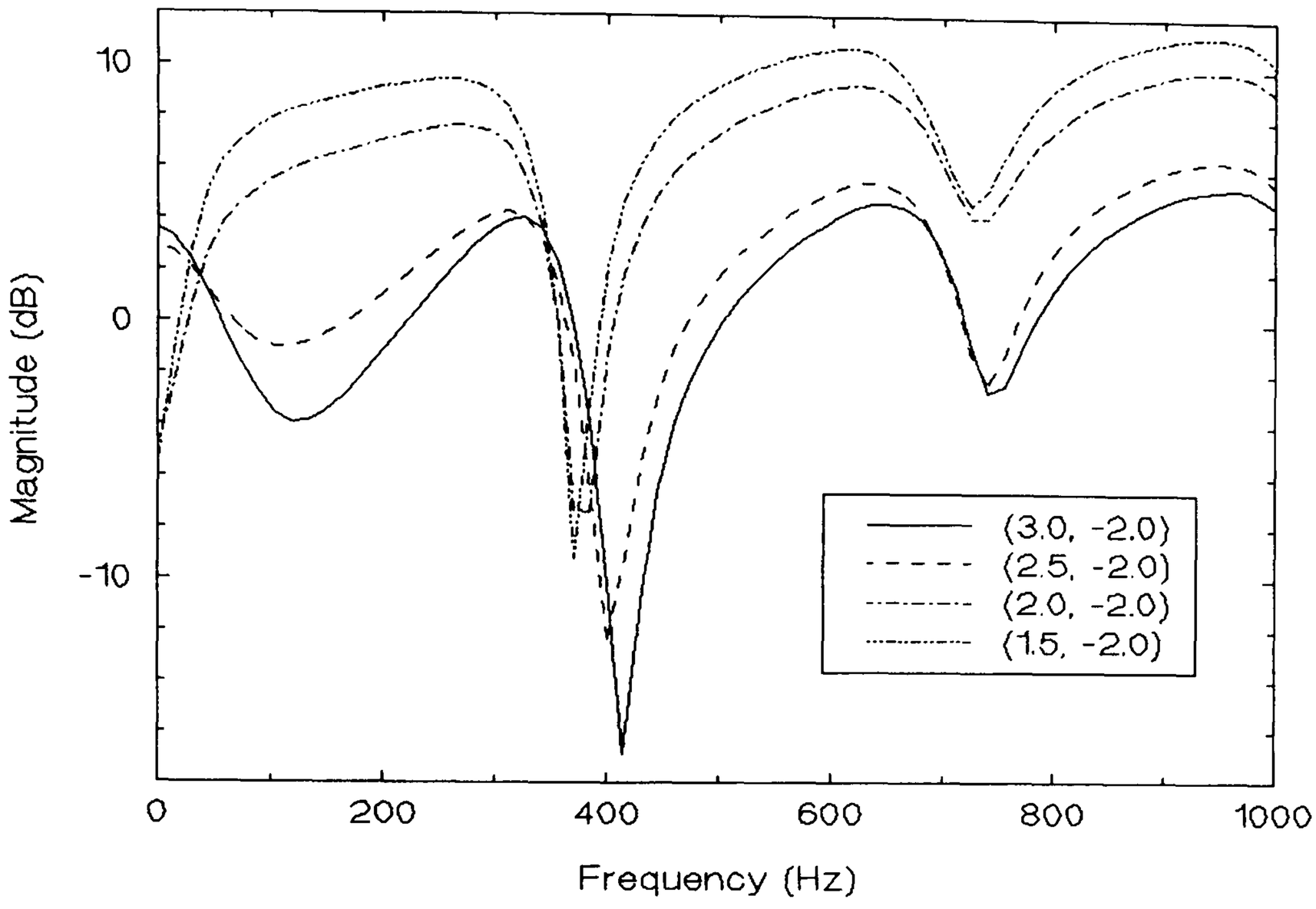

Figure 9.7: Prediction of effect of z_s (in $\rho_0 c$ units) on seat dip attenuation (6 rows back, m=1.14 metres, θ=85° , z_f=(2.0, -10.0), s=0.73 metres, h=0.77 metres).

seat tops. There is limited scope for doing this in an occupied concert hall chair, of course, but drilling the back to form a low-frequency resonant Helmholtz absorber might be worth investigating.

The comparatively large change in spectra when z_s is decreased from (2.5, -2.0) to (2.0, -2.0) in figure 9.7 occurs because one of the seat top reflections in the impulse response changes sign. This is due to the use of the geometric reflection coefficient in equation 9.2: for a given angle α, z_n can be increased so that R changes from negative to positive.

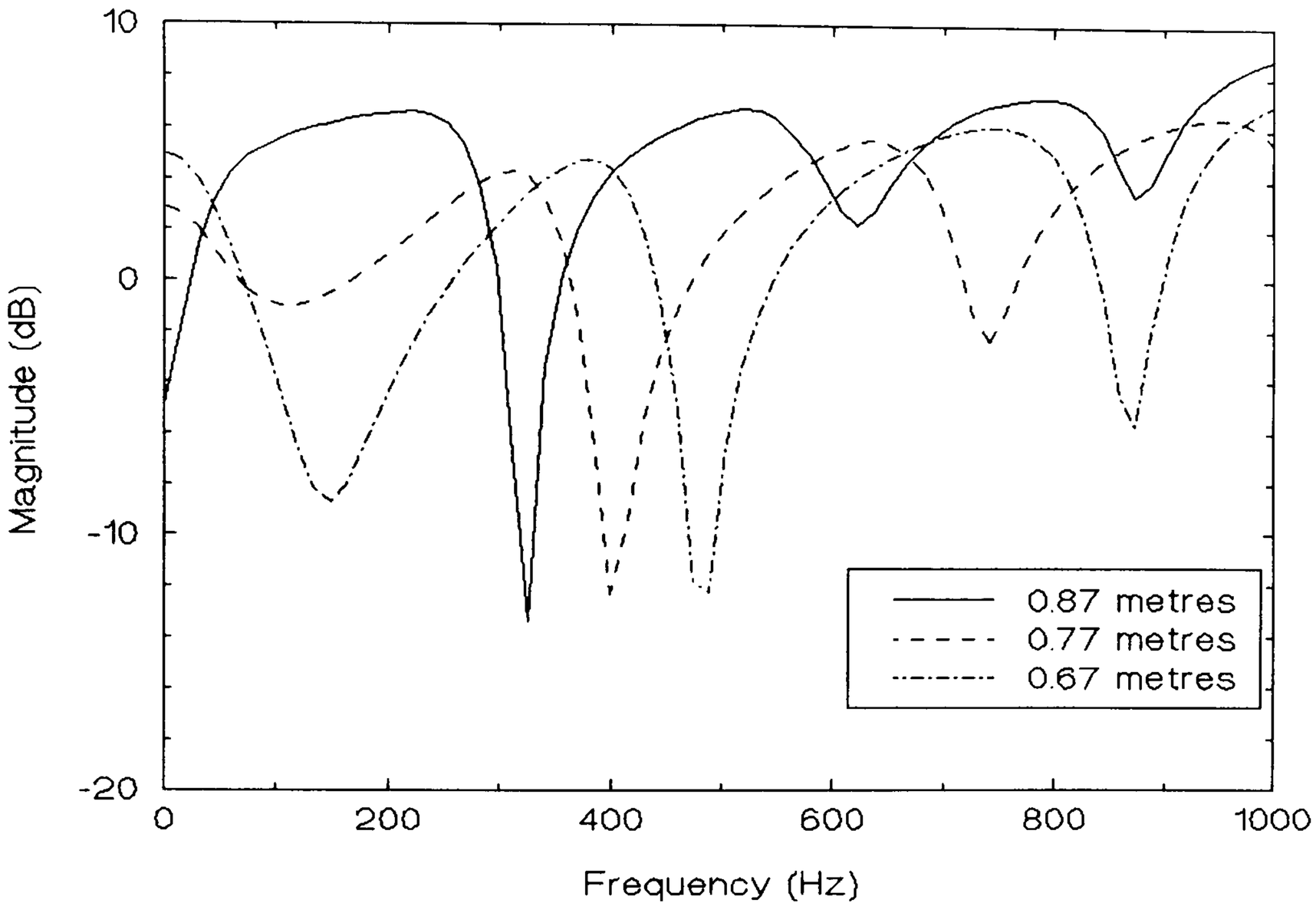

Figure 9.8: Prediction of effect of seat height h on seat dip attenuation (6 rows back, m = 1.14 metres, $\theta = 85°$, $z_s = (2.5, -2.0)$, $z_f = (2.0, -10.0)$, s = 0.73 metres).

9.3.6 Seat Height (h)

The model predicts that the effect of increasing the height of the seats will be to move the main attenuation frequency downwards, as in figure 9.8. This is in agreement with 1:10 scale model data in Sessler and West (1964). Though there is no significant change in the magnitude of the attenuation, this effect could be used as part of a strategy whereby the dip is reduced (say, with floor absorbers and resonant chair backs) and shifted to a lower, subjectively less important, frequency by increasing the seat height.

The dip frequencies in figure 9.8, and those in the real data in chapter 6, are in disagreement with a common proposition in the literature that seat dip attenuation is the product of a vertical resonance between the seat rows resulting in an attenuation dip when the seat backs are a quarter of a wavelength high (see Bradley (1991) for example). In the Free Trade Hall, the chairs are 0.77 metres high, so one might expect a main dip centred around 110 Hz. This is appreciably lower than most of the measured dips. If one adopts the view taken here, that the attenuation process is best thought of in the time domain, then changing the seat height changes the arrival times of some of the seat reflections, thus altering the main dip frequency. The change in frequency in figure 9.8 is not inversely proportional to the seat height, however, nor is there any reason why it should be, according to the time domain explanation.

9.3.7 Inter-row Spacing (s)

In figure 9.9, the model predicts that the effect of increasing the inter-row spacing from the rather cramped 0.73 metres used in the Free Trade Hall to a more typical 0.93 metres will be to reduce the first dip at 400 Hz and increase the size of a second at 800 Hz. Two 1:10 scale model measurements in the literature, due to Schultz and Watters (1964) and Sessler and West (1964), both show smaller effects than this, though there is some disagreement. In Schultz and Watters' paper, increasing s reduces the attenuation, whilst in Sessler and West's it increases the attenuation at one frequency and decreases it at another. Though the experimental situation is not clear, it must be concluded that the performance of the simple theoretical model is not adequate in this respect.

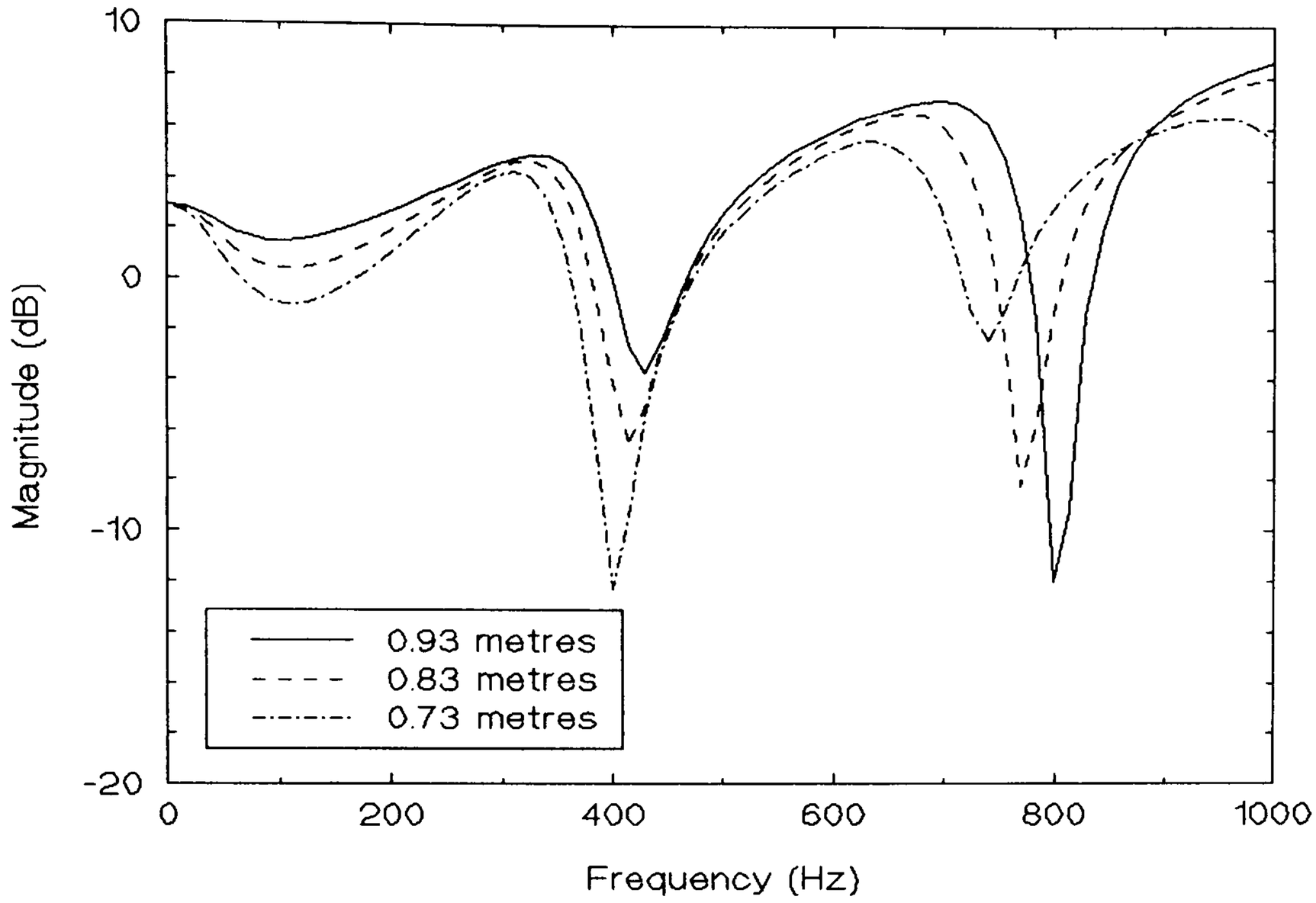

Figure 9.9: Prediction of effect of inter-row spacing s on seat dip attenuation (6 rows back, m=1.14 metres, θ=85° , z_s=(2.5, -2.0), z_f=(2.0, -10.0), h=0.77 metres).

9.4 Changes in Predicted Attenuation Over Time

Though the simple theory is only capable of modelling the very early sound field over seating, the predicted seat dip spectra can change considerably over this period, as do the measured spectra in chapters 6 and 7. Figure 9.10(b) plots the results of program Longfft tracking the minimum of two predicted spectra over time. These can be related to features of the predicted impulse responses in figure 9.10(a). Both graphs have been normalised to the magnitude of the direct impulse. The values of floor impedance chosen for figure 9.10 make the results analogous to the measured data in figure 7.4, where the floor absorption was provided by

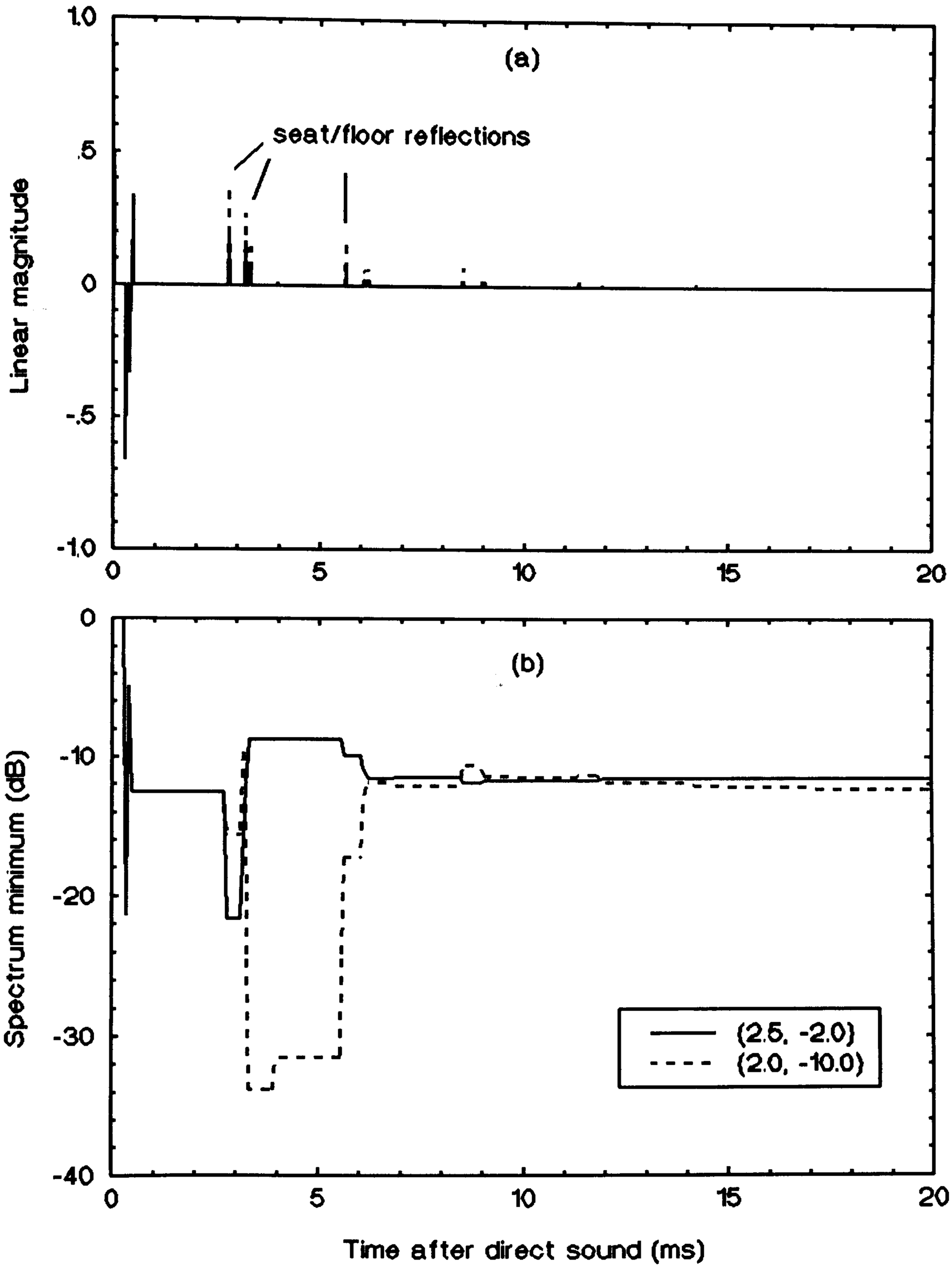

Figure 9.10: Prediction of (a) broadband impulse response and (b) narrowband spectrum minimum versus time for two values of floor impedance (6 rows back, m = 1.14 metres, $\theta = 85°$, $z_s = (2.5, -2.0)$).

carpet only and then by resonant absorbers. The theory predicts that reducing z_f considerably attenuates the principal seat/floor reflections, marked in figure 9.10(a). In a similar fashion to the measured data though, this has a significant effect on the spectrum minimum for only 3 to 6 ms after the direct sound arrival. The reflections arriving later than this reduce the attenuation, and a change in floor impedance from "carpet" to "seating foam" makes little further difference to the spectrum minimum.

Though the theory seems adequate in predicting spectrum variation over time in the early field, the predicted impulse responses peter out at around 15 ms. They do not include any simulation of the process identified in part 8.1 whereby sound reflects many times between surfaces and arrives at up to 20 ms. It would be difficult to incorporate such complicated paths into the present model.

Another way in which figure 9.10(b) could be improved is by the use of a more realistic impulse shape. At the moment, the predicted impulse response is composed of delta functions, causing the spectrum minimum to change sharply over time. It would perhaps be more realistic to represent sound which has diffracted over a barrier as a triangular impulse, thus smoothing out attenuation changes.

9.5 Conclusion

Prompted by observations of measured seat dip impulse responses and changes in their associated spectra over time, a theoretical model for seat dip attenuation was devised. It is based on a representation of the seats and floor as a set of discrete

nodes at which impulses from a loudspeaker either reflect or diffract before eventually reaching a microphone. The model has the advantage of simplicity and hence high computational speed over two others in the literature. The algorithm is perhaps fast enough to be incorporated into more general programs which attempt to predict the total impulse response in an auditorium.

In spite of its simplicity, the new model successfully predicts the most important qualitative effects of varying: the number of seat rows propagated over, the vertical angle of incidence, the microphone height, the floor impedance, the seat top impedance, and the seat height. The only real failure occurs with the effect of inter-row spacing. Most of its shortcomings would probably be improved by incorporating a more sophisticated treatment of diffraction and impedance into the model.

Chapter 10

A Concert Hall Simulator for Subjective Tests

10.1 Previous Experiments in Subjective Auditorium Acoustics

In order to place the present work in context, a brief survey is made of its antecedents, emphasising the methods used to obtain the subjective data and any findings relevant to the subjective experience of seat dip attenuation.

The earliest work of interest here is due to Haas (1951 and 1972), who conducted a pioneering experiment into the effects of reflection delay, level and spectrum on subjective annoyance. This was mostly done using two loudspeakers and a speech source in a room with a 0.8 s reverberation time. Among other results, his paper showed that subjects were less annoyed by echoes when they were low-pass filtered. This may have been the basis for the subsequent opinions of Schultz and Watters (1964) that seat dip attenuation might be compensated by increasing reverberant bass energy, because it seems that the ear is less sensitive to delay at low frequencies. The possibility of such a compensation is contradicted implicitly by more recent work (see below), and explicitly by the results in part 11.3.

Beranek and Schultz (1965) simulated a concert hall sound field in an ordinary, non-anechoic room by using anechoic music with one loudspeaker exciting room reflections to simulate all the early sound field. Reverberation was provided by

several loudspeakers distributed throughout the room, but no artificial echoes were added. They used this arrangement to investigate the preferred range of early to late energy ratio. An experiment was also conducted to show that listeners more readily detected removal of reverberant bass rather than early bass energy. Since many loudspeakers provided reverberant signals and only one provided direct and early reflections, perhaps this is not surprising. The lack of control over the veracity of this simulation means that these results are unlikely to have serious implications for the perceptibility of seat dip attenuation in concert halls.

Hawkes and Douglas (1971) were the first experimenters to apply the statistical technique of factor analysis to subjective auditorium data. The data was obtained by surveying concert audiences with questionnaires using bipolar scales. That is, the subjects had to rate a hall property by placing one mark somewhere on a continuous line labelled, say, "Dead" at one end and "Live" at the other. Their paper includes an extensive criticism of Beranek's scheme for rating concert halls, which had assumed that all subjective factors were linearly additive (so that good reverberance could compensate for poor definition, for example). Hawkes and Douglas showed that listening to a concert is a multidimensional experience, with between four and six independent factors, such as "Resonance" and "Blend". This finding does further damage to the idea that strong bass reverberance may compensate for early field defects.

Hawkes and Douglas' method has the fundamental advantage of the real impulse response provided by the hall with its appropriate early reflection density. The

method also has the disadvantage common to all those using real halls of restricting the range over which the parameters of the impulse response can be changed. This makes it hard to design an experiment to give clear results, and complicated analysis methods must be used.

The other main experimental method reported in the literature involves a fully simulated sound field. Ando and Gottlob (1979) used five loudspeakers to provide direct sound and four delayed reflections, thus simulating a concert hall in an anechoic chamber. Paired comparison tests were used to find preferred values for IACC and initial time delay gap with different musical motifs. Though Ando was not the first to use this method, his paper represents the start of a shift towards the use of completely synthesised sound fields. These offer greater flexibility and ease of control than the method of surveys in real halls typified by Hawkes and Douglas. The appearance of commercially-available high-quality digital delay systems probably accounts partly for the growing popularity of the method.

Barron and Marshall (1981) simulated up to two reflections and reverberation using loudspeakers in an anechoic chamber, in experiments to investigate the effects of reflection delay, direction, level and spectrum on spatial impression. The results were used to propose the definition of Early Lateral Energy Fraction. An attempt was made to determine the effects of seat dip attenuation on spatial impression, but the presence of several possible subjective reflection masking mechanisms prevented firm conclusions from being drawn.

Blauert and Lindemann (1986) synthesised a sound field with two early lateral reflections and reverberation in an anechoic chamber. A dummy head was used to record binaural music samples in this field so that the samples could then be replayed to subjects over headphones. Blauert and Lindemann then ran a paired comparison test where subjects were asked to say which was the more spacious of two samples with different reflection and reverberation level and spectra. The main findings were that early lateral reflections are the primary cause of spaciousness, and that below 3 kHz depth effects predominate with breadth being caused by higher frequencies. This means that it is likely that seat dip attenuation will affect the depth part of spaciousness. The authors note that their method gives rise to errors (thought to be small) due to differences in the head-related transfer function between subjects.

Barron (1988b) has also conducted a subjective survey of UK concert halls by questionnaire. Preference judgements on nine scales were extracted and compared with objective measurements in the same halls. The main findings were that subjects fall into two groups: those that prefer "Intimacy" and those that prefer "Reverberance". If subjects differ on such fundamental subjective attributes, this raises the unfortunate possibility that no consensus opinion might be discernable for secondary defects such as seat dip attenuation. The overall preference was found to best related to mean reverberation time across frequency. Barron notes the advantages of using real concerts in real concert halls: incorporation of the realistic effects of entertainment and visual cues, and the lack of reproduction distortion.

This last point is probably still valid at the state of the art of reproduction equipment available today.

Olive and Toole (1989) investigated, amongst other situations, the effect of low-pass filtering a lateral reflection on its subjective threshold. The familiar loudspeakers-in-anechoic-chamber simulation was used, except that the space simulated was a typical listening room, and not a concert hall. They found that reducing the low-pass filter cut-off to 500 Hz had little effect on threshold. This is in contrast to the quite large above-threshold effect on subjective annoyance measured by Haas (see above). Both results can be accommodated if we infer that the ear is not significantly less sensitive to delay at low frequencies (Olive and Toole), and that high frequencies are more subjectively annoying than low (Haas).

Morimoto *et al.* have conducted several useful investigations into the factors governing auditory spaciousness. In the first, by Morimoto and Maekawa (1988), band limited white noise samples were presented to subjects using three loudspeakers in an anechoic chamber, in such a way that the IACC and cut-off frequency of the samples could be varied independently. Paired comparison tests were conducted in which listeners had to determine the wider of two samples. For the present work, the most interesting finding was that "an increase of spaciousness caused by the components of 100 - 200 Hz is great, and is equivalent to an increase of spaciousness caused by the reduction of IACC from 0.8 to 0.5". Since the Göttingen subjective study reported by Schroeder *et al.* (1974) established the importance of a low value of IACC and since 100 - 200 Hz sound can be strongly

attenuated by the seat dip effect, this is indirect evidence of the subjective importance of seat dip attenuation. In another paper Morimoto and Posselt (1989) describe the use of a similar system with a source of music, and with reverberation added. The method of average error (see part 11.1.1) was used to obtain the point of subjective equality between spaciousness caused by early reflections and that caused by reverberation. It was found that reverberation could independently create the same degree of spaciousness as early reflections. These findings have now been refined by Morimoto and Maekawa (1989). This time, essentially similar experiments were performed, except that subjects were to detect two effects: spaciousness, defined as "the width of an auditory event perceived temporally and spatially to be fused with the auditory event of the direct sound" and envelopment, defined as "the fullness of (the) auditory event around a listener, excluding (the) auditory event relating to spaciousness". Some listeners were able to tell the difference: spaciousness depended on the IACC of the total field and envelopment was affected by the IACC of the reverberant field. Taken together, these three papers mean that seat dip attenuation may noticeably affect spatial attributes of the listening experience caused by early reflections. Reverberation can also produce a spatial effect, but since this is not the same as that caused by early reflections, it probably would not compensate for the seat dip effect.

10.2 A Completely Simulated Sound Field

A brief description of the simulator and its impulse response will be given, before going on to a more detailed examination of important parameters of its sound field. The arrangement was of the now familiar type involving nine independent digital

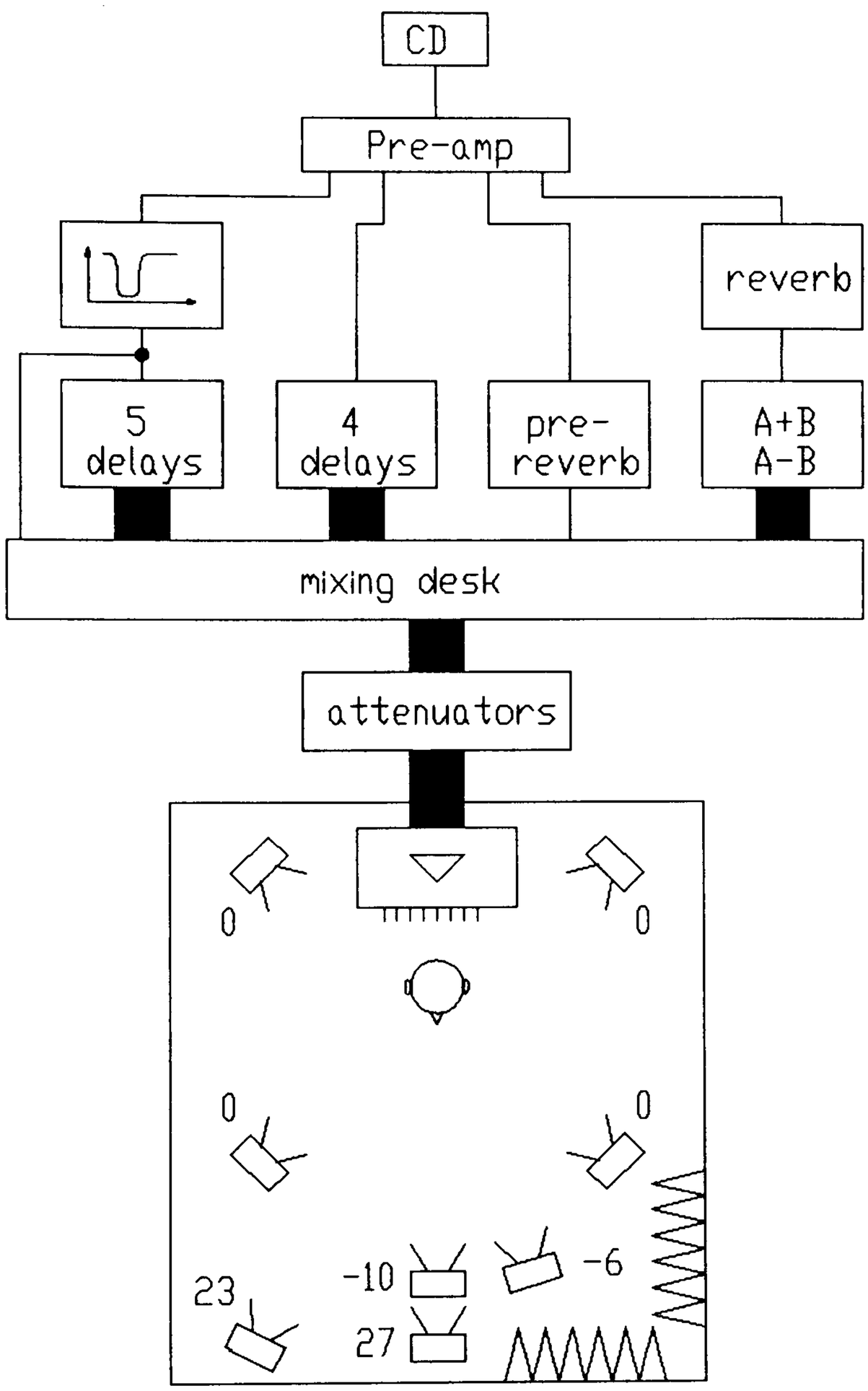

Figure 10.1: Block diagram of the simulator. The angle of elevation (in degrees) of each loudspeaker is given.

delay units simulating reflections from anechoic music, as shown in figure 10.1. The reflections could be individually attenuated, and five of them and the direct sound could also be subjected to a seat dip filter with variable attenuation. Each reflection was sent to one of eight loudspeakers spaced in three dimensions in an

anechoic chamber. Reverberation was provided by a stereo digital unit, from which the sum and difference of the outputs was formed. These four channels of reverberation were sent to the four horizontal loudspeakers. A "pre-reverb" signal consisting of a 110 ms reflection was also used to smooth the transition from early reflections to reverberation. Figure 10.3 is a photograph of a subject in position.

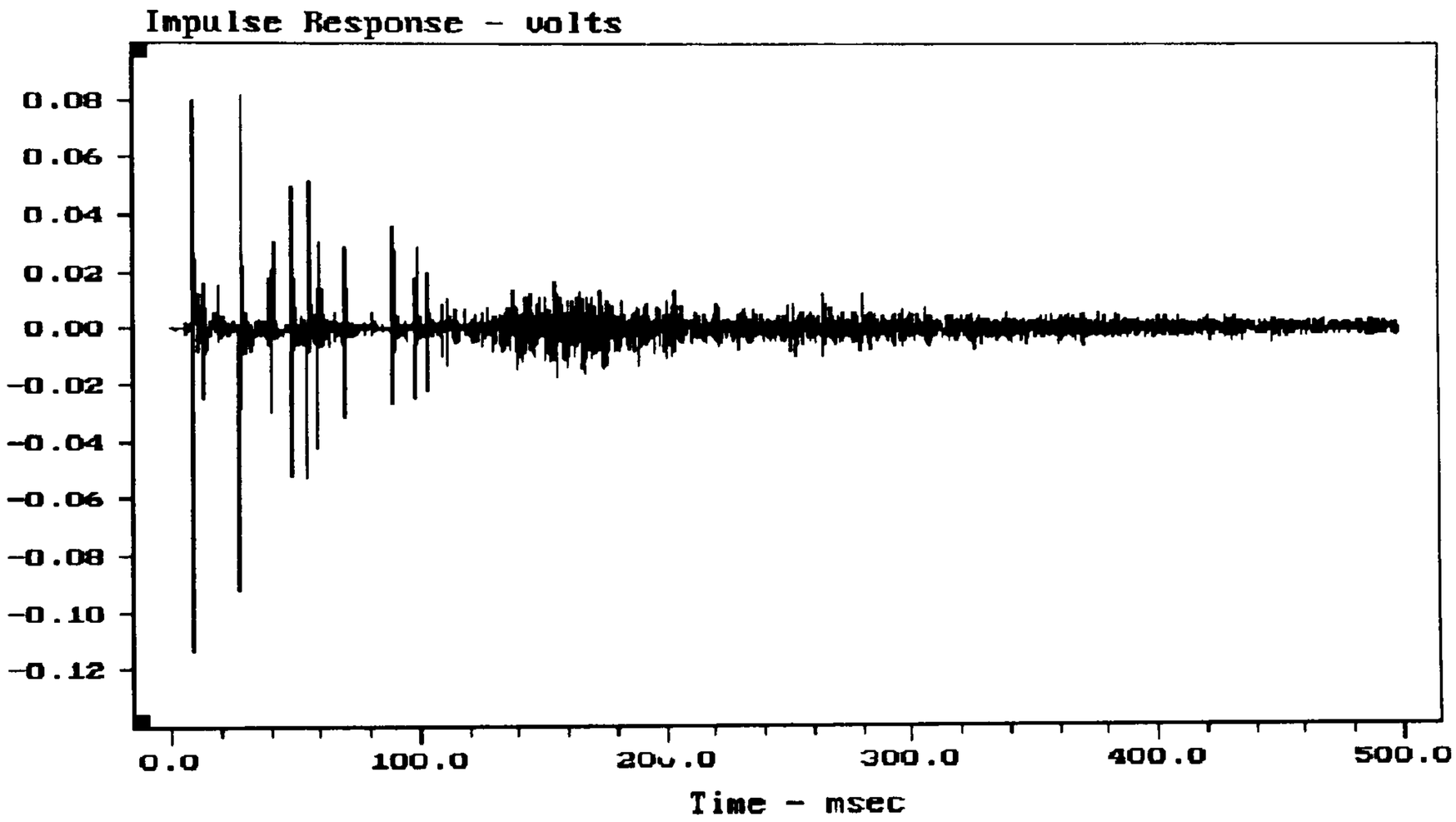

Figure 10.2: Broadband impulse response at listening position in simulator.

The broadband impulse response at the listening position is shown in figure 10.2. This figure emphasises the most important criticism of this type of simulator, namely, that sound energy is discretised into too few early reflections to be realistic. It is true that this impulse response is a simplified version of several produced by a computer model, which must themselves be less complex than that of a real concert hall. However, the subjects used in the difference limen tests (chapter 11)

Figure 10.3: A subject in the concert hall simulator, seen from the rear right-hand loudspeaker.

reported that the sound field was certainly three-dimensional, and that, while it would not be mistaken for a real hall, it had all the features of one. Although the simulation could no doubt have been improved by using more reflections, the greater expenditure in time and money was not felt to be warranted.

The second justification of this form of simulation is necessity. Though using real hall impulse responses is attractive, it is hard to see how variable amounts of seat dip attenuation could be incorporated into them. Perhaps it would be possible to construct digital filters approximating real seat dip transfer functions and use these to modify anechoic music, but it would still be hard to obtain a large range of instantly-reproducible attenuations.

10.3 Target Values for Room Acoustic Parameters in the Simulator

While setting up the simulator, a survey was made of the literature for values of the following parameters: RT, Early Decay Time (EDT), Clarity (C_{80}), Centre Time (T_s), Deutlichkeit (D), Early Lateral Energy Fraction (L_f), and total sound level (L_{tot}). The first six are defined, respectively, in Sabine (1923), Jordan (1968), Reichardt and Lehmann (1981), Cremer and Müller (1982a), Thiele (1953) and Barron and Marshall (1981). Both subjectively preferred values and those measured in real concert halls were sought. While there is a large database of RT values to be found, the other parameters, though by now well-accepted, are not so common in the literature. However, the following range of extremes measured in halls were obtained from Barron (1988a), Beranek and Schultz (1965), Bradley and Halliwell (1989), Gade (1990), Tachibana *et al.* (1986) and Tachibana *et al.* (1989):

-5 < C_{80} < 6.9 dB

0.15 < D < 0.53

76 < T_s < 210 ms

0.9 < RT < 3.1 s

0.75 < EDT < 3.2 s

0.05 < L_f < 0.44

(In order to avoid unnecessarily lengthening the list of different quantities, the less common quantity $10\log(E_R/E_E)$ in Beranek and Schultz (1965), which is the same as M in Gottlob (1973), was converted directly to D using Gottlob's definition. No reliable total level figures from real halls were found; several authors give levels normalised to the source-receiver distance, but do not quote the distance.)

Subjectively optimum values for these quantities are even fewer in the literature. There is only one source each for most of the measures, as follows:

0 <	C_{80}	< 8 dB	Reichardt and Lehmann (1981)
	D	≈ 0.34	Gottlob (1973)
	T_s	< 140 ms	Cremer and Müller (1982a, p. 628) after Lehmann
0.8 <	RT	< 3.0 s	Ando (1985, p. 75)
1.4 <	RT	< 2.8 s	Jordan (1980, p. 188)
1.8 <	EDT	< 2.6 s	(*ibid.*)
	L_f	≈ 0.74	Williamson (1989)
77 <	L_{tot}	< 79 dBA	Ando (1985, p. 67) (Gibbons motif)

$$79 \quad < L_{tot} \quad < 80 \text{ dBA} \qquad \text{Ando (1985, p. 67) (Arnold motif)}$$

It should be noted that all of the above hall values are from unoccupied auditoria. With the introduction of an absorbing audience to a hall, reverberant energy should decrease, and so C_{80} and D should increase, while T_s decreases. Bradley (1991) has estimated that the mid-frequency values of C_{80} for Boston Symphony Hall, Amsterdam Concertgebouw and Vienna Grosser Musikvereinssaal increase by between 2 and 3 dB with occupation. This would help explain why many published measured values of C_{80} are close to 0 dB, whereas the middle of Reichardt's subjectively preferred range is 4 dB. Because it was important that the simulator sound "natural" to subjects, the most important target value governing the early sound field was Reichardt's one of Clarity.

The starting point for fixing the impulse response of the simulator was a computer model of the Royal Festival Hall described by Rindel (1991). The Odeon program was used to predict the delay, level and direction of the principal early reflections. This program is a commercial package using an image-source algorithm with a ray-tracing pre-check for the early sound field and a simple statistical algorithm for the reverberant field. It is thus close to the state of the art for such models identified in a review by Stephenson (1990). This was done for several mid-stalls seats, and the results combined by eye into the nine delays and eight directions available in the simulator. Because this computer program did not incorporate the effects of diffuse reflection and diffraction, additional use was made of the global tour of concert halls by Tachibana *et al.* (1989). This showed significant reflections

in several halls arriving from the seating in front of and below the horizontal plane of the listener.

Slight adjustments were made to the simulator until it sounded "natural" to the experimenters and to some of the subjects used later. This was thought to be important, since the difference limen tests (chapter 11) would require the subjects to listen intently to the sound field. It was felt that making the simulator sound as realistic as possible to them would reduce the chance of fatigue and perceptual errors. The level, direction and delay of the reflections fixed on is shown in table 10.1.

Delay (ms)	Level (dB)	Azimuth (°)	Elevation (°)	Seat dip filtered ?
0	0	0	-10	y
19	-3	45	0	y
32	-12	135	0	n
41	-6	-1	27	n
46.5	-7.5	21	23	n
50.5	-10	315	0	y
61	-12	225	0	y
81	-12	-12	-6	y
90	-12	-1	27	n
95	-14	135	0	y

Table 10.1: Reflection Parameters used in Concert Hall Simulator.

10.4 Simulating Seat Dip Attenuation

Comparison of spectra in the literature shows that the shape of the seat dip attenuation spectrum varies considerably from hall to hall. Some of the graphs in chapters 6 and 7 show that it also varies from seat to seat and over time in one hall. It was decided, therefore, to generalise the problem to that of a low-frequency octave-band attenuation. This might be more meaningful to hall designers than a filter which attempts to represent a particular seat in a particular hall. 200 Hz was chosen as the centre frequency of the octave; this falls roughly in the middle of the spread of seat dip frequencies in the literature. Two ⅓-octave graphic equalisers were therefore cascaded and set so that the 200 Hz octave was maximally attenuated, and the attenuation was evenly applied across the octave. A mixer was then constructed so that the signal sent through the equalisers could be combined with an unattenuated signal, in such a way that the octave band attenuation could be varied in roughly 1 dB steps, while the pass-band level remained constant. Some typical spectra from the filter are shown in figure 10.4. The maximum attenuation of 18.2 dB across the octave is sufficient to represent a very severe seat dip attenuation of the direct sound. In practice, the pass-band level did not vary by more than 0.3 dB across the range of attenuation settings.

The choice of which reflections to apply the filter to was guided by the original computer simulation of the Royal Festival Hall. In the first ten arrivals, the computer gives six lateral reflections and four frontal ones. Of these ten, six are near grazing incidence (two frontal and four lateral). Table 10.1 shows that the simulator had six lateral reflections and four frontal ones, including the direct

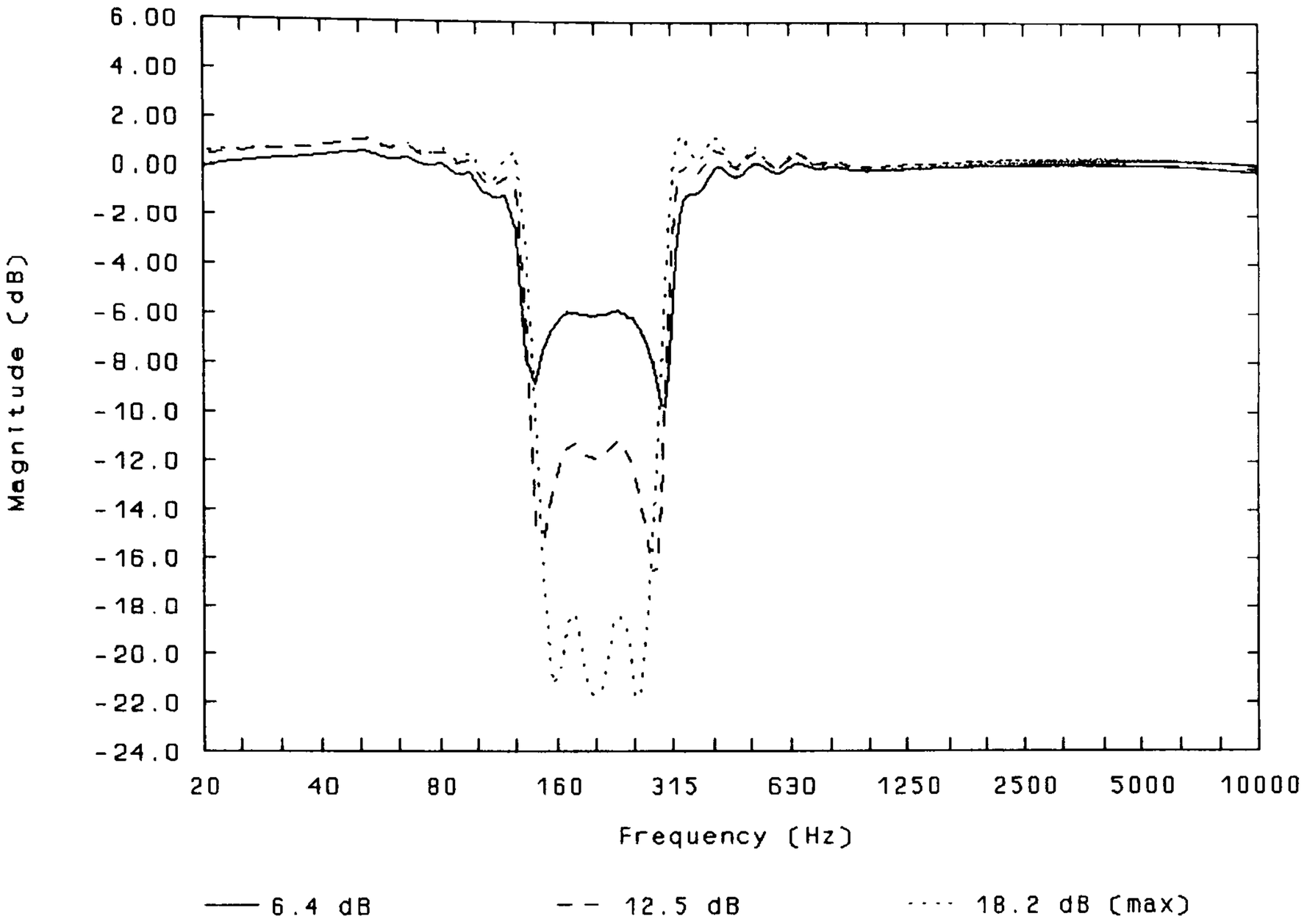

Figure 10.4: Frequency response, at three levels of attenuation, of the variable seat dip filter used in the simulator.

sound. Seven of these ten were near grazing (two frontal and five lateral). Because of the circuitry of the delay lines, it was only possible to apply seat dip attenuation to the direct sound and five delay paths. The one grazing reflection which was picked not to be seat dip filtered was the low-level one at 32 ms. It should be emphasised that all these six reflections are attenuated by the same filter. This is a compromise, but a reasonable one: certainly the vertical angle of incidence of early lateral reflections in a rectangular hall will be close to that of the direct sound. The horizontal angles would of course be different, but we might expect the seat dip attenuation to be very similar over an octave.

10.5 Room Acoustic Parameters Measured in the Simulator

10.5.1 Single-figure Values

The total level for the music motif specified in chapter 11 was set at 79 dBA ("slow" setting on measuring amplifier), with the direct sound alone being 75 dBA. This falls in the middle of Ando's specifications for preferred values of L_{tot}. 79 dBA is also within the range of levels used by Barron (1974, p. 34 and p. 68) in his simulator experiments: 81 dB, 73 dB (slow Wagner motif), and 77 dB. Once the level had been set, mid-frequency values of the other parameters could be found. These were measured across a double octave centred on 1 kHz (i.e. 500 - 2000 Hz):

$RT = 2.3$ s

$EDT = 1.8$ s

$C_{80} = 3.2$ dB

$T_s = 80$ ms

$D = 0.62$

$L_f = 0.28$

The values for RT and EDT are reasonable, though 2.3 seconds is more typical of European than of British concert halls. An EDT of 1.8 seconds is at the bottom of Jordan's recommended range, but plenty of good concert halls have an EDT significantly shorter than their RT (see Bradley and Halliwell (1989) for example). A Clarity of 3.2 dB is nearly in the middle of Reichardt's subjectively optimum range, and would seem reasonable for an occupied hall. The centre time is rather short, at 80 milliseconds. This is a consequence of the limited number of early reflections being balanced against the comparatively dense, statistically-produced,

reverberation (see figure 10.3). Because the simulator is different from real halls in this respect, this apparently low value of T_s may not adequately reflect the satisfactory balance of clarity and reverberation experienced by the subjects. (It should be borne in mind that most subjects were regular attenders at concerts in British halls, which have a reputation for favouring clarity at the expense of reverberation according to Barron (1988b).)

A Deutlichkeit of 0.62 in the simulator also seems extreme, and the low reflection density from 50 to 120 milliseconds may also be part of the explanation here. This value of D is almost twice Gottlob's recommended value, and is the only parameter outside the extremes measured in real, unoccupied, halls. However, there is some disagreement between Gottlob's value of D and Reichardt's range of C_{80}. This may be demonstrated as follows: using an image-source model, it is possible to calculate the total sound intensity I_t^{∞} arriving at a receiver in a hard rectangular room, t seconds after a pulse was emitted. After Barron (1974, p. 128), it is

$$I_t^{\infty} = 312\frac{T}{V}e^{-13.82\frac{t}{T}} I_{01} \qquad (10.2)$$

where T is the reverberation time of the room, V its volume, and I_{01} is the intensity of the direct sound at unit distance from the source. Theoretical values of C_{80} and D are then:

$$C_{80} = 10\log_{10}(e^{\frac{1.1}{T}} - 1)\ dB \qquad (10.4)$$

$$D = 1 - e^{\frac{-0.69}{T}} \qquad (10.5)$$

Using these relationships, Reichardt's range of C_{80} implies an acceptable range for D of 0.35 to 0.71. Given that there is some conflict between these recommended values and that of Gottlob, it was decided that Reichardt's was the more important. C_{80}, with its 80 ms limit, was originally proposed as a more suitable measure of useful early energy for music than D, with its limit of 50 ms. This is because the limit of perceptibility of the ear appears to be longer for music than for speech (Cremer and Müller, 1982a, p. 431).

A value of 0.28 for the Early Lateral Energy Fraction indicates that the spatial distribution of reflections in the simulator is realistic. It is close to the middle of the range measured in real halls. While 0.28 falls a long way short of the optimum value proposed by Williamson, above, so does every other value of L_f in the literature. Williamson notes that, whilst a very high value may be preferred, it cannot be achieved without artificial sound reinforcement. Significantly louder lateral reflections were rejected as subjectively unnatural in the initial listening tests in the simulator.

10.5.2 The Effect of the Seat Dip Filter on Room Acoustic Parameters

All of the parameters discussed above, except Deutlichkeit, were also measured in octave bands either side of 200 Hz, at every setting on the variable seat dip filter. The results appear in figures 10.5 - 10.9, where the arrow points in the direction of increasing attenuation.

Figure 10.5 shows that increasing the seat dip attenuation affects C_{80} substantially. This is to be expected: the seat dip filter removes early energy, so decreasing Clarity. This graph is in good agreement with the C_{80} versus frequency graph for the Free Trade Hall (figure 6.12(a)), where C_{80} at 200 Hz was 3.0 dB lower than that at 1.6 kHz. That Free Trade Hall seat had an octave attenuation (at 40 ms) of -8.1 dB. In the simulator, when the seat dip filter is set so that an octave attenuation of -8 dB (at 40 ms) is measured at the listening position, C_{80} at 200 Hz is 4.0 dB lower than C_{80} at 1.6 kHz. Now, because the simulator is not an attempt to model the Free Trade Hall *per se*, but rather a representation of a generic rectangular hall, exact agreement between C_{80} values is not sought. It is enough to say that the effect of increasing seat dip attenuation in the simulator is of the expected order of magnitude. The implications for the perceptibility of such a large change in low-frequency Clarity will be discussed in the light of the results for the perception of seat dip attenuation in chapter 11.

The effect of increasing seat dip attenuation on centre time (figure 10.6) is analogous to the effect on C_{80}; this time, the value rises dramatically with increasing attenuation at 200 Hz, and remains nearly constant elsewhere. Again, this is in good qualitative agreement with the profile of T_s against frequency in the Free Trade Hall (figure 6.11(b)).

The graph of EDT versus frequency (figure 10.7) shows a slight increase at 200 Hz as the attenuation is increased. This is to be expected: EDT only covers the first 10 dB of decay, and so is more sensitive to changes in the early sound field than the

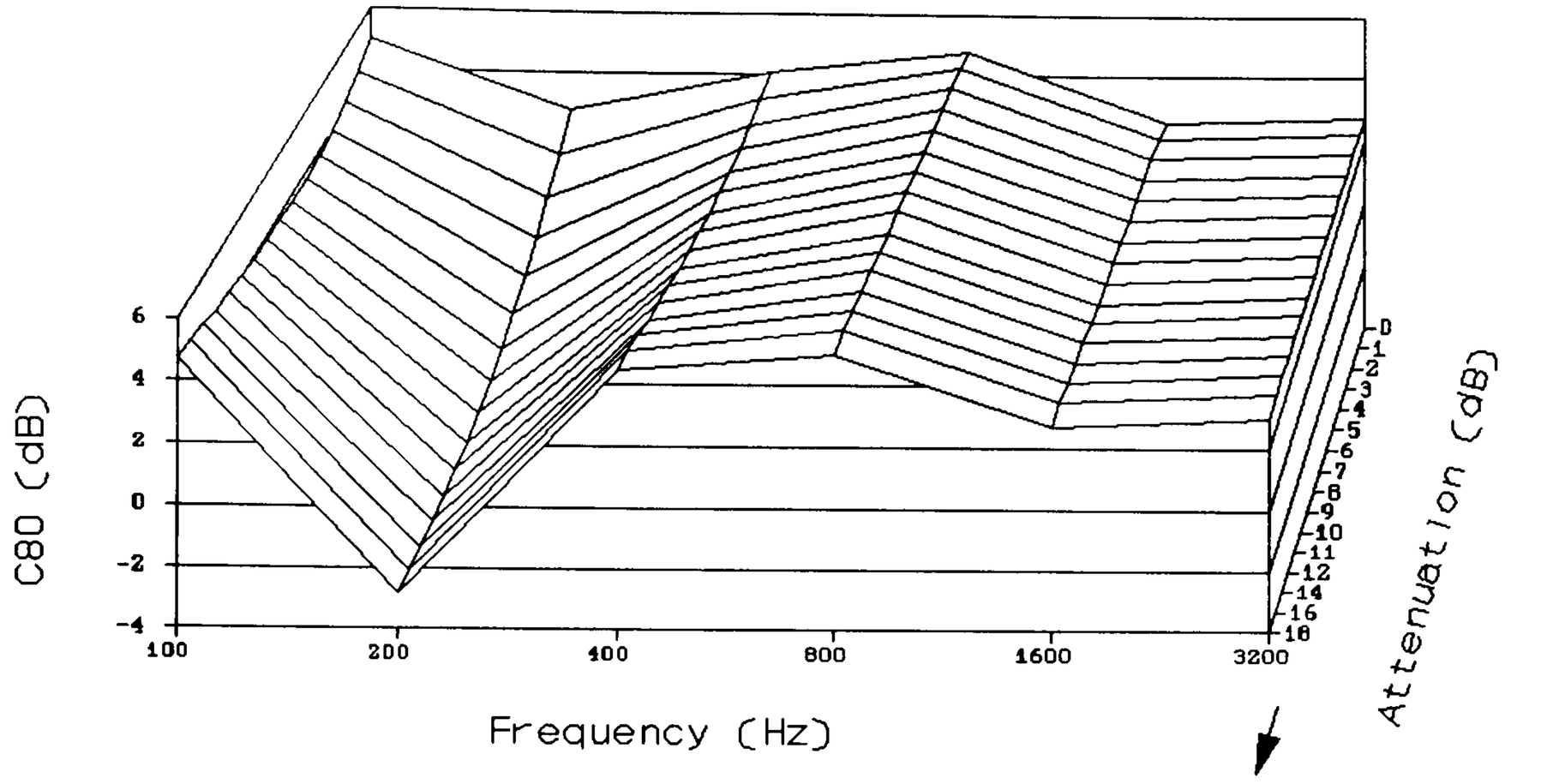

Figure 10.5: Effect of 200 Hz seat dip attenuation on Clarity (C_{80}) in the simulator.

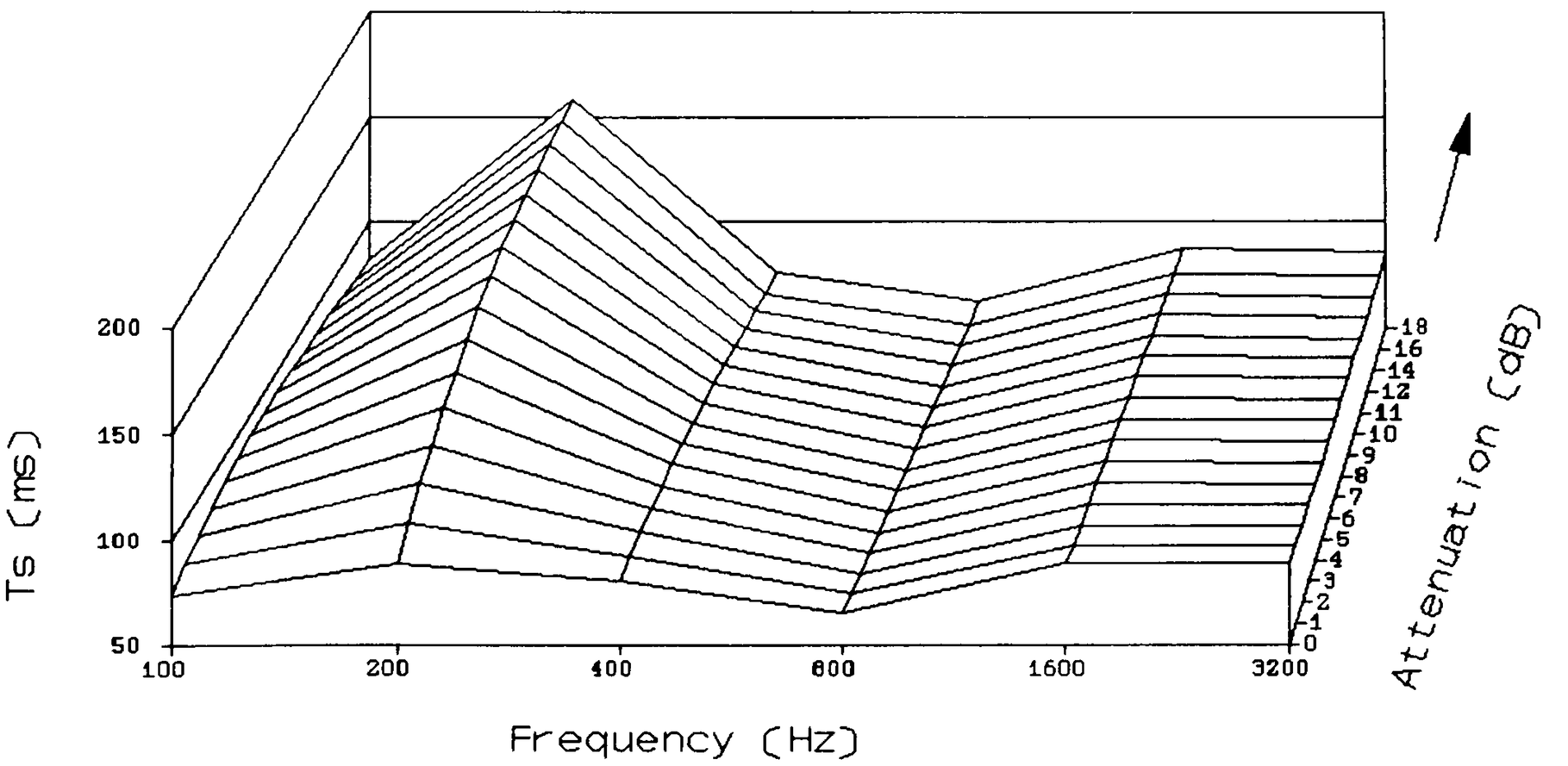

Figure 10.6: Effect of 200 Hz seat dip attenuation on Centre Time (T_s) in the simulator.

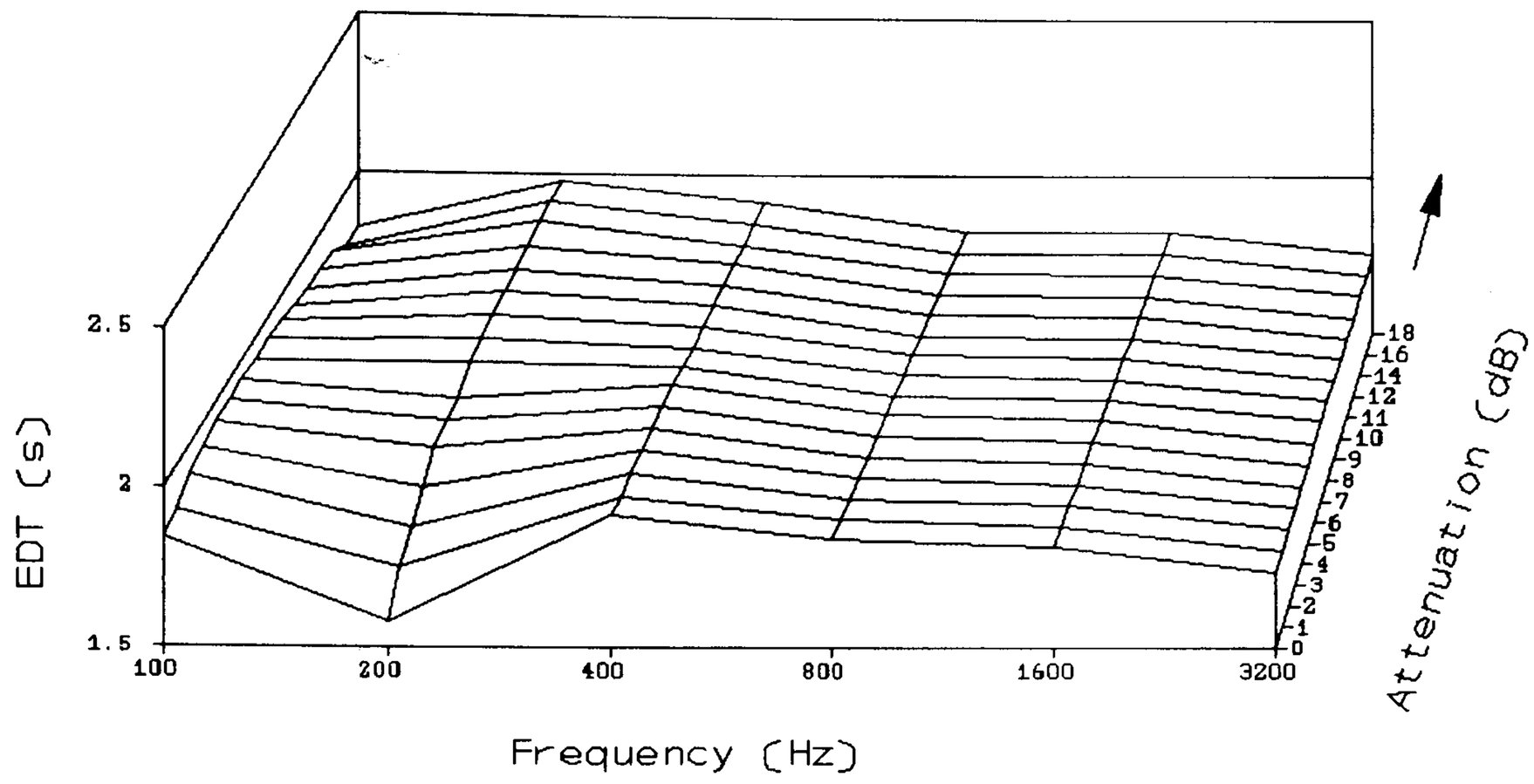

Figure 10.7: Effect of 200 Hz seat dip attenuation on Early Decay Time in the simulator.

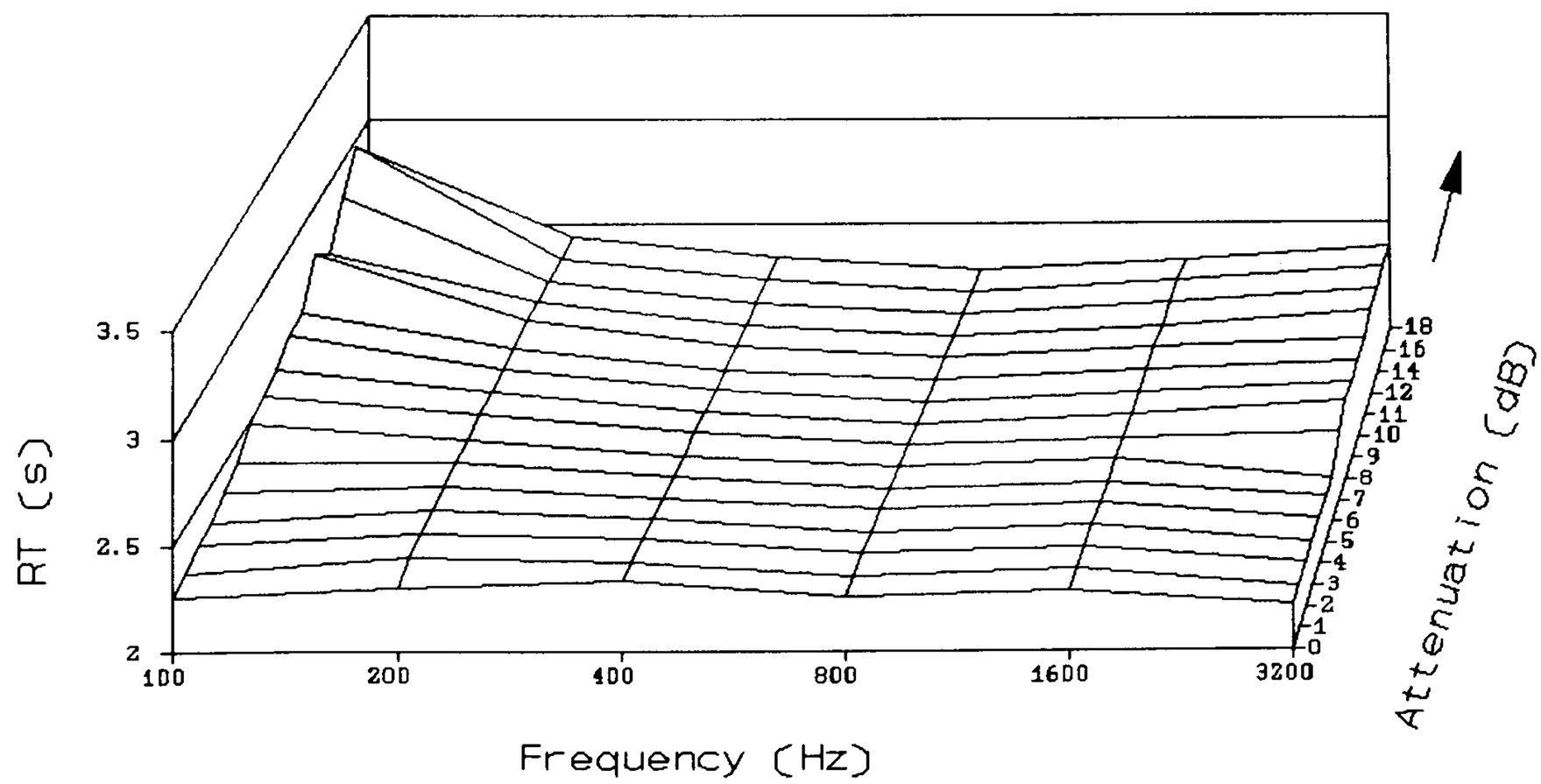

Figure 10.8: Effect of 200 Hz seat dip attenuation on Reverberation Time in the simulator.

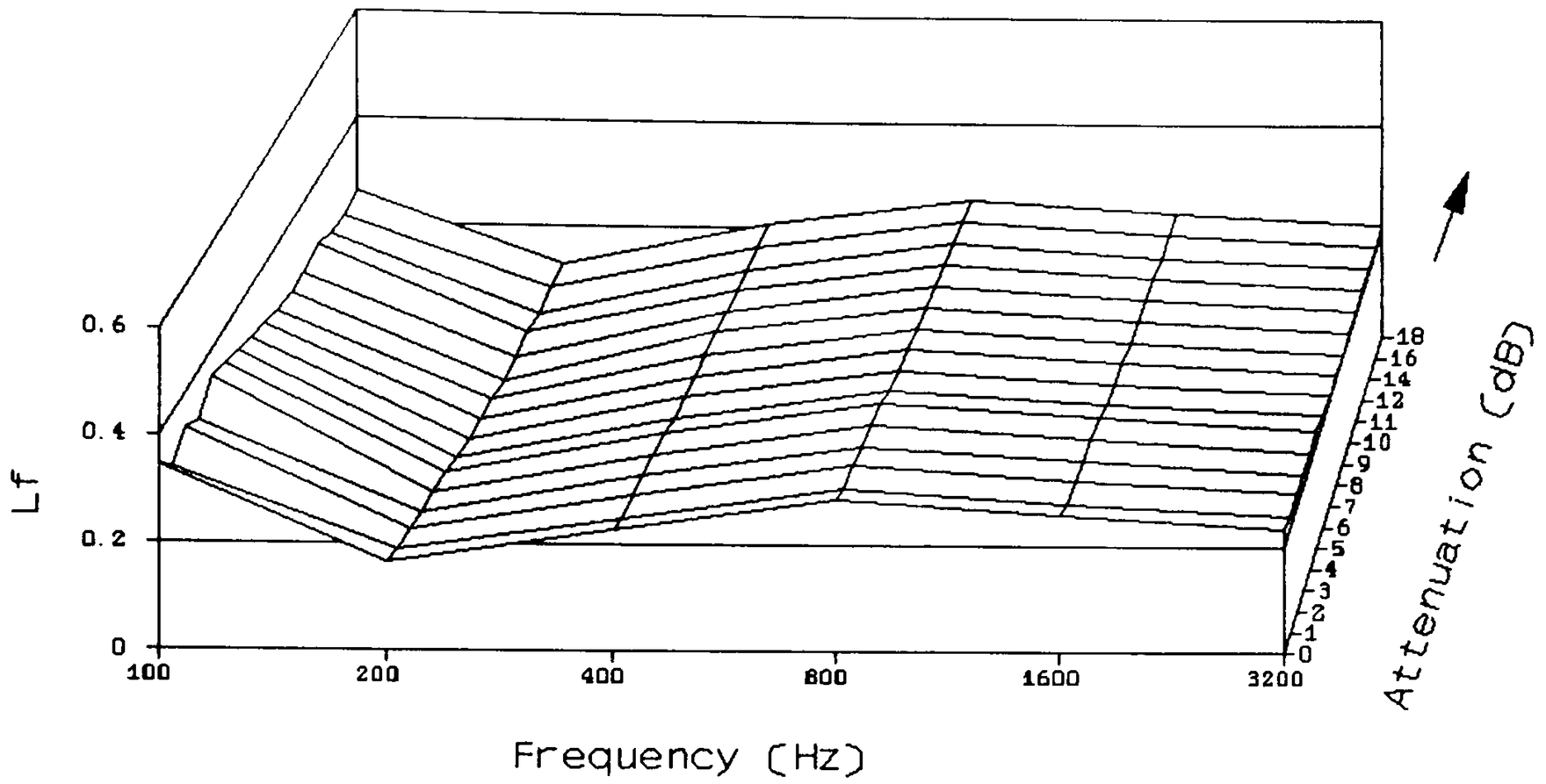

Figure 10.9: Effect of 200 Hz seat dip attenuation on Early Lateral Energy Fraction (L_f) in the simulator.

30 dB RT. The change is in the expected direction, too, as removing early energy would tend to tilt the integrated decay curve to a shallower gradient, thus increasing EDT.

A similar plot for reverberation time, figure 10.8, shows no such effects. RT does not change significantly in any frequency band except 100 Hz over the range of seat dip attenuations applied. The ripple in RT for large attenuations is due to the decay curve becoming progressively non-linear as more energy is removed. Low-frequency decays in real halls are often uneven, and hence hard to fit a straight line to in order to estimate RT. Large seat dip attenuations have exacerbated this.

Finally, figure 10.9 shows that Early Lateral Energy Fraction also remains unchanged when seat dip attenuation is applied. This is because the frontal and lateral sound is being attenuated by the same filter.

10.5.3 Room Acoustic Parameters with Different Reverberant Fields

For part of the investigation into the subjective effects of seat dip attenuation (chapter 11), it was necessary to measure difference limens with much less, and much more, reverberation than that described above. This was done in the first case by switching the digital reverberator off, and in the second by increasing its level and the RT set on the device. The total sound level with music was held at 79 dBA for both sound fields. For the field with no reverberation, the mid-frequency parameters measured in the simulator were:

RT = 0.2 s

EDT = 0.4 s

C_{80} = 11.4 dB

T_s = 23 ms

For the highly reverberant field, the same parameters were:

RT = 3.1 s

EDT = 2.9 s

C_{80} = 0.2 dB

T_s = 152 ms

Whilst the non-reverberant field represents an unnatural extreme, the other was thought by subjects (several of whom were postgraduate students of acoustics) to be a realistic representation of a hall with little absorption present. This is to be expected: because the timing of the early reflections was not altered, the hall sounds highly reverberant for its "size".

For both these non-standard fields, the effects of increasing seat dip attenuation were very similar to those portrayed in figures 10.5 - 10.9. The effects were slightly less pronounced in the non-reverberant field, and very nearly the same in the highly reverberant one.

10.6 Change of Seat Dip Attenuation in Simulator with Time

The final analysis of the performance of the simulator is an examination of its impulse response using program Longfft (described in chapter 6). Figure 10.10 is for a filter attenuation of -7.8 dB attenuation, and shows how the levels in the 100, 200 and 400 Hz octave bands change from 0 to 50 ms after the direct sound arrival. In comparison with figure 7.9, which depicts the same data for a typical seat in the Free Trade Hall, it can be seen that this aspect of the simulator is also realistic. The only difference stems from the lower early reflection density in the simulator. In figure 10.10, the effect of the first few reflections can be clearly seen, particularly when the 200 Hz level starts to climb after the arrival of the ceiling reflections (which have no seat dip attenuation applied) at 41 and 46.5 ms. Though this effect is not quite so apparent in the Free Trade Hall graphs, it does occur.

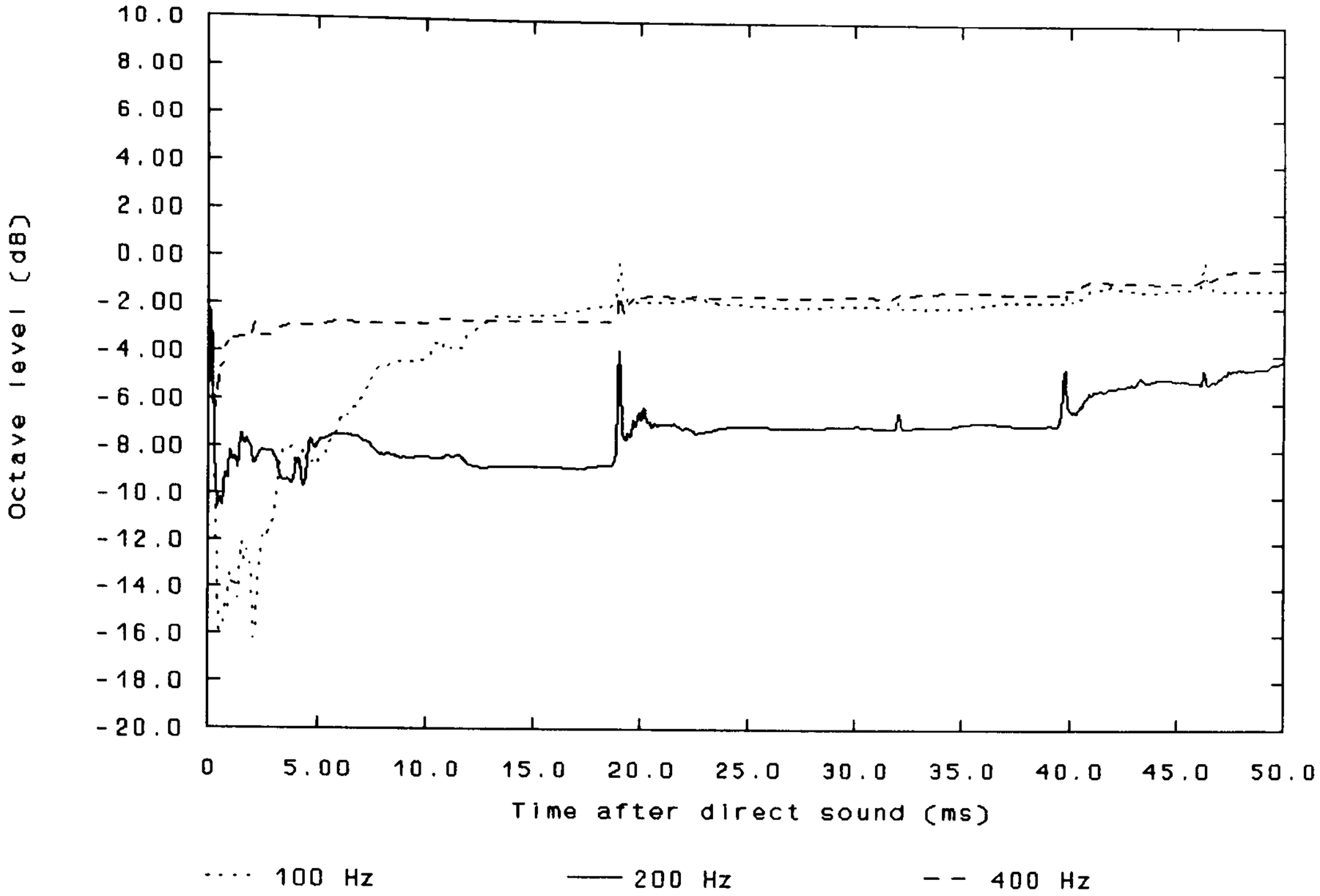

Figure 10.10: Change in octave band levels over time in simulator.

10.7 Conclusion

Seven room acoustic parameters have been measured in the simulator and shown to be in reasonable agreement with subjectively preferred ones. The simulator values also fall within the range of extremes in the literature, in all but one less important case. In comparisons with a computer model, data in the literature, and from subjective impression, the timing, level and direction of the reflections of the simulator also seem realistic. Finally, the form of the synthetic seat dip attenuation used has been shown to be accurate enough to have the expected effects on five room acoustic parameters. It is thought that the change in the level of the 200 Hz octave band of the early sound will also be a variable general enough to be meaningful to hall designers.

Chapter 11

The Subjective Effect of Seat Dip Attenuation

In the preceding chapter, the physical arrangement of the concert hall simulator was considered and its veracity was established. The method used to obtain data from subjects sitting in the simulator can now be considered. There are three main psychometric test methods commonly used for this purpose with artificial sound fields. Their advantages and disadvantages for the task of measuring the smallest perceptible change, or difference limen (DL), for seat dip attenuation are outlined below. Guilford (1954) is a good source of more detailed information on the methods used for subjective experimentation in many disciplines.

11.1 Possible Methods for Subjective Tests

11.1.1 The Method of Average Error

This was used by Barron (1974), where he described it as the self-testing comparison technique. The subject is presented with a fixed, standard sound field and a variable sound field, different from the standard one in some respect. The subject can adjust the variable field in that respect, and switch between the two fields. She adjusts the variable field until it seems equivalent to the standard one. This is repeated many times, and a DL is estimated from the interquartile range of the data.

The main advantages of the method of average error are speed and "naturalness". The subject feels in control of the experiment, and this may improve her motivation and concentration. The main disadvantage here is that strictly the method dictates finding a DL for the *level* of the seat dip frequency band in both the "boost" and "cut" directions, rather than a DL for the amount of attenuation. This would entail a rather complex filter capable of adding energy in the seat dip band as well as removing it. This problem arises because the method of average error is unusual in asking for a judgement of equality rather than one of "different" or "not different".

11.1.2 The Method of Minimal Changes

This entails finding a just noticeable difference (*jnd*), and a just not noticeable difference (*jnnd*). In the first instance, the experimenter sets a variable sound field to be equal to a standard sound field. Both are presented serially to the subject. Some aspect of the variable field is then changed and the presentation repeated. This continues until the subject reports a *jnd*. To obtain the *jnnd*, the procedure begins with the variable field definitely different from the standard one; the difference is decreased until the subject reports a *jnnd*. The DL for this method is then thought to lie somewhere between the *jnd* and *jnnd*. This DL is likely to be larger than that obtained by the method of average error, because the subject cannot switch quickly and repeatedly between sound fields.

In finding a DL for seat dip attenuation, the method of minimal changes needs only a relatively simple filter, capable of changing attenuation in a particular band by

small, well-defined amounts. The two main errors likely to arise are those of habituation (where a subject continues to give the same judgement in a series, past the point of subjective equality) and anticipation (where heightened attention and expectation cause the subject to report a change before one actually occurs). If both these errors are present, they will tend to cancel out when the *jnd* and *jnnd* are averaged.

11.1.3 The Method of Constant Stimuli

In this method, a fixed number of different sound fields are chosen, and each paired with the standard field. Each pair is presented to the subject a large number of times in a prearranged order unknown to the subject. The subject judges whether one of the pair is "greater" or "less" than the other; "uncertain" is also allowed. In a so-called "full paired comparison", a sequence of every possible pair of fields is presented. Because the order of presentation is unknown to the subject, reversal of judgement is possible: the subject may say that A is greater than B when the reverse is true. Hence this method is likely to give a higher DL than either of the two methods above.

The obvious disadvantage of paired comparison tests is the length of time needed for each run. In the present experiment, the differences between even the most extreme sound fields, though audible, were small, so that the probability of subject fatigue occurring increased considerably with test length.

11.2 A Threshold of Perception for Seat Dip Attenuation

The method of minimal changes was used to find a DL for the level of attenuation in the 200 Hz octave band under different conditions of reverberation in the simulator described in chapter 10. This method was chosen because it seemed to represent a good compromise between accuracy, time and complexity of equipment. Ten subjects, all experienced listeners, were used: all either worked in acoustics or were musicians; some were both. The motif used was the first two bars of an anechoic recording of Handel's Water Music Suite produced by Hidaka *et al.* (1988), which lasts for four seconds. This was played to the subject four times, in the format ABAB, where A or B was randomly chosen to be attenuated. There was a one second gap between every presentation. After each ABAB block, the subject had to say whether there was a difference between A and B. If they could not tell, the ABAB block could be repeated at the same level of attenuation (and in the same order). This continued for as many times as the subject wished, at a given attenuation level. Each test run started either at maximum attenuation or no attenuation, giving, respectively, either a *jnnd* or a *jnd*. No special lighting conditions were used in the anechoic chamber, as Morimoto *et al.* (1990) have shown that visual stimulus has little effect on echo threshold. Though extrapolating from threshold to above-threshold effects is not always valid, it was not felt that the lighting would be a significant source of variation. Subjects were allowed to close their eyes to aid concentration.

Once it had been established (see following analysis) that the *jnd* and *jnnd* could be averaged, their mean gave the DL for the level in the 200 Hz octave band.

Because this difference is from 0 dB downwards, the DL is effectively a threshold for seat dip attenuation. That is, the smallest perceptible change from 0 dB downwards is the absolute threshold of perception for seat dip attenuation. Of course, it was important that this attenuation threshold could be realistically compared with the concert hall measurements of attenuation in earlier chapters. To this end, the maximum octave band attenuation in the simulator was measured at the listening position for each level on the seat dip filter. This was done 40 ms after the arrival of the direct sound, in exactly the same way as single-figure attenuations were evaluated for the Free Trade Hall for comparison with the subjective data. The correct measured level was substituted for the nominal filter level recorded for each test run, so that every *jnd* and *jnnd* represented the real attenuation experienced by the subject.

To start with, two reverberant conditions were investigated: one comprised the standard sound field as described in chapter 10; the other used the same sound field with all reverberation turned off, but with the direct sound and all nine early reflections present. These fields are characterised by mid-frequency centre times of 80 and 23 ms respectively. After allowing some runs for training, each subject was tested three times for each run direction. This was done at both values of centre time, giving a total of 120 individual difference limens (60 *jnd*'s and 60 *jnnd*'s). The impulse response of the simulator was recorded and checked after each run to ensure that the equipment performed correctly throughout.

11.3 Statistical Analysis Method and Results

An analysis of variance was performed for the factors centre time (T_s), subject and run direction. This involved constructing a matrix containing every valid DL recorded. The variance of the whole set of data is explained in terms of variances due to the factors, their interactions, and a residual variance. The use of a residual variance is possible because the values of DL at each combination of factors were assumed to be repeat values. Any variation between three such values was due to factors not controlled in the experiment: for the purpose of the analysis these are assumed to be random. This treatment is referred to as a two-way analysis of variance (Chatfield, 1983, pp. 248-256). Its purpose is to establish how significant the variances due to the factors and their interactions are compared to that due to the residual variance.

The first step in the analysis was to calculate the sum of the squares of the data for each factor and interaction. For the factor direction, for example, the mean DL for the whole matrix was subtracted from all the "up" DLs and these values were then summed. The same was done with all the "down" DLs. These two numbers were then squared and added to give the sum of the squares for direction. Next, the mean square for the factor was found by dividing the sum of squares by the number of degrees of freedom for that factor. For direction, which can take two values, the number of degrees of freedom is one; for the factor subject it is nine. The mean square is proportional to the variance in the data due to the factor.

For an interaction between two factors, the procedure was similar except that each combination of factor values was considered when forming the sum of squares. The sum of squares due to each factor in the interaction was then subtracted to give the sum of squares for the interaction between the factors alone. The number of degrees of freedom for the interaction is equal to the product of the number for each factor. The residual sum of squares was finally found by subtracting all the factor and interaction sums of squares from the sum of the squares of the whole data matrix. The degrees of freedom attributed to the residual are all those of the data matrix which are not explained by the factors and their interactions.

To test each factor and interaction mean square against the residual, an F-test was used. This is a probability distribution which gives, at various percentage confidence levels, the answer to the question of whether the ratio of a factor mean square to the residual mean square is significantly greater than one. A table of the F distribution at a particular percentage confidence level was consulted. If the F ratio of the two mean squares was greater than the value in the table for the particular degrees of freedom of the two mean squares, then the factor being tested was significant at that level. For example, if a factor was significant at the 5% level, then there is a 5% probability that the effects attributed to the factor are random. The 5% level is usually termed "possibly significant", the 1% level "significant" and the 0.1% level "highly significant".

In this analysis, the factor subject was a special case: it represents a sample from the whole population of concert-goers, and is therefore termed "random", in contrast

to the other factors which are "fixed". In an analysis of variance with mixed types of factors it can be shown (Wetherill, 1981) that if a random factor is involved in a significant first-order interaction its F-value must be formed by dividing the factor mean square by the interaction mean square, and not by the residual mean square. The results of the analysis are shown in table 11.1

Type	Source	Sum of squares	Degrees of freedom	Mean square	F ratio	signif-icance
fixed	T_s	47.8	1	47.75	17.40	0.1?
fixed	direction	160.3	1	160.31	58.40	0.1
random	subject	828.2	9	92.02	6.32	1?
	T_s x dir	1.7	1	1.73	0.63	n.s.
	T_s x subject	131.0	9	14.56	5.30	0.1
	dir x subject	47.4	9	5.27	1.92	n.s.
	T_s x dir x subject	69.8	9	7.75	2.82	1
	Residual	219.6	80	2.75		
	Total	1505.9	119			

Table 11.1: Analysis of variance of recorded difference limens.

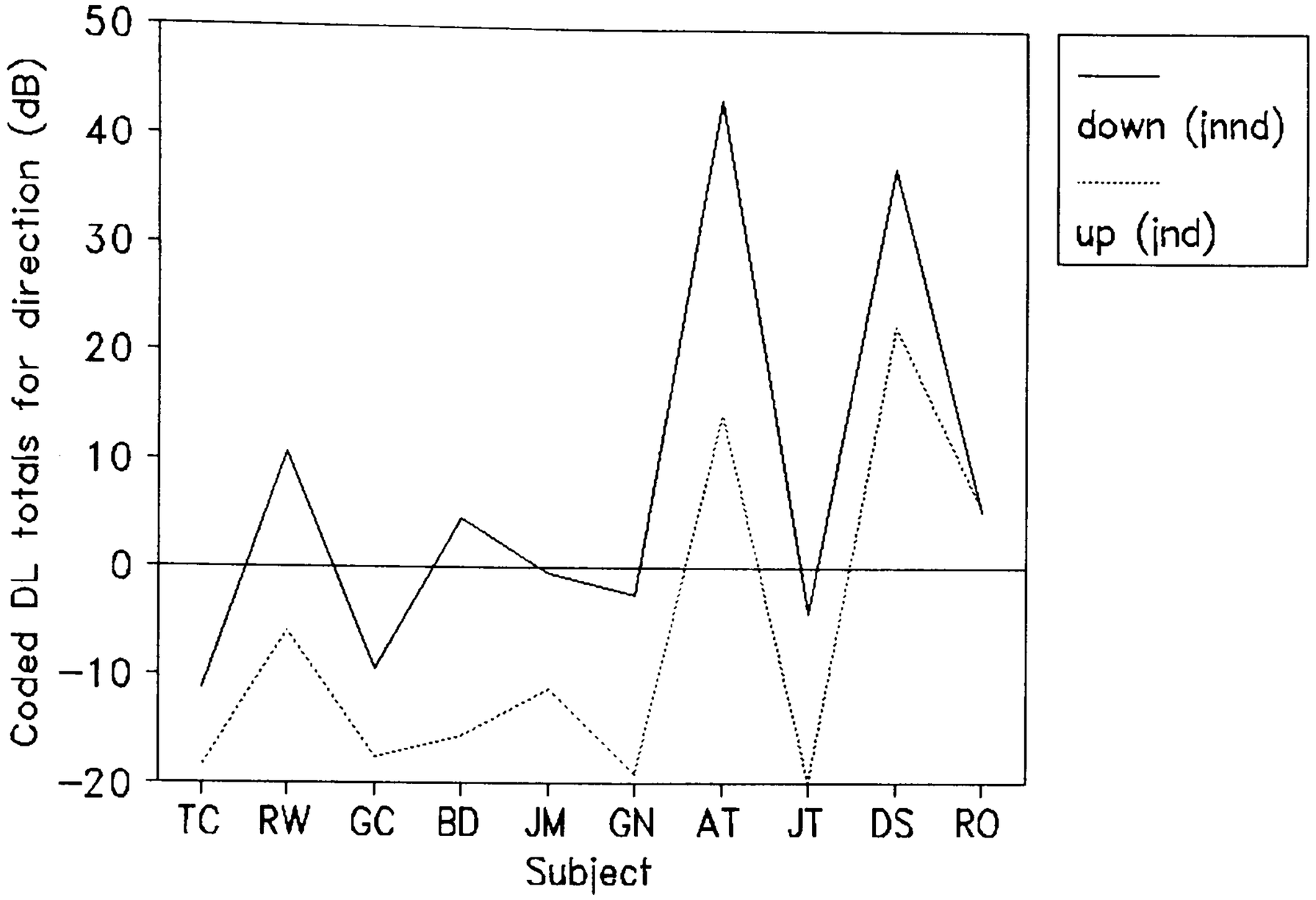

Figure 11.1: Variance of difference limen for seat dip attenuation: direction by subject.

There is a highly significant interaction between the factors centre time and subject (at the 0.1% level). Run direction does not seem to interact with the other factors. This is clearly shown in figures 11.1 and 11.2. The first graph plots the coded difference limen totals for run direction against subject. That is, each point on the graph is the sum of two coded limens, one for each value of T_s. (Coding refers to a constant subtracted from the raw data to reduce the size of the sums of squares.) The two lines are a similar shape and do not cross - the effect of direction seems to be the same for each subject. That the *jnd*'s are lower than the *jnnd*'s indicates that the errors of anticipation are greater than those of habituation. This is a product of the experimental method, and the true limen is likely to lie between the two.

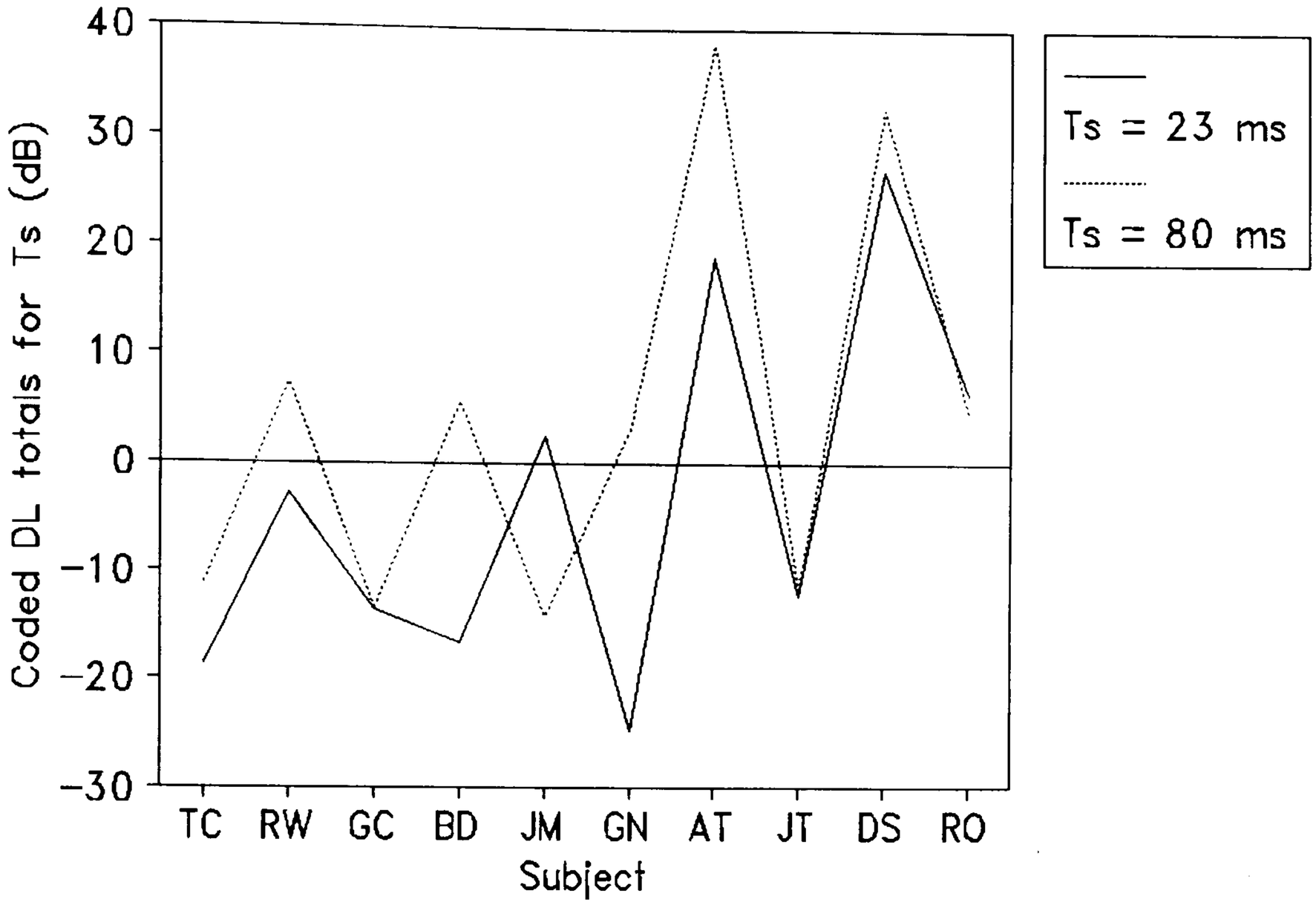

Figure 11.2: Variance of difference limen for seat dip attenuation: centre time by subject.

The second graph is a similar plot, this time of the coded limen totals for centre time against subject. This time, the two lines cross, indicating that the effect of different centre times is quite different for different subjects. This is not surprising. Some subjects commented that they sometimes found it harder to hear differences between presentations in the less "natural" field without reverberation. Others said that, though the effect of seat dip attenuation was similar in both fields, the addition of reverberation made it more difficult to pick out. However, there are no obvious sub-groups in this graph; musicians do not perceive the effect of centre time differently from acousticians, for example. Hence, a breakdown analysis was not conducted.

Because of this significant first-order interaction, it is not possible to be precise about the effects of the factors centre time and subject. F-values have been calculated for these factors in table 11.1, though. Though these F-values must be interpreted tentatively, they indicate that the factor "subject" is significant, and centre time is very significant.

The factor "direction" is not involved in any first-order interactions, so its F-value is less ambiguous. It shows that direction is very significant (at the 0.1% level). However, as mentioned above, this is a product of the experimental method. It is reasonable to assume that the most physically meaningful difference limen will be obtained by averaging out the direction effect (Guilford, 1954). We are therefore left with a threshold which seems to depend on subject and centre time. Because "subject" is a random effect, it is not sensible to present separate limens for each subject and centre time. Hence we proceed to calculate thresholds L_{crit} for each value of centre time, averaged across direction and subject. These are

$$L_{crit}\ (T_s{:}23ms) = 6.4 \pm 0.9\ dB \qquad (11.1)$$

$$L_{crit}\ (T_s{:}80ms) = 7.7 \pm 1.0\ dB \qquad (11.2)$$

The uncertainties are two standard errors. Because these values are so close together it seems reasonable to say that, for practical purposes, the presence of reverberation has little effect on the threshold, which is then

$$L_{crit} = 7.1 \pm 0.6\ dB \qquad (11.3)$$

11.4 A Further Investigation of the Effect of Reverberation

To obtain further evidence for the effect of reverberation on the threshold, two subjects were tested several times with a new sound field. This was identical to the standard field, except the reverberant level was increased, and the RT was increased to 3.0 seconds. Though this increase in reverberant level was broadband, it had the effect of increasing the level in the 200 Hz octave of the late sound (at 500 ms) by 2.8 dB, while a seat dip attenuation of 7.2 dB was being applied to the early sound. This new field is characterised by a mid-frequency centre time of 150 ms (see section 10.5.3). This represents an extreme among measured real concert halls; it is close to the mid-frequency values in the Vienna Grosser Musikvereinssaal measured by Bradley (1991). The two subjects used were chosen because they had the lowest intra-subject variances in the group (i.e. they were the most consistent). This seemed the best way of representing the group, and of obtaining reasonably accurate results, given that there was not enough time to retest more subjects.

A new analysis of variance was then performed on these two subjects, as above, except that this time, centre time had the values 23, 80 and 150 ms. This time, there were no significant interactions between the factors. Only two main effects were found to be possibly significant: direction, at the 5% level; and subject, at the 0.1% level. Centre time was not found to be significant for these two subjects.

From all the above results, it seems as if reverberant energy in a hall would probably not significantly mask the subjective effects of seat dip attenuation. This contradicts the hypothesis of some earlier seat dip researchers, Schultz and Watters

(1964), who were partly influenced by the work of Haas (1951). Haas showed that listeners were less disturbed by a speech echo when a low-pass filter was applied to it. This implies that the integrating time of the ear may be longer at lower frequencies. There is, however, no data in the literature for integration time with music, as a function of frequency. Whilst it is reasonable from signal theory to suppose that the ear has a longer "processing" time at lower frequencies, there seems to be enough information in the first 100 ms for it to detect seat dip attenuation.

The significance of the interaction between centre time and subject is an indication of possible differences in perception mechanisms between subjects. Perhaps some subjects integrate longer passages of music than others. This raises the possibility that compensation by reverberation may be more effective for some listeners than for others. On the other hand, if the group of subjects used here is representative, any resultant differences in threshold are probably too small to be significant when averaged across a population.

11.5 An Investigation of the Effect of Music Motif

The two subjects chosen above were also used in tests to indicate the effect of the source music used. The tests in part 11.2 were repeated, using the standard sound field (T_s = 80 ms only), except that a four-second Mendelssohn motif was used (bars 398 - 399 of the fourth movement of symphony no. 3 from the same compact disc recorded by Hidaka *et al.* (1988)). Though the Mendelssohn is slower than the Handel, it has a similar spectrum when measured at the listening position in the

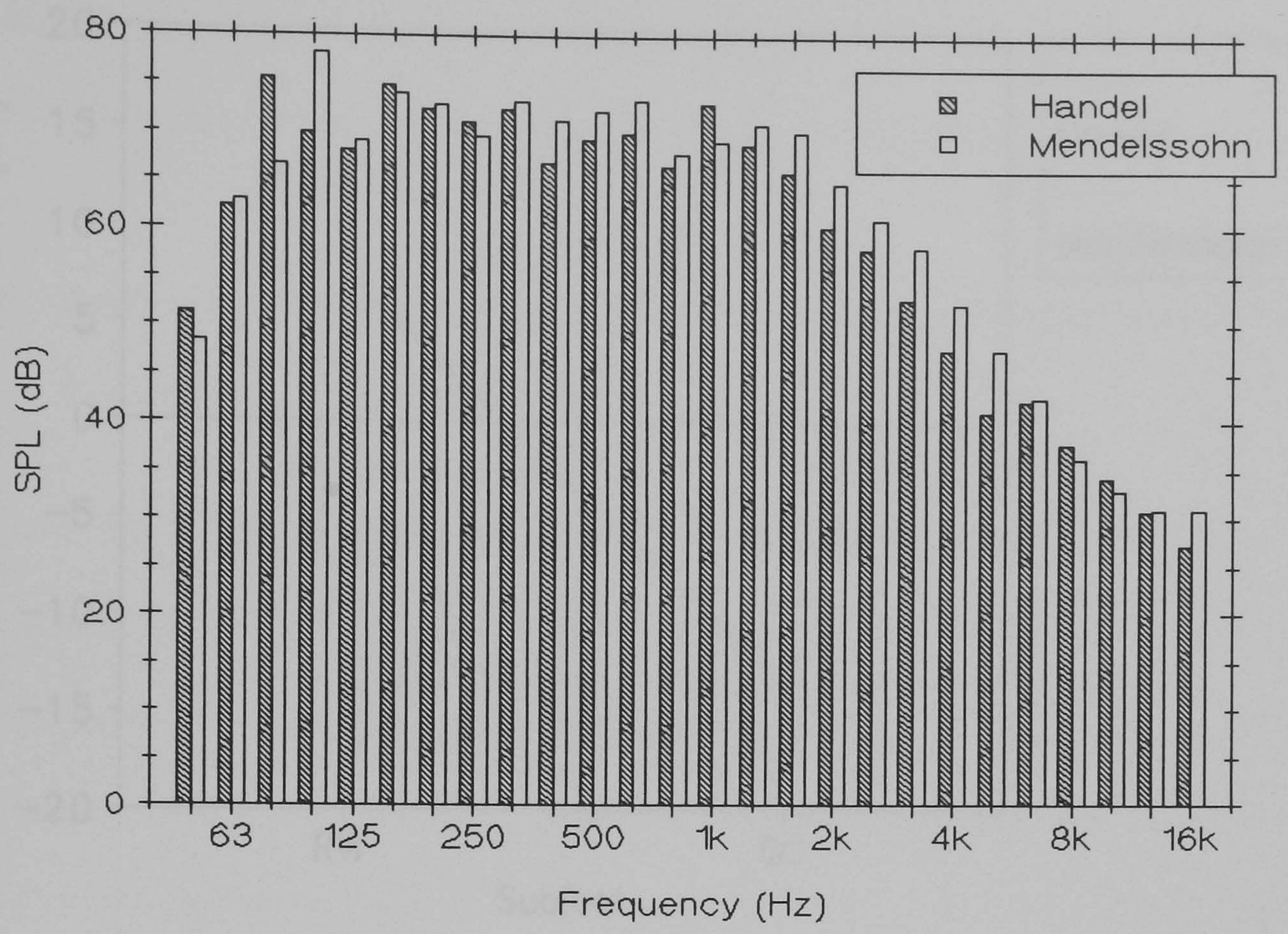

Figure 11.3: Spectra of two different music motifs measured at listening position in simulator and averaged over four seconds.

simulator, as shown in figure 11.3.

Another analysis of variance was then performed on the results from the two subjects, for the factors motif (Handel or Mendelssohn), direction (up or down), and subject. The results table is dominated by the first-order interaction between motif and subject. This is significant at the 0.1% level, whilst all the other effects have no significance. The interaction is illustrated by figure 11.4, which plots the coded difference limen totals for motif against subject. It is clear that the two subjects each found seat dip attenuation "easier" to hear on a different motif. That is, subject RW has a much lower DL for the Mendelssohn motif than for the

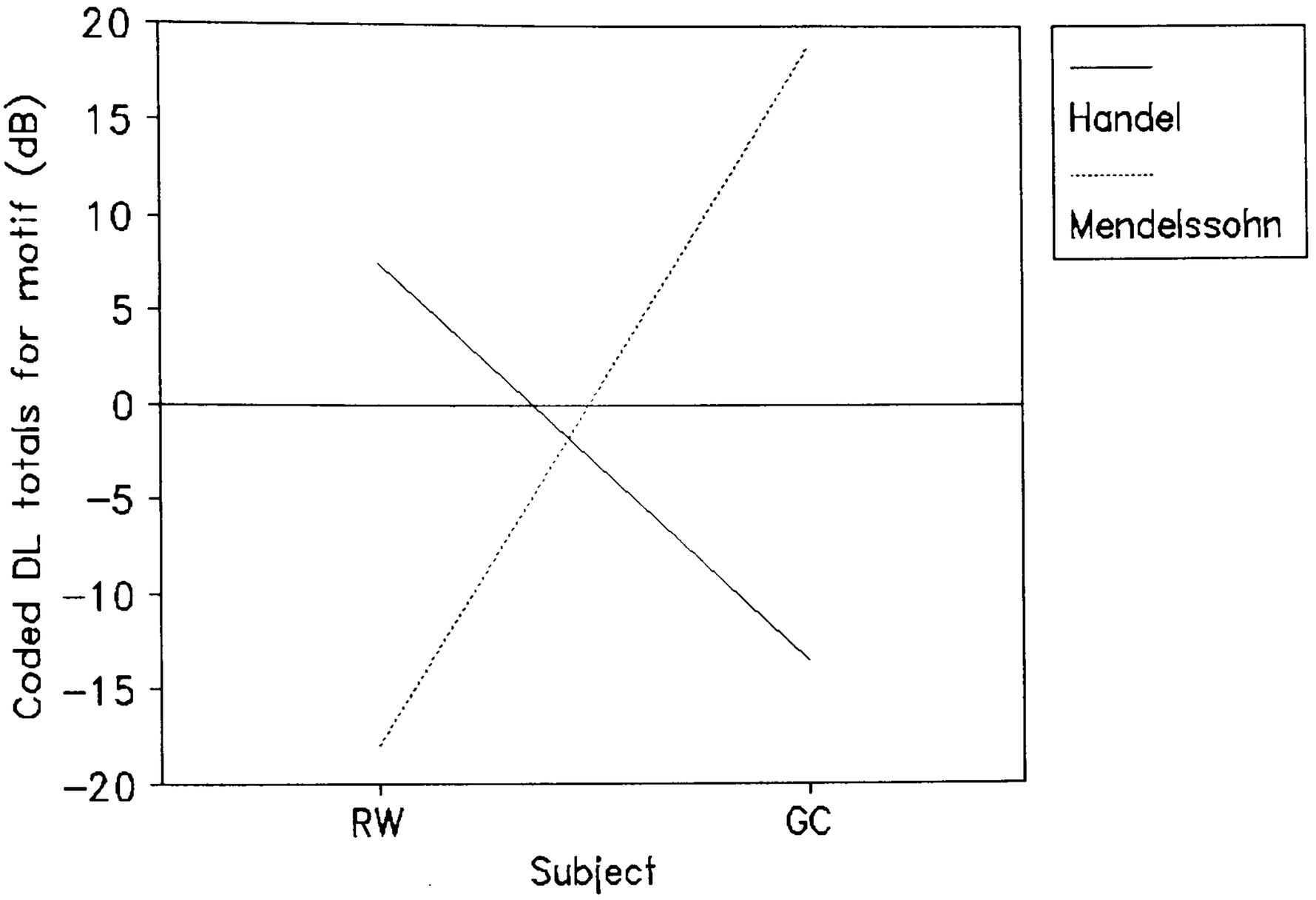

Figure 11.4: Variance of difference limen for seat dip attenuation: motif by subject.

Handel, and vice versa for subject GC.

Though these results are for only two subjects, they reflect those from the whole group of 10 in part 11.2, where subject interactions were also significant. If a threshold is calculated for each motif, averaged across these two subjects only, we obtain

$$L_{crit}\ (T_s{:}80ms;\ Handel) = 6.5 \pm 1.7\ dB \qquad (11.4)$$

$$L_{crit}\ (T_s{:}80ms;\ Mendelssohn) = 7.1 \pm 2.2\ dB \qquad (11.5)$$

Again, we see that, though the motif x subject interaction seems statistically significant, it may not affect the estimate of a threshold greatly.

11.6 Implications for the Usefulness of Low-Frequency Monaural Early Energy Parameters

In part 10.5.2 the variation of five room acoustic parameters with seat dip attenuation in the simulator was examined. It was found that the monaural early energy measures C_{80} and T_s were greatly affected at low frequencies by the attenuation, and RT, EDT and L_f hardly at all. Although these experiments were not designed to change these two parameters specifically, the change is so marked compared with that for the other parameters that we might assume that whatever subjective mechanism was used to detect seat dip attenuation is the same as that used to detect changes in low-frequency C_{80} and T_s. The threshold of 7.1 dB from equation (11.3) can then be used to estimate a DL for low-frequency C_{80} or T_s. (Both are considered together because they are so closely related.)

From figures 10.5 and 10.6, when the seat dip attenuation changes in the "standard" field in the simulator from 0 to 7 dB, C_{80} and T_s change according to the values in tables 11.2 and 11.3 respectively. The largest changes occur, not surprisingly, in the 200 Hz octave band. In this band, C_{80} decreases by 4.2 dB and T_s increases by 51 ms up to the threshold. These are very large changes. Cox (1992, pp. 253-257) has found (in the same simulator) that the average mid-frequency DL for C_{80} is only 0.67 ± 0.13 dB and that for T_s is only 8.6 ± 1.6 ms. It therefore seems that the ear is an order of magnitude less sensitive to monaural early energy indices at low

frequencies than it is at mid frequencies. Whilst the mid-frequency values of these parameters are known to be subjectively important, this result means that the collection and prediction of such low-frequency data in halls is of questionable worth. It should be emphasised that *binaural* parameters such as L_f are different in this respect: if anything, low frequencies are the most important range for spaciousness.

C_{80} (dB)	Frequency (Hz)					
Attenuation (dB)	100	200	400	800	1600	3200
0	5.0	2.9	4.1	4.8	2.6	2.7
7	3.8	-1.3	3.6	5.0	2.7	2.9

Table 11.2: Change in C_{80} recorded in octave bands in simulator for threshold of seat dip attenuation.

T_s (ms)	Frequency (Hz)					
Attenuation (dB)	100	200	400	800	1600	3200
0	74	89	80	65	89	89
7	90	140	85	64	87	87

Table 11.3: Change in T_s recorded in octave bands in simulator for threshold of seat dip attenuation.

11.7 Conclusion

The subjective phenomenon most affected by seat dip attenuation is probably auditory spaciousness. Morimoto and Maekawa (1988) have found that "an increase of spaciousness caused by the components of 100 - 200 Hz is great, and is equivalent to an increase of spaciousness caused by the reduction of inter-aural cross-correlation from 0.8 to 0.5." Furthermore, there is now good evidence from Blauert and Lindemann (1986) that early lateral reflections are a more important cause of auditory spaciousness than is bass reverberation. Of course, although seat dip attenuation may not greatly decrease the Early Lateral Energy *Fraction* (see figure 10.9), it does decrease the absolute level of early laterals, and Keet (1968) shows that this will affect spaciousness.

It was shown above that the threshold of perception of seat dip attenuation does not change significantly with large changes in reverberation. Certainly, it would not be practical to increase by "passive" means the bass reverberant level in a real hall by more than 3 dB (this would require that bass absorption be halved, for instance). A very large increase in reverberant level might be possible by using an electroacoustic system, of course, but such a gross change would be out of proportion to what is probably a small perceived defect for most listeners.

If anything can mask seat dip attenuation, it is likely to be unattenuated early energy provided by non-grazing reflections. However, Barron (1974, pp. 75-83) found it difficult to design an experiment to isolate the exact masking mechanism. During the training of the subjects here, the first step was to establish that a listener

could detect the application of seat dip attenuation when only the direct sound was played. Other reflections were then added gradually. As soon as the first unattenuated reflection was added, most subjects reported that it became much harder to detect the presence of any attenuation of the remaining reflections. This suggests that a way of increasing the subjective threshold would be to increase the strength of the first non-grazing reflection.

In any case it seems that if the seat dip attenuation at a seat is greater then the threshold, there is a danger of reduced spaciousness, no matter how strong the reverberation. The best estimate of the threshold is the all-over average given in equation (11.3). This is a fairly large attenuation, indicating that seat dip attenuation in a typical concert hall need not be an over-riding concern. The threshold is also probably a severe one: it was obtained, like most subjective test results, from a small group of trained "expert" listeners. It must also be remembered that the experiments on only two test subjects give indications at best. It is conceivable that large-scale tests, on many more subjects, could identify groups of subjects with different mechanisms or "preferences" for detecting seat dip attenuation under different test conditions. Given the current data, however, the best design estimate for the threshold of perception of seat dip attenuation is 7.1 ± 0.6 dB.

Chapter 12

Comparison of Objective and Subjective Data; Design Remedies for Seat Dip Attenuation

12.1 Single-figure values for Measured Attenuations

Many measurements of sound travelling at grazing incidence over auditorium seating have been presented in chapters 6, 7 and 8. These have demonstrated that the low-frequency attenuation at a seat is dependent on several factors. In particular, the received level is a function of both frequency and time. In chapter 11 subjective experiments were described which resulted in a figure for the smallest perceptible attenuation in a 200 Hz octave applied to the early sound field of a concert hall simulator. In order to ease the instructive exercise of comparing objective and subjective data, the time and frequency dependencies of this data will be removed to produce a single-figure attenuation level L_{min}.

12.1.1 Constant-frequency values

In chapter 10 it was stated that seat dip attenuation was simulated by applying a certain attenuation across the 200 Hz octave band. A given spectrum measured in the Free Trade Hall will therefore now be considered by looking at the total attenuation in the worst octave band only. Of course, because of the effects of parameters such as the vertical angle of incidence on the narrowband spectrum, the frequency of this octave will be different for different measurements. Because the

subjective data is only available for 200 Hz octave attenuations, the assumption must be made that the difference limen would not vary greatly across the range of frequencies of maximum octave attenuation in the objective data investigated. A second assumption is also made that the shape of the narrowband spectrum is not as subjectively important as its maximum octave attenuation. The final assumption, related to the second, is that one octave is the most sensible percentage bandwidth to use. Though the sharpness of the attenuation dip varies across the measured data, typical total octave band levels around the worst band are: +1.7, -9.1, and -1.7 dB. ⅓ octave band figures around the worst band for the same measurement are: +0.2, -8.6, -14.8, -9.4 and -3.6 dB. Thus a width of one octave is enough to contain most of the attenuation due to the seat dip effect.

These are reasonable assumptions because the ear seems to integrate energy within "critical bands" of frequencies. Zwicker and Feldtheller (1967) found that if the bandwidth of a narrowband noise signal was decreased below a certain critical bandwidth the perceived loudness did not decrease. Hence, changing the shape of a spectrum inside a critical band is probably insignificant if the energy in the band remains constant. Zwicker and Feldtheller found that the width of the critical band increases with its centre frequency. At 200 Hz, the critical bandwidth is a little less than that of an octave. This means that the filter shape within the 200 Hz octave is probably not very important. A rectangular filter shape was used in the subjective experiments (see figure 10.4) because it is an easily specified and reproduced shape. A standard octave band was used for this work rather than a

critical band because it was thought that octave band results would allow others to make use of the results with published hall data more readily.

12.1.2 Constant-time values

In part 6.3.2, it was shown that the level of the 200 Hz octave varied over time up to 400 ms after the direct sound arrival for a typical measurement in the Free Trade Hall. Different measuring positions (see figures 7.8 - 7.11) exhibit different amounts of variation. The octave levels in the concert hall simulator also changed over time. Because the simulator spectrum and any given hall spectrum may change differently over time, both need to be reduced to a single time-invariant figure for simple comparison.

The choice of time value to use is governed by several factors. One might decide to evaluate the attenuation when it is no longer changing; at 500 ms, say. This is certainly too late, however. In the experiment described in part 11.3, the reverberation in the simulator was increased until the 200 Hz octave level at 500 ms was +2.8 dB when a 7.2 dB attenuation had been applied to the early field. Because this made little difference to the subjective detection of the attenuation, a subjectively relevant comparison between objective and subjective data must use a shorter time limit.

A lower limit for possible comparison times is established by the 1:10 scale model tests in part 8.1. These showed that the attenuation due to a single impulse propagating across seating can vary at the receiver over at least 20 ms for full scale

seats. A sensible value for a comparison point should include at least all the effects due to the direct sound and then as many room reflections as are thought necessary.

Once the range of possible comparison times has been set at greater than 20 and considerably less than 500 ms, it becomes more difficult to specify a sensible figure. One candidate might be at the integrating limit of the ear at low frequencies for a music source. Unfortunately no such data could be found in the literature. It seemed best, therefore, to estimate the time interval in which all the arriving sound energy would be integrated. This is likely to be a function of the reflection levels in a hall. Barron (1971) has provided a useful chart for the subjective effects of a single lateral reflection with a music source, and this is reproduced in figure 12.1. Broadband energy-time curves (i.e. squared impulse responses) from several of the Free Trade Hall measurements were compared with the chart: a typical one is plotted in figure 12.1.

Clearly, any reflection touching the "disturbance" line in figure 12.1 might be perceived as a separate echo. There is one such reflection at 75 ms in the energy-time curve shown. Any reflection close to 0 dB, even if it arrives less than 50 ms after the direct sound may also not be fully integrated by the ear. If all such reflections are to be excluded from the part of the impulse response used for the single-figure attenuation, it was found that a limit of 40 ms was a safe one. After this time interval, some measured impulse responses in the hall (mostly those close to the rear wall) had reflection levels close to 0 dB. It is thus possible to show that

all the reflections up to 40 ms in any impulse response measured in the Free Trade Hall would probably be fused into a single auditory event by the ear.

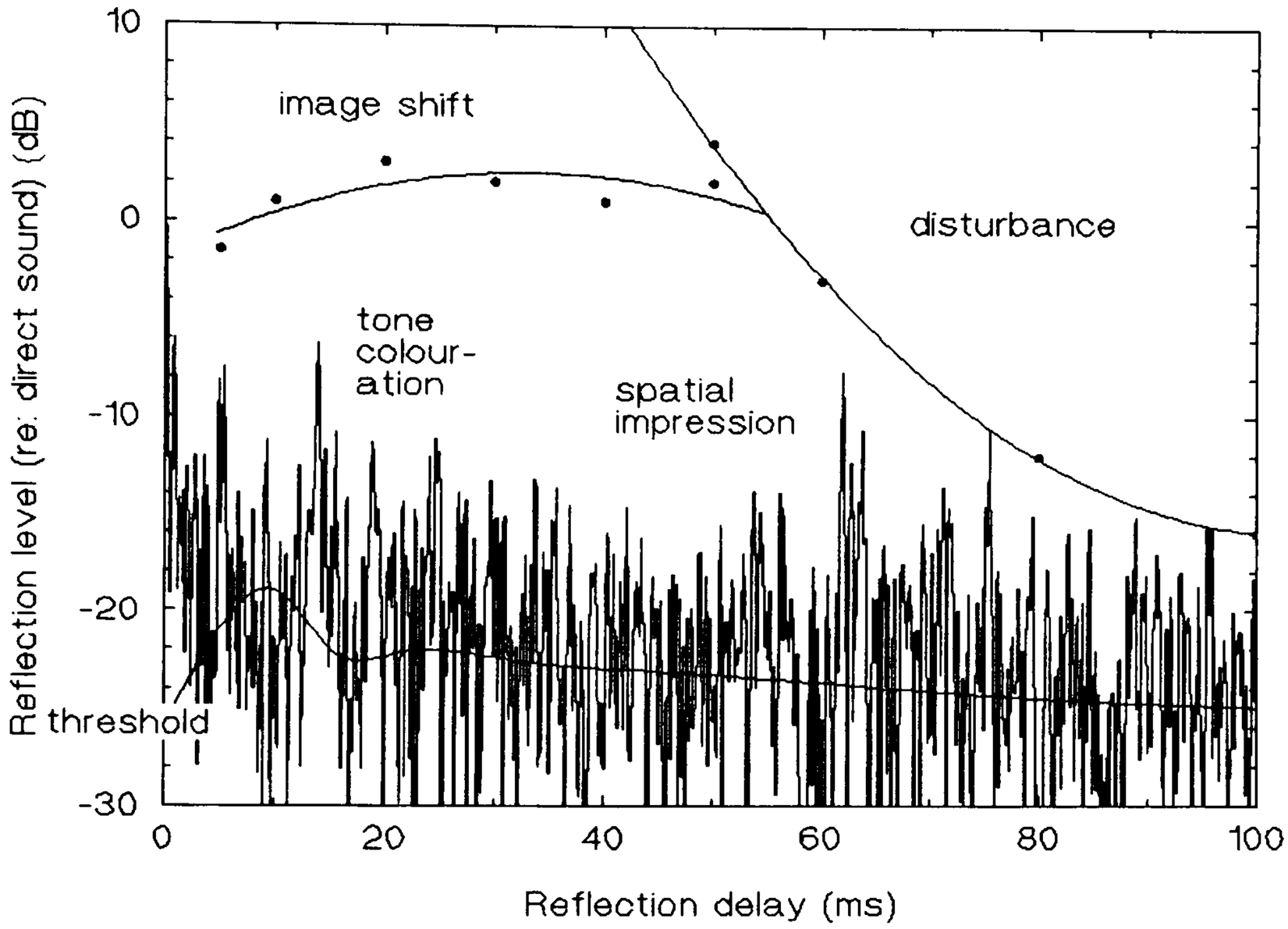

Figure 12.1: Broadband energy-time curve of typical seat dip impulse response plotted over Barron's chart for the subjective effects of a single lateral reflection (after Barron (1971)).

Of course, not all the energy arriving at a seat in the Free Trade Hall in the 40 ms period is at the zero elevation and 40° azimuth for which the chart in figure 12.1 is valid; in particular, the ceiling reflection arrives before 40 ms. Barron (1974, p. 32) notes that it is easier to produce image shift and tonal coloration effects with a ceiling reflection than with a lateral one. An equivalent chart for the subjective effects of a ceiling reflection would therefore have lower thresholds. However, the

given chart also does not show the effects of the forward and backwards reflection masking which would occur in a real hall with many reflections. This phenomenon would tend to raise all the thresholds in the chart. Overall, these two effects will tend to cancel out, so that comparing real energy-time curves with Barron's chart is a realistic test.

There are other points in favour of a 40 ms single-figure attenuation measurement. One is that although the seat dip attenuation in most Free Trade Hall seats fluctuates for a long time, it is fairly stable at 40 ms. This is because the most important early reflections, the first lateral and the ceiling, have already arrived. The final point in favour of a 40 ms comparison time is that it has already been used by Bradley (1991) as an integration limit for his variant of Strength, denoted G_{40}. Whilst 40 ms was deliberately chosen in his case to exclude non-grazing (e.g. ceiling) reflections, Bradley notes that low-frequency G_{40} seems subjectively significant because reductions in it correlate with reductions in the low-frequency strength of the whole impulse response.

To summarise, the single-figure attenuation level L_{min} for a given seat dip impulse response is calculated by taking a Fourier Transform of the portion of the response from 0 to 40 ms after the direct sound, and finding the worst octave attenuation in it. The centre frequency of this octave will be denoted by f_{min}.

12.2 Single-Figure Seat Dip Data from the Free Trade Hall

Having chosen a 40 ms time point and a one octave bandwidth to characterise seat dip spectra, some typical values from a real hall can now be presented and compared with the subjective threshold from chapter 11. As described in section 11.2, the attenuation for the subjective threshold was evaluated from measured impulse responses in the simulator using exactly the same single-figure method, so that it is directly comparable with L_{min} from the Free Trade Hall. A comparison of the data appears in figure 12.2(a) as a function of θ and the number of seat rows. Figure 12.2(b) presents data for the same measuring positions with floor absorbers added. Data for all three types of absorber are shown together in order that the graph be sufficiently general for design purposes. Because the 95% confidence limit range for the subjective threshold is -7.1 ± 0.6 dB octave attenuation, it seems appropriate to present this as one limit of -6.5 dB, above which any attenuation is probably inaudible, and one of -7.7 dB, below which attenuation probably could be heard. The problem for a hall designer is to maximise the number of seats where the single-figure attenuation level L_{min} falls into the inaudible region.

12.2.1 Improving Early Bass Level by Decreasing θ

Figure 12.2(a) shows that there is no simple linear relationship between L_{min} and θ which encompasses all the values of θ investigated. This is in contrast to the very early narrow-band spectra 10 ms after the direct sound arrival in figure 6.5, where it seemed that θ might be a good predictor of attenuation depth. L_{min} does in general worsen with increasing θ, particularly above 85° . A more significant factor,

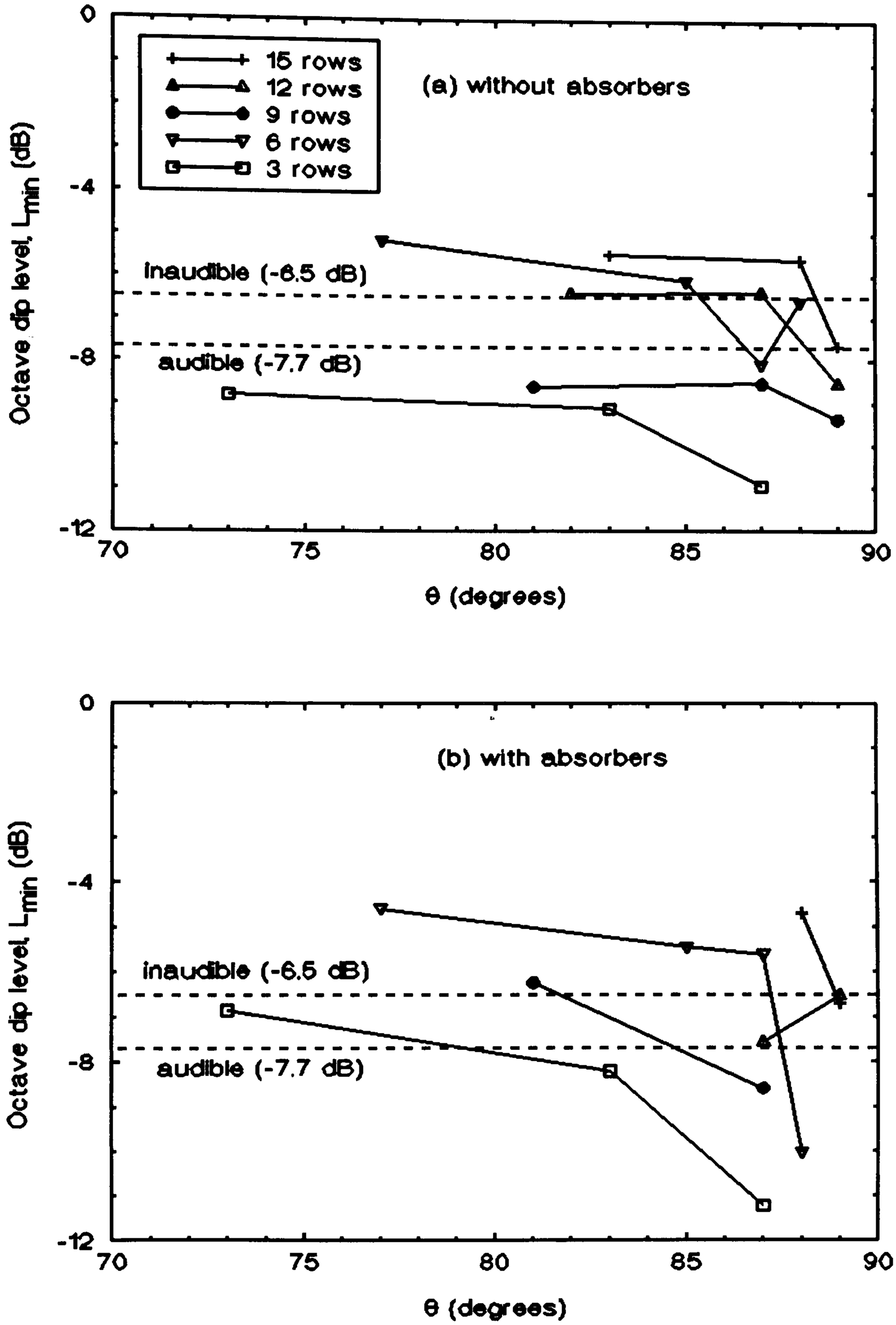

Figure 12.2: Octave dip level L_{min} versus θ, at 40 ms for 3 - 15 rows back, (a) without floor absorbers and (b) with absorbers.

however, is the number of seat rows the sound travels over. This is because the further back the measuring position is, the closer it is to the balcony front, which provides quite strong non-grazing reflections. This effect takes precedence over the worsening attenuation shown in figure 6.2 which is experienced by the direct impulse only as it travels over each successive seat row. This point is reinforced by the fact that all of the three values of L_{min} recorded only three seats back are below the -7.7 dB "audible" line. To give an estimate for designers of how much L_{min} might be improved with θ, it is perhaps valid to average the gradients of the shallow, lower-θ portions of the connecting lines in figure 12.2(a). This gives an approximate gradient of -0.057 dB/° , implying the rather hopeless prescription that to reduce L_{min} by 1 dB requires a decrease in θ of 18° . Achieving this would require very steeply-raked seats.

12.2.2 Improving Early Bass Level with Non-Grazing Reflections

Since larger reductions than 1 dB seem to be afforded by moving the measuring position closer to a source of non-grazing reflections, then the hall designer might decide to combat seat dip attenuation by adding reflecting surfaces, as proposed by Bradley (1991). This option must be followed carefully, however. Some of the smallest values of L_{min} in figure 12.2(a) are exhibited by a seat 15 rows back. This seat is 2.2 m behind the lip of the balcony overhang and so suffers from the defect usually associated with under-balcony seats of high-frequency comb filtering due to interference from overhead reflections. This can result in tonal coloration and a listener at this seat is also likely to experience poor spaciousness due to a low value of L_f. Figure 12.3 shows the increasing comb-filter distortion as the

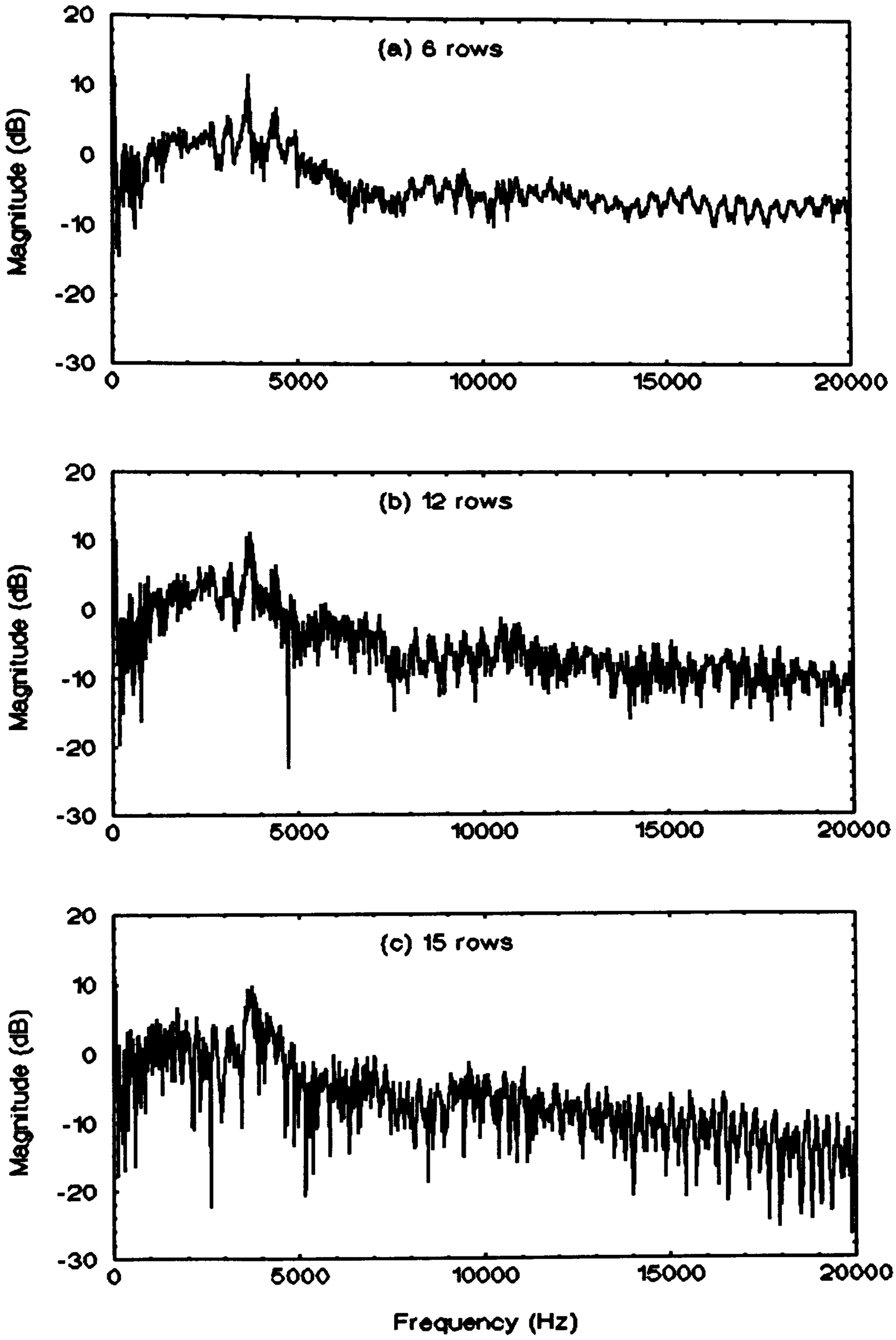

Figure 12.3: The comb filter effect in the spectrum at 40 ms increases as the measuring position is moved further back, towards the balcony front.

measuring position is moved further back, towards the balcony overhang. Similar detrimental effects can be attributed to large areas of purpose-built overhead reflectors (Barron (1974, p. 32) and Kuttruff (1991, pp. 184-186)), so it seems that progressively introducing reflectors to supply non-grazing sound until L_{min} is below -6.5 dB is not an easy answer for the designer. Careful design of lateral reflectors to maximise their low-frequency efficiency and minimise high-frequency specular reflections onto the audience may offer a partial solution. The triangular plates advocated by Nakajima *et al.* (1990 and 1991) seem to be useful in this respect, or perhaps one might use the quadratic residue diffusers invented by Schroeder (1975) to provide diffuse reflections.

12.2.3 Improving Early Bass Level with Floor Absorbers

Figure 12.2(b) shows that subjectively significant improvements in L_{min} have been obtained by using floor absorbers at some seats. As discussed in chapter 7, the improvement is greatest for mid-range values of θ. In general, the improvements are not large, so that a seat must already have a value of L_{min} not far into the audible range for it to become inaudible on the installation of floor absorbers. The possibly undesirable effect of floor absorbers in increasing low-frequency random incidence absorption, and thus decreasing the reverberant bass level, must also be borne in mind.

12.2.4 Improving Early Bass Level by Changing Seat Design and Layout

In part 9.3.5, a simple computer model was used to show that seat dip attenuation may be reduced by decreasing the low-frequency impedance of the seat tops. This

might be achieved in practice by thickening the upholstery on the seat backs and drilling them to effect a resonant Helmholtz absorber in the relevant frequency band. This was not attempted practically in the present study, and would be a good candidate for further work.

Other authors - Ishida *et al.* (1989) and Sessler and West (1964) - have shown that eliminating the seat underpass can help reduce attenuation and shift it to a lower frequency. This seems to work by removing possible paths for some of the multiple reflections arriving after the direct sound. Combining both these ideas might produce an auditorium seat less prone to seat dip attenuation.

Finally, the 1:10 scale model measurements in part 8.1 showed that it might be possible to make seat dip attenuation less audible by restricting the width of the seating blocks. Since a width of only five chairs would be needed to make the attenuation inaudible, this is unlikely to be a solution on its own, however.

12.2.5 Reducing Attenuation Frequency by Decreasing θ

As well as trying to reduce the level of seat dip attenuation, the hall designer might also attempt to shift it to a lower, perhaps subjectively less significant, frequency. Figure 12.4(a) shows that this can be done by decreasing θ, and that, for the hall investigated, there is a linear relationship between the octave frequency of greatest attenuation at 40 ms, f_{min}, and θ. All the measuring positions investigated fall on the same regression line, apart from the outlier 15 rows back. As was noted above, this position is a special case due to the strength of the balcony reflections from

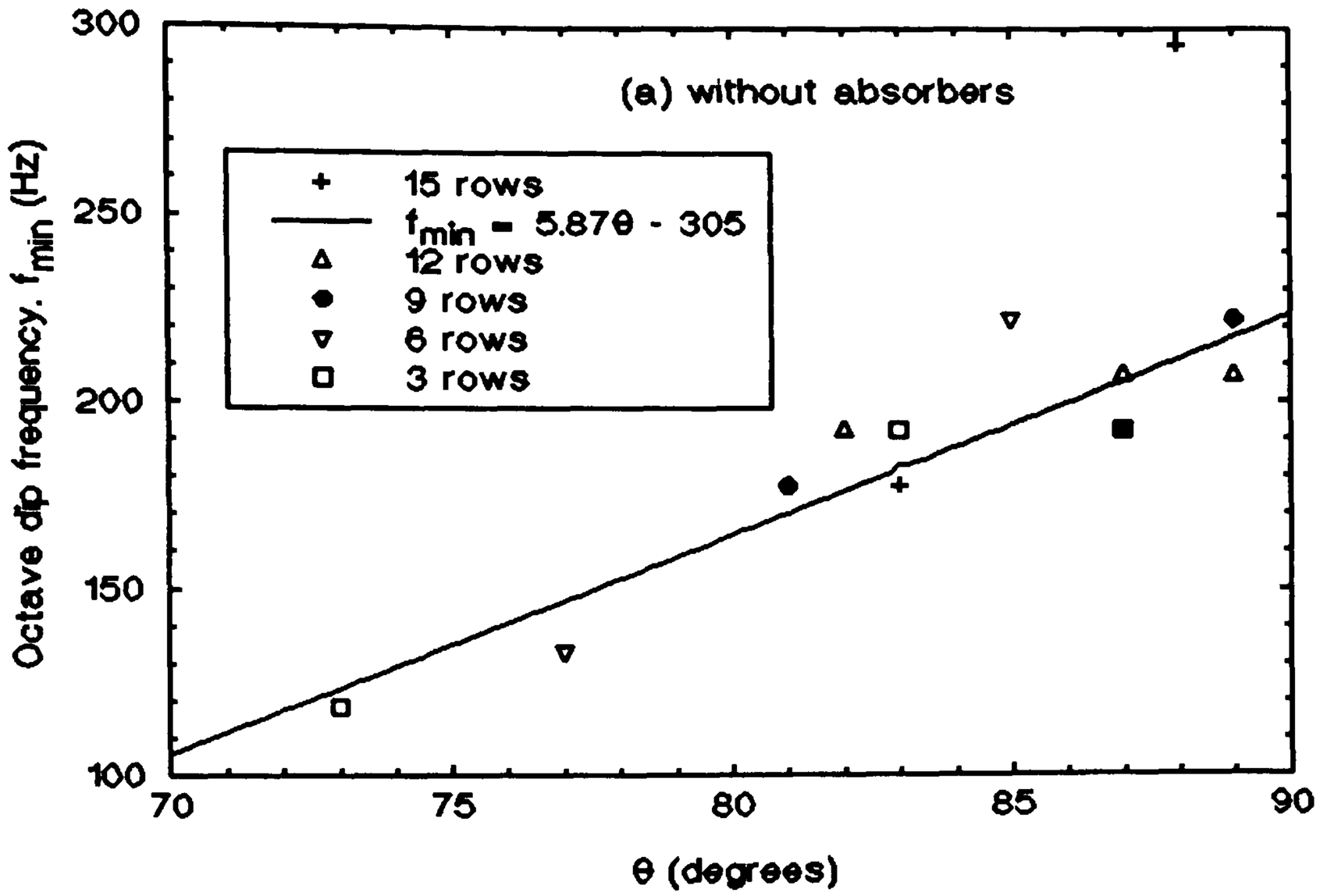

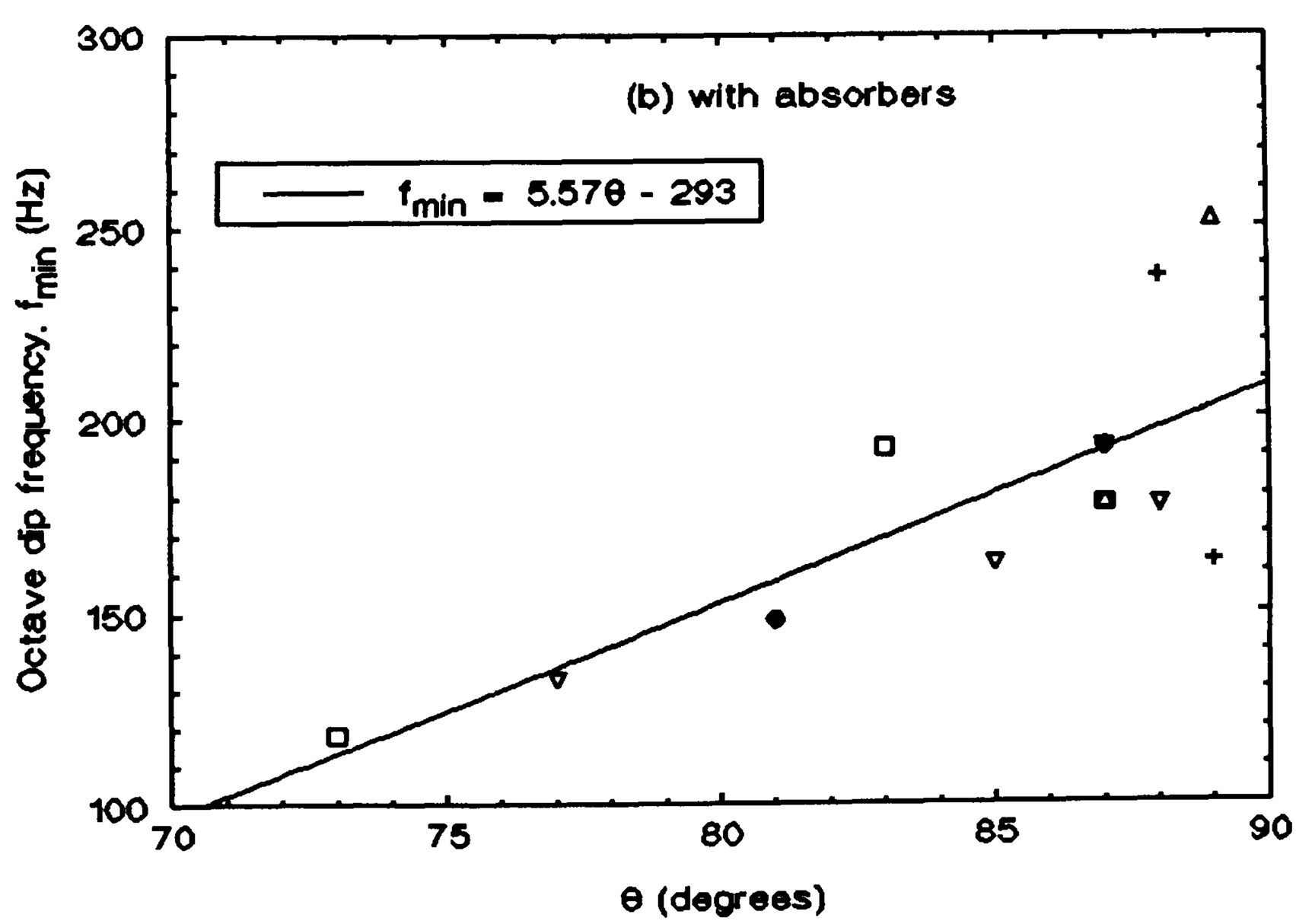

Figure 12.4: Octave dip frequency f_{min} versus θ, at 40 ms for 3 - 15 rows back, (a) without floor absorbers and (b) with absorbers.

immediately overhead. The relationship is essentially similar if floor absorbers are used, as figure 12.4(b) shows, though the frequencies are slightly lower.

This linear relationship is in contrast to the second order ones which Bradley (1991) found between ⅓ octave levels at 20 ms and θ for a particular hall. If the present linear relationship exists in other halls, then it might be a useful design tool. As with using θ to improve L_{min}, figure 12.4 shows that one would have to make large changes to make the attenuation insignificant, however; θ would have to be reduced to 60° to place the octave dip at 50 Hz, for instance.

12.3 A Design Guide

A hall designer has several methods available for reducing seat dip attenuation to a subjectively insignificant magnitude and frequency. Since none of these are inherently satisfactory and without any drawback, using a combination of them will probably be the best course. The majority of the single-figure data from the Free Trade Hall which fall into the "inaudible" range combine more than one factor from a low θ, close reflecting surface, and floor absorbers.

Ensuring good sightlines and hence low values of θ by raking seating and perhaps raising the stage will help to lessen the attenuation slightly and move it to a lower frequency. Incorporating resonant absorbers into the floor of the seating area can be achieved as part of a ventilation system, and this can significantly reduce attenuation and shift it downwards in frequency, at the cost of increasing random incidence audience absorption. Supplying non-grazing energy via overhead

reflectors can also reduce attenuation, at the possible cost of affecting the transfer function at higher frequencies. If this early energy is supplied laterally on paths above the audience plane it would coincide with a design goal for auditory spaciousness. Changing the seat design may also help, as might restricting the width of critical blocks of seating. Finally, boosting the reverberant level is unlikely to make much difference to the perceived early bass attenuation. Changing the design value of what is the subjectively most important acoustic parameter (as Schroeder *et al.* (1974) confirmed) is in any case too gross a strategy for dealing with defects in part of the early field.

Chapter 13

Conclusion

This thesis has encompassed two main studies. The first comprised an examination of the methods available for measuring the acoustic absorption of seating and audiences in the laboratory. This was necessary because a search of the literature revealed a lack of agreement on the best way to achieve the accuracy necessary for a reliable prediction of the reverberation time of an auditorium. The method commonly used at present tends to overpredict seating absorption. Comparisons were therefore made between seating absorption measured in a diffuse reverberation chamber and that calculated from *in-situ* reverberation time measurements in ten auditoria with and without the seats present. It was found that the best procedure in the reverberation chamber was the following:

A rectangular array of approximately 24 seats should be placed in the corner of the chamber at the auditorium row spacing and surrounded by unabsorbent barriers 0.9 m high for unoccupied seats and 1.2 m high for occupied seats. The absorption of the plan area of the array should be measured and corrected for pressure doubling. Two more measurements should be made, with barriers covering the side and front of the array only. A separate measurement of low-frequency barrier absorption may be

subtracted from all the data. The absorption coefficients of the exposed front and sides of the array may now be calculated.

The accuracy of this method was found to be satisfactory for predicting auditorium seating absorption. When calculating the absorption of a particular layout of seats in a hall, the correct amount of side area absorption seems to be obtained by counting all the exposed sides and treating aisles bounded by seating on both sides as one exposed side area, not two. This area should then be assigned the side area absorption coefficient calculated from the reverberation chamber measurements. The use of an edge correction strip with a frequency-constant width to account for side area absorption in halls was found not to be justified in general. This is because the absorption coefficient of the side area of an array of seats can be quite different from that of the plan area. Errors of 5 - 10% can easily be introduced into reverberation time predictions at high frequencies by using a constant strip width.

The accuracy of the reverberation chamber measurement can be marred by anomalous low-frequency absorption contributed by the barriers. This is due at least partly to a lossy transfer of energy from the room modes, a resonant force, to the barrier, a resonant panel. This unwanted absorption is reduced if the seat array is situated in the corner of the reverberation chamber rather than the centre, because only two barriers are required for the corner placing. Accuracy may also be lost because of diffraction at the free edges of the seating array causing the measured absorption coefficient to vary with the array size. Due to mirroring at the

adjacent chamber walls, this edge effect is reduced if the seat array is placed in the corner of the chamber. The effect will become more significant if very small numbers of seats are used.

Some further work remains to be done if seating absorption in auditoria is to be correctly predicted in every case without fail. The variation caused by edge diffraction of the measured absorption coefficient of seating with E, the ratio of perimeter length to array area, remains to be completely investigated. It would be useful to examine the edge effect in direct absorption measurements on blocks of seating over a large range of E, say $0.2 < E < 2$ m^{-1}. (This range is from approximately 1000 to 10 seats). This might be done with careful measurements on 1:10 scale model seats, though a problem would arise in finding a diffuse space big enough to accommodate 1000 seats and where the addition of just 10 seats could be reliably measured. Secondly, it would be useful to obtain more rigorous experimental evidence of the effect of aisles. The scale model experiment could be extended to include an examination of the effects of subdividing large seating blocks and the proximity of one block to another. Thirdly, confirmation of the variation of measured absorption with seating rake could also easily be carried out on scale model seats.

Another area in need of further study is the effect of any differences in diffusion between auditoria and reverberation chambers. Poor auditorium diffusion was suspected as the reason for unusual dips in the *in-situ* absorption coefficient of seating in two of the halls used in this work, and it has been suggested that concert

halls exhibit a preponderance of lateral energy in the reverberant field compared to reverberation chambers. This might be investigated by obtaining the effect of ceiling height on measured seat absorption, since auditoria generally have proportionally lower ceilings than reverberation rooms. Alternatively, direct measurements of the proportion of lateral reverberant energy in halls might be made, and the results used to weight side area absorption coefficients for auditorium seat absorption prediction. Finally, a study of different barrier materials should be made, to determine if the anomalous low-frequency absorption can be further reduced.

The second area of study in this thesis was the low-frequency attenuation of sound passing over seating. Measurements of this seat dip effect in a concert hall were combined with subjective tests in a simulated auditorium sound field to establish the subjective significance of the phenomenon.

In the concert hall, the attenuation spectrum of the direct sound in unoccupied stalls was found to depend on: the number of seat rows between source and receiver; the height of the receiver; and the angles of elevation and azimuth of the sound path. The effect of these parameters largely confirms other seat dip attenuation data in the literature. The attenuation was also found to change considerably over time, due to the influence of many small reflections from the seating and floor. With measurements on scale model seats under anechoic conditions, it was shown that the attenuation depth measured at the receiver varies over 20 ms for the direct sound alone. This means that the attenuation was

influenced by diffraction from seats outside the direct line of propagation and it was reduced when the width of the seating block was reduced.

A scheme for reducing the attenuation using floor-mounted resonant absorbers was tried practically and was found to offer some reduction, by affecting some of the reflections from the floor. One of the absorbers used was an outlet box from an underfloor ventilation system. The use of such a system offers a way of combining a treatment for seat dip attenuation with essential building services in a concert hall.

A model to explain the seat dip effect in the time domain was developed in terms of multiple reflections from the seats and floor. The combined effect of these in the frequency domain is the characteristic notch filter of seat dip attenuation. This model was developed into a computer program which produces a rudimentary time response corresponding to an impulse propagating over a series of seats. The program was found to give reasonable qualitative predictions of the effects of most of the important parameters governing the effect. Some of its results suggested that the attenuation might be reduced by making the backs of the seats resonantly absorbing as well as the floor.

A simulated concert hall sound field was then devised to determine the subjective absolute threshold of perception of seat dip attenuation in a typical auditorium. Using a panel of ten subjects and the method of minimal changes, the threshold was found to be 7.1 ± 0.6 dB attenuation in the 200 Hz octave band of the early sound

field. Seat dip attenuation changes over time in an auditorium impulse response, so this attenuation was evaluated at a fixed time after the arrival of the direct sound. 40 ms was the evaluation time, since there was confidence that all sound energy (including two major reflections) would be integrated by the ear of the listener up to this point.

The subjective threshold is quite large, indicating that the seat dip effect is probably a relatively minor defect in many concert halls. The perception of the attenuation was not found to be greatly affected by the presence of reverberant energy, in contradiction to ideas expressed previously in the literature. It has been reported elsewhere that the early sound field creates an impression of auditory spaciousness independently of reverberation, and it seems that this mechanism is responsible for the detection of seat dip attenuation. One ramification of the value of the threshold is that low-frequency values of monaural early energy measures like C_{80} and T_s are of little subjective significance. In the simulator, it was observed that these parameters changed greatly over the interval of the attenuation threshold. The size of these changes was an order of magnitude greater than the difference limen for the same quantities at mid frequencies.

When the subjective data was compared with the concert hall measurements, it was found that the audibility of the seat dip attenuation in the hall varied with seat position. The attenuations measured for different positions were spread in a range about the subjective threshold, and were affected by several factors. The most important factors in reducing the audibility of the attenuation were: a close,

elevated, reflecting surface; a low angle of vertical incidence of the direct sound; and the use of floor absorbers. In general, more than one of these factors was needed to place the attenuation at a seat in the "inaudible" range. Hence, it is possible to reduce the chance of seat dip attenuation being detected by a listener, but a combination of methods will probably be necessary in most cases. All the methods may have drawbacks for a particular hall design. It is useful, however, that the design criteria for promoting auditory spaciousness coincide with those for ameliorating seat dip attenuation to some extent. This is in the provision of high levels of early lateral energy, which must arrive at paths remote from the audience plane. Hence designs for wide auditoria where much of the seating is on a flat floor far from a reflecting surface should be doubly discouraged.

There is some further work to be done in the understanding and reduction of the seat dip effect. The first quantitative reports in the literature showed that it seemed to depend very little on the presence of an audience. Further experimental confirmation of this would be desirable. A programme of measurements of seat dip attenuation in more existing auditoria would also be useful to confirm its subjective significance in different types of hall. Though the simple computer model which was developed offered some useful insights, accurate quantitative prediction of seat dip attenuation for real concert halls is still some way off. The concept of modelling the effect in the time domain is worth pursuing, however, and more realistic treatments of diffraction and reflection in the time domain could be incorporated into the program. The model may also have to be extended into three dimensions to simulate the effect of the width of the finite seating plane in real

halls. Finally, the possibility of changing the design of the seats themselves to reduce the seat dip effect should also be examined.

Appendix A

Calculation of Standard Error in Reverberation Chamber Absorption Coefficient

The absorption coefficient calculated for the results in Part I is a compound quantity:

$$\alpha = \frac{0.161V}{S}\left[\frac{1}{\overline{T}_f} - \frac{1}{\overline{T}_e}\right] \qquad \text{(A.1)}$$

where the suffix f denotes that the sample is in the room and e that it is empty. However, T_f and T_e are themselves compound quantities, derived from sets of measurements made at five microphone positions for each of two source locations, A and B. Consider first the empty room, and drop the e suffix for clarity. For position A, measurements are made at five microphone positions, so the mean RT is

$$\overline{T}_A = \frac{1}{5}\sum_{i=1}^{5} T_{A_i} \qquad \text{(A.2)}$$

Now in general, for n observations, the standard error in the mean is (Chatfield, 1983, p. 112)

$$s = \frac{\sigma_{n-1}}{\sqrt{n}} \qquad \text{(A.3)}$$

Hence, for the five measurements at position A,

$$s_A = \sqrt{\frac{\sum_{i=1}^{5} T_{A_i}^2 - 5(\overline{T_A})^2}{5 \times 4}} \qquad \text{(A.4)}$$

$$\Rightarrow \quad \sum_{i=1}^{5} T_{A_i}^2 = 20 s_A^2 + 5 \overline{T_A}^2 \qquad \text{(A.5)}$$

and similarly, for position B,

$$\sum_{i=1}^{5} T_{B_i}^2 = 20 s_B^2 + 5 \overline{T_B}^2 \qquad \text{(A.6)}$$

Now, T_{Ai} and T_{Bi} are equivalent (though their means and standard errors are not).

So equations (A.5) and (A.6) may be added to give

$$\sum_{i=1}^{10} T_i^2 = 20(s_A^2 + s_B^2) + 5(\overline{T_A}^2 + \overline{T_B}^2) \qquad \text{(A.7)}$$

Now the empty room process can be considered as a whole to arrive at the empty room standard error. Reasserting the e suffix,

$$s_e = \sqrt{\frac{\sum_{i=1}^{10} T_{e_i}^2 - 10 \overline{T_e}^2}{10 \times 9}} \qquad \text{(A.8)}$$

$$\text{where} \quad \overline{T_e} = \frac{\overline{T_A} + \overline{T_B}}{2} \qquad \text{(A.9)}$$

Substituting for the summation in (A.8) from (A.7),

$$s_\theta = \sqrt{\frac{20(s_{\theta_A}^2 + s_{\theta_B}^2) + 5(\overline{T_{\theta_A}}^2 + \overline{T_{\theta_B}}^2) - 10\overline{T_\theta}^2}{90}} \qquad \textbf{(A.10)}$$

This is the standard error in the empty room RTs. s_{eA} and s_{eB} are found from equation (A.4), T_{eA} and T_{eB} from equation (A.2), and T_e from equation (A.9). Exactly the same measurement procedure is followed with the sample in the room, so s_f is found from equation (A.10), with suffix f substituted for e.

Now in general, the standard error of any compound function $f(m_1, m_2, ..., m_n)$ is s, where

$$s^2 = \left[\frac{\partial f}{\partial m_1}\right]^2 s_1^2 + \left[\frac{\partial f}{\partial m_2}\right]^2 s_2^2 + \ldots + \left[\frac{\partial f}{\partial m_n}\right]^2 s_n^2 \qquad \textbf{(A.11)}$$

and so the total standard error in the absorption coefficient of equation (A.1) is finally given by

$$s_\alpha = \frac{0.161V}{S}\sqrt{\left[\frac{s_f}{\overline{T_f}^2}\right]^2 + \left[\frac{s_\theta}{\overline{T_\theta}^2}\right]^2} \qquad \textbf{(A.12)}$$

Appendix B

Example Output from Absorption Coefficient Comparison Program

Table B.1 contains an example of the results from the automated procedure for comparing many absorption coefficients derived from reverberation chamber measurements on a seat type with the one in-situ auditorium absorption coefficient for the same seat. In this table, all the absorption coefficient sets from the measurements on seat B2 have been used. They are ranked according to the "envelope diff" entry in the table. This is the sum (from 125 - 4 kHz) of the squares of the differences between the error envelopes (± one standard error) of the auditorium measurement and the particular reverberation chamber data set. The meaning of some of the reverberation chamber parameters is as follows:

"array posn" - the seats are laid out in the corner (c) or centre (m) of the chamber;

"barriers cover" - barriers obscure the front (f) or side (s) of the array, or nothing (n);

"array config" - the layout of the array relative to the chamber, as in figure 2.8;

"p corr" - if yes (y), a correction for pressure doubling at the chamber walls has been used, as in equation (2.7);

"f corr" - if yes (y), the absorption for the front and side areas has been added in the correct proportions for the auditorium, to model a large finite area of seating, as in equation (2.10).

	Reverberation chamber parameters							
Rank	array posn	row sp (mm)	barriers cover	barrier height (mm)	array config	"p" corr	"f" corr	envelope diff
1	c	900	f	900	1	n	n	0.0001
2	c	820	s	900	1	n	n	0.0025
3	c	1000	n	-	1	n	n	0.0036
4	c	820	f,s	900	1	n	y	0.0049
5	c	820	f	900	1	n	n	0.0050
6	c	900	f,s	900	1	n	y	0.0065
7	c	820	s	900	1	y	n	0.0068
8	c	1000	f	900	1	n	n	0.0081
9	c	900	s	900	1	n	n	0.0081
10	c	820	f	1200	1	y	n	0.0084
11	c	820	f,s	900	1	n	n	0.0089
12	c	820	f,s	900	3	n	n	0.0094

Table B.1: A comparison of many reverberation chamber seating absorption coefficients with one auditorium seating absorption coefficient for hall B2. The meaning of the column headings is given in the text.

	Reverberation chamber parameters							
Rank	array posn	row sp (mm)	barriers cover	barrier height (mm)	array config	"p" corr	"f" corr	envelope diff
13	c	820	f,s	900	2	n	n	0.0097
14	m	820	f,s	900	2	-	n	0.0101
15	c	1000	n	-	1	y	n	0.0101
16	c	820	f	900	1	y	n	0.0106
17	c	820	f	1200	1	n	n	0.0106
18	c	1000	f,s	900	1	n	y	0.0121
19	c	820	n	-	1	y	n	0.0125
20	c	900	f,s	900	2	n	n	0.0130
21	m	820	f,s	900	1	-	n	0.0139
22	c	820	f,s	1200	3	n	n	0.0140
23	c	1000	s	900	1	n	n	0.0144
24	c	820	f,s	900	1	y	y	0.0145
25	c	820	f,s	1200	1	n	y	0.0151
26	c	820	n	-	1	n	n	0.0159
27	c	820	s	1200	1	y	n	0.0166
28	c	1000	f	900	1	y	n	0.0169
29	c	900	f,s	900	1	y	y	0.0171
30	c	900	s	900	1	y	n	0.0173
31	c	820	f,s	900	2	y	n	0.0179
32	c	820	f,s	1200	2	n	n	0.0180
33	c	1000	f,s	1200	1	n	n	0.0182
34	c	820	s	1200	1	n	n	0.0183

Table B.1 (continued).

	Reverberation chamber parameters							
Rank	array posn	row sp (mm)	barriers cover	barrier height (mm)	array config	"p" corr	"f" corr	envelope diff
35	c	820	f,s	900	1	y	n	0.0189
36	c	900	f,s	900	1	n	n	0.0195
37	c	820	f,s	900	3	y	n	0.0207
38	c	820	f,s	1200	1	n	n	0.0210
39	c	1000	s	900	1	y	n	0.0236
40	c	820	f,s	1200	3	y	n	0.0250
41	c	900	f,s	900	2	y	n	0.0251
42	c	900	f,s	900	3	n	n	0.0257
43	c	820	n	-	2	y	n	0.0265
44	c	820	f,s	1200	1	y	n	0.0277
45	c	820	f,s	1200	1	y	y	0.0293
46	c	1000	f,s	1200	1	y	n	0.0306
47	c	820	f,s	1200	2	y	n	0.0308
48	c	900	f,s	900	1	y	n	0.0323
49	c	820	n	-	2	n	n	0.0367
50	c	1000	f,s	900	1	y	y	0.0393
51	c	900	f,s	900	3	y	n	0.0406
52	c	1000	f,s	900	1	n	n	0.0477
53	c	1000	f,s	900	1	y	n	0.0686
54	m	820	n	-	1	-	n	0.0759

Table B.1 (continued).

Appendix C

Source Code for Seat Dip Prediction Program

```
c       The following FORTRAN 77 code calculates an impulse
c       response for sound propagating over seating according
c       to the theory described in chapter 9.  Each
c       reflection/diffraction node is input from a text file
c       containing details of position, impedance, and a list
c       of nodes obscured from the current one.
c       The impulse response is 4096 points long, at 0.0165
c       ms spacing: when an FFT is applied this will give a
c       spectrum with a resolution of 14 Hz.
c
c       The code listed here requires routines for
c       calculating a FFT and displaying the spectrum.
c       With these included, it compiles, links and runs with
c       version 4.01 of the Microsoft FORTRAN compiler, on an
c       80386-based PC under Microsoft DOS.
c
c       ------------------------------------------------------------
c
c
c                          ----------------
c                            Initialisation
c                          ----------------
c
c
c       Parameters
        INTEGER*4 max_nodes, num_points, one_plusnum
        INTEGER*4 two_plusnum
        INTEGER*4 num_lessone, pow_nodes
        REAL*4 sample_interval
c       max_nodes needs to be at least 8 for 3 rows, or 14
c       for 6 rows; and pow_nodes should be 2**(max_nodes-1)
        PARAMETER (max_nodes = 14)
        PARAMETER (pow_nodes = 8192)
        PARAMETER (num_points = 4096)
        PARAMETER (one_plusnum = 4097)
        PARAMETER (two_plusnum = 4098)
        PARAMETER (num_lessone = 4095)
        PARAMETER (sample_interval = 0.0165)

c       Variables
        INTEGER*2 num_nodes, node, num_obscured(0:max_nodes)
        INTEGER*2 list_obscured(0:max_nodes, max_nodes), i, j
        INTEGER*2 k, num_hits, index
        INTEGER*2 num_seq, list_seq(0:max_nodes, pow_nodes)
        INTEGER*2 current_node, prev_node, next_node
        REAL*4 pos_x(0:max_nodes), pos_y(0:max_nodes)
        REAL*4 dist(max_nodes, 0:max_nodes)
```

```
      REAL*4 dx, dy, source_rec, tantheta, theta, pi
      REAL*4 time, R_dir, pathlength, mag
      REAL*4 impulse_response(0:one_plusnum)
      REAL*4 cos_theta(max_nodes, 0:max_nodes), inc_angle
      REAL*4 ref_angle
      COMPLEX*8 z(0:max_nodes), z_cos_th, one
      COMPLEX*8 R(max_nodes, 0:max_nodes), R_current
      CHARACTER*72 header
      CHARACTER*40 nodes_filename, time_filename
c     Initialise some important variables
      DATA impulse_response / two_plusnum * 0.0 /
      one = CMPLX(1.0, 0.0)
      pi = 4.0 * ATAN(1.0)
      num_hits = 0


c                    ________
c                     Input
c                    ________

      PRINT*,'Name of file containing node data ?'
      PRINT*,'(example is seatray.dat)'
      READ(*,201) nodes_filename
      OPEN(10,FILE=nodes_filename)
      WRITE(*,207) 'Node data input from file ' //
     +  nodes_filename
      READ(10,201) time_filename
      READ(10,200) num_nodes
      READ(10,201) header
      WRITE(*,207) header
      DO 5 i=0,num_nodes
        READ(10,202) node, pos_x(node), pos_y(node),
     +    z(node), num_obscured(node),
     +    (list_obscured(node,j), j=1, num_obscured(node))
        WRITE(*,202) node, pos_x(node), pos_y(node),
     +    z(node), num_obscured(node),
     +    (list_obscured(node,j), j=1, num_obscured(node))
5     CONTINUE
      CLOSE(10)


c                    ____________________
c                     Precalculation
c                    ____________________
c
c     The distances between all possible node pairs are
c     calculated, and also specular coefficients for all
c     possible reflections (not yet taking notice of
c     obscured combinations):
c
c                    z.cos(theta) - 1
c          R   =     ----------------
c                    z.cos(theta) + 1
```

```
      DO 20 i = 1, num_nodes
        DO 10 j = 0, i-1
          dx = (pos_x(i) - pos_x(j))
          dy = (pos_y(i) - pos_y(j))
          dist(i,j) = SQRT(dx*dx + dy*dy)
          cos_theta(i,j) = ABS(dy) / dist(i,j)
          z_cos_th = z(j) * CMPLX(cos_theta(i,j), 0.0)
          R(i,j) = (z_cos_th - one) / (z_cos_th + one)
10      CONTINUE
20    CONTINUE
      source_rec = dist(num_nodes, 0)
      R_dir = ABS(R(num_nodes, 0))

c     This call generates all possible ray sequences
c     (including obscured ones)
      CALL SEQGEN(num_nodes, num_seq, list_seq)

c     Put up headers etc for output
      tantheta = (pos_y(num_nodes) - pos_y(0)) /
     +           (pos_x(num_nodes) - pos_x(0))
      theta = 90.0 - ABS(180.0 * ATAN(tantheta) / pi)
      WRITE(*,205) 'Source - receiver distance (m):',
     +  source_rec
      WRITE(*,205) 'Theta (degrees):                ', theta
      WRITE(*,207) 'Magnitude      time (ms)         ' //
     +  'path (m)   sequence'

c                    ------------------------------------
c                     Impulse response calculation
c                    ------------------------------------
c
c     The predetermined reflection sequences are followed;
c     those which are obstructed are eliminated, and the
c     impulse contributions of the rest are calculated.
c
c     Loop 50 is for all the possible reflection sequences.
c     Loop 40 is for each node in a particular sequence.
c     Loop 30 checks to see if the current node in a
c     particular sequence is obscured from the previous
c     node.  mag is the ray magnitude, pathlength its
c     pathlength.

      DO 50 j = 1, num_seq
        pathlength = 0.0
        mag = 1.0
        prev_node = list_seq(0,j)
        DO 40 i = 1, num_nodes
          current_node = list_seq(i,j)
          DO 30 k = 1, num_obscured(prev_node)
            IF(current_node .EQ.
     +         list_obscured(prev_node,k)) GOTO 50
30        CONTINUE

c         If the end of a valid sequence has not been
```

```
c           reached, then the magnitude is multiplied by the
c           absolute value of the reflection coefficient.
c           The sign of the reflection coefficient is used
c           only for approximately geometric interactions
c           (i.e. the incident and leaving angles are close).

            R_current = R(prev_node, current_node)
            mag = mag * ABS(R_current)
            IF (i .NE. num_nodes) THEN
              next_node = list_seq(i+1,j)
              inc_angle = cos_theta(prev_node, current_node)
              ref_angle = cos_theta(current_node, next_node)
              IF (ABS(inc_angle - ref_angle) .LT. 0.35) THEN
                mag = SIGN(mag, REAL(R_current))
              ENDIF
            ENDIF

c           If the current node is 0, then this sequence has
c           reached the receiver so it only remains to modify
c           the magnitude with the pathlength and normalise
c           to the direct sound.

            pathlength = pathlength +
     +        dist(prev_node, current_node)
            IF(current_node .EQ. 0) THEN
              num_hits = num_hits + 1
              mag = (mag / R_dir) * (source_rec /
     +                               pathlength)**2
              time = (pathlength - source_rec) / 0.344
              index = NINT(time / sample_interval)
              impulse_response(index) =
     +          impulse_response(index) + mag
              WRITE(*,203) mag, time, pathlength,
     +          (list_seq(k,j), k=0, num_nodes)
              GOTO 50
            ENDIF
            prev_node = current_node
 40       CONTINUE
 50     CONTINUE

        WRITE(*,204) 'Number of paths resulting in a hit:',
     +  num_hits
        WRITE(*,204) 'Number of paths discarded:         ',
     +  num_seq-num_hits

c                              ----------
c                               Output
c                              ----------

        WRITE(*,207) 'Wait: writing impulse response to file'
        OPEN(11, FILE=time_filename)
        WRITE(11,*) 0
        WRITE(11,*) sample_interval
        WRITE(11,*) num_points
```

```
      WRITE(11,208) (impulse_response(i), i=0, num_lessone)
      WRITE(11,201) 'Impulse Response - volts'
      CLOSE(11)

200   FORMAT(I2)
201   FORMAT(A)
202   FORMAT(I2,8X,F6.3,1X,F6.3,4X,F6.2,1X,F6.2,1X,I2,21X,
     +  20(:,I2))
203   FORMAT(2X,F6.3,9X,F6.3,11X,F5.2,3X,20(I3,:))
204   FORMAT(/,1X,A,I5)
205   FORMAT(/,1X,A,F5.2)
206   FORMAT(20(I3,:))
207   FORMAT(//,1X,A)
208   FORMAT(1X,F6.3,:)

      END


c     ------------------------------------------------------------------
      SUBROUTINE SEQGEN(n, total_refl, sequences)

c     Generate reflection sequences
c
c     Input:      n             -  number of nodes
c
c     Output:     total_refl    -  number of reflection
c                                  sequences for n
c                 sequences     -  array containing the
c                                  reflection sequences
c     ------------------------------------------------------------------

      INTEGER*2 n, total_refl, sequences(0:14, 8192)
      INTEGER*2 i, j, k, dj

      total_refl = 2**(n-1)

c     First, set all sequences to: n, n-1, n-2, .., 2, 1, 0
      DO 20 j = 1, total_refl
        DO 10 i = 0, n
          sequences(i,j) = n-i
10      CONTINUE
20    CONTINUE

c     Now copy blocks above and to the right, within the
c     array of sequences
      DO 50 k = 1, n-1
        dj = 1 + 2**(k-1)
        DO 40 j = dj, 2**k
          DO 30 i = n-k, n-1
            sequences(i,j) = sequences(i+1, j-dj+1)
30        CONTINUE
40      CONTINUE
50    CONTINUE
      END
```

References

ALRUTZ, H. and SCHROEDER, M. R. (1983). "A fast Hadamard transform method for the evaluation of measurements using pseudorandom test signals," *Proc. 11th I.C.A.* 6, 235-238.

ANDO, Y. (1985). *Concert Hall Acoustics*. Berlin: Springer.

ANDO, Y. and GOTTLOB, D. (1979). "Effects of early multiple reflections on subjective preference judgements of music sound fields," *J. Acoust. Soc. Am.* 65, 524-527.

ANDO, Y. and KATO, K. (1976). "Calculations on the sound reflection from periodically uneven surfaces of arbitrary profile," *Acustica* 35, 321-329.

ANDO, Y., TAKAISHI, M. and TADA, K. (1982). "Calculations of the sound transmission over theater seats and methods for its improvement in the low-frequency range," *J. Acoust. Soc. Am.* 72, 443-448.

ARAU-PUCHADES, H. (1988). "An improved reverberation formula," *Acustica* 65, 163-180.

ASAYAMA, H., KIMURA, S. and SEKIGUCHI, K. (1989). "Revised finite sound ray integration method based on Kirchoff's integral equation," *J. Acoust. Soc. Jpn. (E)* 10(2), 93-100.

B.S.I. (1987). *Measurement of sound absorption in a reverberation room*. BS 3638: 1987.

BARRON, M. (1971). "The subjective effects of first reflections in concert halls - the need for lateral reflections," *J. Sound & Vib.* 15, 475-494.

BARRON, M. (1988a). "Equivalent absorption coefficient in unoccupied British halls," *unpublished*.

BARRON, M. (1988b). "Subjective study of British symphony concert halls," *Acustica* 66, 1-14.

BARRON, M. and MARSHALL, A. H. (1981). "Spatial impression due to early lateral reflections in concert halls: the derivation of a physical measure," *J. Sound & Vib.* 77, 211-232.

BARRON, M. F. E. (1974). *The effects of early reflections on subjective acoustic quality in concert halls*. Ph.D. Southampton University.

BARTEL, T. W. (1981). "Effect of absorber geometry on apparent absorption coefficients as measured in a reverberation chamber," *J. Acoust. Soc. Am.* 69, 1065-1074.

BASS, H. E., SUTHERLAND, L. C. and ZUCKERWAR, A. J. (1990). "Atmospheric absorption of sound: update," *J. Acoust. Soc. Am.* 88, 2019-2021.

BERANEK, L. L. (1960). "Audience and seat absorption in large halls," *J. Acoust. Soc. Am.* 32, 661-670.

BERANEK, L. L. (1962). *Music, Acoustics, and Architecture*. New York: Wiley.

BERANEK, L. L. (1969). "Audience and chair absorption in large halls. II," *J. Acoust. Soc. Am.* 45, 13-19.

BERANEK, L. L. and SCHULTZ, T. J. (1965). "Some recent experiences in the design and testing of concert halls with suspended panel arrays," *Acustica* 15, 307-316.

BLAUERT, J. and LINDEMANN, W. (1986). "Auditory spaciousness: some further psychoacoustic analyses," *J. Acoust. Soc. Am.* 80, 533-542.

BORISH, J. and ANGELL, J. B. (1983). "An efficient algorithm for measuring the impulse response using pseudorandom noise," *J. Audio. Eng. Soc.* 31, 478-487.

BRADLEY, J. S. (1991a). "A comparison of three classical concert halls," *J. Acoust. Soc. Am.* 89, 1176-1192.

BRADLEY, J. S. (1991b). "Some further investigations of the seat dip effect," *J. Acoust. Soc Am.* 90, 324-333.

BRADLEY, J. S. (1992). "Predicting theater chair absorption from reverberation chamber measurements," *J. Acoust. Soc. Am.* 91, 1514-1524.

BRADLEY, J. S. and HALLIWELL, R. F (1989). "Making auditorium acoustics more quantitative," *Sound and Vibration* Feb, 16-23.

CHATFIELD, C. (1983). *Statistics for Technology*, 3rd ed. London: Chapman and Hall.

COX, T. J. (1992). *Objective and subjective evaluation of reflecting and diffusing surfaces in auditoria*. Ph.D. Salford University.

CREMER, L. (1989). "Early lateral reflections in some modern concert halls," *J. Acoust. Soc. Am.* 85, 1213-1225.

CREMER, L. and MÜLLER, H. A. (1982a). *Principles and Applications of Room Acoustics*, Vol. I. Barking, England: Applied Science Publishers.

CREMER, L. and MÜLLER, H. A. (1982b). *Principles and Applications of Room Acoustics*, Vol. II. Barking, England: Applied Science Publishers.

DANIEL, E. D. (1963). "On the dependence of absorption coefficients upon the area of the absorbent material," *J. Acoust. Soc. Am.* 35, 571-573.

DEKKER, H. (1974). "Edge effect measurements in a reverberation room," *J. Sound & Vib.* 32, 199-202.

DOWELL, E. H. (1978). "Reverberation time, absorption and impedance," *J. Acoust. Soc. Am.* 64, 181-191.

EMBLETON, T. F. W. (1971). "Absorption coefficients of surfaces calculated from decaying sound fields," *J. Acoust. Soc. Am.* 50, 801-811.

EYRING, C. F. (1930). "Reverberation time in "dead" rooms," *J. Acoust. Soc. Am.* 1, 217.

GADE, A. C. (1990). "The influence of architectural design on the acoustics of concert halls," *Appl. Acoustics* 31, 207-214.

GOLOMB, S. W. (1967). *Shift Register Sequences*. San Francisco: Holden Day.

GOMPERTS, M. C. (1965). "Do the classical reverberation formulae still have a right for existence?," *Acustica* 16, 255-268.

GOTTLOB, D. (1973). *Comparison of objective acoustic parameters in concert halls with results of subjective experiments*. Ph.D. Gottingen University.

GUILFORD, J. P. (1954). *Psychometric Methods*. New York: McGraw-Hill.

HAAS, H. (1951). "Uber den Einfluss eines Einfachechos auf die Horsamkeit von Sprache," *Acustica* 1, 49-58.

HAAS, H. (1972). "The influence of a single echo on the audibility of speech," *J. Audio. Eng. Soc.* 20, 146-159.

HAWKES, R. J. and DOUGLAS, H. (1971). "Subjective acoustic experience in concert auditoria," *Acustica* 24, 235-250.

HEGVOLD, L. W. (1971). "The sound absorption of an audience on unupholstered seating," *Applied Acoustics* 4, 257-278.

HIDAKA, T., KAGEYAMA, K. and MASUDA, S. (1988). "Recording of anechoic orchestral music and measurement of its physical characteristics based on the auto-correlation function," *Acustica* 67, 68-70.

IIDA, K. and ANDO, Y. (1986). "Expansion of the image method for acoustical design of auditoria," *Proc. 12th I.C.A.*, paper E11-3.

ISHIDA, K., SUGINO, K. and MASUDA, I. (1989). "On the sound reflection of the auditorium seats," *Proc. 13th I.C.A.* 2, 157-160.

JAROCH, A., JURKIEWICZ, J. and RUDNO-RUDZINSKA, B. (1990). "A geometrical analysis of reflected-diffracted sound rays in three dimensional space," *Proc. Inter-noise 90*, 239-242.

JORDAN, V. L. (1968). "Einige Bemerkungen uber Anhall und Anfangsnachhall in Musikraumen," *Applied Acoustics* 1, 29-36.

JORDAN, V. L. (1980). *Acoustical Design of Concert Halls and Theatres*. Barking, England: Applied Science Publishers.

KATH, U. and KUHL, W. (1961). "Einfluss von Streuflache und Hallraumdimensionen auf den Gemessenen Schallabsorptionsgrad," *Acustica* 11, 50-64.

KATH, U. and KUHL, W. (1964). "Messungen zur Schallabsorption von Personen," *Acustica* 14, 49-55.

KATH, U. and KUHL, W. (1965). "Messungen zur Schallabsorption von Polsterstuhlen," *Acustica* 15, 127-131.

KAWAI, Y. and TERAI, T. (1991). "Calculation of sound fields over audience seats by using integral method," *Trans. A.S.M.E., J. of Vibration and Acoustics* 113, 22-27.

KEET, W. D. V. (1968). "The influence of early lateral reflections on the spatial impression," *6th I.C.A.* E, 53-56.

KLEINER, M., SVENSSON, P. and DALENBACK, B.-I. (1990). "Auralization: experiments in acoustical CAD," *AES 89th Convention*, paper I-I-3.

KOLMER, F. and KRNAK, M. (1961). "Der Einfluss der Flache des Prufmaterials auf die Diffusitat des Schallfeldes im Hallraum und auf den Scallabsorptionsgrad," *Acustica* 11, 405-413.

KOSTEN, C. W. (1960). "International comparison measurements in the reverberation room," *Acustica* 10, 400-411.

KOSTEN, C. W. (1965). "New method for the calculation of the reverberation time of halls for public assembly," *Acustica* 16, 325-330.

KUTTRUFF, H. (1991). *Room Acoustics*. London: Elsevier.

LAM, Y. W. and HODGSON, D. C. (1990). "The prediction of the sound field due to an arbitrary vibrating body in a rectangular enclosure," *J. Acoust. Soc. Am.* 88, 1993-2000.

MEIROVITCH, L. (1967). *Analytical Methods in Vibrations*. New York: Macmillan.

MORIMOTO, M., ISHII, M. and MAEKAWA, Z. (1990). "Influence of a visual stimulus on echo-threshold," *J. Acoust. Soc. Jpn. (E)* 11, 198.

MORIMOTO, M. and MAEKAWA, Z. (1988). "Effects of low frequency components on auditory spaciousness," *Acustica* 66, 190-196.

MORIMOTO, M. and MAEKAWA, Z. (1989). "Auditory spaciousness and envelopment," *13th I.C.A.*, 215-218.

MORIMOTO, M. and PÖSSELT, C. (1989). "Contribution of reverberation to auditory spaciousness in concert halls," *J. Acoust. Soc. Jpn. (E)* 10, 87-92.

NAGATA, M. (1990). "What we have learned from the listening experiences in concert halls - physical properties and subjective impressions of five concert halls in Tokyo," *Applied Acoustics* 31, 29-45.

NAKAJIMA, T., ANDO, Y. and FUJITA, K. (1990). "Strong lateral low-frequency components reflection from canopy complex comprising triangle plates in concert halls," *J. Acoust. Soc. Am.* 88 (Suppl. 1), S185.

NAKAJIMA, T., ANDO, Y. and FUJITA, K. (1991). "Fujita Hall 2000 with adjustable IACC and reverberation time," *J. Acoust. Soc. Am.* 90, 2280.

NORTHWOOD, T. D. (1963). "Absorption of diffuse sound by a strip or rectangular patch of absorptive material," *J. Acoust. Soc. Am.* 35, 1173-1177.

OLIVE, S. E. and TOOLE, F. E. (1989). "The detection of reflections in typical rooms," *J. Audio Eng. Soc.* 37, 539-553.

REICHARDT, W. and LEHMANN, U. (1981). "Optimierung von Raumeindruck und Durchsichtigkeit von Musikdarbeitungen durch Auswertung von Impulsschalltests," *Acustica* 48, 174-185.

RIFE, D. D. (1987). "Maximum-length sequences optimize PC-based linear systems analysis," *Personal Engineering and Instrumentation News* May, 35-43.

RIFE, D. D. and VANDERKOOY, J. (1989). "Transfer-function measurement with maximum-length sequences," *J. Audio. Eng. Soc.* 37, 419-444.

RINDEL, J. H. (1991a). "Modelization of the angle-dependent pressure reflection factor," *Computer Modelling Symposium*, Copenhagen, 19 - 22 August.

RINDEL, J. H. (1991b). "Odeon - a hybrid computer model for room acoustic modelling," *Western Pacific Regional Acoustics Conference IV*, Brisbane, 26 - 28 November.

SABINE, W. C. (1923). *Collected papers on acoustics*. Cambridge, Mass.: Harvard University Press.

SCHROEDER, M. R. (1975). "Diffuse sound reflection by maximum-length sequences," *J. Acoust. Soc. Am.* 57, 149-150.

SCHROEDER, M. R. (1979). "Integrated-impulse method measuring sound decay without using impulses," *J. Acoust. Soc. Am.* 66, 497-500.

SCHROEDER, M. R., GOTTLOB, D. and SIEBRASSE, K. F. (1974). "Comparative study of European concert halls: correlation of subjective preference with geometric and acoustic parameters," *J. Acoust. Soc. Am.* 56, 1195-1201.

SCHULTZ, T. J. and WATTERS, B. G. (1964). "Propagation of sound across audience seating," *J. Acoust. Soc. Am.* 36, 885-896.

SEKIGUCHI, K. and KIMURA, S. (1991). "Calculation of sound field in a room by finite sound ray integration method," *Applied Acoustics* 32, 121-148.

SESSLER, G. M. and WEST, J. E. (1964). "Sound transmission over theatre seats," *J. Acoust. Soc. Am.* 36, 1725-1732.

STEPHENSON, U. (1990a). "Comparison of the mirror image source method and the sound particle simulation method," *Applied Acoustics* 29, 35-72.

STEPHENSON, U. M. (1990b). "A sound particle scattering model simulating sound propagation in factory halls," *Proc. Inter-noise 90*, 243-246.

SUBAGIO (1986). *Acoustic absorption of auditorium seating*. M.Sc. Salford University.

TACHIBANA, H., YAMASAKI, Y., MORIMOTO, M., HIRASAWA, Y. and MAEKAWA, Z. (1986). *The acoustical data of European concert halls obtained by survey with new methods*. Institute of Industrial Science, University of Tokyo, 7-22-1, Roppongi, Minato-ku, Tokyo, 106 Japan.

TACHIBANA, H., YAMASAKI, Y., MORIMOTO, M., HIRASAWA, Y., MAEKAWA, Z.-I. and PÖSSELT, C. (1989). "Acoustic survey of auditoriums in Europe and Japan," *J. Acoust. Soc. Jpn. (E)* 10, 73-85.

TAYLOR, E. W. (1985). *Room modes and sound absorption: some practical measurements compared with theoretical predictions*. B.B.C. report RD 1985/11.

TEN WOLDE, T. (1967). "Measurements on the edge-effect in reverberation rooms," *Acustica* 18, 207-212.

TERAI, T. and KAWAI, Y. (1989). "Calculation of steady and transient sound fields by using integral equation," *Proc. Kobe Symposium*, 75-97.

THIELE, R. (1953). "Richtungsverteilung und Zeitfolge der Schallruckwurfe in Raumen," *Acustica* 3, 291-302.

WATERHOUSE, R. V. (1955). "Interference patterns in reverberant sound fields," *J. Acoust. Soc. Am.* 27, 247-258.

WETHERILL, G. B. (1981). *Intermediate Statistical Methods*. London: Chapman and Hall.

WILLIAMSON, R. P. (1989). "Optimisation of variable lateral energy for spatial impression in a hall," *Applied Acoustics* 26, 113-134.

ZWICKER, E. and FELDTHELLER, R. (1967). *Das Ohr als Nachrichtenempfanger*. Stuttgart: Hirzel.